Phenotypic and Proteomic Analysis of 5-Fluorouracil Treated Normal and Carcinoma Cells

A thesis submitted for the degree of Ph.D.

Dublin City University

By

William Bryan, B.Sc.

The research work described in this thesis was performed under the supervision of

Prof. Martin Clynes

National Institute for Cellular Biotechnology

Dublin City University

2006

I hereby certify that this material, which I now submit for assessment on the programme of study leading to the award of Ph.D.... (insert title of degree for which registered) is entirely my own work and has not been taken from the work of others save and to the extent that such work has been cited and acknowledged within the text of my work.

Signed: William Bryson (Candidate) ID No.: 98572032

Date: 22-11-06

Acknowledgements

Firstly, I'd like to thank Prof. Martin Clynes and Dr. Paula Meleady for the opportunity to pursue this Ph.D. in the National Institute for Cellular Biotechnology at Dublin City University and for their mentoring over the years – it's very much appreciated.

Also I'd like to thank the proteomics crew, Andrew, Paul, Jon and Mick for all the technical discussions on casting the perfect 2D gels and mastering of the mass spectrum. Also I'd like to thank the proteomics/toxicology crew, Lisa and Joanne, for the useful discussions over the years. Also I have to thank Lisa for the friendly 'slagging' towards the end of our Ph.D.'s, I guess you won the Ph.D. race, barely, by just 30 minutes.

Cheers to Bella and Eadaoin for making those otherwise painful weekends pleasant.

Also I have to thank the old Differentiation lab, Finbar, Brendan, and Jason for showing me the ropes when I started and for the many crazy surreal moments. I can't forget the diabetes lab, cheers, particularly Elaine and Irene – always up for a bit of craic. Thanks to Helena and Annemarie for the useful invasion assay discussions. Cheers Toxicology folk particularly Vanessa for helpful discussions on drug metabolism and Molecular folk particularly Paudie, Mohan and Jai for all the Bioinfomatics tips.

Thanks to Bella for all the help at the end of my Ph.D. especially during my crazy scientist stage. Thanks to Paul for the games of pool and the use of the office while writing up the thesis – it helped maintain my sanity.

Thanks to Joe, Ultan, Mairead, Carol and Yvonne, the crucial cogs in the machine that is the NICB, especially to Carol and Yvonne for the help at the end, cheers.

-ABBREVIATIONS-

5-FU	-	5-Fluorouracil
52FdU	-	5-Fluoro-2'deoxyuridine
55FdU	-	5-Fluoro-5'deoxyuridine
Adr	-	Adriamycin
ATCC	-	American Type tissue Culture Collection
ATR	-	ataxia-telangiectasia-and-RAD3-related
ATM	-	ataxia telangiectasia mutated
BrdU	-	Bromodeoxyuridine
DMEM	-	Dulbeccos modified Eagle Medium
DMSO	-	Dimethyl sulphoxide
ECM	-	Extracellular Matrix
eIF	-	eukaryotic Initiation Factor
EEF	-	Eukayotic Elongation Factor
ER	-	Endoplasmic Reticulum
FAK	-	Focal Adherence Kinase
FCS	-	Fetal Calf Serum
HSPB1	-	Heat shock protein 27
IC	-	Inhibitory concentration
ID	-	Inhibitor of DNA binding
kDa	-	KiloDaltons
PBS-A	-	Phosphate Buffered Saline – Autoclaved
NSCLC	-	Non-Small Cell Lung Carcinoma
MMP	-	Matrix Metalloproteinase
MALDI-ToF	-	Matrix Assisted Laser Desorption/Ionisation – Time of Flight

MS	-	Mass Spectrometer
RNA	-	ribonucleic acid
SDS	-	Sodium Dodecyl Sulphate
PAGE	-	Polyacryamide Gel Electrophoresis
mRNA	-	messenger RNA
rRNA	-	Ribosomal RNA
tRNA	-	transcriptional RNA
RT	-	Room temperature
TP	-	Thymidine Phosphorylase (Platelet Derived Growth Factor)
TS	-	Thymidylate Synthetase
UHP	-	Ultra high pure water
UPR	-	Unfolded protein response
v/v	-	volume/volume
w/v	-	weight/volume
XBP1	-	X-Box binding protein 1
rpm	-	revolutions per minute

-Abstract-

The anti-metabolite - 5-Fluorouracil (5-FU) – is the most widely used chemotherapeutic drug. It exerts its anti cancer effect through incorporation into DNA and RNA. Characterisation of this drugs mode of action is crucial in the development of future therapies. There have been many DNA microarray experiments performed in order to gain such information. However, only two proteomic experiments have been performed to date that look at the effect of 5-FU treatment. Here the proteomic alterations induced by IC_{80} 5-FU treatment of normal and cancer cells of epithelial origin of the lung and breast are investigated. These cell lines include a lung adenocarcinoma (A549), a non small cell lung carcinoma cell line (DLKP), normal bronchial epithelial cell line (NHBE), a breast adenocarcinoma (MCF-7) and human mammary epithelial cells (HMEC). Phenotypes were characterised and 5-FU was found to induce and reduce invasion in various cell lines. Adherence was altered in one of the three cancer cell lines to the extracellular matrix proteins collagen type IV and fibronectin. Differential regulated proteins were quantified using 2 dimensional difference gel electrophoresis (2D-DIGE) and differentially regulated proteins were identified using matrix-assisted laser desorption/ionization time of flight mass spectrometry (MALDI-ToF MS). Data shows the NHBE showed a dose dependent response to 5-FU treatment. Proteins that were found regulated are discussed in terms of microtubule dynamics and future drug combinations, translation control and stress, cytosketetal dynamics and invasion, and inhibition of apoptosis.

5-Fluorouracil is being increasing replaced in clinical trials with 3rd generation 5-FU drugs such as capecitabine. Capecitabine is converted in the liver to 5-fluoro-5'-

deoxyuridine (55FdU) and this is converted to 5-FU by thymidine phosphorylase whose over expression is induced by radiotherapy. 5-FU is converted to 5-fluoro-2'-deoxyuridine in the cytoplasm. A comparison using 2D-DIGE between DLKP treated 5-FU and the fluoropyrimidines – 52FdU and 55FdU at IC_{80} cocentrations to determine similar proteomic alterations. Results demonstrated that the down regulation of Stathmin as a common fluoropyrimidine response. Furthermore this data may indicate a role for the use of vinca alkoloids or taxanes in combination with 5-FU.

Resistance to 5-FU is a major clinical problem as mediated predominantly by over expression of Thymidylate Synthetase. A variant of DLKP was generated by pulse selection with 55FdU and showed a ~4 fold resistance to 5-FU. Proteomic analysis using 2D-DIGE identified several proteins involved in uracil metabolism and oxidative metabolism differentially regulated between DLKP and DLKP-55.

DLKP is a heterogeneous cell line composed of at least three subpopulations. These subpopulations were isolated and were assigned the names DLKP-SQ, DLKP-I and DLKP-M. In this thesis data is presented demonstrating highly significant differences in motility and invasion between the clonal subpopulation. Analysis of proteomic alteration was carried out using 2D-DIGE on both the total cell lysate and the hydrophobic proteomes. Proteins were identified in the total cell lysates that suggest that DLKP-M is mesenchymal-like in nature as originally described and that the interconversion process observed between the clones is regulated at least by key proteins involved in protein metabolism. Analysis of the hydrophobic proteome found at least 300 proteins that correlated with motility/invasion and collagen synthesis. Identification of these proteins demonstrated increased association of microfilaments to

the cellular membranes a process important in cellular motility. Furthermore 3 poorly described proteins were identified that correlated with motility/invasion and collagen synthesis. In addition data generated by these experiments indicates that fluoropyrimidine treatment of DLKP does not result in the selection of one of the subpopulations of DLKP and that DLKP-55 is not a subpopulation of DLKP. Data also shows the presence of protein in the heterogeneous population that are not present or are over expressed in the clonal populations indicating cell-cell communication.

Table of contents

1.0 Introduction

1.1 Fluorouracil

1.1.1 Development of the fluoropyrimidines and 5-Fluorouracil

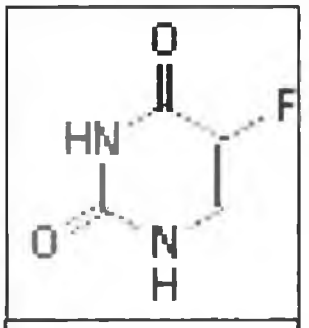

Figure 1.1: Chemical structure of 5-FU

In 1957 Heidelberger created the anti-metabolite group of drugs referred to as the fluoropyrimidines and is the first example of a rationally designed drug. The group of fluoropyrimidines include 5-Fluorouracil (5-FU) {Heildelberger *et al.*, 1957} and it has become the most commonly used chemotherapeutic drug used today {Longley *et al.*, 2003}. The development of the fluoropyrimidines was based on the observation that rat hepatomas utilised far greater amounts of the pyrimidine - uracil {Rutman *et al.*, 1954}. The molecular structure of 5-FU can be seen in figure 1.1 and is essentially a uracil molecule with a fluorine atom substituted for a hydrogen atom in position 5, hence the name 5-Fluorouracil {Heidelberger *et al.*, 1957}.

1.1.2 Clinical usage of 5-FU

In the 1980's the most commonly dosage schedules with 5-FU were a monthly course with 5 daily doses given as intravenous bolus infusions of 400-600mg/ml^2, or of one bolus infusion at same concentration on a weekly basis. Dosage is generally limited by myelosuppression or mucositis. Alternatively a continuous infusion is employed intravenous infusion is used, a higher dosage is required of 1000-2000 mg/m^2/d to achieve a steady state concentration of 1-5μM of 5-FU in plasma where the steady state concentration can vary as much as 10 fold during treatment. This treatment regimes side effect is mucositis with minimal myelosupression. Continuous infusion was found to be superior over bolus infusion (Erlichman, C. *et al.* 1988}. The 5-FU half life in plasma is in the order of 10 to 20 minutes {Diasio, 1989}.

Dihydropyrimidine dehydrogenase is responsible for catabolic degradation of 5-FU in the clinic and modern therapies include the use of Eniluracil, a dihydropyrimidine dehydrogenase inhibitor, and allows for the clinically lower dosage of 300mg/ml/d in combination with Eniluracil these trials failed and use of clinical trials is discontinued (Malet-Martino and Martino, 2000). Other dosage regimes in include combination with the salt of folinic acid called commercially as Leucovorin {Adjei *et al.* 2002}.

Second generation 5-FU prodrugs were developed with the intention for oral administration and include 1-(2-tetrahydrofuryl)-5-fluorouracil (Tegafur or Futraful), 5-fluoro-5'-deoxyuridine (doxifluridine or Furtulon®, abbrev. 55FdU) but caused intestinal toxicity, which lead to the generation of third generation drugs and include capecitabine (discussed later) and the dihydropyrimidine dehydrogenase inhibitory compounds Eniluracil used in combination with uracil and Futraful and S-1 a combination of Futraful plus 5-chloro-2,4-dihydroxypyridine plus potassium oxonate (Malet-Martino and Martino, 2000).

1.1.3 5-Fluorouracil metabolism and method of action

Like most metabolites two pathways referred to as catabolism and anabolism process 5-FU. The anabolic route gives rise to the active metabolites and the catabolic leads to 5-FU degradation and elimination from the organism (Malet-Martino and Martino, 2000).

Anabolism

5-FU is processed by a series of enzymatic reactions that are normally utilised by uracil and its derivatives and thus results in 5-FU incorporation into RNA and DNA, and to the formation of 5-FU nucleotide sugars (Malet-Martino and Martino, 2000).

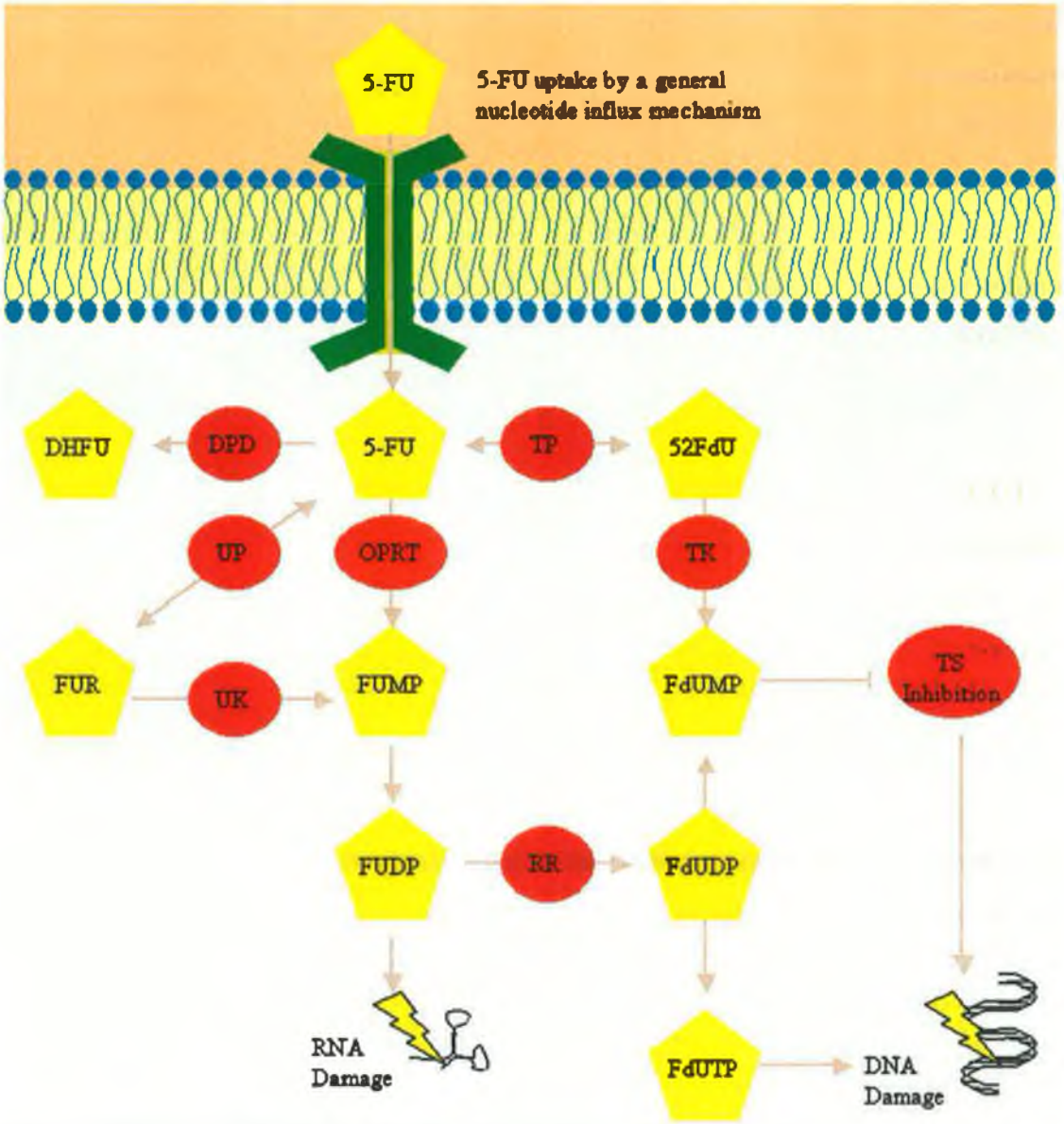

Figure 1.2: Metabolism of 5-FU results in the production of its active metabolites; FdUMP, FdUTP and FUTP, that result in DNA and RNA damage. Enzymes are represented by red ovals; DPD dihydrodyrimidine dehydrogenase; UP (uracil phosphorylase; UK (uridine kinase); TP (thymidine phosphorylase); TK (thymidine kinase); RR (ribonucleotide reductase); OPRT (Orotate phosphoribosyl transferase).

Upon entry into the cells 5-FU is converted through a series of enzymatic reaction into fluorouridine monophosphate which is incorporated into RNA and can inhibit polyadenylation of RNA and prevent pseudouridine maturation preventing correct folding of tRNA. The anabolism of 5-FU is summarised in figure 1.2.

5-FU is also converted into fluorodeoxyuridine monophosphate (FdUMP) by a series of enzymatic steps. FdUMP irreversibly binds to thymidylate synthetase (TS). This inhibition prevents TS from replenishing the thymidine pool during DNA synthesis of

the S-phase of the cell cycle. As a result other nucleotides are incorporated into DNA. The DNA excision repair mechanism excises these misincorporated bases from the DNA backbone. At this point there is little thymidine available for DNA synthesis (Malet-Martino and Martino., 2000). DNA synthesis is effectively stopped at

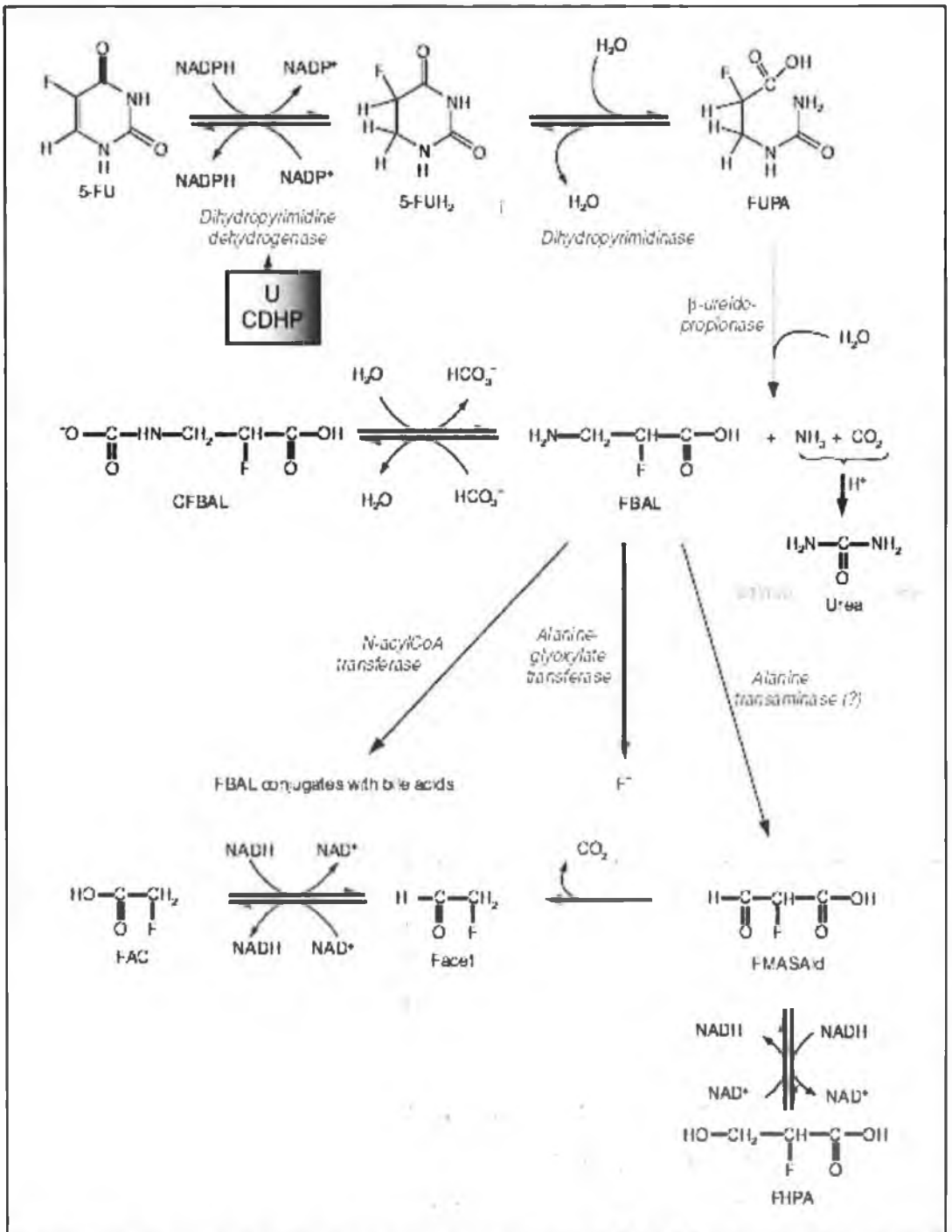

Figure 1.3: The catabolic route for the degradation of 5-FU (Malet-Martino and Martino, 2000)

this point and at the molecular level this would appear as stalled replication forks. FdUMP may be further anabolized to the triphosphate, FdUTP, which serves as an

alternative substrate for dTTP in DNA replication. Once incorporated into DNA, this is a substrate for the base repair enzyme, uracil glycosylase. If multiple analog residues are incorporated in close proximity, the attempts to remove them may result in DNA fragmentation (Ingraham *et al.*, 1982). The ribonucleoside triphosphate of 5-fluorouracil, FUTP, may be incorporated into RNA, and affect the function of RNA transcripts (Longley *et al.*, 2003).

1.1.4 Mode of action of 5-FU

The anabolism of 5-FU results in the production of the metabolic derivates - FdUMP, FdUTP and FUTP. These compounds are responsible for the cytotoxic effects induced by 5-FU. FdUMP irreversibly binds to TS causing its inactivation leading dTTP depletion causing stalling of DNA replication during S phase of the cell cycle. FdUTP is incorporated into DNA leading to uracil glycosylase excision, since dTTP is depleted this results in a series of nucleotide misincorporations, if multiple FdUTP residues are incorporated in close proximity it may result in DNA fragmentation. FUTP is incorporated in to RNA and leads to RNA instability.

Clinically the mode of action of 5-FU is dependent upon administration regimen – bolus or continuous infusion. Studies have shown that bolus infusions predominantly cause RNA damage leading to cell death whereas continuous infusions lead to TS inhibition and DNA damage (Malet-Martino and Martino, 2000).

1.1.4 DNA damage and repair

How cells exactly detect DNA lesions caused by 5-FU mediated stalling of replication forks is poorly understood. However, both ATR and Chk1 have a role in maintaining the potential functionality during stalled replication of DNA or stalled replication forks. It is thought that the proteins that respond first to DNA replication stresses are the DNA clamp loading proteins Rad17 and the heterotrimeric clamp Rad9-Hus1-Rad1 (9-1-1 complex). (Clamp proteins are DNA binding proteins essential for DNA repair) Rad 17 preferentially binds to nicked DNA and recruits the 9-1-1 complex which then enables ATR to recognize it substrates which leads to cell cycle arrest and to either DNA repair or apoptosis (Renton *et al.*, 2003).

ATM and DNA-PK are serine/threonine kinases that represent a second set of DNA damage sensors, and their role in the detection of 5-FU induced DNA damage is

unclear (Sampath *et al.*, 2003). Recent research found that MCF-7 cells exposed to 5-FU under conditions that induce p53 accumulation in the presence of the ATM inhibitor, caffeine, found that p53 failed to accumulate indicating the genotoxic response triggered by 5-FU is mediated by ATM recognition of DNA damage. However, the exact role of ATM, other than phosphorylation of p53 on serine residues is unknown (Renton *et al.*, 2003). The involvement of DNA-PK or ATR signal transduction in response to 5-FU genotoxicity is unknown.

1.1.5 RNA damage and RNA Decay

All RNA species snRNA, mRNA, tRNA and rRNA during transcription in the presence of FUTP will result in the incorporation of the fluorinated residues. The RNA molecules rRNA, tRNA and snRNA require the conversion of uracil into pseudouridine for maturation. If FUTP is incorporated in this location formation of pseudouridine is prevented and the RNA secondary structure and function is disrupted (Gu *et al.*, 1999; Longley *et al.*, 2003). Functionality of snRNA can be impaired when synthesised in the presence of FUTP (Lenz *et al.*, 1994).

The nuclear RNA processing exosome, a complex of 10 exoribonucleases, plays an important role in rRNA processing as it is required for proper 3′-end processing of rRNA and for the degradation of abnormal pre-rRNA processing intermediates. RNA is surveyed by exosomes and they detect structurally abnormal mRNAs. There are few studies done to date that have investigated the role of fluorinated RNA and exosome surveillance. However microarray experiments on yeast treated with 5-FU suggest that 5-FU inhibits an exosome-dependent surveillance pathway that degrades polyadenylated precursor rRNAs (Fang, F. 2004).

Protein synthesis requires aminoacylation of amino acids to the elongating peptide by ribosomes attached to mRNA. In rat models aminoacylation rates vary depending on 5-FU dose and amino acid and is a result of fluorinated tRNA (Vulimiri *et al.*, 1993).

1.1.6 Catabolism

In vivo, approximately 80% of 5-FU is degraded by the catabolic pathway. The degradation of 5-FU is mediated through the alanine aspartate metabolic route. The first step of this process is governed by dihydropyrimidine dehydrogenase (DPD) and

is the rate-limiting step in determining how much 5-FU is converted to 5,6-dihydro-5-fluorouracil and requires NADPH. 5,6-dihydro-5-fluorouracil is further broke down by a series of enzymatic steps to form fluoracetate, 2-fluoro-3-hydrxypropanic acid, fluorine ion and α-fluoro-β-alanine conjucated to bile acids (Malet-Martino and Martino, 2000).

1.1.7 5-Fluorouracil clinical treatment

Fluorouracil is often used in combination with many drugs, which include Leucovorin, Methotrexate and interferons. The generation of second and third generation fluorouracil derivatives such as UFT, S-1 and capecitabine that have been designed to lessen the burden on patients. These drugs produce a more targeted response when used in combination with radiation. Thus the use of 5-FU is being replaced with the next generation of 5-FU derivatives in clinical trials. However, 5-FU still remains the most commonly used chemotherapeutic today. 5-FU and second and third generation analogue drugs are used to treat colorectal, head and neck, gastric, cervical, kidney, basal skin, lung, pancreatic, and breast cancers (Malet-Martino M. and Martino R., 2000).

1.1.8 Global mRNA analysis 5-Fluorouracil treatments

Several microarray experiments have done on *in vitro* models investigating growth inhibition induced by 5-FU (Hernandez-Vargas, 2006; Troester, 2005).
Hernandez-Vargas *et al.* (2006) identified a list of genes that respond in a dose dependent manner in MCF-7 cells. Dose dependent regulation was observed; genes regulated in the IC50 48 hour dose include CCNG2, CCNB2, AURKA/STK15 and TNFRSF11B and in the IC80 48 hour dose regulation of SFN, BAK1, TP53I3/PIG3, BCL2 and APAF1 was observed. Genes that were not previously reported regulated in response to 5-FU induced DNA damage include BAK1, CCNG2, SFN and TP53I3/PIG3. A set of genes belonging to the E2F pathway were regulated by 5-FU treatment (Hernandez-Vargas, 2006). The E2F pathway involves the regulation of transcription through phosphorylation of Retinoblastoma binding proteins which interacts with Inhibitor of DNA binding proteins and promotes angiogenesis and invasion (Galbellini *et al.*, 2006). Follow up promoter analysis of direct p53 DNA binding sites revealed the existence of novel p53 targets after 5-FU treatment and included inhibitors of DNA binding 1 (ID1) and 2 (ID2) and provides a mechanistic connection between p21, ID1 and ID2 overexpression and p53 regulation (Hernandez-

Vargas, 2006). Work performed in our laboratory demonstrated that the halogenated pyrimidines induce a similar up-regulation of ID1, and ID2 and analysis of data established as well a functional link between p21 and the ID proteins (McMorrow, Ph. D. Thesis, 2004).

Troester *et al.* (2005) performed a thorough experiment comparing the response of two immortalised normal cell lines, and two breast cancer cell lines to exposure to 5-FU. A common normal cell line response, a common tumour cell line response and a cell-type (basal versus luminal) response were observed. The common overall expression pattern in the two luminal cell lines included well-characterized cell cycle regulators such as cyclin A2, cyclin B1, cell division cycle 2, and many genes involved in specific phases of the cell cycle and include Ki-67, ribonucleotide reductase M2, polo-like kinase, and topoisomerase IIA. This cluster also included pituitary tumor-transforming 1, a gene that is overexpressed in many cancers, is tumorigenic in vivo, and has been shown to bind p53. The gene product of serine/threonine kinase 6 (STK6) is also present and has cell-cycle-dependent expression, with maximum expression in G2-M; in addition, STK6 has been shown to bind chromosome 20 open reading frame 1, which is also repressed. Squalene epoxidase was downregulated in the luminal cell lines and is a gene that was differentially expressed between luminal and basal tumors in vivo. A large list of genes that include DNA-damage and stress response genes was up regulated in response to treatment in the luminal lines. The genes $p21^{waf1}$ and the DNA-damage response gene GADD45 were induced strongly in both lines. Also present were a number of genes involved in xenobiotic metabolism including carboyxlesterase 2, epoxide hydrolase, and ferredoxin reductase (Troester *et al*,. 2005)

Differences between basal and luminal cell lines in response to 5-FU were identified and among these genes was X-box binding protein 1 (XBP1), a gene whose expression was previously shown to be highly expressed in luminal tumors in vivo. XBP1 is a transcription factor involved in mediating the unfolded protein response, which may represent a stress response that is more prominent in secretory luminal cells. HER2 also appeared to be induced more distinctly in luminal cells treated with 5-FU (Troester *et al*,. 2005)

Maxwell *et al.* (2003) performed a microarray experiment to identify genes that are transcriptionally activated by 5-FU treatment in the MCF-7 breast cancer cell line. Of 2400 genes analyzed, 619 were up-regulated by >3-fold. Genes that were consistently found to be up-regulated were spermine/spermidine acetyl transferase (SSAT), annexin II, thymosin-ß-10, chaperonin-10, and MAT-8. The 5-FU-induced activation of MAT-8, thymosin-ß-10, and chaperonin-10 was abrogated by inactivation of p53 in MCF-7 cells, whereas induction of SSAT and annexin II was significantly reduced in the absence of p53. Basal expression levels of SSAT, annexin II, thymosin ß-10, and chaperonin-10 were increased and MAT-8 expression dramatically increased in a 5-FU-resistant colorectal cancer cell line (H630-R10) compared with the parental H630 cell line, suggesting these genes may be useful biomarkers of resistance {Maxwell *et al.*, 2003}.

1.1.9 Global Protein expression analysis of 5-Fluororuacil treatment

There are only 2 proteomic studies published to date that have looked at the anti-proliferative effect of 5-FU. Neither publication used the fluorescent Cy dye chemistry for protein detection and quantification and instead used silver staining techniques and colloidal commassie Blue staining to quantify protein expression trends. CCB lacks sensitivity and thus fewer proteins are detected while silver stained gels are sensitive they display poor linearity and gives poor statisitcs.
Chen *et al.* 2006 investigated the apoptotic effect of 5-FU on gastric cancer (MGC-803) cells and identified using MALDI-ToF MS a selection of proteins related to metabolism, oxidation, cytoskeleton and signal transduction.

Yim *et al.*, (2006) treated HeLa cells with 5-FU and identified differentially regulated proteins using colloidal commassie blue stained 2DE gels. The results indicate that 5-FU engaged the mitochondrial apoptotic pathway involving cytosolic cytochrome c release and subsequent activation of caspase-9 and caspase-3 as well as the membrane death receptor-mediated apoptotic pathway involving activation of caspase-8 with an Apo-1/CD95 (Fas)-dependent fashion. Yim *et al.* (2006) conclusion suggests that 5-

FU suppresses the growth of cervical cancer cells not only by antiproliferative effect but also through antiviral regulation.

1.1.10 Environmental stress mechanisms

A cell encounters a wide variety of stresses and must be capable of dealing with these appropriately manner. There are a variety of stresses that impact a cell. These include genotoxins leading to DNA damage, hypoxia and various stresses that lead to incorrect folding of protein. These general stress conditions lead to activation of either genotoxic stress or endoplasmic reticulum stress. As demonstrated above 5-FU has impacted upon the expression of genes involved in both processes.

1.1.11 Genotoxic stress

As already stated ATM and probably ATR detect 5-FU induced DNA damage and can lead to accumulation of p53 in cells exposed to 5-FU due to stalled replication forks and possibly double strand breaks depending on the degree of 5-FU exposure. The DNA damage signal from double strand breaks replication stress is primarily recognized by ATM (ataxia telangiectasia mutated) or the ATR–ATRIP (ataxia-telangiectasia-and-RAD3-related–ATR-interacting-protein) complex, respectively. Chromatin structure changes can lead to the autophosphorylation-mediated activation of ATM, which is subsequently recruited to the double strand breaks. The site of damage contains the MRN complex (composed of RAD50, MRE11 (meiotic-recombination-11) and NBS1 (Nijmegen breakage syndrome-1)) and BRCA1 (breast-cancer-susceptibility protein-1). H2AX (histone-2A family, member X), 53BP1 (p53-binding protein-1), MDC1 (mediator of DNA-damage checkpoint protein-1) and SMC1 (structural maintenance of chromosomes-1) are phosphorylated by ATM, and are the key proteins that are involved in transducing a double strand break-induced signal. The ATR–ATRIP complex is recruited to the replication forks by the single-

stranded DNA–RPA (replication protein A) complex. The RAD9–RAD1–HUS1 complex and its loading factor RAD17 facilitate recognition of the stalled fork. BLM (Bloom syndrome protein) and H2AX are phosphorylated in an ATR/CHK1-dependent manner in response to replication stress. CHK1 and CHK2, the respective targets of ATR and ATM, also phosphorylate the transducer proteins. The transducer proteins transmit the signal to effector proteins such as p53, which is phosphorylated at specific residues by ATM, ATR, CHK1 and CHK2. p53 is involved in cell-cycle arrest, DNA repair, apoptosis or senescence. p53 has roles that do not involve its transactivation functions during DNA repair — nucleotide-excision repair, base-excision repair, mismatch repair, non-homologous end-joining — and homologous recombination. The repair processes are also partially influenced by the transactivation function of p53 (Sengupta *et al.* 2005).

1.1.12 ER stress/Unfolded protein response

When eukaryotic cells encounter physiologically taxing conditions that impact on protein folding in the endoplasmic reticulum, a signal-transduction cascade is activated; this is termed the unfolded protein response (UPR). The UPR is a multi pronged response that is largely cytoprotective, but under conditions of prolonged stress apoptosis is induced. The UPR can be activated in tumours and is apparently due to their inadequate vascularization. This results in limited oxygen and nutrients, which interfere with the normal maturation of secretory-pathway proteins. Activation of the UPR might promote dormancy, aid tumour growth or protect the host by inducing apoptosis. *in vitro* activation of the UPR alters the sensitivity of tumour cells to chemotherapeutic agents. Several tentative observations have been made to implicate the UPR in tumour growth and resistance to treatments, more comprehensive *in vivo* studies are required to establish which components of the pathways are responsible for these undesirable out comes (Mori, 2004).

The mammalian UPR is an expansion of the basic yeast UPR. Two inositol-requiring gene 1 (Ire1) homologues are expressed in mammalian cells: IRE1α and IRE1β. Activated IRE1 removes 26 bases from the XBP1 transcript through its endonuclease activity and allows the synthesis of a highly active transcription factor with a more potent transactivation domain than the one encoded by the unspliced form of XBP1. A transient inhibition of protein synthesis during the UPR, which is achieved by

activation of PKR-like endoplasmic reticulum (ER) kinase (PERK) that phosphorylates the eukaryotic translation initiation factor-2α (eIF-2α). This leads to the loss of cyclin D1 from cells, causing a G1 arrest that prevents the propagation of cells experiencing ER stress. The block in translation specifically allows the activating transcription factor 4 (ATF4) to be synthesized and transactivate downstream genes, like GADD34, which is the regulatory subunit of the PP1 phosphatase that acts on eIF-2α and reverses the translation arrest, and C/EBP-homologous protein (CHOP), which has been implicated in apoptosis. PERK is also required for NF-κB activation, which positively regulates anti-apoptotic proteins like BCL2 (important in inhibiting cytochrome c release from the mitochodria) during ER stress, so contributing to the balance between survival and death signals. The ATF6α/ATF6β transcription factors are synthesized as ER-localized transmembrane proteins, which are cleaved by the Golgi localized S1P and S2P proteases during activation of the UPR, liberating the cytosolic transcription-factor domain. ATF6 induces XBP1 transcription, which is then spliced by the activated IRE1 endonuclease domain to produce a highly active transcription factor leading to the upregulation of ER chaperones such as ERdj3 and folding enzymes such as peptidylprolyl isomerase B (PPIase B). If ER stress conditions are not resolved, apoptotic pathways are initiated. Procaspase-12 in mice is localized to the cytosolic face of the ER membrane and is activated in response to ER stress by IRE1-dependent mechanisms. In humans it is likely that capase 4 is activated and not caspases 12. Similar to the situation in yeast, BiP binds to the luminal domain of all three mammalian UPR transducers (IRE1, PERK and ATF6) and keeps them inactive in the absence of ER stress. The accumulation of unfolded proteins in the ER results in the release of BiP from the luminal domains of the transducers and the dimerization and activation of the kinases. In the case of ATF6, the release of BiP from the luminal domain allows its transport to the Golgi, where the transcription-factor domain is liberated from the membrane and transported to the nucleus (Mori, 2004).

1.1.13 Genotoxic stress and ER stress

During ER stress the accumulation of p53 is prevented by Glycogen synthase kinase-3β (GSK3β). GSK3β was found to phosphorylate nuclear localized p53 at serine 315.

This phosphorylation was found to relocalize p53 to cytoplasm and mediate its degradation. It is believed that ER stress can protect cells from apoptosis by preventing p53 accumulation (Qu *et al.* 2004). The exact mechanism is not defined.

1.1.14 HSPs and apoptosis

Reactive oxygen species (ROS) are produced during exposure to toxin including 5-FU. The main source of ROS in a cell is the mitochondria and are produced by by the occasional loss of an electron from the conversion of NAD(H) to NADPH in the mitochondria. Cellular stress place a high rewuirement on the metabolism and cause increased metabolism thus causing dangerously high levels of ROS and trigger apoptosis pathways (Chen *et al.*, 2003; Scafer *et al.*, 2006; Screeder *et al.*, 2006).
Cell death signals induce the release of cytochrome c from the mitochondria that then binds to the APAF-1, inducing oligmerization and eventual recruitment of procaspase-9 and activation of the caspase cascade and cell death. HSPs have emerged recently that are known to regulate activation of apoptosis (Takayama *et al.* 2003).

1.1.14.1 HSPB1 (Heat shock protein 27) in apoptosis

In unstressed cells HSPB1 (Heat shock protein 27) exists as a large oligiomeric unit of up to 800KDa usually comprising of 6 tetrameric subunits of HSPB1. During a stress response HSPB1 is phosphorylated on 3 known sites and are at serine residues 15, 78 and 82. During stress MAPK is activated and phosphorylates MAPKAP 2 and 3 which subsequently phosphorylates HSPB1. Protein Kinase C may also phosphorylate HSPB1. HSPB1, during stress, facilitates the repair and destruction of damaged proteins during stress. HSPB1 was shown to bind eIF4G under *in vitro* conditions and suggests it may inhibit translation initiation and other data indicates that HSPB1 may also stimulate the recovery of transcription and translation after heat shock {Concannon, C.G. 2003}. Over expression of HSP27 increases resistance to various forms of apoptopic signaling. One mechanism by which HSP27 can inhibit apoptosis is by the sequestering of cytochrome c in the cytoplasm preventing binding to APAF-1 thus preventing activation of the caspase cascade {Gorman *et al.* 2005}. HSPB1 has

also been found to protect cells from reactive oxygen species produced during mitochondrial disfunction prior to induction of apoptosis. HSPB1 induces the increased expression of Glucose-6-phosphate dehydrogenase which produces NADPH and modulates intercellular RADOX potential. Other roles for HSPB1 indicate that the non-phosphorylated non-oligiomerised isoforms can contribute to F-actin stabilization while phosphorylated and oligiomerised isoforms do not interact with F-actin or actin (Concannon, 2003). See figure 1.4.

1.1.14.2 Other HSPs

HSP70 shows a similar mode of apoptosis inhibition and involves the sequestering of APAF-1 at the procaspase-9 binding site {Beere, *et al.* 2000}. HSP60 is bound to procaspase-3 in the mitochondrial matrix and is involved in its maturation. Under hypoxic stress these proteins are released into the cytosol and dissociate from each other (Concannonm 2003).

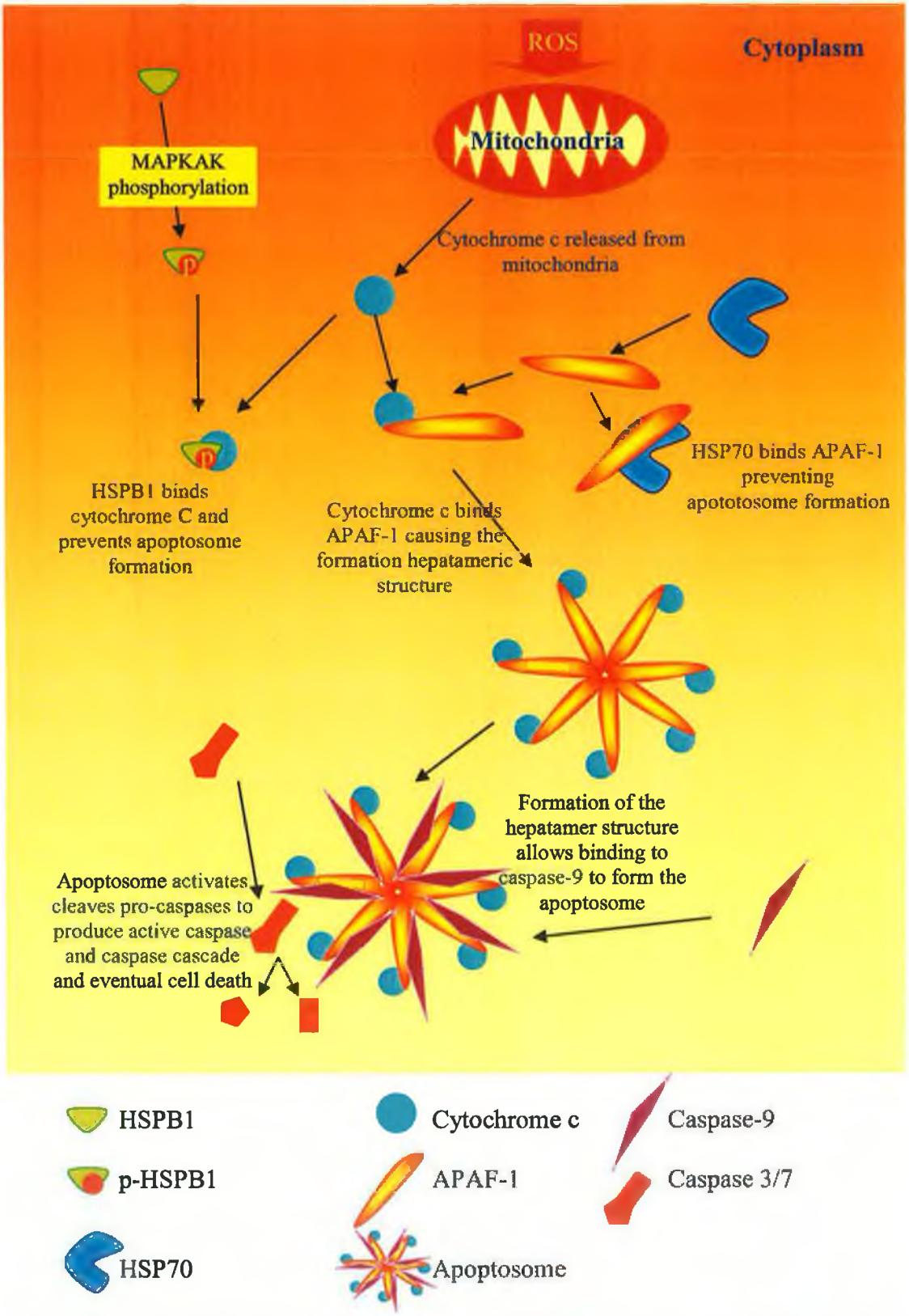

Figure 1.4: Heat shock protein inhibition of apoptosome formation (Scafer et al., 2006; Screeder et al., 2006)

1.1.15 Translation initiation and elongation

Translational initiation begins by first the dissociation of the 80S ribosome into 40S and 60S subunits followed by forming the 43S pre-initiation complex containing the 40S ribosome subunit, eIF1, eIF1A, eIF3, eIF5, and the ternary complex composed of eIF2, Met-tRNAi^{Met} and GTP. mRNAs bound with eIF4F and eIF4B at their 5′-end caps then join the 43S pre-initiation complex followed by scanning along the mRNA for the physiological AUG translational initiation codon and forming the 48S pre-initiation complex. Finally, with the release of eIFs, the 60S subunit joins the 48S complex to form the 80S ribosome for elongation, completing the initiation steps for cap-dependent translation. In all these steps of initiation, eIF3 plays a central role. eIF3 is also important for cap-independent translational initiation, such as the internal ribosome entry site (IRES) mediated translation initiation of viral RNAs and by analogy of cellular mRNAs (Holcik and Sonenberg, 2005).

eIF3 is the most complex translational initiation factor with a molecular weight of about 550–700 kDa in mammalian cells consisting of thirteen putative subunits known as eIF3S1–eIF3S13. The eIF3S5 (eIF3Se) has been identified as a negative oncogene where its down regulation has been associated with oncogenic transformation. The expression of eIF3e is reduced in 37% breast cancers and 31% non-small cell lung cancers. Furthermore the eIF35 plays an important role in recruiting eIF-4G (a component of eIF4F) to the translation initiation complex (Dong *et al.*, 2006).

1.1.16 5-FU and translation control

As stated previously 5-FU treatment was found to increase expression of the eIF2B protein, and decrease expression of the mRNA transcript of the protein eIF3 subunit 3. The translation initiation factor eIF2B exchanges GDP for GTP on eIF-2α allowing for an additional amino acid to be added to growing peptide. The translation initiation factor eIF3 directly recruits the 40S ribosomal subunit into the translation initiation

complex and the eIF3 subunits have recently been shown to play important roles in regulating translation (LeFebvre *et al.*, 2006).

1.1.17 5-FU and mRNA decay

The effect of FUTP (5-FU metabolic derivative) incorporation into mRNA to form fluorinated mRNA and investigation of translation efficiencies on a small set of mRNA's revealed no change in translation efficiency (Glazier *et al.*, 1981). However it is worth noting that bolus infusion of 5-FU induces cell death through incorporation of FUTP into mRNA. Although there is no direct evidence it is likely that fluorinated mRNA is repaired or destroyed by the cellular machinery and when in excess causes cell death.

1.1.18 Translation during stress

ER stress has been shown to phosphorylate eIF2α and inhibit translation initiation. Data discussed above would suggest that 5-FU treatments can cause ER stress as indicated by accumulation of the XBP-1 transcript a hallmark of ER stress. Thus in some instances 5-FU can lead to translation repression. Alternatively 5-FU treatment of Hela cells caused down regulation of eIF3 subunits 3 mRNA. This data may indicate reduced formation of translation initiation complexes.

During cellular stress conditions a cell needs to focus on dealing with the stress effector and as discussed previously there are different mechanisms that deal with the detection of cellular injury such as ER stress for dealing with protein damage and genotoxic response that deals with DNA lesions. During ER stress cells repress translation by phosphorylation of eIF2α and induction of XBP-1 transcript (Holcik and Sonenberg 2003. DNA damage or genotoxicity has been shown in general to cause the down regulation of RNA polymerase I and II and thus reduce the rate of ribosomal RNA and tRNA production (Schultz *et al.*, 2003). Both mechanisms cause a down regulation of global translation initiation rates. Under such condition translation of proteins is believed to be regulated by a mechanism called internal ribosome entry sites (IRES) mediated translation. IRES translation is better under stood during ER stress but is still poorly described.

1.1.19 Summary of 5-FU mode of action

The anti-metabolite 5-FU enters the cell and is metabolized to produce its active derivatives – fluorodeoxyuridine triphosphate, fluorodeoxyuridine monophosphate and fluorouridine triphosphate. These products are incorporated into DNA and RNA where they exert their anti-neoplastic effects. RNA incorporation can lead to interference in RNA maturation and degradation. DNA incorporation can lead to accumulation of p53 through activation of ATR/ATM DNA repair mechanisms. Proteomic data and microarray data on 5-FU treatments show the following; 5-FU effects the expression of translation initiation factors, and causes differential regulation of genes involved in the E2F pathway (potentially inducing differentiation effects such as angiogenesis and metastasis). Normal and cancer cell lines were found to respond to 5-FU in different manners.

1.2 Fluoropyrimidines

There are numerous fluoropyrimidines and here only 5-fluoro-2'deoxyuridine (52FdU) and 5-Fluoro-5'deoxyuridine (55FdU) are introduced. 52FdU is a metabolic derivative of 5-FU and as such should have a similar mode of action.

Capecitabine is a third generation 5-FU drug, developed from 55FdU a second generation 5-FU drug. 55FdU was designed for oral administration but caused unacceptable intestinal toxicity. Capecitabine is a further modified so that it is converted to 5'-deoxy-5-fluorocytidine (dFCR) by carboxylesterase in the liver thus avoiding intestinal toxicity. Cytdine deaminase in the liver or tumour converts dFCR to 55FdU. Thymidine deaminase converts 55FdU to 5-FU in the liver or tumour (Malet-Martino M. and Martino R., 2000). Radiotherapy works well with 55FdU as it promotes the increased expression of TP at the site of the tumour during therapy. Combination therapies with 55FdU or Capecitabine and radiation result in increased production of 5-FU localised to the tumour.

1.3 Fluorouracil resistance

As already stated 5-FU is used in the treatment of Breast, Colon, and other cancers and development of resistance to 5-FU is a major obstacle to be overcome.

1.3.1 *In vitro* resistance to 5-FU

In vitro resistance to 5-FU has been linked to TS and TP over expression (Longley, 2003).

Shin *et al.* 2005 investigated resistance in a selection of colon cancer cell lines using a proteomics based approach and there findings show that ATP synthase down-regulation may not only be a bioenergetic signature of colorectal carcinomas but may also lead to cellular events responsible for 5-FU resistance. Yoo *et al.* (2004) using proteomics techniques to analyse 5-FU-resistant human colon cancer cells (resistant variant developed from SNU-769A) were found to overexpress metabotropic glutamate receptor 4 (mGluR4) and tentatively linked it to 5-FU resistance. PARK *et al.*, (2002) identified 5 proteins differentially regulated between resistant and parental cell lines using proteomic silver stain based quantification. These proteins are HNRPK, transcription factor II, FLJ11122, Hook3 protein and TCP-1.

Wang *et al.* (2004) compared five 5-FU resistant cell lines to their five parental cell lines and identified 91 genes associated with 5-FU sensitivity. Key genes involved in 5-FU activation were significantly down-regulated (thymidine kinase, orotate phosphoribosyltransferase, uridine monophosphate kinase, pyrimidine nucleoside phosphorylase) in resistant cells. Overexpression of thymidylate synthase and its adjacent gene, c-Yes, was detected in the resistant cell lines. The mRNA and protein overexpression of nuclear factor _B (NF_B) p65 and related anti-apoptotic c-Flip gene was detected in resistant cells. The 5-FU– resistant cell lines also showed high NF_B DNA-binding activity. Cotransfection of NF_B p50 and p65 cDNA induced 5-FU resistance in MCF-7 cells. Both NF_B- and 5-FU–induced resistant cell lines manifested reduced expression of genes governing G1-S and S-phase transition. Expression of genes involved in DNA replication was also down regulated in resistant cell lines. These findings were consistent with the slower growth rate, higher proportion of G1, and lower proportion of S-phase cells in the resistant cell lines. This phenotype may protect resistant cells from cell death induced by incorporation of 5-FU derivatives into DNA chains, thus allowing time to repair 5-FU –induced damage (Wang *et al.* 2004).

Expression levels of SSAT, annexin II, thymosin ß-10, and chaperonin-10 were increased and MAT-8 expression increased in a 5-FU-resistant colorectal cancer cell line (H630-R10) compared with the parental H630 cell line, suggesting these genes may be useful biomarkers of resistance {Maxwell *et al.*, 2003}.

Research by Klampfer *et al.* (2005) indicate that Ras mutations promote apoptosis in response to 5-FU treatment and imply that tumors with Ras mutations and/or reduced expression of gelsolin may show enhanced apoptosis in response to 5-FU also in vivo.

1.3.2 Clinical (*in vivo*) resistance to 5-FU

High TS expression has consistently been shown to cause resistance to 5-FU (Longley, 2003). Thymidine phosphorylase however has shown conflicting data between preclinical and clinical data, however this data may be explained by the fact that TP is also an angiogenic endothelial growth factor and high TP expression in colorectal cancer has been correlated with poor prognosis. Dihydropyrimidine dehydrogenase (DPD) mRNA expression in colorectal tumours has been linked to 5-FU resistance and this correlation presumably leads to higher levels of Dihydropyrimidine dehydrogenase and thus higher rates of 5-FU degradation (Longley, D.B. 2003). Salonga *et al.* (2000) showed that responsiveness to 5-FU was dependent on the independent expression of Dihydropyrimidine dehydrogenase, TS and TP and measurement of all three markers accurately predicted the responsiveness to 5-FU based chemotherapy.

1.3.3 Thymidylate synthetase

Thymidylate synthase (TS) is an E2F1-regulated enzyme that is essential for DNA synthesis and repair. TS protein and mRNA levels are elevated in many human cancers, and high TS levels have been correlated with poor prognosis in patients with colorectal, breast, cervical, bladder, kidney, and non-small cell lung cancers (Rathman *et al.* 2004).

TS is regulated at both transcriptional and post-transcriptional levels and functions as a RNA binding protein. The translation of human TS mRNA is regulated by its own protein product via a negative autoregulatory mechanism whereby the binding of TS

protein to at least two distinct sequences on its own TS mRNA results in translational repression. TS is also capable of interacting with several other cellular mRNAs including the mRNA of the transcription factors p53 and c-Myc (Xi *et al.* 2006). An acute increase in TS expression after 5-FU treatment is often observed and is regulated at the translational level (Xi *et al.* 2006). Long-term resistance to 5-FU is related to transcriptional activation and gene amplification of TS (Xi *et al.* 2006). Xi *et al.* (2006) conducted experimentations to determine proteins regulated by TS at a post-transcriptional level during 5-FU exposure. Microarray profiling of His Tagged TS immunoprecipitated from polysomes fractions was investigated to identify mRNA that was regulated at a post-transcriptional level by TS. These include SPRR1A, RRM2, KRT6A, B, C, SPRR1B, GPIBB, CDKNIA, SEII, KRT17, PLAU, DDB2, SFN (Xi *et al.* 2006).

A recent report suggested that TS may also function as an oncogene as transfection with the gene transformed NIH3T3 cells {Rahman *et al.*, 2004}

As mentioned the mode of action of 5-FU is the irreversible binding and inhibition of its activity leading to DNA lesions. Interestingly other halogen pyrimidine metabolites have not been reported to irreversibly bind to TS.

1.3.4 5-Fluorouracil as differentiating agents

As discussed previously 5-FU has been shown to impact upon various cellular stresses and potentially causes the regulation of gene expression at the transcriptional and post-transcriptional levels. The role of 5-FU in modulating TS expression has been shown not only to assist in DNA repair but also have additional roles in post-transcriptional regulation of proteins involved in differentiation such as KRT6A and KRT17 (Xi *et al.* 2006). 5-FU has also been shown to increase expression of TP also known as platelet derived growth factor and plays a role in promoting angiogenesis (Griffin *et al.*, 2002).

1.3.5 5-Fluorouracil and the cellular microenvironment

As explained previously 5-FU has been shown to impact upon a wide variety of cellular processes with in the cell, here the literature is explored to investigate the role in which 5-FU has on the cellular phenomenon such as adherence and invasion.

Integrin $\alpha_5 \beta_1$ is expressed on activated endothelial cells and plays a critical role in tumor angiogenesis. A novel integrin $\alpha_5 \beta_1$ antagonist, ATN-161, was assessed in combination with 5-FU to determine if it would inhibit angiogenesis and growth of liver metastases in a murine model. Targeting integrin $\alpha_5 \beta_1$ in combination with 5-FU infusion reduced liver metastases formation and improved survival in this colon cancer model when compared to 5-FU alone. The enhancement of antineoplastic activity from the combination of anti-angiogenic therapy and chemotherapy may be a promising approach for treating metastatic colorectal cancer {Stoeltzing *et al.*, 2003}. This data demonstrated the role of integrin $\alpha_5 \beta_1$ in promoting cell survival and metastasis during 5-FU treatment.

RhoB is a small GTPase important in promoting cellular motility. Jiang *et al.* (2004) demonstrated that Ras/PI3K/Akt pathway inhibited RhoB induction and inhibited tumor survival, transformation, invasion, and metastasis. Treatment with 5-FU was also found induce RhoB expression. This data suggests that 5-FU treatment may have a modulating effect on invasion (Jiang *et al.* 2004).

Induction of apoptosis in fludarabine (5-FU analogue) treated human leukaemia cells was prevented by integrin-mediated adhesion to ECM on the basis of upregulation of Bcl-2-like proteins in parallel to downregulation of proapoptotic proteins such as Bax or Bim (Helhgans *et al.*, 2006)

1.4 The cell line DLKP and its subpopulations

Previous work in our laboratory established the cell line DLKP. It was histologically diagnosed as a 'poorly differentiated squamous carcinoma' or Non-Small cell Lung Carcinoma (NSCLC) and is of lung epithelial origin (McBride *et al.*, 1998}. NSCLC are characterized by a remarkable degree of cellular heterogeneity. The present studies indicate that practically all NSCLC samples yield, together with a fraction of diploid cells, one or more than one aneuploid subpopulations (Teodori *et al.*, 1983). DLKP contains three morphologically distinct subpopulations. Three clonal populations were isolated from this cell line that displayed the morphology of these morphologically distinct populations, and DNA fingerprinting established that they were derived from the parental population. Based on there morphologies two clones were designated DLKP-M (mesenchymal-like) and DLKP-SQ (squamous-like) and as these two population were observed to interconvert with the third population and was designated DLKP-I (intermediate). DLKP-SQ and DLKP-M do not interconvert with each other. The heterogeneous population of DLKP is composed of ~70% DLKP-SQ, ~25% DLKP-I and ~5% DLKP-M. The growth characteristics of DLKP and its subpopulations were investigated and were found to have distinct growth curves under various culture conditions and DLKP-M was found to have a significantly lower growth rate of all the subpopulations. The attachment properties of this cell line were assessed with the ECM proteins collagen type IV, fibronectin and laminin. It was observed that the four cell lines displayed a high affinity to collagen type IV compared to other cell lines and that DLKP-M displayed higher initial attachment to fibronectin. The presence of tight junctions was found to be absent (assessed by electrical resistance) and therefore DLKP and its subpopulations are unpolarised epithelial cells. Marker expression determined that the DLKP clones did not express cytokeratins although it was observed that in DLKP a few cells (<1%) stained positive with a pan-cytokeratin antibody (detects cytokeratins 1, 4 - 6, 8, 10, 13 18 and 19). These 4 cell lines were found to be positive for Vimentin, Desmin and neurofilaments amongst other protein however no specific protein markers of each population were identified (McBride *et al.*, 1998).

1.4.1 Epithelial-Mesenchymal transition

Epithelial and mesenchymal cells differ from each other in various functional and phenotypic characteristics. Epithelial cells form layers of cells that are adjoined by specialized membrane structures, such as tight junctions, adherens junctions, desmosomes and gap junctions. In addition, epithelial cells have apical–basolateral polarization, which manifests itself through the localized distribution of adhesion molecules such as cadherins and certain integrins, the organization of cell–cell junctions as a lateral belt, the polarized organization of the actin cytoskeleton, and the presence of a basal lamina at the basal surface. Epithelial cells are motile and can move away from their nearest neighbours, while remaining within the epithelial layer. Mesenchymal cells do not form an organized cell layer, nor do they have the same apical–basolateral organization and polarization of the cell-surface molecules and the actin cytoskeleton as epithelial cells. They contact neighbouring mesenchymal cells only in a focal manner, and are not typically associated with a basal lamina. In culture, mesenchymal cells have a spindle-shaped, fibroblast-like morphology, whereas epithelial cells grow as clusters of cells that maintain complete cell–cell adhesion with neighbouring epithelial cells. Cultured mesenchymal cells tend be highly motile, but this is not necessarily the case in vivo. Indeed, there is plasticity in the way that mesenchymal cells migrate — they might migrate together as chains, or as individual cells that exhibit either cyclic extension–adhesion–retraction translocation or amoeboid-type crawling (Thiery, 2006}.

Epithelial cells can convert into mesenchymal cells through a process known as the epithelial–mesenchymal transition. The term epithelial–mesenchymal transition describes a series of events during which epithelial cells lose many of their epithelial characteristics and take on properties that are typical of mesenchymal cells, which require complex changes in cell architecture and behaviour). The transition from epithelial- to mesenchymal-cell characteristics encompasses a spectrum of inter- and intracellular changes, not all of which are always seen during epithelial–mesenchymal transition. Epithelial–mesenchymal transition does not therefore necessarily refer to a lineage switch. The precise spectrum of changes that occur during epithelial–mesenchymal transition is probably determined by the integration of extracellular signals the cell receives, although this is still unclear. The reverse process, known as mesenchymal–epithelial transition has also been reported (Thiery, 2006}.

Mesenchyme tissue (cells, matrix and soluble factors) influence the morphogenesis, proliferation and differentiation of a variety of embryonic epithelia, e.g. in the tooth, skin, mammary and salivary glands. Mesenchyme derivatives also 'maintain' adult epithelia, e.g. the local proliferation rate and cytokeratin composition of oral mucosa. Abnormalities in such epithelial-mesenchymal interactions lead to a variety of pathologies such as premalignant lesions, e.g. leukoplakia, tumours and psoriasis (Sharpe, 1988). Stromagenesis is a host reaction of connective tissue that, when induced in cancer, produces a progressive and permissive mesenchymal microenvironment, thereby supporting tumour progression. The stromal microenvironment is complex and comprises several cell types, including fibroblasts, the primary producers of the non-cellular glycoprotein scaffolds known as extracellular matrices. The events that support tumour progression during stromagenesis are for the most part unknown due to the lack of suitable, physiologically relevant, experimental model systems (Amatangelo, 2005).

A homologue of the tumour suppressor p53, p63, is critical for the development and maintenance of squamous epithelia. p63 is specifically expressed in the basal layers of stratified epithelial tissues and is considered a specific marker for cells of this type. The role of p63 in tumorigenesis remains poorly defined. Numerous studies have highlighted the oncogenic potential of the predominant p63 isoform DeltaNp63alpha; however, data suggest that other p63 proteins can act as tumor suppressors or alter the metastatic potential of tumors. DeltaNp63alpha can act as a transcriptional repressor, but the link between the transcriptional functions of p63 and its biological role is still unclear. Disruption of p63, using siRNA, in squamous cell lines resulted in down-regulation of transcripts specifically expressed in squamous tissues and a significant alteration of keratinocyte differentiation. Disruption of p63 led to up-regulation of markers of nonepithelial tissues (mesenchyme and neural tissue) in both primary and immortalized squamous cells. Many of these up-regulated genes are associated with increased capacity for invasion and metastasis in tumors. Loss of p63 expression caused a shift toward mesenchymal morphology and an increase in motility in primary keratinocytes and squamous cell lines. This suggests that loss of endogenous p63 expression results in up-regulation of genes associated with invasion and metastasis, and predisposes to a loss of epithelial and acquisition of mesenchymal characteristics. These findings have implications for the role of p63 in both development and tumorigenesis {Barbieri, 2006}.

Throughout the entire process of cancer aetiology, progression and metastasis, the microenvironment of the local host tissue can be an active participant. Invasion occurs within a tumour-host microecology, where stroma and tumour cells exchange enzymes and cytokines that modify the local extracellular matrix, stimulate migration, and promote proliferation and survival. A new class of cancer therapies that targets this pathological communication interface between tumour cells and host cells is currently under development {Liotta, 2001}.

Recently, a view of the tumour as a functional tissue interconnected with the microenvironment has recently been described. For many years, the stroma has been studied in the context of the malignant lesion, and only rarely has its role been considered before carcinogenic lesions appear. Recent studies have provided evidence that stromal cells and their products can cause the transformation of adjacent cells through transient signalling that leads to the disruption of homeostatic regulation, including control of tissue architecture, adhesion, cell death, and proliferation. It is now well established that tumor progression requires a continually evolving network of interactions between neoplastic cells and extracellular matrix. A relevant step of this process is the remodeling of microenvironment which surrounds tumors leading to the release of ECM-associated growth factors which can then stimulate tumor and/or endothelial cells. Finally, tumor cells reorganizing the extracellular matrix to facilitate communications and escape the homeostatic control exerted by the microenvironment modify response to cytotoxic treatments (Pupa, 2002}.

Integrin-mediated cell adhesions provide dynamic, bidirectional links between the extracellular matrix and the cytoskeleton. Besides having central roles in cell migration and morphogenesis, focal adhesions and related structures convey information across the cell membrane, to regulate extracellular-matrix assembly, cell proliferation, differentiation, and death. (Geiger, 2001}

1.4.2 Cell Matrix interactions

Adherence proteins regulate migration, invasion and ECM remodelling and assembly. These adherence proteins include members of the integrin and syndecan family.

1.4.3 Integrins

As cancer cells become metastatic and as endothelial cells become angiogenic, they develop altered affinity and avidity for their ECM and is mediated by alterations in the expression of integrins, release of proteases that remodel the ECM and the deposition of new ECM molecules. These activate signaling cascades that regulate gene expression, cytoskeletal organization, cell adhesion and (more importantly in terms of cancer) cell survival. Cellular invasion and migration are governed at both the extracellular and intracellular levels by several factors that include ECM composition, adjacent cells, and the presence of soluble and insoluble gradients (Hood, J.D. 2002; Anderson *et al.*, 2006).

During migration, cells project lamellipodia that attach to the ECM whilst simultaneously breaking existing ECM contacts at their trailing edge allowing the cell to pull itself forward. Extension of lamellipodia is induced by actin polymerization. Retraction of the cell edge is dependent on fracturing the cell–ECM linkage in highly adhesive environments or by simple dissociation of integrins (the cellular receptors for ECM molecules). Integrins are glycoproteins that form heterodimeric receptors for ECM molecules. The integrin family can form at least 25 distinct pairings of the 18 α-subunits and 8 β-subunits. Each αβ pairing is specific for a unique set of ligands. Integrins relay molecular cues regarding the cellular environment and through signal transduction that influences cell shape, survival, proliferation, gene transcription and migration. Upon binging to ligand, integrins cluster into focal contacts that contain different actin-associated proteins, such as α-actinin, vinculin, tensin and paxillin, which form a link between the focal contact and the cytoskeleton. . Integrin binding to ligands in the extracellular matrix (ECM) activates focal adhesion kinase (FAK), which binds and activates multiple signalling proteins. FAK autophosphorylation at tyrosine 925 causes it to bind growth-factor-receptor-bound protein 2 (GRB2) and activate another small G protein, RAS. FAK activation also promotes SRC-dependent phosphorylation of SHC, leading to GRB2 recruitment and RAS activation. Activated RAS recruits RAF to the cytoplasmic membrane, where it can be activated by protein kinases such as SRC, thereby leading to mitogen-activated protein kinase kinase (MEK) and extracellular-signal-regulated kinase (ERK) activation. Once activated by FAK or SHC, RAS can activate phosphatidylinositol 3-kinase (PI3K) and RAF.

Activated SRC can also phosphorylate CRK-associated substrate (CAS), enabling it to bind CRK and dedicator of cytokinesis 180 (DOCK-180), leading to RAC activation. Activated RAC, in conjunction with activated CDC42, can regulate numerous biochemical pathways, including activation of p21-activated kinase (PAK). PAK affects numerous pathways, and also activates RAF's kinase activity. MEK, once activated by RAS and RAF, can phosphorylate and activate ERK. ERK activation leads to transcriptional activity, alterations in integrin affinity for ligand, and myosin-light-chain kinase (MLCK) activity. Independent of FAK activation,

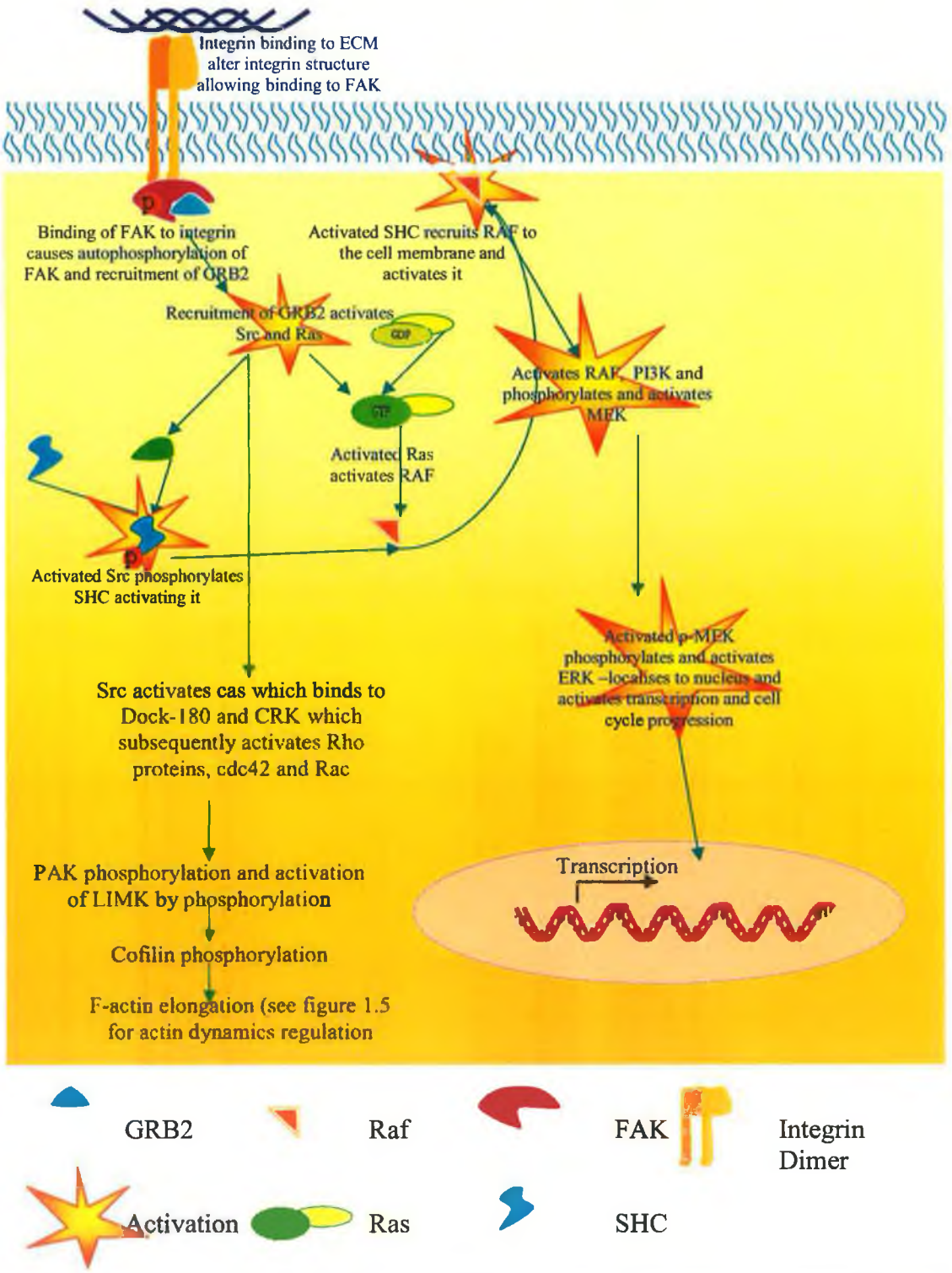

Figure 1.4: Integrin signalling regulates actin dynamics and transcription

signaling molecules such as SHC and PKC are also activated by integrin adhesion events. Activating these molecules can also eventually lead to RAS and RAF activation, along with the alterations in the cytoskeleton that are necessary for the migratory phenotype (Hood, J.D. 2002; Anderson *et al.*, 2006).

1.4.4 Rho family members and actin dynamics

Most of the functional information on Rho-family proteins has come from studies of RhoA, Rac1 and Cdc42. All share common growth-promoting and anti-apoptotic functions, as well as regulation of gene expression, through activation of signaling molecules such as serum response factor, NF-κB, the stress-activated protein kinases and cyclin D1. All three promote actin cytoskeleton reorganization, but have distinct effects on cell shape and movement (see figure 1.5). RhoA promotes actin-myosin contractility and, thereby, the formation of stress fibers and focal adhesions, regulating cell shape, attachment and motility. Rac1 promotes actin polymerization and the formation of lamellipodia, which are curtain-like extensions that consist of thin protrusive actin sheets at the leading edge of migrating cells. Cdc42 causes formation of filopodia, which are thin, finger-like cytoplasmic extensions that contain tight actin bundles and might be involved in the recognition of the extracellular environment (Weenerberg *et al.*, 2004).

1.4.5 Integrin and proteases

Integrins are involved in regulating proteolytic enzymes that degrade the basement membrane (the initial barrier to surrounding tissue). The basement membrane forms a non-cellular scaffold for cells and is made up of a complex mix of ECM proteins, including laminins, collagens and proteoglycans. Cancer cells produce, activate and release several types of proteases that specifically cleave ECM molecules. Two members of the matrix metalloproteinase (MMP) family, MMP-2 (gelatinase A) and MMP-9 (gelatinase B) have the highest activity against type IV collagen, which is the main constituent of the basement membrane {Hood, J.D. 2002}. Other proteases involved in ECM remodeling include the cysteine proteases (Cathepsin B) and aspartic proteases (Cathepsin D) (Pupa *et al* 2002).

1.4.6 Syndecans

The syndecan family are transmembrane proteoglycans expressed on adherent cells. The family of four proteins (sdc-1, -2, -3, -4) participate in cell-matrix adhesion, the regulation of growth factors (FGFs, VEGF, HGF) binding and signaling. The syndecans are composed of an extracellular domain (contains heparan sulfate and chondroitin sulfate glycosaminoglycan chains), a transmembrane region and a short cytoplasmic domain. The cytoplasmic domain attaches activated protein kinase C alpha, phosphatidyl-inositol-4,5-bisphosphate, syntenin, beta-catenin and many others molecules and is important in focal contacts. Syndecans bind numerous ligands present in extracellular matrix and include growth factors, enzymes, and ECMs such as fibronectin and laminin. They form connections with actin cytoskeleton in focal contacts. The changes in syndecan expression influence cell adhesion and migration, structure of focal contacts and cytoskeleton and participate in cell differentiation and tissue regeneration {Brzoska, 2005}. Syndecan-2 have been shown to participate in focal adherence and induce regulation of rho stimulating actin nucleation (Irie *et al.* 2004).

1.4.7 Cytoskeletal alteration during migration

The cytoskeleton of eukaryotic cells is composed of actin microfilaments, microtubules, and intermediate filaments. An important property of actin is its ability to produce movement. Microfilament assembly at the cell membrane protrudes the membrane forward producing the ruffling membranes in actively moving cells. Microfilaments can also play a passive structural role by providing the internal stiffening rods in microvilli, maintaining cell shape, and anchoring cytoskeletal proteins.

1.4.7.1 Assembly of Actin Filaments

Actin polymerization is a condensation reaction. The main features of this process are first a slow initial association to an actin dimer that is more likely to rapidly dissociate to monomers than to assemble, secondly the formation of a stable actin trimer that represents the nucleus of polymerization, a state where actin assembly is more likely than is disassembly and thirdly the elongation phase during which actin monomers are rapidly assembled.

1.4.7.2 The Arp2/3 Complex

The Arp2/3 complex is a stable complex of seven-subunits — two actin-related proteins (Arp2 and Arp3) and five additional novel proteins (p40, p35, p19, p18, and p14). ARP2/3 activity requires binding to activated WASP protein which contains two actin-profilin binding domain. Thus ARP2/3 complex is important in the stimulation of actin nucleation (Anton *et al.*, 2006). The principal function of Arp2/3 is to create branch points by nucleating the assembly of filaments near ruffling membranes, a process that needs ATP. Arp2/3 is also considered to be a cross-linking protein, and some authors believe it can cap the pointed (depolymerizing) ends of actin filaments, although this is still controversial (dos Remedios *et al.* 2003}.

1.4.7.3 Elongation and Annealing of F-actin

Elongation involves association and dissociation of monomers from the filament and can occur at either end of the filament. However, association predominantly occurs at the barbed end and dissociation at the pointed end. An ATP binding site is required for the extension of actin filament by hydrolysis producing actin filaments (F-actin) containing ADP. During depolymerization of ADP-actin subunits in F-actin rapidly exchange their bound ADP for ATP in solution and is accelerated by profilin. Due to the cycling nature of actin elongation and polymerisation the process is referred to as "treadmilling" (dos Remedios *et al.* 2003; des Marais *et al.*, 2005).

Actin Binding proteins (ABP) present *in vivo* regulate different aspects of the assembly/disassembly process. These include filament stabilizers (e.g., tropomyosin), capping proteins (e.g., CapZ, tropomodulin), ABPs that promote branching (e.g., Arp2/3), and ABPs that sequester G-actin and thus maintain a pool of monomers in solution (e.g., thymosin β4, profilin) (dos Remedios *et al.* 2003; des Marais *et al.*, 2005).

Actin filament lengths are affected by fragmentation and annealing. Fragmentation can arise from thermal motion in vitro, but *in vivo* much of this will be constrained by the other contents of the cytoplasm. Annealing occurs when an existing filament binds to the appropriate end of a second filament. Arp2/3 is believed to create branch points in actin microfilaments by "capturing" existing filaments (dos Remedios *et al.* 2003; des Marais *et al.*, 2005).

1.4.7.4 ADF/Cofilin

The actin depolymerizing factors ADF/cofilin family of proteins are ubiquitously expressed in all eukaryotic cells and are relatively small (15-19 kDa) proteins that exist in multiple isoforms. Their main functions include the rapid recycling of actin monomers associated with membrane ruffling and with cytokinesis. Different genes encode for ADF and cofilin, but although it is common to regard them as synonymous, they are distinctly different (dos Remedios *et al.* 2003; des Marais *et al.*, 2005).

Cofilin accelerates the dissociation of monomers from the pointed ends of filaments. Phosphorylation of cofilin dissociates it from ADP-actin. Cofilin cycles through

phosphorylation and dephosphorylation in order to allow it to function in its depolymerising role during actin threadmilling (dos Remedios *et al.* 2003; des Marais *et al.*, 2005).

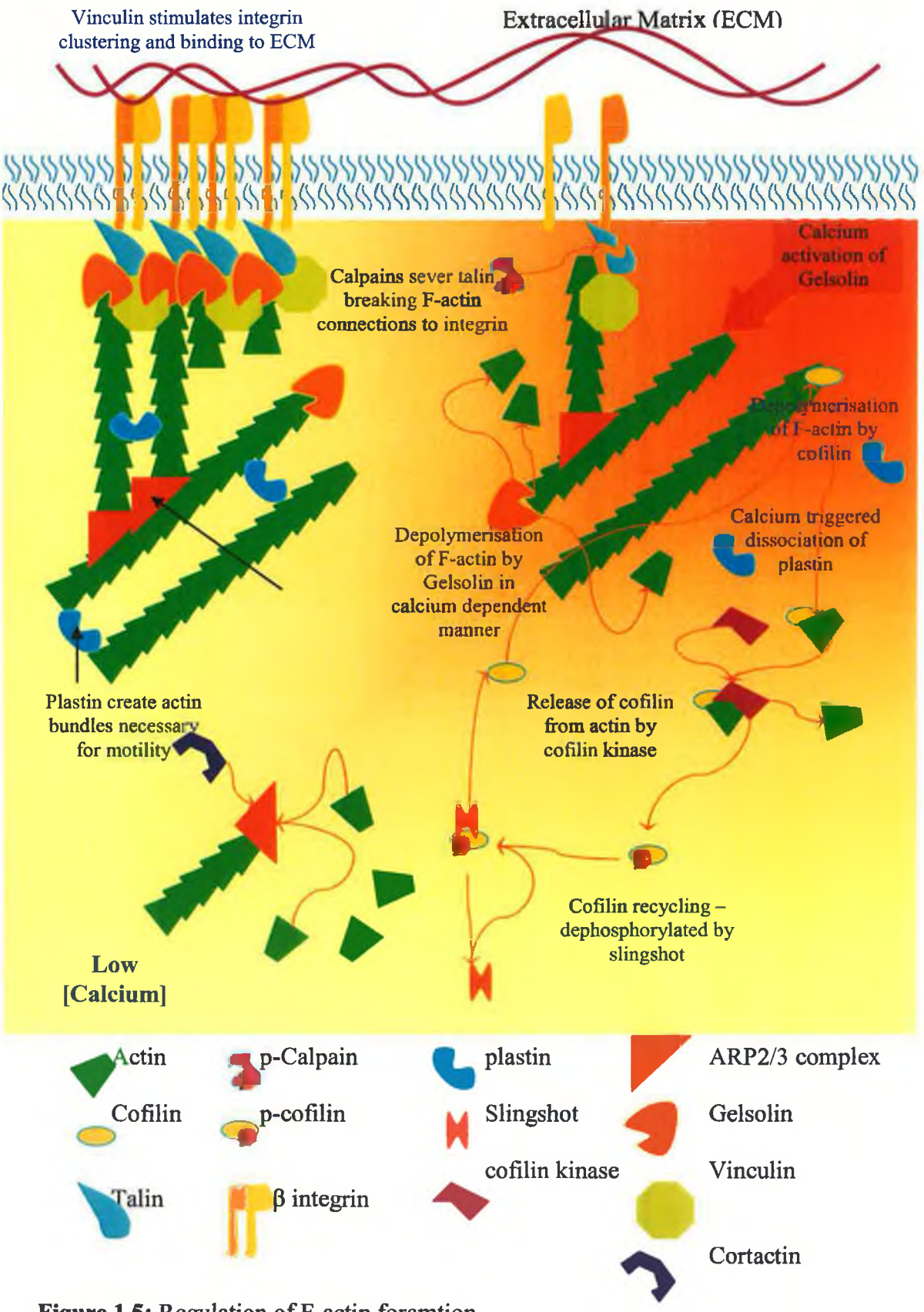

Figure 1.5: Regulation of F-actin foramtion

1.4.7.5 Profilin

Profilin promotes the exchange of ADP for ATP that facilitates the addition of profilin-ATP-actin at the barbed end of F-actin and thus is important in F-actin elongation (dos Remedios *et al.* 2003; des Marais *et al.*, 2005).

1.4.7.6 Gelsolin Superfamily

Gelsolin is part of a superfamily of ABPs expressed in all eukaryotes. The grouping includes gelsolin, villin, adseverin, CapG, flil, and severin. Unlike coflin and profilin, an isoform of intracellular gelsolin can circulate in plasma where it severs and caps actin filaments released into the circulation. Gelsolin is an important ABP because of its high affinity for actin filaments. Binding of gelsolin initiates the severing, but while binding to filaments is rapid, its severing action is slow. Gelsolin is also involved in capping and is calcium dependent (dos Remedios *et al.* 2003; des Marais *et al.*, 2005).

After severing, gelsolin remains attached to the barbed end of the filament as a cap, thereby preventing the reannealing of actin fragments. Capping prevents rapid growth at the barbed ends while disassembly proceeds unchecked at the pointed ends, resulting in the rapid disassembly until equilibrium is established between capped filaments and free gelsolin. Dissociation (uncapping) of gelsolin from these filaments generates numerous polymerization-competent ends that seed the rapid assembly of new filaments. Thus the cytoskeleton can be rapidly rebuilt in a new direction and cell movement can be redirected (dos Remedios *et al.* 2003; des Marais *et al.*, 2005).

1.4.7.7 CapZ, a barbed-end capping protein

The reported biological roles of CapZ include nucleation of actin assembly, capture of pre-existing filaments, regulation of actin assembly at the barbed ends of filaments, elimination of annealing at the barbed ends of filaments. CapZ does not affect the rate

of fragmentation of actin filaments and does not bind to their pointed ends (Sept D *et al* 1999; dos Remedios *et al*. 2003; des Marais *et al*., 2005).

1.5 Aims of thesis

1.5.1 5-Fluorouracil treatments and proteomic analysis

Previous work performed in the NICB found that the halogenated pyrimidine, Bromodeoxyuridine (BrdU), was capable of inducing markers of epithelial differentiation in the poorly differentiated cell line DLKP {McBride,S. *et al.* 1999}. Specifically, the up-regulation of Keratins 8, 18 and 19 were observed and investigation of mRNA and proteins expression levels indicated regulation at a post-transcriptional level (McBride *et al.*, 1999; Meleady *et al.*, 2001; Walsh *et al.*, 2003}.

Further research with other halogen pyrimidines (Fluoro-, chloro-, and iodo-pyrimidines) was found to induce similar effects (O' Sullivan F, Thesis, 1999; McMorrow J, Thesis, 2004). Of these fluoropyrimidines investigated the chemotherapeutic, 5-Fluorouracil (5-FU), was found to induce expression of keratin 8 and 18 and was regulated at a post-transcriptional level (O' Sullivan F, Ph.D. Thesis, 1999; McMorrow J, Ph.D. Thesis, 2004).

As regulation of keratin 8 and 18 was observed to occur at a post transcriptional level by halogenated pyrimidine treatment investigation of alterations induced by 5-FU was to be carried out at a proteomic level in order to investigate possible mechanisms of translation control and identify proteins differentially regulated that may be controlled at a post-transcriptional level.

Transfection of the simple epithelial markers keratin 8 and 18 were found to induce invasion and its expression is found to correlate with invasion (Chu *et al.* 1996). Work performed in our laboratory demonstrated that pulse selection of many cell lines to chemotherapeutic drugs including 5-FU often induced a more invasive phenotype (Liang Ph. D. Thesis, 2002). Thus 5-FU has been shown to induce an increase in invasion and it may be linked to increased expression of keratin markers associated with increased invasion. To assess if 5-FU treatments could alter the invasive status of various cell lines invasive status the degree of invasion was assessed post 5-FU treatment. Proteomic data was performed on these cell lines in order to characterise potential mechanisms induced by 5-FU treatment that lead to increased or decreased

invasion post 5-FU treatment. Normal cell lines were included in this experiment. A characteristic of epithelial is an invasive phenotype (Barbieri *et al.*, 2006; Liotta *et al.*, 2001). The normal cell lines human mammary epithelial cells (HMEC) and normal human bronchial epithelial (NHBE) cells are used in these experiments. NHBE cells require retinoic acid to induce epithelial differentiation and would be expected to induce invasion (Lotan, 2003). To assess the role of 5-FU as a promoter of markers of epithelial differentiation and invasion these cells were cultured with out retinoic acid.

1.5.2 Fluoropyrimidine treatments and proteomic analysis

As previously mentioned work performed in our laboratory found that the fluoropyrimidines are capable of inducing a differentiation effect in DLKP (O' Sullivan F, Ph.D. Thesis, 1999; McMorrow J, Ph.D. Thesis, 2004). Further characterisation of this phenomenon is to be investigated at a proteomic level to further characterise the effect of these drug and to determine a common mode of action between these drugs. Adherence profiles were determined after 7 days treatment with the fluoropyrimidines and analysis of differential protein expression was investigated.

1.5.3 Development of a 5-FU resistant cell line and proteomic analysis

Understanding resistance to 5-FU and comparison to 5-FU treatments is important in the understanding of how cancer cell may develop resistance. Development of resistant variants of DLKP and A549 by pulse selection with the fluoropyrimidine drugs in order to develop a stable 5-FU resistant variant of DLKP or A549. Resistant variants developed were then characterised at a proteomic level to determine possible resistance mechanisms.

1.5.4 Further characterisation of invasion and motility rates in DLKP and its subpopulations and characterisation of total and membrane proteomes

The heterogeneous cell line DLKP is composed of at least three morphologically distinct populations and these have been designated DLKP-SQ, DLKP-I and DLKP-

M (McBride *et al.*, 1998). Investigation of these cell lines determined that the -SQ and -M populations interconverted with the -I population (McBride *et al.*, 1998). Investigation of adherence profiles indicated that DLKP-M adhered more readily to fibronectin and had a slower growth rate when compared to the other populations (McBride *et al.*, 1998). No distinct protein markers of these populations could be determined (McBride *et al.*, 1998). Invasion and motility rates are to be determined using DLKP and clones of the same passage as described by McBride, S. 1998. Investigation of the interconversion between these populations is investigated using two dimensional difference gel electrophoresis (2D-DIGE) analysis of total cell lysate proteome and hydrophobic proteomes.

Comparison DLKP clonal 2D-DIGE experiment and DLKP treated with 5-FU in combination with invasion assays results would allow for identification of protein trends that parallel invasion trends and this would help identify proteins potentially involved in progression of invasion. This data may also show if 5-FU treatment caused the selection of subpopulation or induced specific alterations associated with 5-FU treatment.

1.5.5 Summary of Aims

5-FU treatments of cancer and normal cells in vitro

- Determination of phenotypic changes (invasion, and adherence to ECM proteins) in cancer and normal cells of the lung post 5-FU exposure
- Proteomic analysis of these cell lines after 7 days exposure to 5-FU at an IC_{80} drug concentration
- Identification of potential mechanisms important during 5-FU treatment that contribute to differentiation, inhibition of growth, prevention of apoptosis, and progression of invasion.

Fluoropyrimidine treatments of DLKP in vitro

- Proteomic analysis of DLKP after 7 days exposure to the fluoropyrimidines at an IC_{80} concentration and determination of common markers of fluoropyrimidine treatment

Development of a 5-FU drug resistant variant

- Pulse selection of DLKP and A549 with the fluoropyrimidine drugs to develop a 5-FU stably resistant variant
- Identification and characterisation of a stable 5-FU resistant variant
- Proteomic analysis of variants versus Parental cell lines
- Assess if an overlap exists between fluoropyrimidine treatments and cell lines pulse selected by the fluoropyrimidines

Characterisation of DLKP and its subpopulations

- Investigation of motility and invasion rates of DLKP and its subpopulations
- Total cell lysate and hydrophobic proteome analysis of DLKP and its subpopulations
- Identification of clonal markers
- Identification of proteins involved in invasion

2.0 Materials and Methods

2.1 Ultrapure water

Ultrapure water (UHP) was used in the preparation of all media and solutions. This water was purified to a standard of 12-18 mΩ/cm resistance by a reverse osmosis system (Millipore MillI-RO 10 Plus, Elgastat UHP).

2.2 Glassware

The solutions used in the various stages of cell culture were stored in sterile glass bottles. All sterile bottles and other glassware required for cell culture related applications were prepared as follows: glassware and lids were soaked in a 2% RBS-25 (AGB Scientific) for 1 hour. After this time, they were cleansed and washed in an industrial dishwasher, using Neodisher detergent and rinsed twice with UHP. The resulting materials were sterilised by autoclaving.

2.3 Sterilisation Procedures

All thermostable solutions, water and glassware were sterilised by autoclaving at 121°C for 20 minutes at 15 p.s.i.. Thermolabile solutions were filtered through 0.22 □m sterile filters (Millipore, Millex-GV SLGV025BS). Larger volumes (up to 10

litres) of thermolabile solutions were filter sterilised through a micro-culture bell filter (Gelman, 12158).

2.4 Preparation of cell culture media

Media for the routine culture of cancer cells was prepared by Joe Carey (technician) Basal media used during cell culture was prepared as follows: 10X media was added to sterile UHP water, buffered with HEPES (N-(2-Hydroxyethyl) piperazine-N-(2-ethanesulfonic acid) and NaHCO3 as required and adjusted to pH 7.45-7.55 using sterile 1.5 N NaOH or 1.5 N HCl. The media was then filtered through sterile 0.22µm bell filters (Gelman, 12158) and stored in sterile 500ml bottles at 4°C. Sterility as described in section 2.5.5.

Basal media were stored at 4°C for up to three months. The HEPES buffer was prepared by dissolving 23.8g of HEPES in 80ml UHP water and this solution was then sterilised by autoclaving. Then 5ml sterile 5N NaOH was added to give a final volume of 100ml. NaHCO3 was prepared by dissolving 7.5g in 100ml UHP water followed by autoclaving. Complete media was then prepared as follows: supplements of 2mM L-glutamine (Gibco, 11140-0350) for all basal media and 1ml 100X non-essential amino acids (Gibco, 11140-035) and 100mM sodium pyruvate (Gibco, 11360-035) were added to MEM. Other basal media were supplied by sigma. Components were added as described in Table 2.1. Complete media was stored at 4°C for a maximum of one week, complete normal cell media was stored for upto 1 month.

Bronchial Epithelial Medium (BEGM®) and Mammary Epithelial Cell Medium (MEGM®) required for culture of normal cells was supplied by Cambrex. This media supplied as a kit and includes supplementary growth factors, cytokines and antibiotics and were stored at –20°C. BEGM was prepared by addition of the following supplements under aseptic techniques. These supplements are

Table 2.1: Additional components in media.

Cell Line	Culture Medium
A549	ATCC Media (Sigma), 5% FCS
DLKP	ATCC Media (Sigma), 5% FCS
DLKP-SQ	ATCC Media (Sigma), 5% FCS
DLKP-I	ATCC Media (Sigma), 5% FCS
DLKP-M	ATCC Media (Sigma), 5% FCS
DLKP-55	ATCC Media (Sigma), 5% FCS
MCF-7	DMEM Media (Sigma), 5% FCS
NHBE	BEGM basal media, plus Bovine pituitary extract (2ml), Epithelial Growth factor (0.5ml), Insulin (0.5ml), hydrocortisone (0.5ml), transferrin (0.5ml), and without Retinoic acid and GA-1000 (Antibiotic mixture). Concentrations not specified by supplier
HMEC	MEGM basal media, plus Bovine pituitary extract (2ml), Epithelial Growth factor (0.5ml), Insulin (0.5ml), hydrocortisone (0.5ml), transferin (0.5ml), and without GA-1000 (Antibiotic mixture). Concentrations not specified by supplier

2.5 Cells and Cell Culture

All cell culture work was carried out in a class II laminar air-flow cabinet (Nuaire Biological Laminar Air-Flow Cabinet). All experiments involving cytotoxic compounds were conducted in a cytogard laminar air-flow cabinet (Gelman Sciences, CG series). Before and after use the laminar air-flow cabinet was cleaned with 70%

industrial methylated spirits (IMS). Any items brought into the cabinet were also cleaned with IMS. At any time, only one cell line was used in the laminar air-flow cabinet and upon completion of work with any given cell line the laminar air-flow cabinet was allowed to clear for at least 15 minutes so as to eliminate any possibility of cross-contamination between the various cell lines. The cabinet was cleaned weekly with industrial disinfectants (Virkon or TEGO) and these disinfectants were alternated every month. Details pertaining to the cell lines used for the experiments detailed in this thesis are provided in Table 2.5.1. All cells were incubated at 37°C and where required, in an atmosphere of 5% CO2. Cells were fed with fresh media or subcultured (see Section 2.5.1) every 2-3 days in order to maintain active cell growth. All of the cell lines listed in Table 2.2 are anchorage-dependent cell lines.

Table 2.2: Addition cell line information.

Cell line	Source	Cell type
A549	NICB	Lung Adenocarcinoma
DLKP	NICB	Non-Small Cell Lung carcinoma
DLKP-SQ	NICB	Non-Small Cell Lung carcinoma,
DLKP-I	NICB	Non-Small Cell Lung carcinoma
DLKP-M	NICB	Non-Small Cell Lung carcinoma,
DLKP-55	NICB	Non-Small Cell Lung carcinoma variant
MCF-7	NICB	Breast Adenocarcinoma
NHBE	Cambrex	Bronchial epithelial cells
HMEC	Cambrex	Mammary epithelial cells

2.5.1 Subculturing of cell lines

Subculturing of cancer cell lines

The waste cell culture medium was removed from the tissue culture flask and discarded into a sterile bottle. The flask was then rinsed out with 1ml of trypsin/EDTA solution (0.25% trypsin (Gibco, 043-05090), 0.01% EDTA (Sigma, E9884) solution in PBS (Oxoid, BRI4a)) to ensure the removal of any residual media.

5ml of trypsin was then added to the flask, which was then incubated at 37°C for approximately 5 minutes, until all of the cells detached from the inside surface of the flask. The trypsin was deactivated by adding an equal volume of complete media to the flask. The cell suspension was removed from the flask and placed in a sterile universal container (Sterilin, 128a) and centrifuged at 1000rpm for 5 minutes. The supernatant was then discarded from the universal and the pellet was suspended in complete medium. A cell count was performed and an aliquot of cells was used to re-seed a flask at the required density.

Subculturing of Normal cell lines

Normal cell lines were subcultured in the following manner using the subculture reagent kit supplied by Cambrex (CC-5034). Cells were rinsed with 5 ml of room temperature Clonetics HEPES Buffered Saline Solution. The HEPES Buffered Saline Solution was allowed to evaporate from the flask. The cells were covered with 2 ml of room temperature Trypsin/EDTA. The cell layer was examined microscopically. The trypsinisation process was allowed to continue until approximately 90% of the cells had rounded up and takes about 2-6 minutes, depending on the cell type. At this point, the flask was rapped against the palm of hand to release the majority of the cells from the culture surface. If only a few cells detached, trypsinisation was allowed to continue for a further 30 seconds, and flask was given a further rap with the palm of the hand. This process was repeated until the majority of cells had detached. The trypsin in the flask was immediately nuetralised by addition of 4 ml of room temperature Trypsin Neutralizing Solution.

2.5.2 Cell counting

Cells were trypsinised, pelleted and resuspended in media. The suspension was incubated for 3 minutes at room temperature. A 10µl aliquot of the mixture was then applied to the chamber of a glass coverslip enclosed haemocytometer. Cells in the 16 squares of the four grids of the chamber were counted. The average cell numbers per 16 squares were multiplied by a factor of 104 and the relevant dilution factor to determine the number of cells per ml in the original cell suspension

2.5.3 Cryopreservation of cells

Cells for cryopreservation were harvested in the log phase of growth and counted as described in Section 2.5.2. Cell pellets were resuspended in a suitable volume of serum. An equal volume of a 10 % DMSO/serum solution was added drop wise to the cell suspension. A total volume of 1ml of this suspension (which should contain approximately 7x106 cells) was then placed in cryovials (Greiner, 122278). These vials were then placed in a polystyrene rack in the –20°C freezer for 1 hour and then subsequently placed in a –80°C freezer for at least 4 hours to overnight. Subsequently vials were removed from the –80°C freezer and transferred to the liquid Nitrogen phase of the liquid nitrogen tank for storage (- 196°C).

2.5.4 Thawing of cryopreserved cells

A volume of 5ml of fresh growth medium was added to a sterile universal. The cryopreserved cells were removed from the liquid nitrogen and thawed by using

gentle pipetting action on the frozen cell suspension in the cryovial. The cells were removed from the cryovial and transferred to the aliquoted media. The resulting cell suspension was centrifuged at 1,000 rpm for 5 minutes. The supernatant was removed and the pellet resuspended in fresh culture medium. Thawed cells were counted as described in section 2.5.2 and then divided amongst $25cm^2$ flasks at $5x10^4$ per flask and allowed to attach overnight. The following day, flasks were refed with fresh media to remove any non-viable cells. The same process was used for both normal and cancer cell lines.

2.5.5 Monitoring of sterility of cell culture solutions

Sterility testing was performed in the case of all cell culture media and cell culture related solutions. Samples of prepared basal media were inoculated on to Colombia blood agar plates (Oxoid, CM331), Thioglycollate broths (Oxoid, CM173) and Sabauraud dextrose (Oxoid, CM217) and incubating the plates at 37°C and 25°C. These tests facilitated the detection of bacteria, fungus and yeast contamination. Complete cell culture media were sterility tested at least four days prior to use, using Columbia blood agar.

2.6 Mycoplasma analysis of cell lines

Cell lines were tested for possible mycoplasma contamination by Mr. Michael Henry. The protocol used is detailed in the following Sections 2.6.1.

2.6.1 Indirect staining procedure for Mycoplasma analysis

Mycoplasma negative NRK (Normal rat kidney fibroblast) cells were used as an indicator cells for this analysis. The cells were incubated with a sample volume of supernatant from the cell lines in question and then examined for Mycoplasma contamination. A fluorescent Hoechst stain was used in this analysis. The stain binds specifically to DNA and so stains the nucleus of the cell in addition to any Mycoplasma present. Mycoplasma infection was indicated by fluorescent bodies in the cytoplasm of the NRK cells.

2.7 In vitro toxicity assays

2.7.1 Miniaturised *in vitro* toxicity assay

Cells in the exponential phase of growth were harvested by trypsinisation as described in section 2.5.1. Cell suspensions containing 1 x 10^4 cells per ml were prepared in cell culture medium. Volumes of 100µl/well of these cell suspensions were added to 96-well plates (Costar, 3599) using a multichannel pipette. Cells were then incubated for 24 hours at 37°C in an atmosphere containing 5% CO_2. Cytotoxic drug dilutions were prepared at 2X their final concentration in cell culture medium. Volumes of the drug dilutions (100µl) were then added to each well using a multichannel pipette. Cells were incubated for a further 7-8 days at 37°C and 5% CO2 until the control wells had reached approximately 80-90% confluency. Following the incubation

period of 7-8 days, media was removed from the plates. Each well on the plate was washed twice with 100µl PBS. This was then removed and 100µl of freshly prepared phosphatase substrate (10mM p-nitrophenol phosphate (Sigma 104-0) in 0.1M sodium acetate (Sigma, S8625), 0.1% triton X-100 (BDH, 30632), pH 5.5) was added to each well. The plates were then incubated in the dark at 37°C for 2 hours. The enzymatic reaction was stopped by the addition of 50µl of 1M NaOH. The plate was read in a dual beam plate reader at 405nm with a reference wavelength of 620nm. Assessment of cell survival in the presence of drug was determined by the acid phosphatase assay (section 2.7.3). The concentration of drug which caused 50% inhibition of cell growth (IC50 of the drug) was determined from a plot of the % survival (relative to the control cells - 0µM drug) versus cytotoxic drug concentration.

2.7.2 Fluoropyrimidine treatments for the determination of approximate IC80 value; an *in vitro* compound toxicity assay

Exponentially growing cells were harvested as described in section 2.5.1. A total of $5x10^4$ cells were seeded into each of ten 25cm^2 flasks and were further cultured for two days at 37°C in an atmosphere containing 5%CO_2 in 5ml of media. On days 2, 4 and 6 media was replaced with fluoropyrimidine-supplemented media at 37°C and in control flasks (untreated) media was replaced with media heated to 37°C. By day 9 cells were harvested as described in section 2.5.1 to determine the degree of growth inhibition.

2.7.3 Fluoropyrimidine IC_{80} treatment cell culture and post treatment cell culture

A total of 5 x 10^5 cells were seeded into 175cm^2 flasks and cultures for 2 days in 25ml of media. Media was replaced with media supplemented with fluoropyrimidine drug at IC_{80} concentration determined as described in section 2.7.2, and confirmed by counting. Cells were cultured for a further 7 days were media was replaced with media supplemented freshly fluoropyrimidine after 2 and 4 days exposure.

For culturing of cells post 5-FU exposure, cells were trypsinised and seeded in to fresh 25cm2 flasks at a concentration 5x10^4 cells in 5ml of media per flask and were fed every 2 days.

2.8 Safe handling of cytotoxic drugs

Cytotoxic drugs were handled with extreme caution at all times in the laboratory, due to their inherent danger. Disposable nitrile gloves (Medical Supply Company Ltd) were worn at all times and all work was carried out in cytotoxic cabinets (Gelman Sciences, CG series). All drugs were stored in a safety cabinet at room temperature or in designated areas at 4°C or -20°C. The storage and means of disposal of the cytotoxic drugs used in this work are outlined in Table 2.3.

Cytotoxic Agent	Storage	Disposal
Adriamycin	4°C in dark	Incineration
Taxol	Room temperature in dark	Incineration

5-FU	-20oC in dark	Incineration
55FdU	-20oC in dark	Incineration
52FdU	-20oC in dark	Incineration

Table 2.3 Storage and disposal details for chemotherapeutic agents (drug disposal carried out by Dr. Robert O Connor).

2.9 Pulse selection process with fluoropyrimidines

The cell lines DLKP and A549 were grown to 50% confluency in 75cm^2 flasks. The cells were then exposed to a low level concentration of 5-FU, 52FdU and 55FdU for 4 hour pulses, and this was gradually ramped in increments of 10-20μM in a series of 10 pulses. Ramping was determined by failure to induce cell death or growth inhibition. Cells culture between pulse selections were then grown in drug-free media for at least 1 week, refeeding every 2-3 days between pulses and pulsing recommenced when cells reached 50% confluency and were seen to be proliferating.

2.10 Western blotting

2.10.1 Whole cell protein extraction

Media was removed and cells were trypsinised as described in section 2.5.1. Cells were washed twice with ice cold PBS. All procedures from this point forward were performed on ice. Cells were resuspended in 100-200μl of NP-40 lysis buffer and incubated on ice for 60 minutes (see tables 2.4 and 2.5).

Table 2.4: below provides the details of the lysis buffer. Immediately before use, 10µl of the 100X stocks listed in table 2.4 were added to 1ml of lysis buffer.

Addition required per 500ml stock	Final concentration
425ml UHP water	-
25ml 1M Tris-HCl (pH 7.5)	50mM Tris-HCl (pH 7.5)
15ml 5M NaCl	150 mM NaCl
2.5ml NP-40	0.5% NP-40

Table 2.5: NP-40 lysis buffer

100X stock	Preparation instructions
100mM Na3 VO4	1.83g Na3 VO4 in 100ml UHP
100mM DTT	154mg in 10ml UHP
100mM PMSF	174mg in 10ml 100% ethanol
100X Protease inhibitors	2.5 mg/ml leupeptin, 2.5 mg/ml aprotinin, 15 mg/ml benzamidine and 1mg/ml trypsin inhibitor in UHP water

Cells were sonicated with 10 pulses lasting 0.5 seconds at 50% power. Lysed cells were transferred to an eppendorf and pelleted at 13,000 r.p.m for 10 minutes. Supernatant was removed and protein concentration quantified as detailed in section 2.10.2. Samples were then stored in aliquots at -80°C.

2.10.2 Protein Quantification

Protein levels were determined using the Bio-Rad protein assay kit (Bio-Rad, 5000006) as follows. A 2mg/ml bovine serum albumin (BSA) solution (Sigma, A9543) was prepared freshly in lysis buffer. A protein standard curve (0, 0.2, 0.4, 0.6, 0.8 and 1.0mg/ml) was prepared from the BSA stock with dilutions made in lysis buffer. The Bio-Rad reagent was diluted 1:5 in UHP water and filtered through Whatman paper before use. A 20µl volume of protein standard dilution or sample

(diluted 1:20) was added to 0.98ml of diluted dye reagent and the mixture vortexed. After 5 minutes incubation, absorbance was assessed at 570nm. The concentration of the protein samples was determined from the plot of the absorbance at 570nm versus concentration of the protein standard.

2.10.3 SDS-PAGE

Proteins for analysis by Western blotting were resolved using SDS-polyacrylamide gel electrophoresis (SDS-PAGE). The stacking and resolving gels were prepared as illustrated in table 2.10.4.1. Gels were cast using the Atto rig system. It consists of two glass plates, one square and the other notched with two fixed 1.5mm spacers. A rubber seal is placed around the spacers and across the base of the notched plate. The other plate is placed on top of this and two clamps are placed on either side to create a tightly sealed mould for the pouring of polyacrylamide gels. The resolving gel is poured into the gel mould and allowed to set while covered with methanol. Once set the methanol is decanted and the gel is rinsed with UHP and subsequently stacking gel is poured. A comb was placed into the stacking gel after pouring in order to create wells for sample loading (maximum sample loading volume of 15-20µl).

Table 2.6: Preparation protocol for SDS-PAGE gels (2 x 0.75mm gels).

Components	7.5% Resolving Gel	12% Resolving Gel	5%Stacking Gel
Acrylamide stock	3.8ml	6.0ml	0.8ml
UHP water	8.0ml	6.0ml	3.6ml
1.875 M Tris-HCl pH 8.8	3.0ml	3.0ml	-
1.25 M Tris-HCl pH 6.8	-	-	0.5ml
10% SDS	150µL	150µL	50µL
10% NH4-persulfate	60µL	50µL	17µL
TEMED	9µL	7.5µL	9µL

The acrylamide stock in Table 2.6 consists of a 30% (29:1) ratio of acrylamide:bis-acrylamide (Sigma, A2792). The molecular weight markers (Biorad, C3437) and protein samples were heated to 95°C for 5 minutes. After heating, equal amounts of protein (10-30µg) were added in to each well. The gels were run at 250V and 45mA until the bromophenol blue dye front was found to have reached the end of the gel, at which time sufficient resolution of the molecular weight markers was achieved.

2.10.4 Western Blotting

Once electrophoresis had been completed, the SDS-PAGE gel was equilibrated in transfer buffer (25mM Tris (Sigma, T8404), 192mM glycine (Sigma, G7126), pH 8.3-8.5) for approximately 30 minutes. Six sheets of Whatman 3mm filter paper were soaked in freshly prepared transfer buffer. These were then placed on the cathode plate of a semi-dry blotting apparatus (Bio-rad). Air pockets were then removed from between the filter paper. Nitrocellulose membrane (GE Healthcare, RPN 303D), which had been equilibriated in the same transfer buffer, was placed over the filter paper on the cathode plate. Air pockets were once again removed. The gels were then aligned on to the membrane. Six additional sheets of transfer buffer soaked filter paper were placed on top of the gel and all air pockets removed. The proteins were transferred from the gel to the membrane at a constant current of 34mA 30-60 minutes, until all colour markers had transferred.

Following protein transfer, the membranes were blocked for 2 hours using 5% milk powder (Cadburys; Marvel skimmed milk) in PBS at 4°C. Membranes were treated with primary antibody in PBS/0.5% tween/5% milk powder overnight at 4oC under gentle agitation. Primary antibody was removed after this period and the membranes rinsed 3 times with PBS containing 0.5% Tween 20 (Sigma P1379) for a total of 30 minutes. Secondary antibody (1 in 1,000 dilution of anti-mouse IgG peroxidase conjugate (Dako) in PBS, 1 in 2,000 dilution of anti-rabbit IgG (Dako) in PBS or, 1 in 1,000 dilution of anti-rat IgG (Dako, P0450) in PBS) was added for 1.5 hour at room temperature. The membranes were washed thoroughly in PBS containing 0.5% Tween for 15 minutes.

Primary Antibody Antigen	Species	Conditions	Supplier
HSPA5	Mouse	1/1000 dilution, O/N, 5% Marvel/0.5% tween/PBS-A	BD
TP53	Mouse	1/1000 dilution, O/N, 5% Marvel/0.5% tween/PBS-A	Oncogene
KRT8	Mouse	1/1000 dilution, O/N, 5% Marvel/0.5% tween/PBS-A	Sigma
KRT18	Mouse	1/1000 dilution, O/N, 5% Marvel/0.5% tween/PBS-A	Sigma
Sdc-2	Rabbit	1/1000 dilution, O/N, 5% Marvel/0.5% tween/PBS-A	Zymed
β1 integrin	Mouse	1/1000 dilution, O/N, 5% Marvel/0.5% tween/PBS-A	BD
α1integrin	Rabbit	1/500 dilution, O/N, 5% Marvel/0.5% tween/PBS-A	Chemicon
α5 integrin	Rabbit	1/500 dilution, O/N, 5% Marvel/0.5% tween/PBS-A	Chemicon
TS	Mouse	1/500 dilution, O/N, 5% Marvel/0.5% tween/PBS-A	ABCAM
GAPDH	Mouse	1/10000 dilution, O/N, 5% Marvel/0.5% tween/PBS-A	ABCAM
GAPDH	Rabbit	1/1000 dilution, O/N, 5% Marvel/0.5% tween/PBS-A	ABCAM
Gelsolin	Mouse	1/1000 dilution, O/N, 5% Marvel/0.5% tween/PBS-A	ABCAM

Table 2.7 List of Primary antibodies, species, conditions, supplier.

2.10.5 Enhanced chemiluminescence (ECL) detection

Immunoblots were developed using an Enhanced Chemiluminescence kit (GE Healthcare, RPN2109) which facilitated the detection of bound peroxidase-conjugated secondary antibody.

Following the final washing nitrocellulose membranes were dipped in 1:1 mixture of ECL reagents to ensure even coverage and were covered with an acetate sheet in a rolling action to ensure exclusion of air pockets. The membrane was then exposed to chemiluminescent film (Roche) for various times (from 10 seconds to 10 minutes depending on the signal). The exposed chemiluminescent film was developed for 3 minutes in developer (Kodak, LX-24). The film was then washed in water for 15 seconds and transferred to a fixative (Kodak, FX-40) for 5 minutes. The film was then washed with water for 5-10 minutes and left to dry at room temperature.

2.11 Extracellular Matrix Adherence Assays

2.11.1 Reconstitution of ECM Proteins

Adhesion assays were performed using the method of Torimura et al. (1999). Collagen type IV (Sigma C-5533), fibronectin (Sigma F-2006) and laminin (Sigma L-2020) were reconstituted in PBS to a stock concentration of 500 μg/ml. Stocks were aliquoted into sterile eppendorfs. Fibronectin and collagen stocks were stored at -20°C, while laminin stocks were stored at -80°C. Matrigel (Sigma E-1270) was aliquoted and stored at -20°C until use. Matrigel undergoes thermally activated polymerisation when brought to 20-40°C to form a reconstituted basement membrane.

2.11.2 Coating of Plates

Each of the ECM proteins, collagen, fibronectin and laminin, was diluted to 25μg/ml while matrigel was diluted to 1mg/ml with PBS. 250μl aliquots were placed into wells of a 24-well plate. The plates were gently tapped to ensure that the base of each well was completely covered with solution. The plates were then incubated overnight at 4°C. The ECM solutions were then removed from the wells and the wells rinsed twice with sterile PBS. 0.5ml of a sterile 0.1% BSA/PBS solution was dispensed into each well to reduce non-specific binding. The plates were incubated at 37°C for 20 minutes and then rinsed twice again with PBS.

2.11.3 Adhesion Assay

Cells were set up in 75cm2 flasks and then harvested and resuspended in serum-free HAM's F12 medium. The cells were then plated at a concentration of 2.5×10^4 cells per well in triplicate and incubated at 37°C for 15, 30 and 60 minutes. A blank control was included for each ECM protein and contained no cells. After each the specified elapsed time, the cell suspension was removed, non-adhered cells were

removed by rinsing with PBS. Subsequently 250µl of freshly prepared phosphatase substrate (10mM p-nitrophenol phosphate (Sigma 104-0) in 0.1M sodium acetate (Sigma, S8625), 0.1% triton X-100 (BDH, 30632), pH 5.5) was added to each well. The plates were then incubated in the dark at 37°C for 2 hours. The enzymatic reaction was stopped by the addition of 100µl of 1M NaOH. 100µl aliquots were transferred to a 96-well plate and read in a dual beam plate reader at 405nm with a reference wavelength of 620nm.

2.12 Invasion Assays

Invasion assay was performed using pre-cast Matrigel invasion chambers supplied by BD Biocoat™ Matrigel™ Invasion Chambers (BD Biosciences 354480) and invasion assays were performed as described by manufacturer. Briefly, Matrigel coated Boyden invasion chambers were reconstituted by addition of 500 µl of DMEM into the boyden invasion chamber sits in a well of 24 well plate containing 750µL of DMEM media. The chamber was subsequently incubated for at least 2 hours at 37°C to ensure complete rehydration of matrigel. Cells to be analysed were harvested by trypsinisation and counted as described in sections 2.5.1 and 2.5.2, respectively. Cell pellets were resuspended and $1x10^5$ cells were prepared in 500µl media per cell line. The DMEM media was removed from invasion chambers and wells and 750µl of complete media was added to the well and cell suspension was added to Boyden chamber. Cells were incubated at 37°C for 24 and 48 hours depending on cell lines degree of invasiveness. After this time period, the inner side of the insert was wiped with a wet cotton bud (Johnson and Johnson) while the outer side of the insert was

stained with 0.25% crystal violet for 10 minutes and then rinsed and allowed to dry. The inserts were then viewed under the microscope. The numbers of invasive cells were counted using a microscope equipped with a raticule. A total of 5 raticule fields were counted per biological replicate at 10x magnification and the average number of cells for this area was determined. No FCS gradients or chemoattractants were used to stimulate invasion. The non-invasive cell line MCF-7 and highly invasive cell line A549 were used as a negative and positive invasion controls.

2.13 Motility Assay

Motility assays were carried out by the addition of 100µl of media containing 1x105 cells into a non-coated boyden invasion chamber (BD biosciences 351154) and were incubated for 48 hours at 37°C. bumber of motile cells were quantified at described in section 2.14.

2.14 Proteomics

2.14.1 Chemicals

The N-hydroxy succinimidyl ester-derivatives of the cyanine dyes Cy2, Cy3, and Cy5, immobilised pH gradient strips and Ampholytes were purchased from GE Healthcare. Urea and iodoacetamide were bought from Fluka Chemical Corp (Milwaukee, WI). All other reagents were supplied by sigma.

2.14.2 Protein Preparation for 2D-elctrophoresis

2.14.2.1 Total cell lysate Proteome Preparation

Cells for 2D analysis were removed from adherent culture by trypsinisation. Trypsin was neutralized by addition of media, and cells were subsequently washed twice in cold PBS and twice with cold sucrose-tris (10mM sucrose, 100mM Tris, pH 8) buffer. Cells were lysed using a buffer containing (4% (w/v) CHAPS, 7M urea, 2M Thiourea, 10 mM Tris-HCl, 5mM Magnesium Acetate pH 8.5 plus DNase) at concentration of 3 x 10^7 cells per ml. Cells were passed through a 18 gauge syringe until solution become homogenous and non-viscous and was incubated at room temperature for 1 hour. Insoluble material was removed by centrifugation at 14,000 rpm for 20 min at 10°C. Protein concentration was determined using the Bradford protein assay kit (Biorad).

2.14.2.2 Membrane fractionation

The fractionation process for the isolation of hydrophobic proteins from the cell lines DLKP and its subpopulations was carried out using ReadyPrep™ Protein Extraction Kit (Membrane I) (Biorad). Samples were prepared as previously described in section 2.5.3 and were lysed in a solution containing 2% precondensed Triton X-114 in TBS (150mM NaCl, 10mM Tris-HCl, pH 7.6) and was incubated for 15 minutes in ice. Samples were centrifuged at 10,000 x g for 10 minutes and the supernatant was collected and incubated at 37°C. The cloudy solution obtained was centrifuged at 1000 x g for 10 minutes. This caused the formation of two liquid phases. The lower liquid phase was collected and is enriched in hydrophobic proteins. Proteins were precipitated using cold acetone. The fractionation process follows Santoni *et al.*, (2000) protocol for the extraction of membrane proteins. Dr. Andrew Dowd carried out this fractionation process.

2.14.3 Cy Dye labelling for 2D-DIGE

Cell lysates prepared as described in section 2.17 were labelled with N-hydroxy succinimidyl ester-derivatives of the cyanine dyes Cy2, Cy3, and Cy5 as follows. Typically, samples yielded 2-10 μg/μL protein and 50 μg of protein from total cell lysate or 25μg of protein from membrane fractionation was minimally labelled with 1μL solution containing 200 pmol of either Cy3 or Cy5 per 50μg of protein for comparison on the same 2D gel. Labelling reactions were performed on ice in the dark for 30 mins and then quenched with a 1μL of 10mM free lysine per 200pmol of Cy Dye for 10 mins on ice. A pool of all samples was also prepared and labelled with Cy2 to be used as a standard on all gels to aid image matching and cross-gel statistical analysis. The Cy3 and Cy5 labelling reactions (50 μg of each) from each lysate were mixed and run on the same gels with an equal amount (50 μg) of Cy2-labeled standard (Alban et al., 2003). In each 2D-DIGE experiment a total of 3 biological replicates were used for each group. Each biological replicate was run as technical duplicates.

2.14.4 2D-electrophoresis and imaging of 2D-DIGE gels

Immobilized 18cm linear pH gradient (IPG) strips, pH 4-7, were rehydrated in rehydration buffer (7M urea, 2M Thiourea, 4% CHAPS, 0.5% IPG Buffer, 50 mM DTT) overnight, according to the manufacturers guidelines. Isoelectric focusing was performed using an IPGphor apparatus (GE Healthcare) for a total of 48 kV/h at 20°C, 50 mA. Strips were equilibrated for 20 mins in 50 mM Tris-HCl, pH 8.8, 6 M urea, 30% (v/v) glycerol, 1% (w/v) SDS containing 65 mM DTT and then for 20 mins in the same buffer containing 240 mM iodoacetamide. Equilibrated IPG strips were

transferred onto 18 cm x 20 cm 12.5% uniform polyacrylamide gels poured between low fluorescence glass plates. Strips were overlaid with 0.5% (w/v) low melting point agarose in 2x running buffer containing bromphenol blue. Gels were run using the Ettan Dalt 6 or Ettan Dalt 12 (GE Healthcare) at 2.5 W/gel for 30 mins then 100 W in total at 10°C until the dye front had run off the bottom of the gels. All the images were collected on a Typhoon 9400 Variable Mode Imager (GE Healthcare).

2.14.5 Statistical analysis and image processing of 2D-DIGE gels

Images collected of 2D-DIGE gels were were examined in Image Quant Tool Box (GE Healthcare) to ensure images were not saturated. Subsequently images were cropped to remove area of gel that does not contain protein spots and cropping area was aligned with a reference protein spot for consistant cropping between gels.

Statistics and quantification of protein expression were carried out using Biological Variation Analysis (BVA) a component of Decyder software (GE Healthcare). Images were manually inspected to ensure accurate spot matching between gels. Generation of protein pick lists for identification using MALDI-ToF MS were determined using filters are described per experiment in section 3.0.

2.14.6 Preparation of plates for spot picking

Low fluorescent plates were polished with lint free wipes soaked in methanol and allowed to dry at room temperature for 10 minutes. During this time the Bind-Silane solution was prepared and is composed of the components listed in table 2.8. A volume of 1.5ml of this solution was pipetted onto one side of each low fluorescent plate using a Pasteur pipette. The solution was spread over each plate using a fresh lint free swab. Plates were placed in a rack and covered with a sheet of aluminium foil

to prevent dust particules adhering to surface of plates and were allowed to dry for at least 90 minutes. Plates were again polished with methanol and allowed to dry for 10 minutes. Low fluorescent plates were placed together with its accompanying spacer plate with the bind-silane surface in contact with the spacers on the spacer plate. Plates were then placed in the DALT 6 or DALT 12 as described in section 2.19. For preparative gels protein samples were prepared as described in section 2.19. A total of 300µg of protein was loaded on to each preparative gel. Loading of protein samples onto IEF strips was the same as with loading of labelled proteins described in section 2.19 with one exception. No 2X running buffer was added to protein solutions prior to addition to IEF strips.

Table 2.8: Components of Bind Silane solution

Reagent	Quantity
Ethanol	8 ml
Glacial Acetic acid	200 µl
Bind-silane	10 µl
double distilled H2O	1.8 ml
Total volume	~10ml (enough for 6 gels)

2.14.7 Colloidal staining of 2D-Gels, imaging, and spot matching to BVA

Preparative 2D gels prepared as described in section 2.21 were removed from the DALT 6 or DALT 12. The spacer plates were removed from the plate/Gel sandwich using wedging action with a "wonder wedge" (GE healthcare). The spacer plate was removed for cleaning later. The polyacryamide gel fixed to the low fluorescent plate was allowed to fix in a solution of 7% glacial acetic acid, 40% methanol for at least 60 minutes in a plastic container under agitation. Brilliant Blue G-Colloidal concentrate (Sigma B2025) was diluted in UHP water at ratio of 1:4 to give a final volume of 1l and was mixed by inversion of bottle. Immediately before staining the

colloidals were activated by addition of 100ml of methanol to 400ml of diluted solution. This solution was mixed with severe agitation for 30 seconds as it is important in order to activate colloidals. The fixing solution was removed from gel and activated colloidal solution waspoured onto gel. Gels were allowed to stain for 1-4 hours under vigorous agitation. Staining was complete when gel appears dark blue and highly abundant protein spots are clearly visible. Decant colloidal staining solution into 1L Duran bottle. Gel and container were quickly rinsed with UHP water to remove as much colloidal staining solution as possible. Destaining solution composed of 10% acetic acid, 25% methanol and 65% UHP water (v/v) was poured onto gel in container and was agitated for 30 seconds. The gel was rinsed with 25% methanol and allowed to destain in 25% methanol for up to 24 hours. Residual colloidal precipitate was removed by wiping swab soaked in 25% methanol. Destaining was stopped as soon as gel background became clear. Two reference marker stickers were placed on the back of the plate and the plate was scanned using Lab Scan software. The image was imported into Image Master and spots were detected. Location of reference markers was assigned (IR1 for left reference marker and IR2 for right reference marker). Using a printed image of the master gel from the BVA experiment were the locations of pick proteins are indicated the locations of proteins colloidal gels that were found to be of interest were selected for robotic picking. See section 2.26 for robotic picking of spots.

2.14.8 Synthesis of Ruthenium (II) tris bathophenanthroline Bisulphonate (RuPBS)

The fluorescent dye RuPBS was synthesised as described by Rabilloud *et al.,* (2001 and 2000). For the synthesis of RuPBS 0.5 g of potassium pentachloro aquo ruthenate

(26.9% Ru) was dissolved in 50 ml boiling water and kept under reflux, resulting in a deep red-brown solution. Three molar equivalents of 1, 10-phenthroline monohydrate, were added and the refluxing continued for 20 min. The solution turned to a deep greenish brown. Meanwhile, a reducing solution containing 12 mM of sodium hydroxide and 8 mM of phosphinic acid (Fluka) in 10 ml water was prepared. This solution was then added to the refluxing mixture and refluxing was continued for another 20 min. The solution turned to a deep orange-brown. After cooling, the pH was adjusted to 7 with sodium hydroxide and the volume was adjusted to 65 ml with water. This gives a 20 mM stock solution, which can be stored in the fridge for several months. RuPBS was synthesized with the assistance of Mr. Gavin Sewell (Chemistry).

2.14.9 RuPBS staining of 2D gels, imaging, and spot matching to BVA

Preparative 2D gels prepared as described in section 2.21 were removed from DALT 6 or DALT 12. The spacer plate was removed from plate/Gel sandwich using wedging action with a "wonder wedge" (GE healthcare). The spacer plate was removed for cleaning later. The polyacryamide gel fixed to the low fluorescent plate was allowed to fix in a solution of 7% glacial acetic acid, 40% methanol for at least 60 minutes in a plastic container under agitation. Staining solution of 123ml of 0.2M acetic acid, 27ml of 0.2M sodium acetate, 120ml ethanol, 120ml Glycerol, 3ml Tween and the volume was adjusted to 600ml by the addition of UHP water. A volume of 15µl of RuPBS stock was added to this solution and the mixture was inverted several times to aid mixing. The fixing solution was removed and staining solution was poured on to the gel and allowed to stain for 4 hours or overnight under gentle agitation. The destaining solution was composed of 123ml of 0.2M acetic acid, 17ml of 0.2M

sodium acetate, and 120ml of ethanol, the volume was adjusted to 600ml by the addition of UHP water. Destaining was performed using 2 washes with the destaining solution for 4 hours each or 4 hours and an overnight destain. Two reference markers were placed on the back of the low fluorescence plates and gels were scanned at excitation wavelength of 488nm and emission wavelength of 605nm using the Typhoon 9400 scanner. Images were imported into Image Quant and cropped appropriately. A single gel DIA file was created for the detection of spots and reference marker locations were assigned. Spot map was exported and imported into the BVA file created for the DIGE experiment for which the preparative gel was part of. Matching mode was selected in the BVA experiment file and landmark mode was activated. Obvious highly abundant spots present in distinct protein patterns were matched manually in this mode. The software was then instructed to match image to experiment using these landmarks. Pick spots were displayed in match mode gel images by alteration of image preferences. Matching of these proteins spots between DIGE images prep gel images were checked individually and proteins that were matched incorrectly were corrected. Where the correct spot could not be found the spot was left unmatched. Pick list was then exported to Spotter. See section 2.26 for spot picking.

2.14.10 Pro-Q diamond staining of 2D gels, imaging, and spot matching to BVA

Preparation and running of 2D gels is the same as described in section 2.24 with the following additional step. Peppermint stick (Molecular Probes) phosphoprotein ladder was prepared by the 1:4 parts dilution in 2x running buffer and was subsequently boiled for 5 minutes. A piece of filter paper of dimensions 1cm+/-0.5 x 3cm was cut. A volume of 5µl diluted ladder was added to filter paper and using a forceps was

placed next to IEF strip on top of gel. Agarose solution was applied and second dimension separation was completed as described in section 2.21. After completion of 2D electrophoresis the spacer plate was removed from the plate/Gel sandwich using wedging action with a "wonder wedge". The spacer plate was removed for cleaning later. Gels were fixed with two 30 minute fixation steps with a solution of 40% methanol, 10% acetic acid made to a volume of 500ml using UHP water. Gels were washed three times with 500ml UHP and stained for 2-hours in 400ml of Pro-Q® Diamond phosphoprotein gel stain (Molecular Probes) solution. Gels were then destained with three 30 minute washes with Pro-Q diamond Destain Solution. Gels were washed in two 5 minute washes with UHP water to rehydrate gels and were scanned with the typhoon 9400 scanner at excitation wavelength of 532nm and emission wavelength of 560nm. Gel destaining was confirmed by analysis of phospho protein ladder. Properly destained gels display only two phospho protein bands in the Peppermint stick phosphoprotein ladder. The image was appropriately saved and the gel was counter stained with RuPBS as described in section 2.24. (The phospho-protein specific stain, Pro-Q diamond, is reported by manufacturer to be compatible with mass spectrometry techniques used for the identification of proteins. Thus such gels can be used as preparative gels and were found to give superior spectra to other techniques). Both fluorescent images were cropped using image quant, and a double image DIA file was created. Images were processed and imported into BVA as described in section 2.24. The RuPBS stained gel image was matched to BVA as described in section 2.24. Spots that appeared on picklist that appeared on both Pro-Q diamond stained gels and RuBPS stained gels were marked as phosphorylated.

2.14.11 Spot picking of protein spot gel plugs from 2D-Gels

Preparative gels stained as described in sections 2.21, 2.22 and 2.23 were placed in plate holder on the Ettan spot picker robot (GE Healthcare). Plates were positioned so that reference markers would appear between the two white strips on plate holder. The plate was secured in position by positioning of clamps on edges of plates and tightening of screws. The solution inlet pipe was removed form the 70% methanol and placed in UHP water. The robot was powered up and the syringe was primed 10 times to replace methanol with UHP water. The pick lists generated were imported into spot picker software and the robot was instructed to automatically detect the reference markers. Upon detection of reference markers the instrument instructs the user to insert an appropriate number of microtitre plates in to robot. Once this done a file directory is created which allows tracking of spots when transferred to the Digester robot and Spotter robot (GE Healthcare). Upon completion of gel picking gels can be scanned with relevant process to ensure picking was done accurately. Microtitre plates containing gel plugs were sealed with foil wrapping and were stored at 4°C until they were ready for digestion.

2.14.12 Destaining of gel plugs and protein digestion

Plates ready for digestion were placed in appropriate positions in Robot digester. The files corresponding to microtitre plates placed in robot that were created in the spot picker robot were uploaded into robot. The UHP water surrounding gel plugs was removed, and destained for three 20 minute washes with 70% methanol 0.1% TFA. Gel plugs were dehydrated by 2 washes with 50% acetonitrile. They were allowed to aspirate for 1 hour. After 30 minutes of aspiration the Trypsin Gold, Mass Spectromoetry Grade (Promega V5280) was prepared. The trypsin was reconstituted by addition of 200µl of acetic acid buffer supplied by manufacturer. The solution was allowed to stand for 5minutes. Subsequently, 1.4ml of 40mM Ammonium

Bicarbonate, 10% Acetonotrile in MS grade water is added to this 200µl of activated trypsin to give a final concentration of 10ug/ml. This solution is vortexed and dispensed equally amongst the 8 disposible plastic trypsin tubes (GE Healthcare). These tubes containing the trypsin are then placed in the robot in the appropriate position. Once at least 60 minutes of aspiration of gel plugs is complete and trypsin is prepared the robot was instructed to dispense 10µl ot trypsin solution on top of each gel plug. The Microtitre plates were then wrapped in foil and incubated at 37°C overnight.

The following day the microtitre plates were removed from incubator and are placed in digester robot as previously described. An equal number of microtitre plates were prepared, labelled, and placed in appropriate extraction positions in robot. The robot was instructed to transfer piptides to the clean microtitre plates. This process involved 20 minute incubation at room temperature in 60µl of 50% acetonitrile, 0.1%TFA and 49.9% MS grade water, which is transferred in to extraction plate, followed by a second extraction cycle of 70µl of same solution for 20 minutes, which was transfered into same well as before. Upon transfer of protein digests to fresh microtitre plate the plates were placed in a speedvac for 60 minutes in order to desiccate peptide. Once solvent was observed to have vaporised completely plates were transferred to the ettan robot spotter.

4.14.13 Identification of differentially expressed proteins using MALDI-ToF Mass spectrometry

2.14.13.1 Preparation of MALDI-ToF slides

MALDI-ToF slides were prepared by scrubbing with detergent, rinsing with UHP water, submerged in ethanol in a beaker and sonicated for two 30 minute intervals in a sonicator bath where ethanol was replaced between sonications. Slides were stored submerged in ethanol in a 50ml universal. Immediately prior to use slides were placed on to lint free tissue and allowed to aspirate until dry, and were subsequently inserted into MALDI-ToF trays using a forceps. Powder free gloves were worn at all times to maintain clean slides.

2.14.13.2 Mass spectrum analysis

Proteins digests (prepared as described in section 2.25) were spotted on to MALDI-ToF slides using sandwich technique. The sandwich technique involves the spotting of each slide with 0.3µl of 7.5mg/ml CHCA in the spotting solution (composed of 50% acetonitrile, 0.5% TFA and 49.5% MS grade water) and was allowed to aspirate for 10 minutes. Peptides created as described in section 2.26 were resuspended in 3µl of spotting solution and 0.3µl was spotted on top of dried CHCA on MALDI-ToF slide. Immediately after this addition 0.3µl of CHCA solution was added to and mixed peptide solution. This was allowed to aspirate for a further 10 minutes before insertion into the MALDI-ToF MS (GE Healthcare). A vacuum of 1.98×10^{-9} pa was pulled and the spotted peptide-CHCA mix was hit by a laser causing peptide ionisation. The conditions are so that each peptide is singly charged upon ionisation. The peptides being singly charged were attracted to the opposite end of the time of flight tube. Since the charge is one on each peptide the mass of the peptide can be determined by the time it takes for the peptide to reach the detector at the other end of the tube. A

typical peptide peak generated by this process is shown in figure 2.1. A peptide peak appears as a series of peaks differing by one mass unit and atomic isotopes of carbon, hydrogen and nitrogen create this phenomenon, however, carbon isotopes predominantly cause this. This information is vital during mass spectrometry as it allows the user to distinguish between peaks created by peptides and those created by non-peptides such as matrix or chemical contaminants.

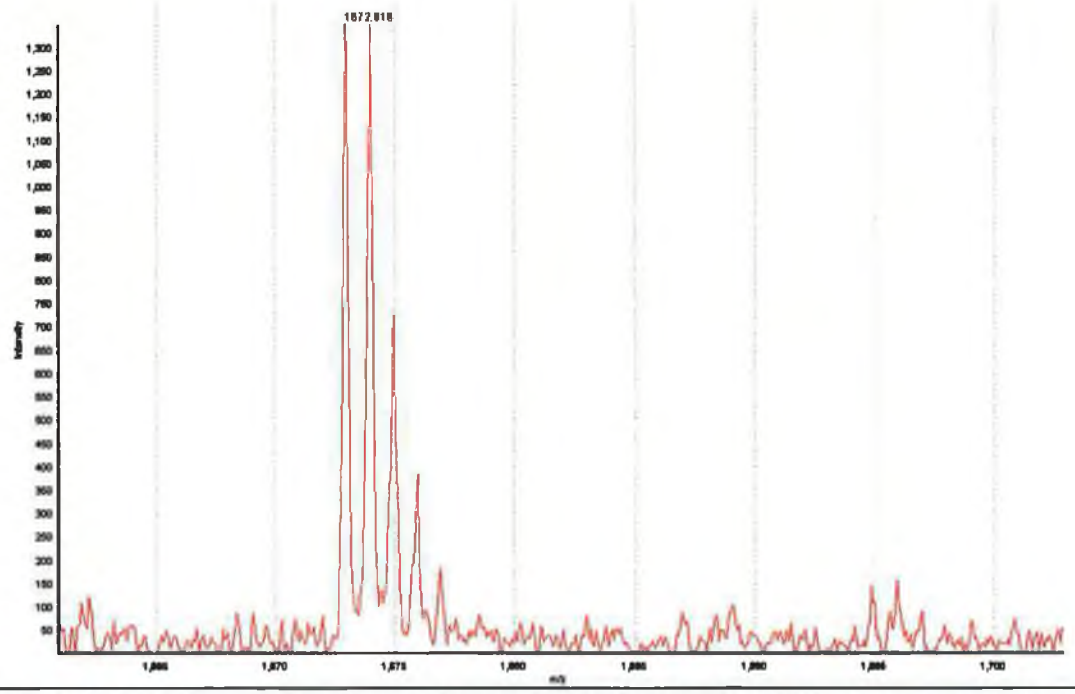

Figure 2.1: A series monoisotopic peptide peak, i.e. a series of peaks differing by one mass unit caused by atomic isotopes (different numbers of neutrons).

However, before proteins can be identified it is important to calibrate the Mass spectrometer in order to assure accurate mass detection. To do this a mixture of 4 peptides of known mass (referred to as Pep 4 mix (Lose Biolabs)) were used to calibrate the instrument. Their masses are listed below in table 2.9. Peptides between 800 and 2500 mass units are predominantly used for identification and thus during calibration peptides of the Pep 4 mix that occur in this region are used for calibration purposes and are indicated in table 2.9.

Table 2.9: The table lists the components of Pep 4 mix and masses. The peptides used to calibrate the instrument are indicated.

Peptide Name	Mass	Used for calibration
Angiotensin 2	1046.542	Yes
Nuerotensin	1672.918	Yes
ACTH fragment 18-39	2456.199	Yes
Insulin B chain oxidized	3494.651	No

Displayed in figure 2.2 is a typical mass spectrum generated by Pep 4 mix used for calibration. Automatic calibrations were checked to ensure the software had detected the correct peaks.

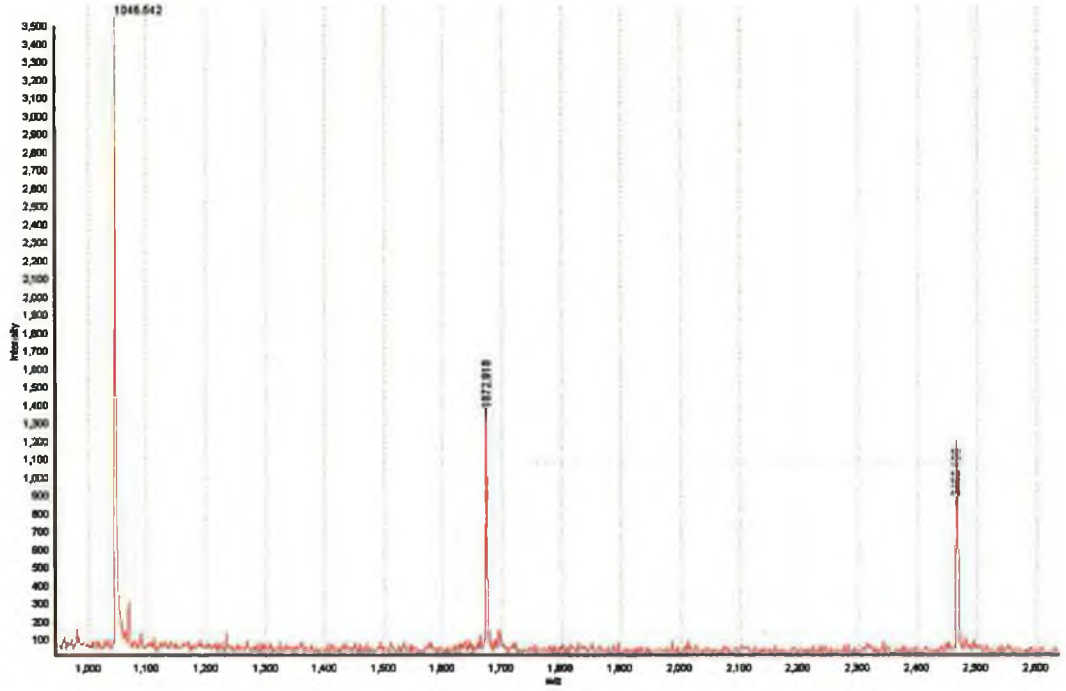

Figure 2.2: A mass spectrum generated by Pep 4 mix used for initial calibration of the MALDI-Tof mass spectrometer.

This calibration is saved as system calibration and is used to accurately measure the peptides measured in subsequent spectra generated on same slide.

For each spectra generated a total of 358 individual spectra are collected, the intensity of each spectra are combined together by addition to create an accumulation spectra. A total of 3 accumulated spectra were created for each spotted peptide-CHCA mix. Calibration can be lost with progression of analysis, to further ensure accuracy of mass spectra the use of internal calibration was used to enhance mass accuracy. Trypsin eventually digests itself during the tryptic digestion process and this creates several peptide peaks that can be used to calibrate individual spectra. Figure 2.3 demonstrates the most common trypsin peaks that may occur in a given mass spectrum. There are three commonn trypsin peaks that result from trypsin self digestion but they may not occur in every spectra and their occurrence depends upon the amount of protein being digested, the abundance of ionisable peptides and the degree of digestion. These products have a m/z of 854.564, 1046.509 and 2211.104

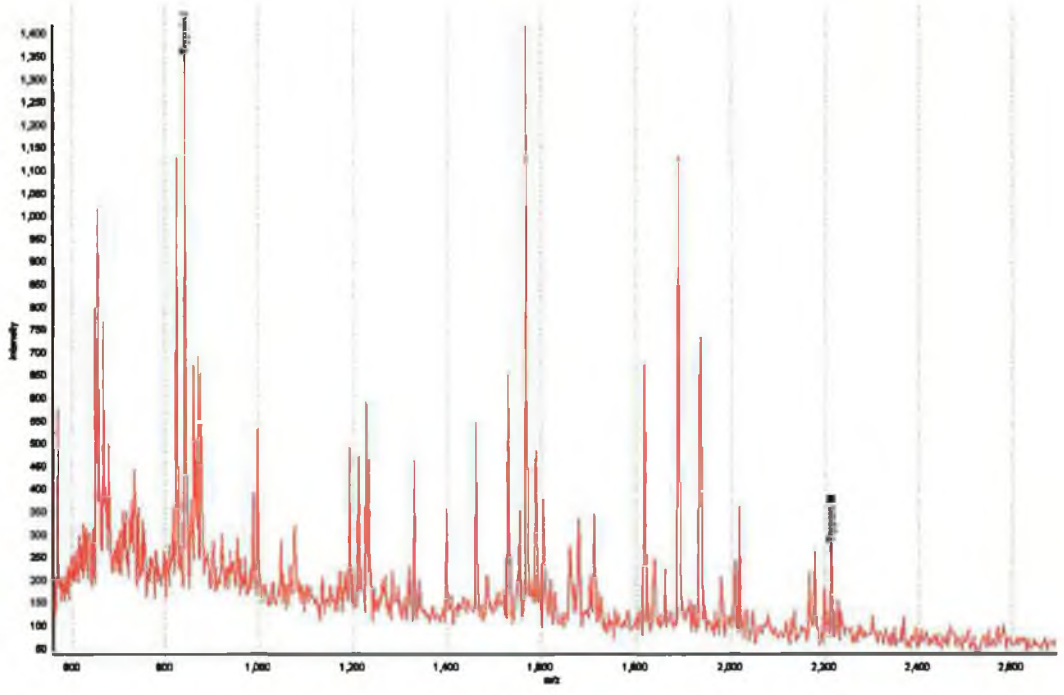

Figure 2.3: A mass spectrum resulting from digestion of a protein showing the location of Trypsin I and Trypsin II peaks used for internal calibration

The software automatically searches and identifies trypsin peaks but these can often

be missed or incorrectly identified and thus it is important to inspect each spectra's calibration.

Once calibration is completed to satisfaction processing of spectrum for protein identification can commence. The software automatically detects and processes the peaks and gives an expectation score for the protein being correctly identified. A spectrum resulting from digestion of the protein BiP/GRP78 is presented in figure 2.4. An expectation score of less than 0.01 is the cut off for protein identification. It is important to inspect a spectrum at this point as the software can miss peaks and they may need to be manually imputed. The criteria for peak detection is as follows; Algorithm centroid, Mass range 800-3500m/z, mono isotopic cut-off 3000m/z mass tolerance 0.2m/z and Average peak 1 m/z. Average peaks are peaks that display peptide pattern but are poorly resolved and the average of all those peaks are used to determine

The laser intensity and the laser target location can be adjusted by user. Adjustment of these paramenters is generally unnesseccary as the software automatically searches and adjusts laser intensity to create the optimal conditions for accurate mass specta accumulation. However on occasion under certain circumstances these parameters need to be manually controlled. Such instances occur when a spectrum contains far too many peaks which the software can confuse with the background, more often than not is fails to collect a spectrum and the mass spectra accumulation needs to be controlled manually. Digestion of low molecular weight proteins results in a mixture of 5-20 peptides. On occasion one or two peptides ionise more readily than the others and can generate peaks with high intensities. The software reduces the laser intensity and thus appearance of other peaks is often missed. In such occasions mass spectrums

collected are manually controlled. Laser intensity in increased until a low level background is observed. Spectrum accumulation is then allowed to continue.

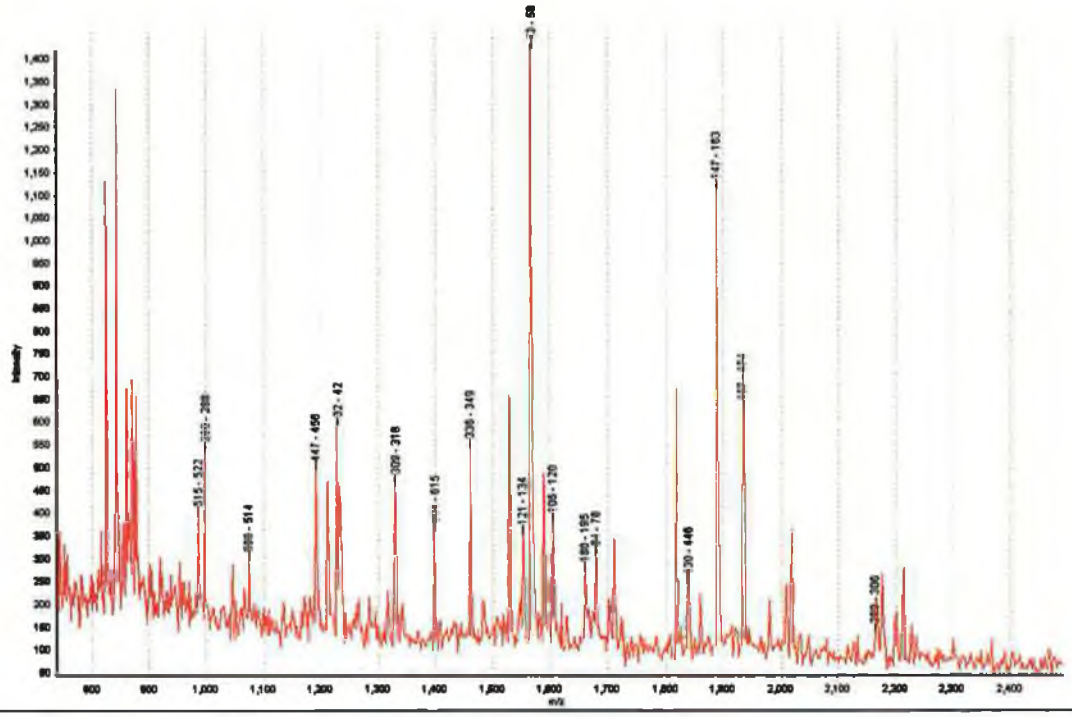

Figure 2.4: A mass spectrum generated by tryptic digestion of BiP/GRP78. Black numbers above each peak indicates locations of peptide peaks in the amino acid sequence of the protein BiP.

2.14.13.3 Bioinfomatic processing of Proteomic data

Protein identification using MALDI-ToF MS results in the identification of a protein with a gene index accession number. "Gene index accession number" for proteins were converted to "gene symbol" using DAVID database ID conversion tool (http://niaid.abcc.ncifcrf.gov/). Not all gene index accession numbers can be converted in this way as some identifications refer to proteins that may be poorly annotated or simple not updated in the database. In such instances the protein name was inputted into swissprot database (http://www.expasy.org/sprot/) and the human protein reference database (www.hprd.org) and the gene symbol was found. In other instances where the protein could not be found in either of the above databases the protein sequence was blasted on the NCBI database using the protein blast tool. Proteins that were found to be 100% identical were used to identify the gene symbol. Such proteins names appear as unknown and the gene symbol found by protein blasting is adjacent to MALDI-ToF identification.

Lists of Gene symbols were imported into Pathway assist. Direct interactions and common pathways were identified using this software. Phosphorylation data was obtained from the human protein reference database. Enzyme location in metabolic pathways sources from the KEGG website (www.genome.ad.jp/kegg/metabolism.html).

2.15 Statistical Analysis

Significance of data presented in section 3.0 was determined using 2 tailed T-tests with 2 unpaired samples with unequal variance.

T-tests were performed on invasion and toxicity assays in order to determine if data was significant

A t-test > 0.05 was deemed not significant

A t-test < 0.05 was deemed significant

3.0 Results

3.1 Analysis of 5-FU treatments

The fluoropyrimidine antimetabolite drug 5-FU is used in the treatment of a wide variety of cancers. It exerts its effect through inhibition of TS activity and inhibition of de novo synthesis of DNA and incorporation of fluoropyrimidine derivatives into RNA and DNA. These result in the inhibition of cell growth and the eventual induction of apoptosis. Understanding how cells respond at a proteomics level is poorly described in the literature and thus identifying molecular mechanisms induced by growth inhibition is key to understanding the mechanisms induced which contribute to cell survival and possible altered phenotypes. To assess this 5-FU treatment of the lung adenocarcinoma, A549, the NSCLC, DLKP, the lung normal bronchial epithelial cell line NHBE, the breast adenocarcinoma, MCF-7, and the normal mammary epithelial cell line, HMEC, were assessed to determine the drug concentration of 5-FU that would induce an inhibition of growth by at least 80% over a 7 day period. Using this drug concentration drug resistance and invasion rates were assessed post 5-FU treatment. Protein was prepared at day 7 of the 5-FU treatment from each cell line in biological triplicates and an exponentially growing untreated control was collected simultaneously. Protein preps were then prepared for the purposes of expression profiling using Cy dye labelling of protein preps and separated using 2D electrophoresis a process referred to as two dimensional difference gel electrophoresis (2D-DIGE).

3.1.1 Growth inhibition induced by 5-FU

In order to assess the anti-proliferative effect of 5-FU it was necessary to determine the concentration at which 5-FU induces an inhibition of growth. An exposure time of 7 days was selected as it was found to induce differentiation effects in DLKP and A549 with similar drugs. The treatment regime involved the replacement of media with drug supplemented media every 2-3 days. For experimental consistency 5-FU supplemented media was replaced on days 2, and 4 of treatment regime (see section 2.7.3). Figures 3.1.1 – 5 demonstrate that the concentration of 10μM inhibited the growth of 5-FU by approximately 80-90%. The normal cell experiments included the additional concentration of 30μM 5-FU as cells appeared to be as healthy microscopically as those exposed to 10μM for 7 days and yielded similar cell numbers. In addition the pharmakokinetics of normal cells is different to that of cancer cells. Specifically cancer cells *in vivo* generally require a higher amount of uracil than normal tissue {Rutman, *et al.,* 1954}and thus 5-FU influx rates would be expected to be higher in cancer than normal cells. However, this may not be evident *in vitro* as cells are allowed to grow exponentially and there requirement for uracil may be equivalent. Figures 3.1.1-5 show that indeed inhibition of growth is comparable between cell lines and suggests that 5-FU consumption rates are related to proliferation and not disease status.

Growth post 5-FU exposure (10μM for 7 days) was assessed in order to determine if cancer cell lines become senescent or apoptopic. Figures 3.1.6-8 demonstrates that all cell lines display an initial decrease followed by a gradual increase in cell number. A549 displays the quickest recovery. All cancer cell lines appear to increase cell number by day 7. Normal cell lines were not assessed. Normal cell lines can only be cultured for 20 doublings and cell division beyond this time point is not guaranteed. Proteomic analysis requires a large amount of cell to generate a sufficient protein mass for 2D-DIGE and protein identification. In light of these difficulties invasion was only assessed at day 7 of 5-FU treatment.

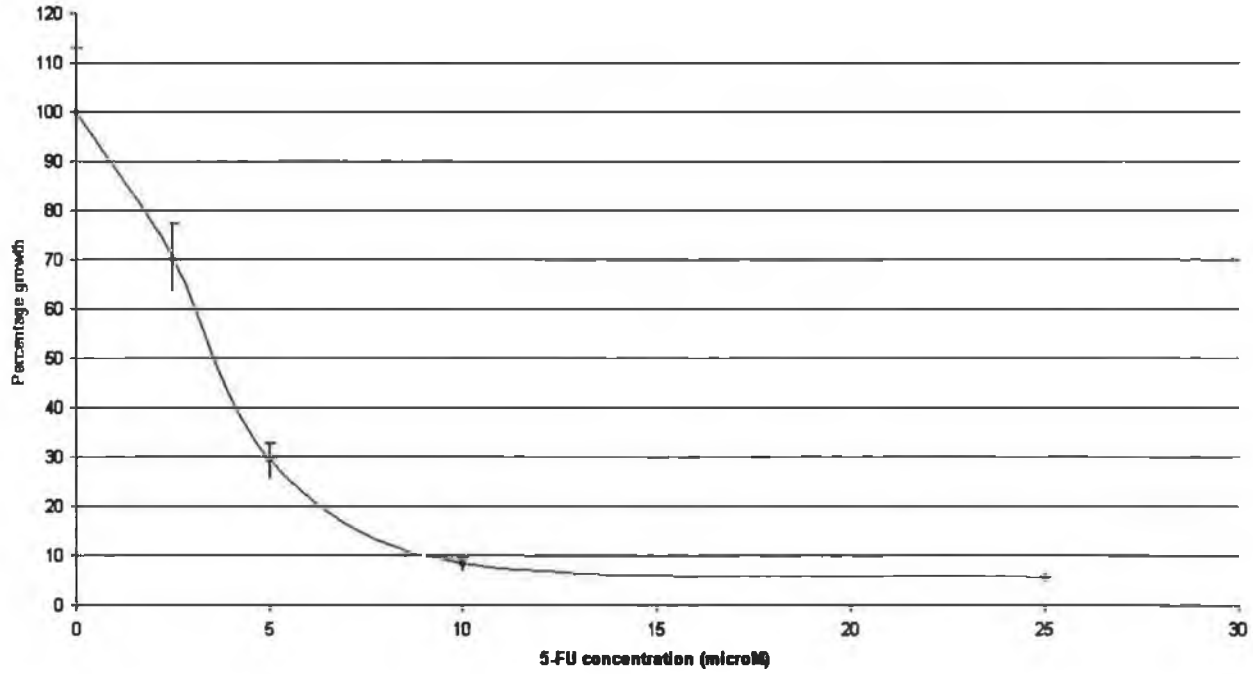

Figure 3.1.1: Number of cells harvested after exposing **A549** cells for 7 days at various 5-FU concentrations. The concentration of 10μM induces an inhibition of growth.

Inhibition of cell growth is inhibited by 90% in A549 by treatment with 10μM over a 7 day treatment with 5-FU. The growth inhibition curve enters a plateau at 10μM and would suggest inhibition of cell growth in the majority of cells per flask. A concentration of 3-4μM 5-FU induces a growth inhibition by 50%.

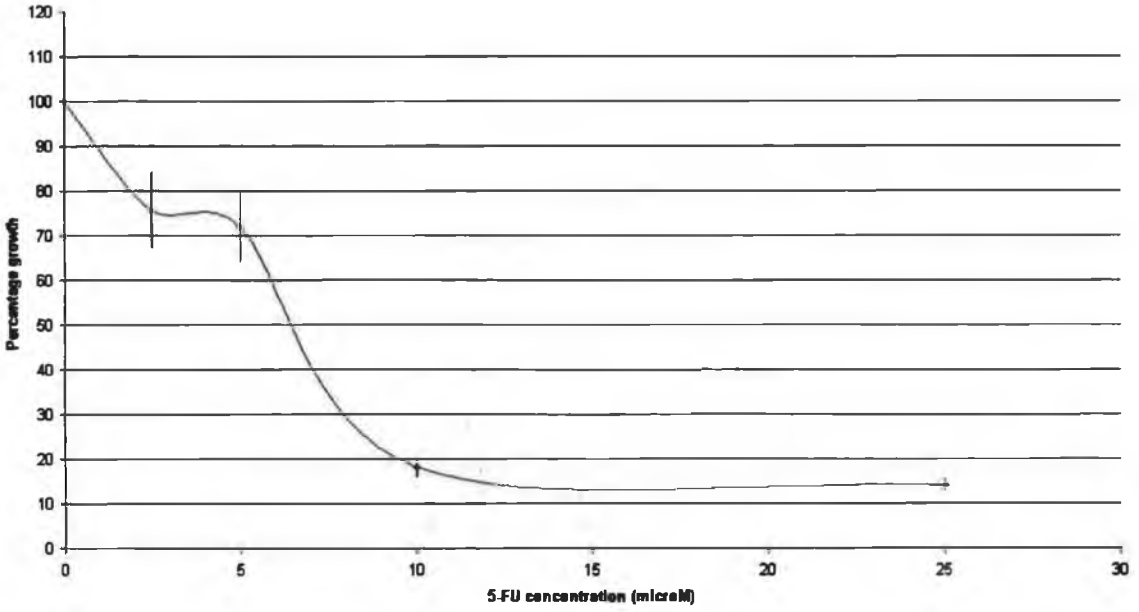

Figure 3.1.2: Number of cells harvested after exposing **DLKP** cells for 7 days at various 5-FU concentrations. The concentration of 10μM induces an inhibition of growth.

Inhibition of cell growth is inhibited by 80% in DLKP by treatment with 10μM over a 7 day treatment with 5-FU. The growth inhibition curve enters a plateau at 10μM and would suggest inhibition of cell growth in the majority of cells per flask. DLKP appears to have a higher tolerance to 5-FU than A549. A concentration of 6-7μM induces a 50% growth inhibition in DLKP an approximate 2 fold increase in tolerance to 5-FU in DLKP over A549.

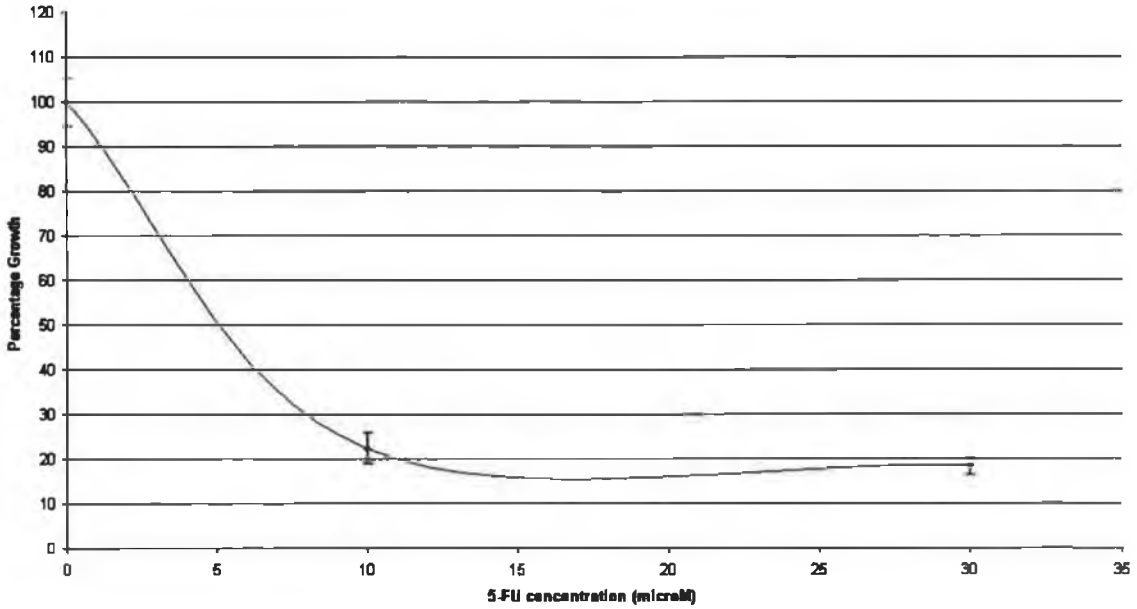

Figure 3.1.3: Number of cells harvested after exposing **NHBE** cells for 7 days at various 5-FU concentrations. The concentration of 10μM induces an inhibition of growth.

Inhibition of cell growth is inhibited by 80% in NHBE by treatment with 10μM 5-FU over a 7 day treatment. The growth inhibition curve enters a plateau at 10μM and would suggest inhibition of cell growth in the majority of cells per flask. Curve would indicate that 5μM 5-FU induces a 50% inhibition of growth suggesting NHBE to be slightly more tolerant than A549 but less tolerant than DLKP to 5-FU treatment. NHBE appears to be similarily tolerant to 5-FU as DLKP and shows a higher tolerance to 5-FU than A549. However it should be noted that this graph contains limited data points due to limited supply of NHBE cells.

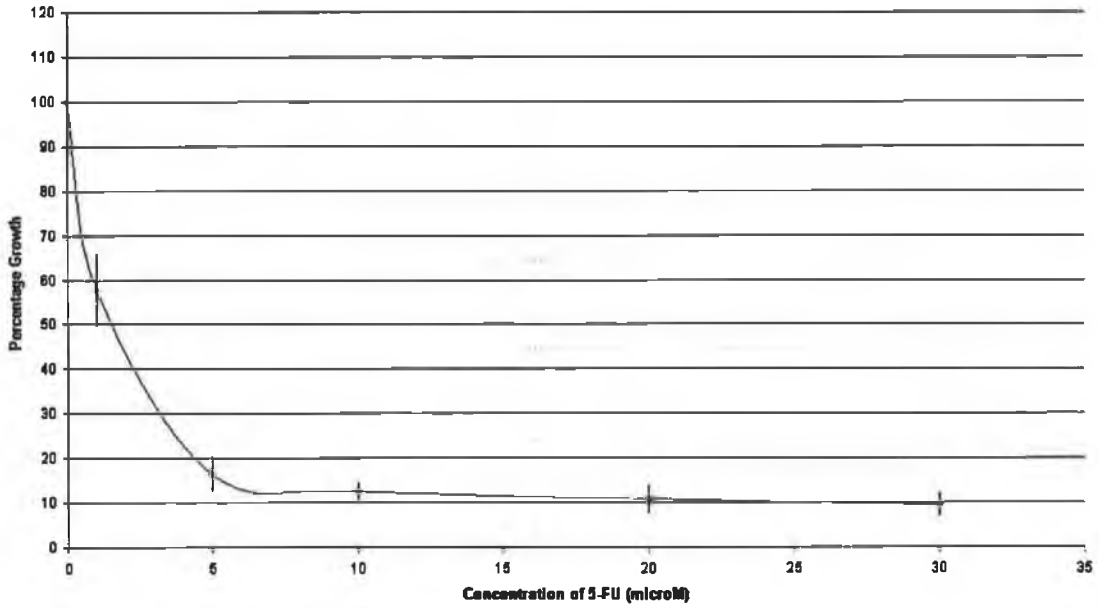

Figure 3.1.4: Number of cells harvested after exposing **MCF-7** cells for 7 days at various 5-FU concentrations. The concentration of 10μM induces an inhibition of growth.

Inhibition of cell growth is inhibited by 90% in MCF-7 by treatment with 10μM over a 7 day treatment with 5-FU. The growth inhibition curve enters a plateau at 10μM and would suggest inhibition of cell growth in the majority of cells per flask. Growth inhibition of 50% is induced by 2-3μM 5-FU and would suggest that MCF-7 is least tolerant to 5-FU of all cell lines.

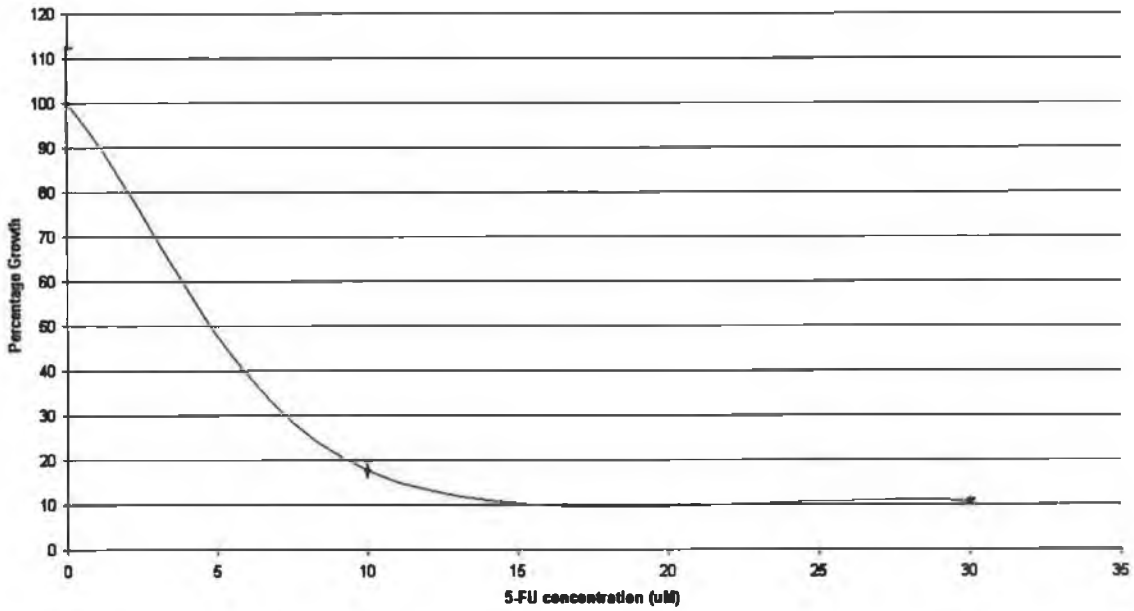

Figure 3.1.5: Number of cells harvested after exposing **HMEC** cells for 7 days at various 5-FU concentrations. The concentration of 10μM induces an inhibition of growth.

Inhibition of cell growth is inhibited by 80% and 90% in HMEC by treatment with 10 and 30 μM, respectively, over a 7 day treatment regime. The growth inhibition curve enters a plateau at 10μM and would suggest inhibition of cell growth in the majority of cells per flask. A concentration of 5μM 5-FU induced growth inhibition by 50% and would suggest that HMEC is more tolerant to 5-FU than MCF-7. However it should be noted that this graph contains limited data points due to limited supply of HMEC cells.

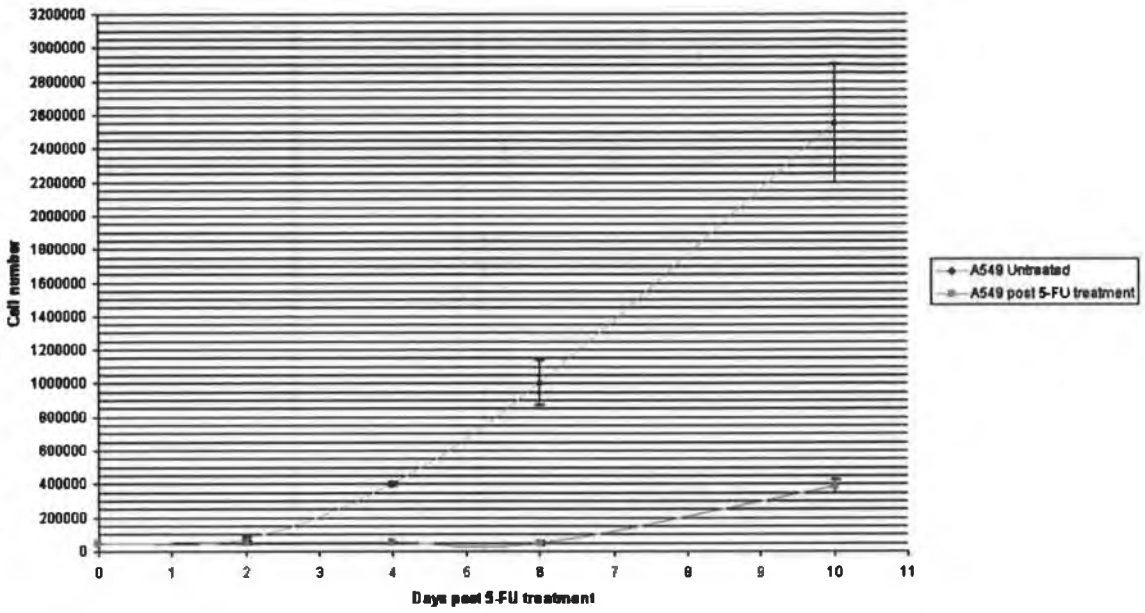

Figure 3.1.6: Growth curves of A549 and A549 post 5-FU treatment over a 10-day period (Gridline factor 50000).

A549 appears to begin proliferating 6 days post 5-FU treatment. Thus toxicity assays may be set up after this time point in order to determine alterations in drug resistance.

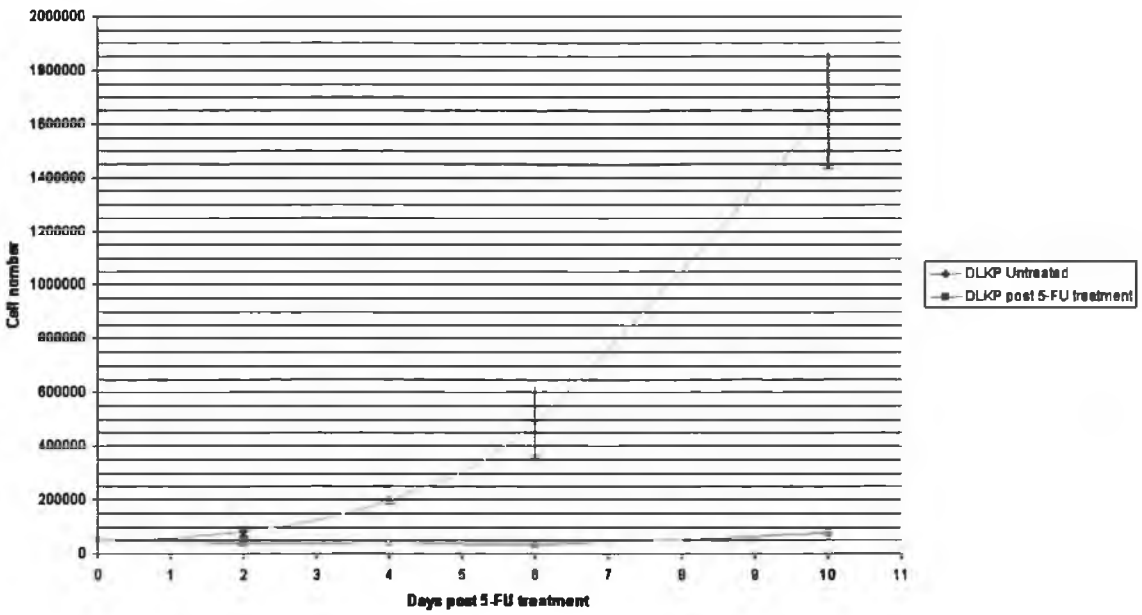

Figure 3.1.7: Growth curves of DLKP and DLKP post 5-FU treatment over a 10 day period (Gridline factor 50000).

DLKP appears to begin proliferating 6 days post 5-FU treatment. Thus toxicity assays may be set up after this time point in order to determine alterations in drug resistance.

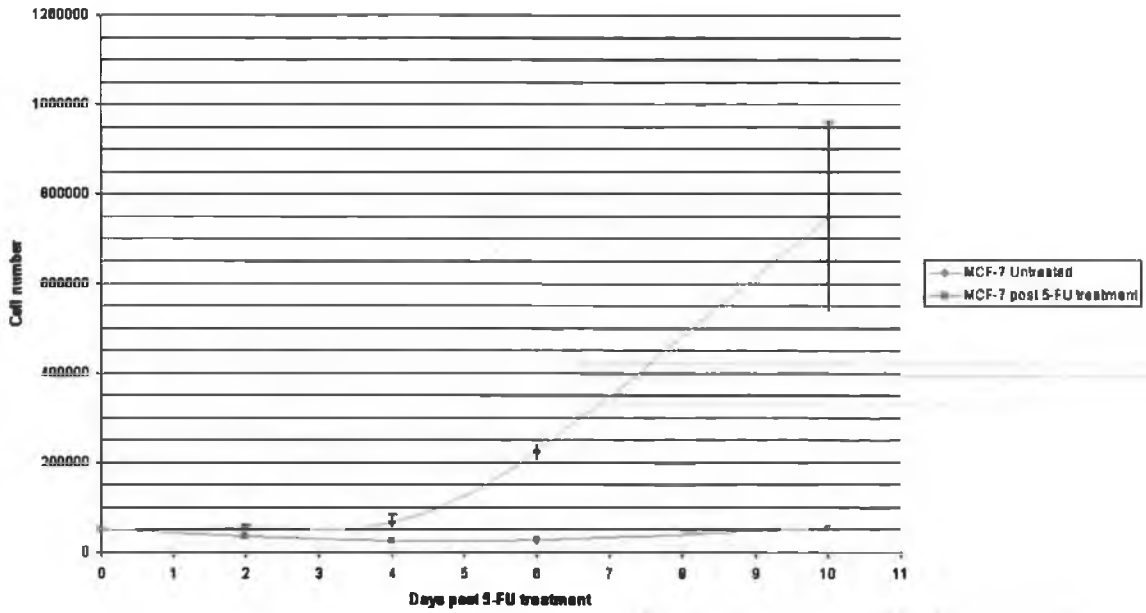

Figure 3.1.8: Growth curves of MCF-7 and MCF-7 post 5-FU treatment over a 10 day period (Gridline factor 50000).

MCF-7 appears to begin proliferating 6 days post 5-FU treatment. Thus toxicity assays may be set up after this time point in order to determine alterations in drug resistance.

Summary of growth curves during and post 5-FU treatment

Growth was inhibited between 80-90% in all cell lines by the concentration of 10μM. The normal cell lines of the breast and lung displayed higher tolerance in general when compared to the adenocarcinomas of the breast and lung. Due to this the 30μM treatment of normal cell lines was included in the proteomic analysis and invasion analysis post treatment where available in order to investigate the effect of similar toxicity. This would allow a comparison between between normal and cancer cells at similar toxicities. All cancer cell displayed recovery of cell growth at 7 days post treatment.

3.1.2 Altered adherence by 5-FU

Previous work performed using the other halogenated pyrimidines modulated the adherence profiles in DLKP and A549 to the ECM proteins collagen type IV, fibronectin and laminin (O' Callaghan, M., unpublished). Specifically BrdU was found to induce increased adherence in DLKP and A549 to these substrates and this found to induced by the post-transcriptional upregulation of α_2 and β_1 integrin subunits (Meleady, M., et al., 2001). Figures 3.1.9-11 shows that 5-FU effected the adherence profile in only A549. Specifically it induced increased adherence to collagen type IV and Laminin. Normal cells were not analysised due to the limited number of cells.

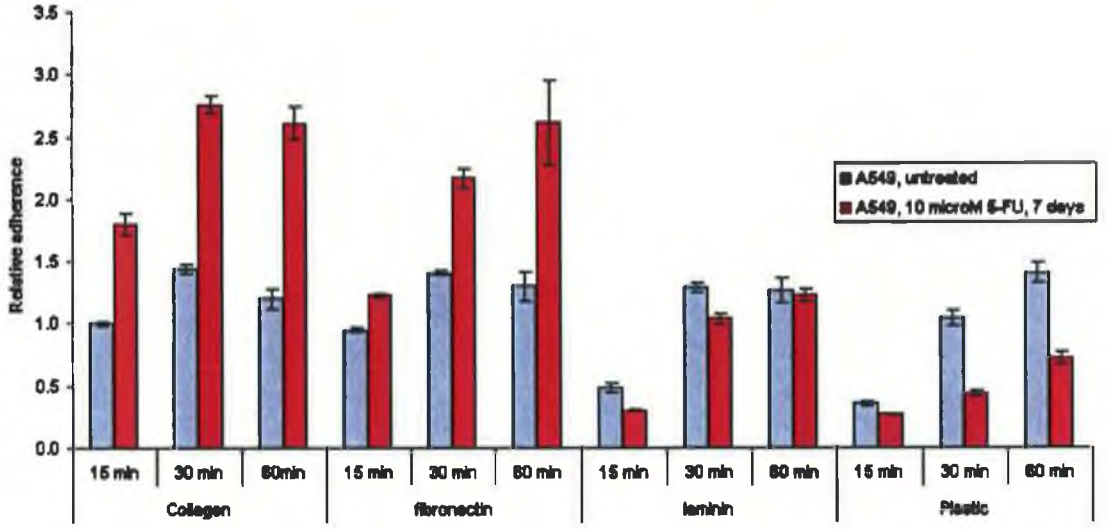

Figure 3.1.9: Adherence profile in A549 and A549 after 7 days exposure to 5-FU to the extracellular matrix proteins collagen type IV, Fibronectin and Laminin over a time period of 15, 30 and 60 minutes.

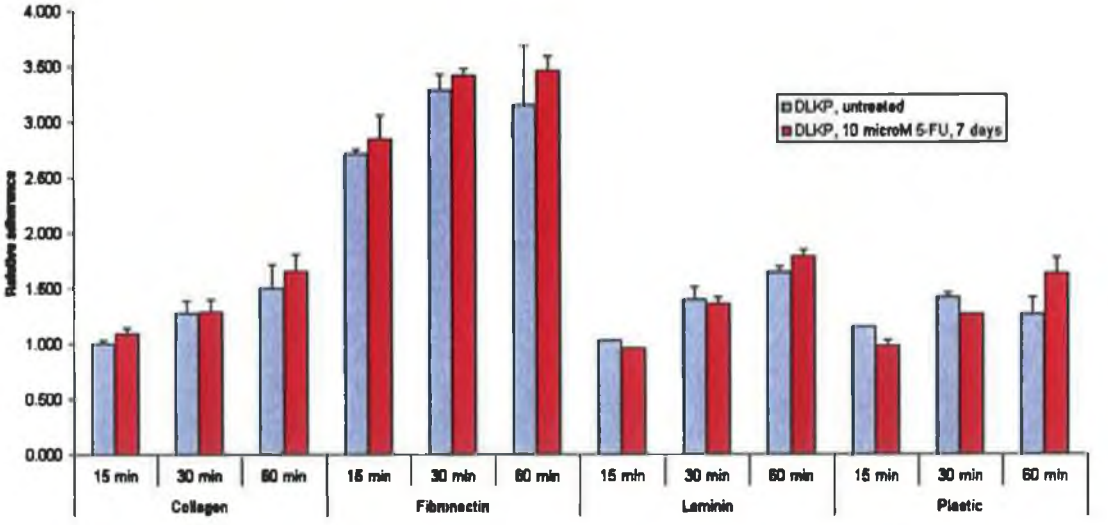

Figure 3.1.10: Adherence profile in DLKP and DLKP after 7 days exposure to 5-FU to the extracellular matrix proteins collagen type IV, Fibronectin and Laminin over a time period of 15, 30 and 60 minutes.

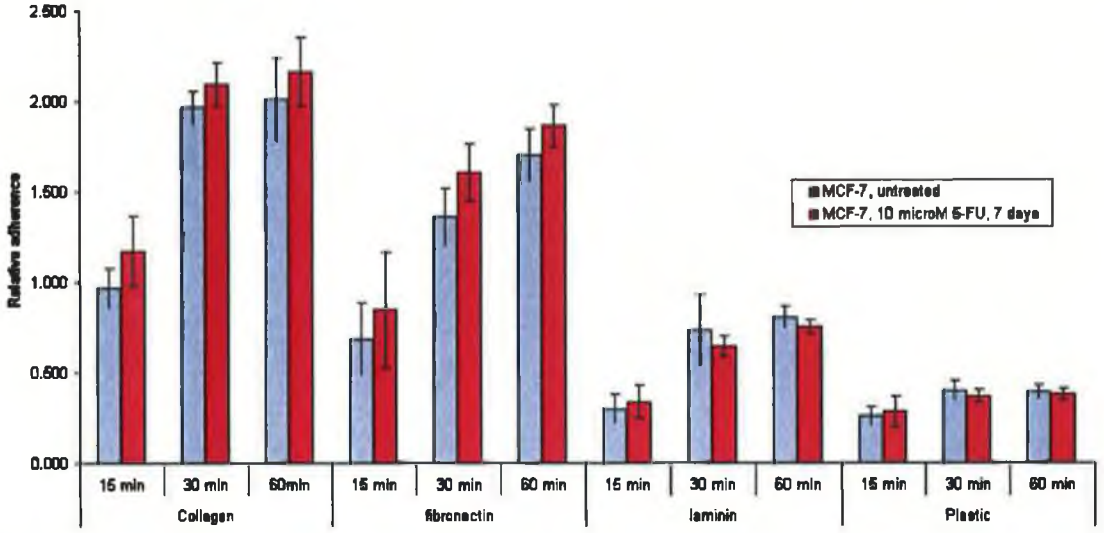

Figure 3.1.11: Adherence profile in MCF-7 and MCF-7 after 7 days exposure to 5-FU to the extracellular matrix proteins collagen type IV, Fibronectin and Laminin over a time period of 15, 30 and 60 minutes.

3.1.2 Altered drug resistance to 5-FU, 55FdU, Adr and BrdU post 5-FU exposure in the cell lines A549, DLKP and MCF-7.

In vitro experiments have demonstrated that exposure to 5-FU results in the short-term sensitisation to 5-FU (). In order to assess if 5-FU sensitisation occurs in this model, drug resistance was assessed up to 21 days post 5-FU exposure. The data in presented in table 3.1.1 and shows that A549 displays a resistance to halogenpyrimidines and a slight sensitisation to Adr by 7 days post treatment, by day 14 there is no significant differences in drug treatment and by day 21 post treatment there appears to be a significant resistance to Adr. DLKP shows a general sensitisation and may be a result of low proliferation rates at this time point as can be seen from figure 3.1.7, by 21 days post treatment DLKP displays a significant resistance to the fluoropyrimidines. MCF-7 shows a sensitisation to 5-FU but not to Adr which suggests that sensitisation is due to a drug specific mechanism. Normal cells were not assessed to due limited number of cells and due to associated problems of high doublings in normal cell lines.

In summary A549 shows a transient resistance to the fluoropyrimidines which is lost after 7 days post treatment, DLKP appear to show resistance to the fluoropyrimidines 21 days post treatment and MCF-7 shows a sensitisation to fluorouracil 14 days post treatment but has not been determined to be transient/stable. The fold changes are small al may not be significant.

Table 3.1.1: Drug resistance profiles in A549, DLKP and MCF-7 at specific time points post 5-FU exposure to chemotherapeutic and anti-metabolite drugs 5-FU, 55FdU, Adr and BrdU.

Cell line comparison	Days post treatment	Fold resistance to			
		5-FU	55FdU	Adr	BrdU
A549 5-FU treated/A549	7	1.220	2.000	0.741	2.016
t-test*		1.1×10^{-2}	3×10^{-4}	2.1×10^{-3}	1×10^{-2}
A549 5-FU treated/A549	14	0.966	1.348	1.070	0.831
t-test*		0.8	2.8 E-1	0.41	0.42
A549 5-FU treated/A549	21	0.987	1.512	1.400	1.024
t-test*		0.4	0.72	1.6×10^{-3}	6.3×10^{-3}
DLKP 5-FU treated/DLKP	7	0.554	0.332	0.580	0.383
t-test*		7.1×10^{-3}	1.3×10^{-3}	3.2×10^{-3}	9.2×10^{-3}
DLKP 5-FU treated/DLKP	14	1.237	1.690	1.088	1.592
t-test*		0.17	0.37	0.51	0.41
DLKP 5-FU treated/DLKP	21	1.389	1.887	1.033	0.987
t-test*		5.1×10^{-3}	1.1×10^{-3}	0.1	0.63
MCF-7 5-FU treated/MCF-7	14	0.528		1.293	
t-test*		5.5×10^{-5}		1.6×10^{-4}	

*t-test is performed on samples compared in above line and consists of 3 biological replicates.

3.1.3 Altered invasion post 5-FU exposure

Invasion assays were performed as described in materials and methods section 2.14. Assays were performed on untreated parental cells compared simultaneously to 5-FU treated cells at 0 and 7 days post 5-FU treatment. Invasion assays were performed over 24 and 48 hour incubation times. Normal cell lines (NHBE and HMEC) were only assessed at 0 days post treatment due to limited supply of cells. Data can be seen in figures 3.1.12 to 3.1.16.

Figure 3.1.12 Invasion assays performed on A549 and A549 post 5-FU treatment. (a) Average number of invading cells per field in A549 and A549 at specified time points post 5-FU treatment. Representative images of (b) untreated A549 invaded cells after 24 hours invasion assays compared to (c) simultaneous 24 hour invasion assay on A549 cells 0 days post treatment. Representative image of (d) untreated A549 invaded cells after 48 hours invasion assays compared to (e) simultaneous 48 hour invasion assay on A549 cells 0 days post treatment.

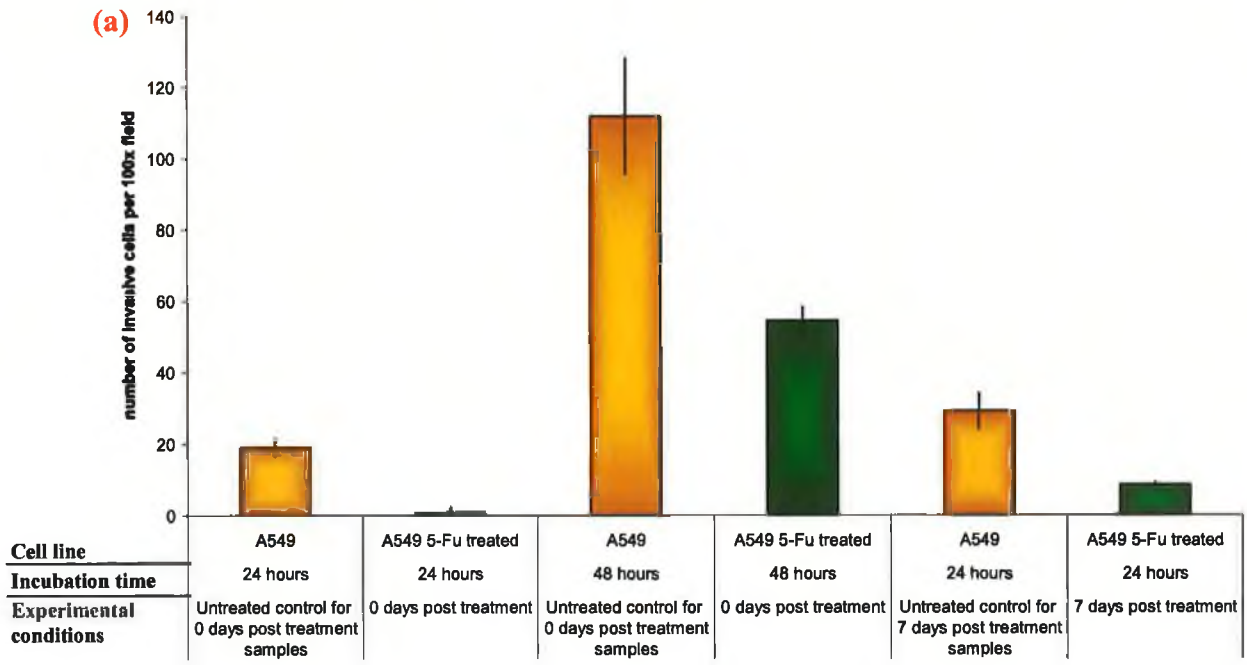

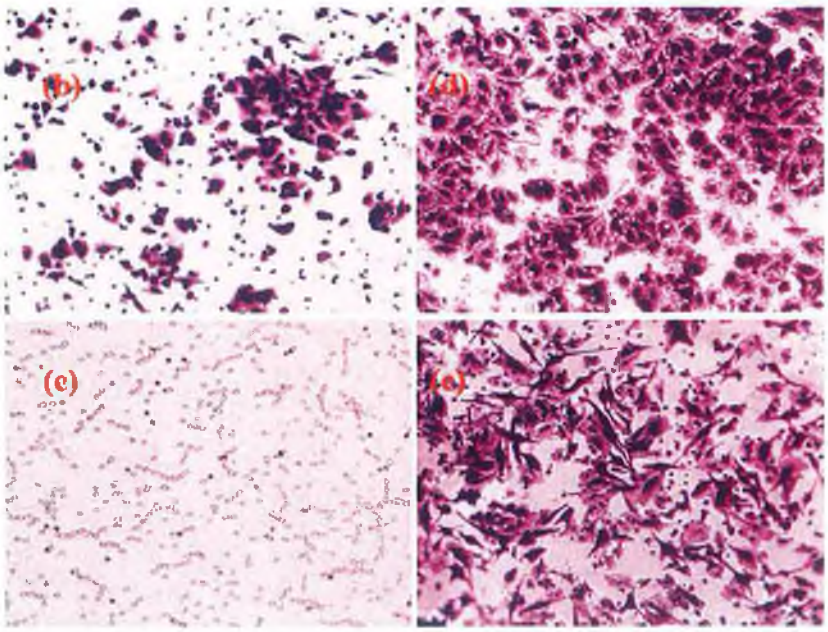

Figure 3.1.13 Invasion assays performed on DLKP and DLKP post 5-FU treatment. (a) A bar chart summarising the invasion trends between DLKP and DLKP at specified time points post 5-FU treatment. Representative images of (b) untreated DLKP invaded cells after 24 hours invasion assays compared to (c) simultaneous 24 hour invasion assay on A549 cells 0 days post treatment.

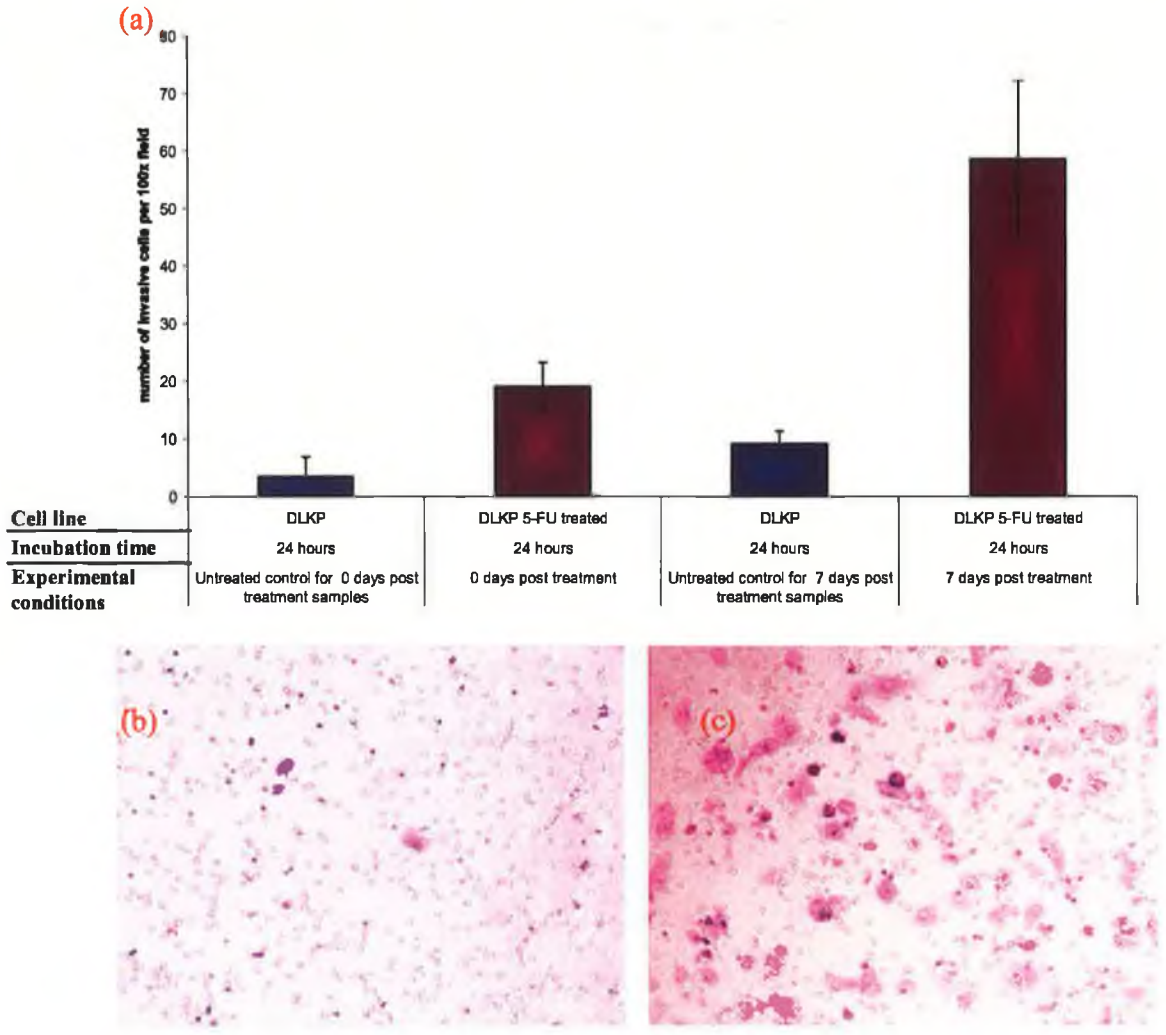

Figure 3.1.14 Invasion assays performed on NHBE and NHBE post 5-FU treatment. (a) Average number of invading cells per field in NHBE and NHBE at specified time points post 5-FU treatment. Representative images of (b) untreated NHBE invaded cells after 48 hours invasion assays compared to (c) simultaneous 48 hour invasion assay on NHBE cells 0 days post treatment.

(a)

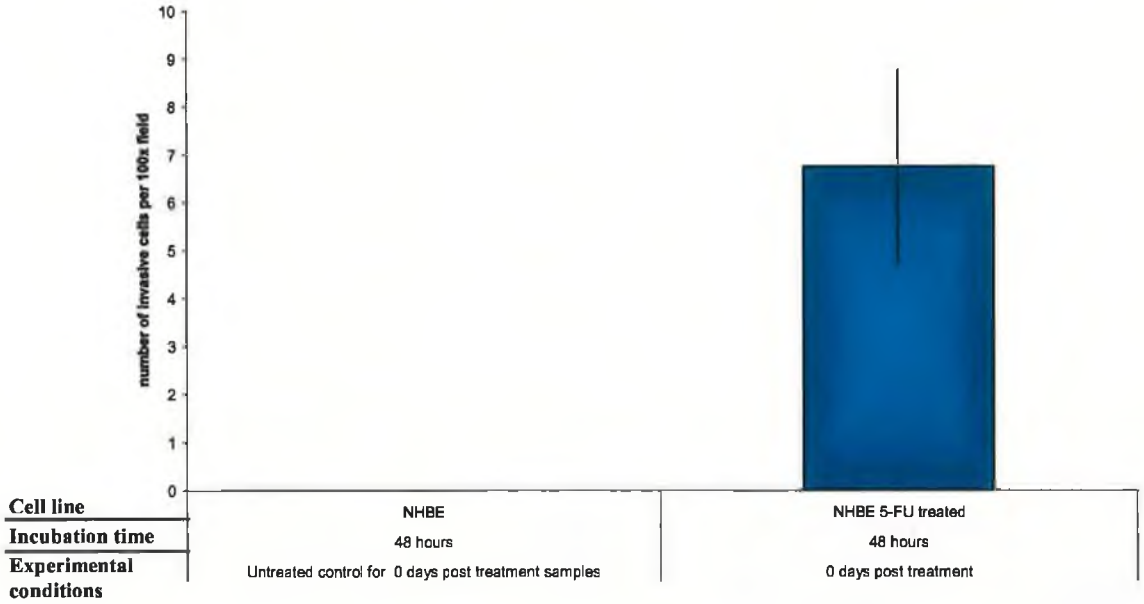

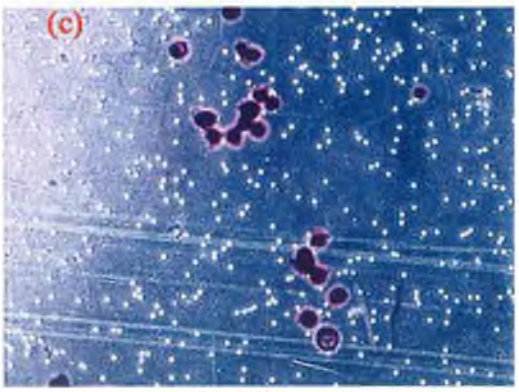

Figure 3.1.15 Invasion assays performed on MCF-7 and MCF-7 post 5-FU treatment. (a) Average number of invading cells per field in MCF-7 and MCF-7 at specified time points post 5-FU treatment. Representative images of (b) untreated MCF-7 invaded cells after 24 hours invasion assays compared to (c) simultaneous 24 hour invasion assay on MCF-7 cells 0 days post treatment. Representative image of (d) untreated MCF-7 invaded cells after 72 hours invasion assays compared to (e) simultaneous 72 hour invasion assay on MCF-7 cells 0 days post treatment.

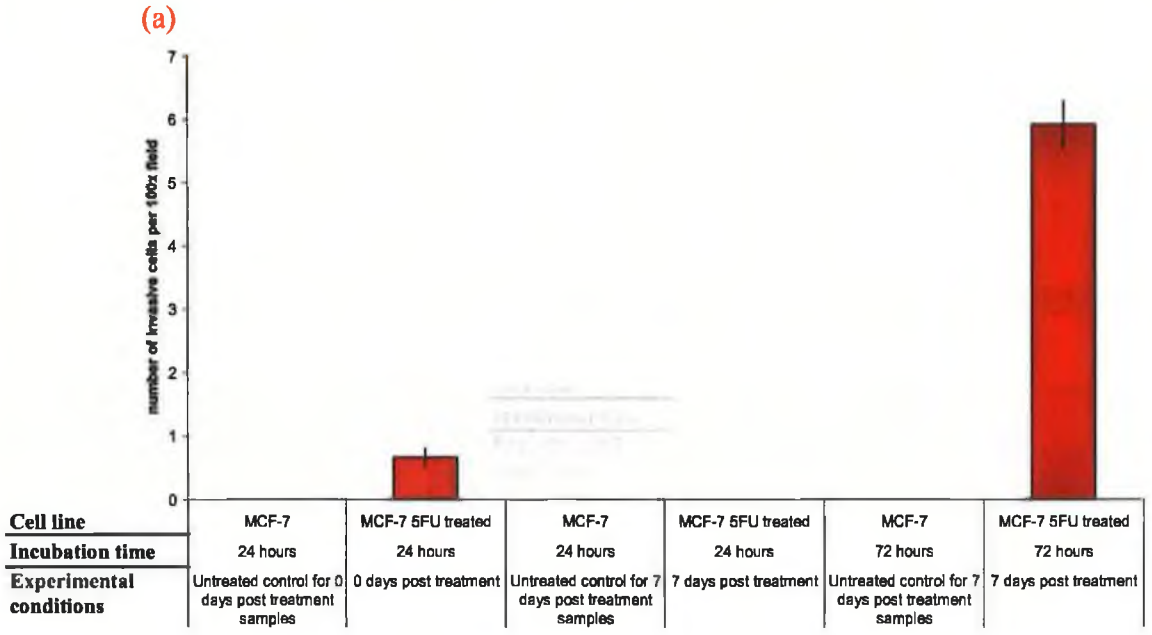

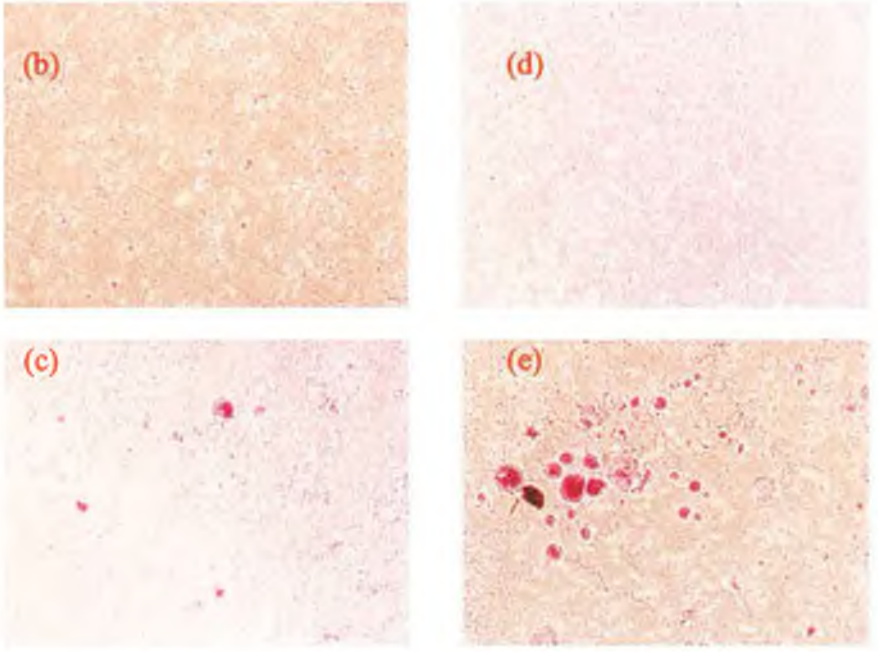

Figure 3.1.16 (a) Bar chart demonstrating apparent altered invasion rates in A549 post 5-FU exposure, (b) image of invaded cells from HMEC after 48 hour incubation, (c) image of invasive cells from HMEC 0 days post 5-FU exposure after 24 hour incubation time, (d) image of invaded cells from HMEC after 48 hour incubation,

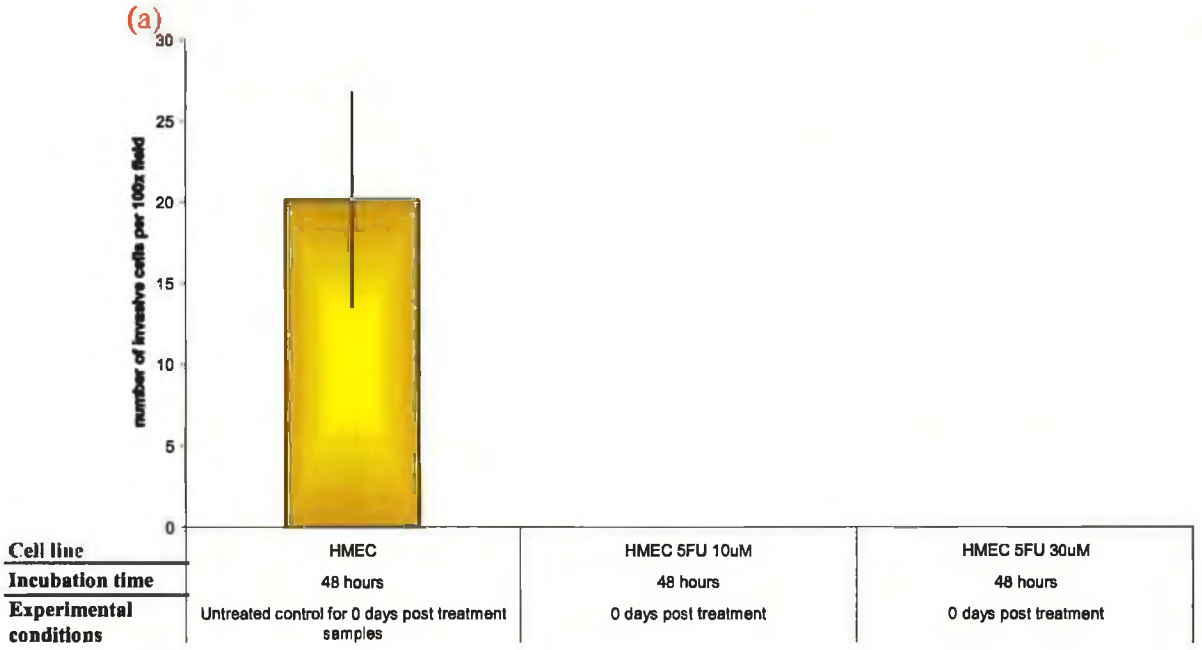

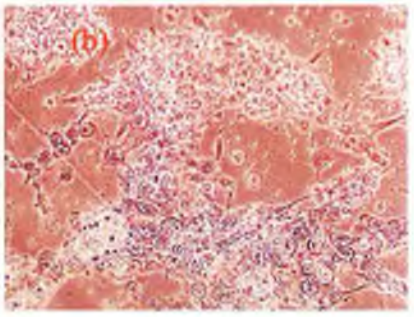

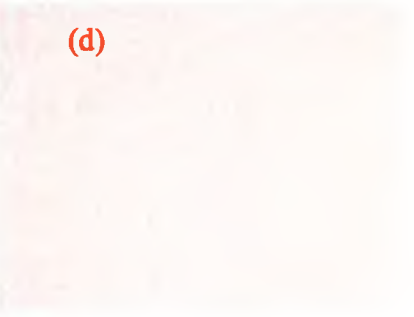

Summary of invasion assays

Table 3.1.2: summary of invasion trends with t-test performed on each analysis showing data to be highly significant

Cell line comparison	Incubation time	Experimental conditions	Fold change in number of invading cells	T-test score (p value =)
A549 10μM 5-FU treated / A549 N=3	24 hours	0 days post treatment	-21 (n=3)	$4.2x10^{-16}$
A549 10μM 5-FU treated / A549 N=3	48 hours	0 days post treatment	-2.1 (n=3)	$2x10^{-11}$
A549 10μM 5-FU treated / A549 N=3	24 hours	7 days post treatment	-3.4 (n=3)	$1.3x10^{-14}$
DLKP 10μM 5-FU treated / DLKP N=3	24 hours	0 days post treatment	5.4 (n=3)	$3.5x10^{-9}$
DLKP 10μM 5-FU treated / DLKP N=3	24 hours	7 days post treatment	6.3 (n=3)	$3.9x10^{-13}$
NHBE 10μM 5-FU treated / NHBE N=3	48 hours	0 days post treatment	Apparent induction of invasive phenotype (n=3)	0*
MCF-7 10μM 5-FU treated / MCF-7 N=3	48 hours	0 days post treatment	Apparent induction of invasive phenotype (n=3)	0*
MCF-7 10μM 5-FU treated / MCF-7 N=3	24 hours	0 days post treatment	1 (n=3)	0*
MCF-7 10μM 5-FU treated / MCF-7 N=3	72 hours	7 days post treatment	Apparent induction of invasive phenotype (n=3)	0*
HMEC 10μM 5-FU treated / HMEC N=3	48 hours	0 days post treatment	Apparent loss of invasive phenotype (n=3)	0*
HMEC 30μM 5-FU treated/HMEC N=3	48 hours	0 days post treatment	Apparent loss of invasive phenotype (n=3)	0*

*This data showed a change from the base line 0 and thus T-test can not be performed on this data but would indicate a 100% confidence in result or a p value of 0.

Invasion assays data presented in figures 3.1.12-16 indicate that MCF-7 and NHBE become invasive as a result of exposure to 5-FU. DLKP invasion rate increases 5 to 6 fold as a result of exposure to 5-FU while HMEC and A549 display apparent decreases of invasion rates.

3.1.4 Investigation of adherence related proteins.

Integrin are important membrane proteins and play a role in communicating to cell its extracellular environment and interactions with the cell and its extracellular environment. Integrins cluster together to form focal contacts and stimulate signal transduction through recruitment of the focal adherence kinase (FAK) and autophosphorylation which can lead to activation of ERK, MAPK, Src and regulation of G-proteins such as rho which play important roles in cell migration.

Syndecans play important roles in cell contractility and are important in stromatogenesis and tissue repair. Regulation of actin dynamics is poorly described by the syndecans but they are involved in regulating of proteins such as rho – a GTPase responsible for regulating actin dynamics (Irie, *et al.*, 2004).

Specifically the integrin subunits β_1, α_2, and α_5 and syndecan 2 were investigated.

Figure 3.1.17: Western Blot for the presence of the integrin subunit α_2 in DLKP and DLKP treated with the fluorouracil for 4 and 7 days (10μg of protein per lane).

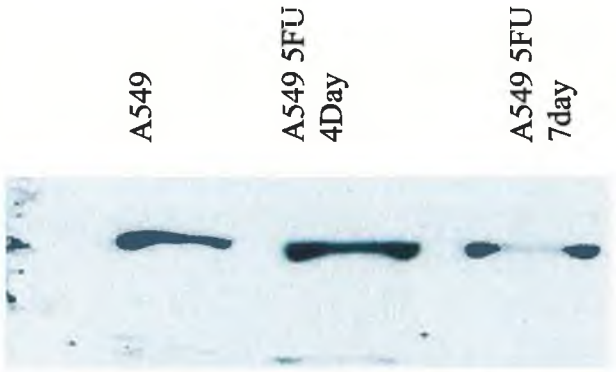

Figure 3.1.18: Western Blot for the presence of the integrin subunit α_2 in A549 and A549 treated with 5-fluorouracil for 4 and 7 days (10μg of protein per lane).

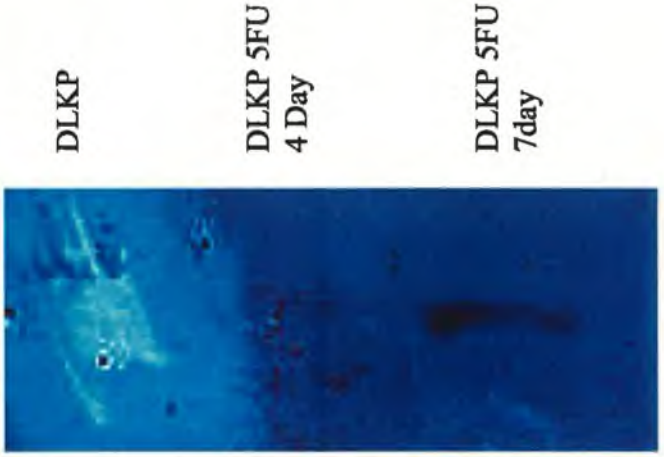

Figure 3.1.19: Western Blot for the presence of the integrin subunit α_5 in DLKP and DLKP treated with the fluorouracil for 4 and 7 days (10µg of protein per lane).

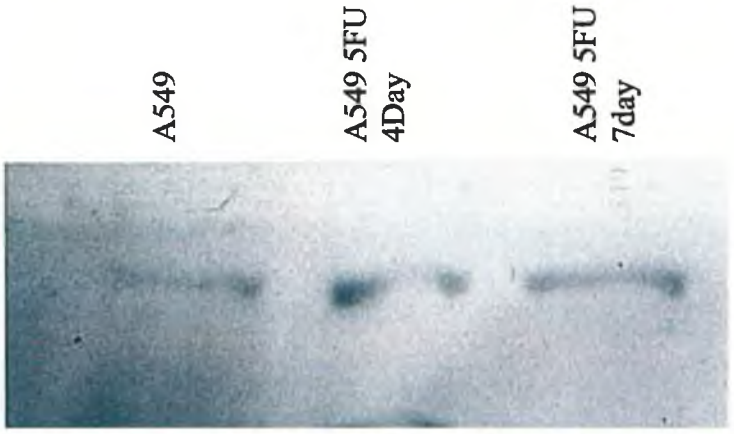

Figure 3.1.20: Western Blot for the presence of the integrin subunit α_5 in A549 and A549 treated with 5-fluorouracil for 4 and 7 days (10µg of protein per lane).

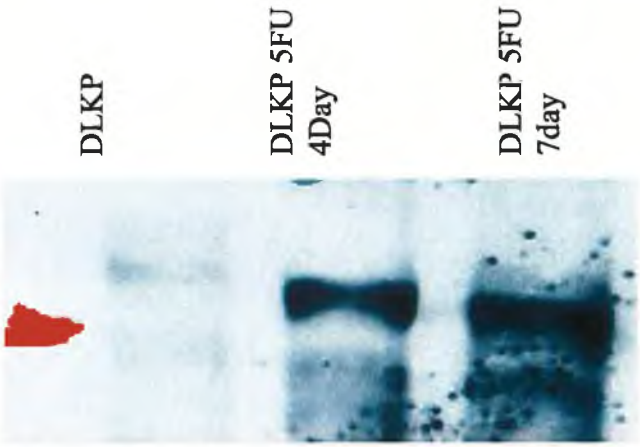

Figure 3.1.21: Western Blot for the presence of the integrin subunit β_1 in DLKP and DLKP treated with the fluorouracil for 4 and 7 days (10μg of protein per lane).

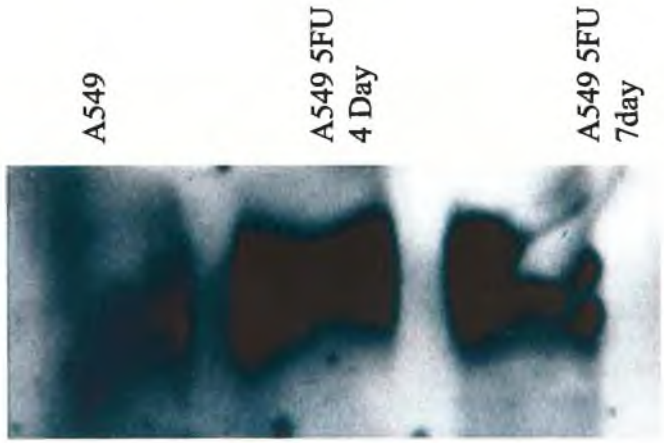

Figure 3.1.22: Western Blot for the presence of the integrin subunit β_1 in A549 and A549 treated with the fluorouracil for 4 and 7 days (10μg of protein per lane).

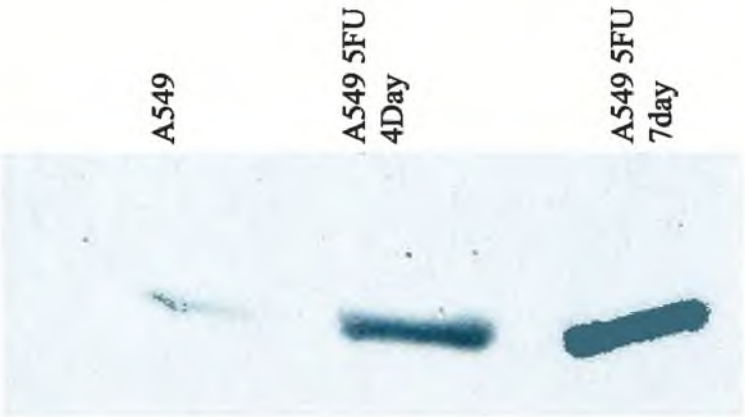

Figure 3.1.23: Western Blot for the presence of adherence related protein syndecan-2 in A549 and A549 treated with 5-fluorouracil for 4 and 7 days (10µg of protein per lane).

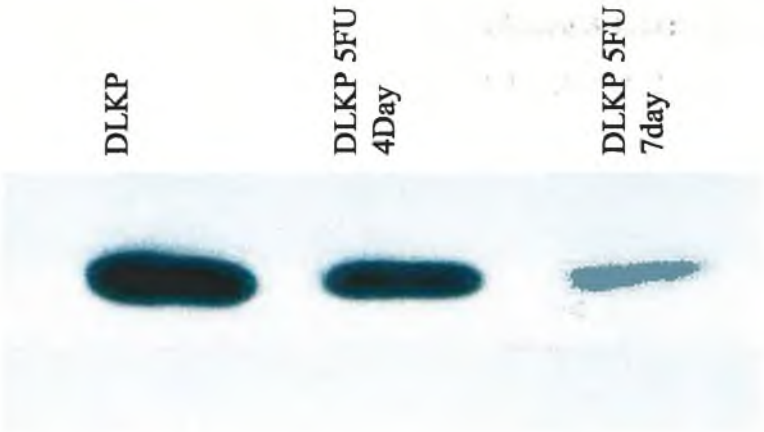

Figure 3.1.24: Western Blot for the presence of adherence related protein syndecan-2 in DLKP and DLKP treated with 5-fluorouracil for 4 and 7 days (10µg of protein per lane).

Investigation of the integrin subunits β_1, α_2, and α_5 and syndecan-2 reveal an up regulation of the integrin subunits β_1, α_2, and α_5 and a down regulation of syndecan-2 in DLKP treated with 5-FU, while in A549 treated with 5-FU the integrin subunits β_1, and α_5, and syndecan-2 are up regulated while the integrin subunit α_2 is down regulated.

The integrin subunits β_1 forms a dimer with α_2, and α_5 integrin subunits. The formation of a dimer allows selective binding to ECM proteins and allow binding of actin filaments via connecting proteins. The formation of integrin dimers contribute to various signal transduction cascades that can inhibit apoptosis, promote motility and the secretion of matrix metaloproteases involved in invasion. Further more integrin signalling in combination with growth factor signalling is required for progression from G1 to S phase of the cell cycle (*Damsky et al. 2002*). Syndecan-2 forms a trimer with $\beta_1\alpha_5$ integrin dimer and promotes binding to Fibronectin, its increased expression was found to reduce invasion (Kusano et al. 2004). Thus the alterations observed in $\beta_1\alpha_5$ integrin dimer in combination with sydecan-2 are important for the regulation of the altered invasion rates. Further more increased expression of syndecan-2 in combination with $\beta_1\alpha_5$ integrin was found to promote stress fiber formation and adherence to fibronectin (Kusano et al. 2000). Thus this expression trend would explain the increased adherence to the the ECM proteins collagen type IV and fibronectin and decreased invasion rate observed in A549 treated with 5-FU and the increased invasion rates observed in DLKP. It is likey that 5-FU induces stress fiber formation in A549 but not in DLKP and that signalling from the $\beta_1\alpha_5$ integrin dimer promotes motility in DLKP.

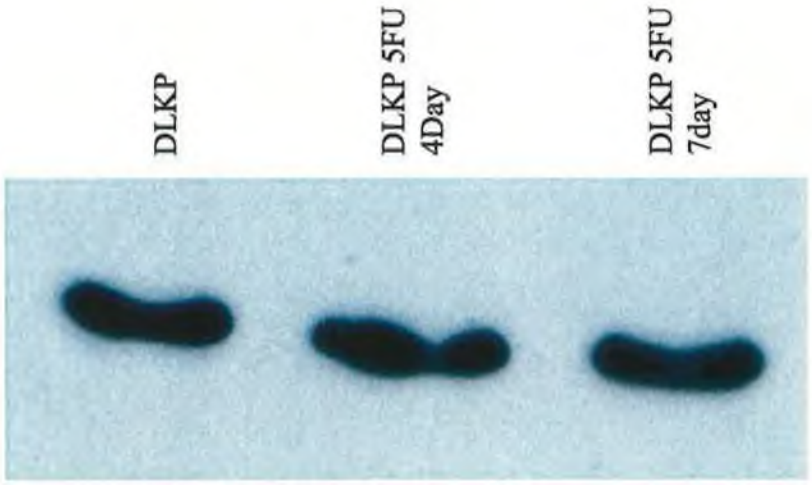

Figure 3.1.25: Western Blot for the presence of endogenous control GAPDH in DLKP and DLKP treated with fluorouracil for 4 and 7 days (10μg of protein per lane).

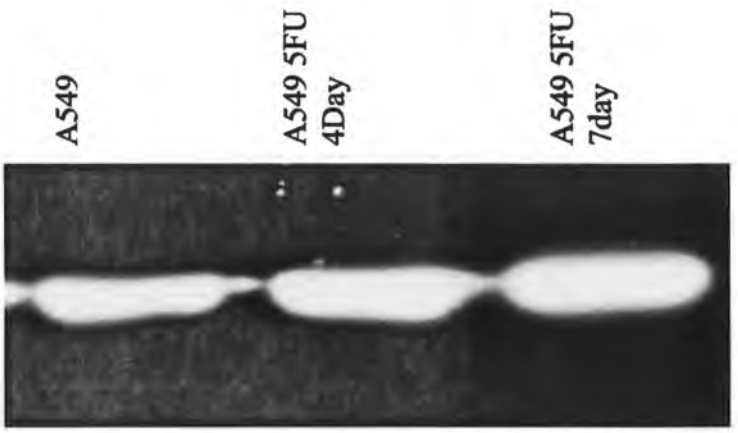

Figure 3.1.26: Western Blot for the presence of endogenous control GAPDH in A549 and A549 treated with the fluorouracil for 4 and 7 days (10μg of protein per lane).

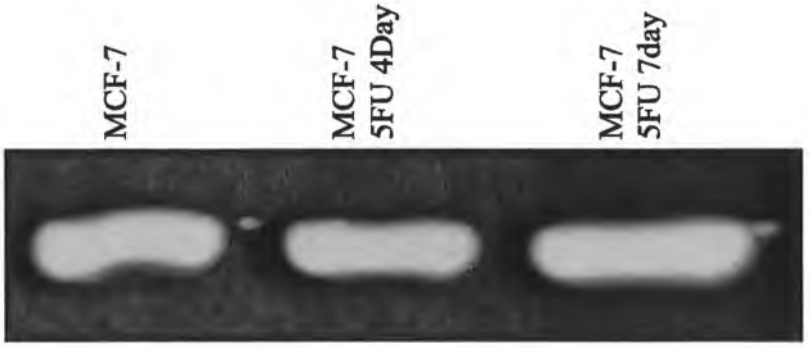

Figure 3.1.27: Western Blot for the presence of endogenous control GAPDH in MCF-7 and MCF-7 treated with the fluorouracil for 4 and 7 days (10μg of protein per lane).

3.1.5 Investigation of p53 expression

The tumour suppression protein p53 is induced by DNA lesions or genotoxic stress as described in section 1.0. The accumulation of p53 suggests detection of DNA lesions, cell cycle arrest and may suggest p53 mediated transcription.

Figures 3.1.28: Expression of p53 in A549 after 4 and 7 days exposure to 5-FU

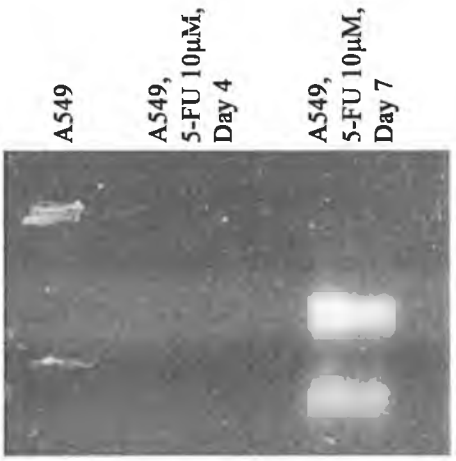

Figures 3.1.29: Expression of p53 in DLKP after 4 and 7 days exposure to 5-FU

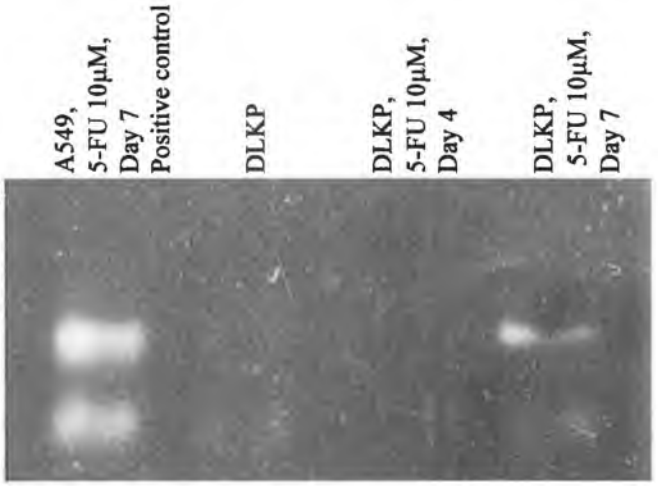

Figures 3.1.31: Expression of p53 in NHBE after 7 days exposure to 10μM 5-FU

Figures 3.1.30: Expression of p53 in MCF-7 after 4 and 7 days exposure to 5-FU

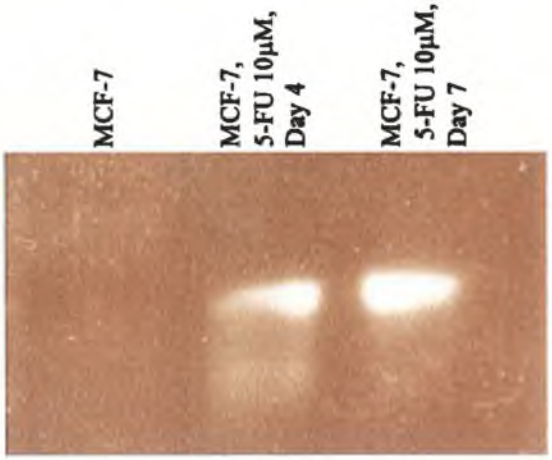

Figures 3.1.31: Expression of p53 in HMEC after 7 days exposure to 10μM 5-FU

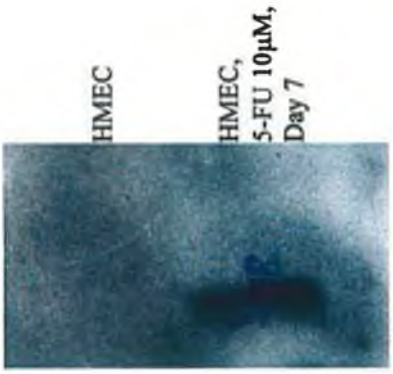

The accumulation of p53 was observed in all cell lines with the exception of NHBE. The accumulation of p53 suggests incorporation of 5-FU derivates into DNA, the formation of DNA lesions and activation of ATR/ATM pathway leading to phosphorylation of p53 and localisation to the nucleus. In NHBE p53 was not observed to increase and suggests that the normal cell line NHBE is tolerant to 5-FU even though its growth rate was inhibited by 80% at both 10 and 30μM. However due to limited sample p53 expression was not assessed in NHBE treated with 30μM 5-FU.

3.1.6 Investigation of the epithelial markers Keratin 8 and 18

The intermediate filament proteins Keratin 8 and 18 were generally found to accumulate as a result of halogenated pyrimidine treatment in DLKP and A549 (McMorrow J, Ph.D. thesis, 2004, O' Sullivan F, Ph.D. thesis 1999). Keratin 8/18 pair are hallmarks of simple epithelial cells (*Gilbert et al. 2004*). Thus this data would suggest that the halogenated pyrimidines promote epithelial differentiation. Further more Keratin 8 and 18 been shown to promote invasion although the exact role in invasion is not clear it is believed to induce alteration in cytoskeletal architecture through the induction of integrin expression and resulting signal transductions (*Chu et al. 1996*).

Figures 3.1.32: Expression of Keratin 8 in A549 after 4 and 7 days exposure to 5-FU

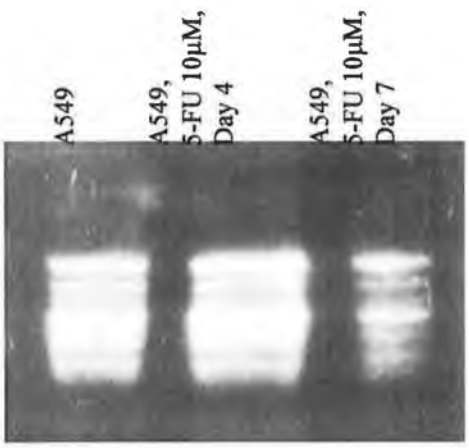

Figures 3.1.33: Expression of Keratin 8 in DLKP after 4 and 7 days exposure to 5-FU

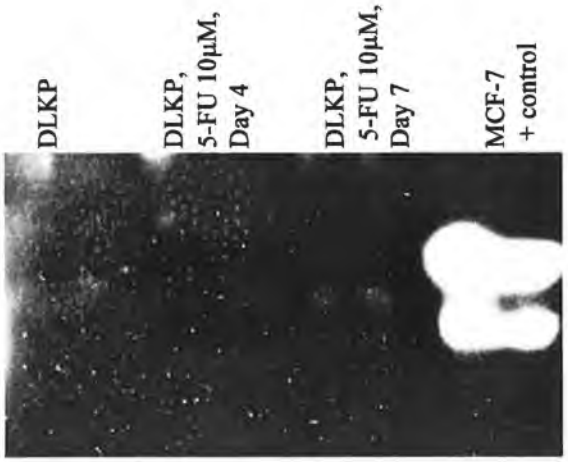

Figures 3.1.34: Expression in of Keratin 8 MCF-7 after 4 and 7 days exposure to 5-FU

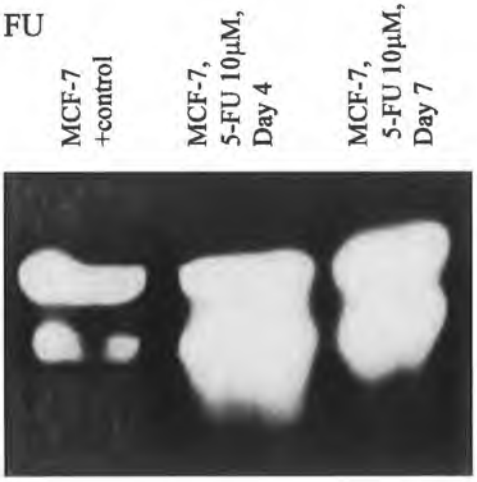

Figures 3.1.35: Expression of keratin 18 in A549 after 4 and 7 days exposure to 5-FU

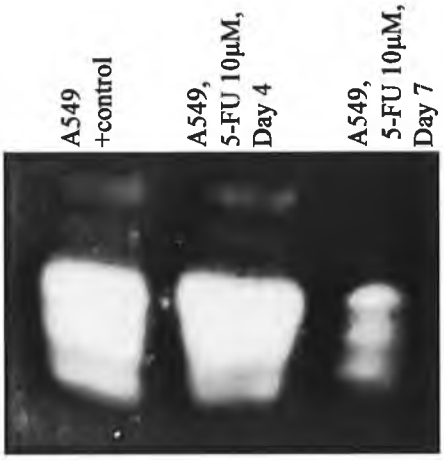

Figures 3.1.36: Expression of keratin 18 in DLKP after 7 days exposure to 5-FU

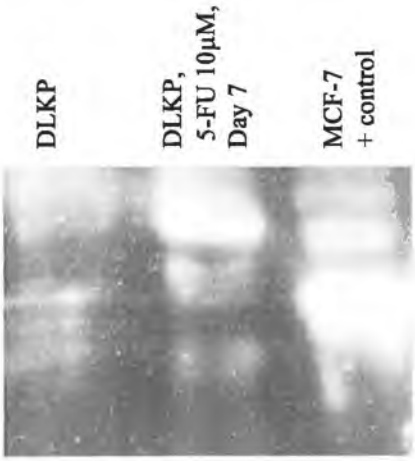

Figures 3.1.37: Expression of Keratin 18 in MCF-7 after 4 and 7 days exposure to 5-FU

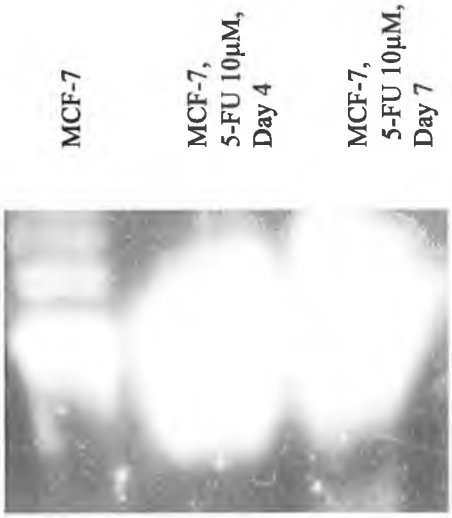

The simple epithelial markers keratin8/18 were found to accumulate in DLKP and MCF-7 while in A549 they were found to decrease. The expression of keratin 8/18 correlates with altered invasion in DLKP, MCF-7and A549 and this data supports a role for keratins in the 5-FU regulation of invasion.

Table 3.1.3: Summary of western blots on the cell lines A549, DLKP, NHBE, MCF-7 and HMEC treated with 5-FU investigating expression of adherence related proteins – integrins and sdc-2-, actin organisation regulating protein – Rho-, intermediate filament proteins keratin 8 and 18, and the genotoxicity related protein p53.

Protein	A549	DLKP	NHBE	MCF-7	HMEC
α_2 integrin	↑	↓	?	?	?
α_5 integrin	↑	↑	?	?	?
β_1 integrin	↑	↑	?	?	?
Sdc-2	↑	↓	?	?	?
KRT8	↓	↑	?	↑	?
KRT18	↓	↑	?	↑	?
p53	↑	↑	-	↑	↑

↑ upregulation, ↓down regulation, - no change, ? not determined

The expression of rho correlated with invasion trends and suggests actin dynamics are important in the regulation of invasion alterations induced by 5-FU treatment. Keratin 8 and 18 regulation and sdc-2 also correlate with invasion and suggest epithelial differentiation is important in invasion. Sdc-2 and integrin subunits in lung cancer cell lines appear to correlate with invasion and suggest a role in regulation of rho and invasion. p53 expression does not correlate with invasion and suggests that its regulation is not a determinant in promoting invasion although can indirectly inhibit invasion through induction of apoptosis.

3.1.7 Proteomic analysis of A549 post 5-FU exposure

As already stated, investigation of the proteomic alterations induced by 5-FU treatments are poorly described in the literature and no studies have been performed on lung cell lines. Investigation of the proteomic alterations induced by 5-FU treatment of A549 may indicate pathways and biological processes activated by 5-FU that would contribute to the understanding of the anti-metabolites mode of action. Furthermore, in conjunction with invasion data presented above an insight into the mechanisms that control alteration in invasion would be elucidated. Finally, identification of proteins involved in the inhibition of apoptosis would lead to the development of drugs that would target such pathways and perhaps lead to enhanced future therapies.

To achieve these goals protein analysis was carried out using 2D-DIGE, phosphorylated proteins were identified using a phosphospecific fluorescent stain called Pro-Q Diamond. Differentially regulated proteins were identified using MALDI-ToF MS.

Cell culture of A549 and A549 treated with 5-FU was carried out as described in section 2.7.3. Total protein extractions were prepared as described in 2.17. These were prepared in biological triplicate. Each biological triplicate was run in technical duplicates. Sample labelling with Cy dyes is shown in table 3.1.3. Differentially regulated proteins were identified statistically important using the following filters. A fold change less than minus 1.2 or greater than plus 1.2 with a t-test score less than 0.01 was deemed significant or a fold change less than minus 1.5 or greater than plus 1.5 with a t-test less than 0.05 was deemed significant. These filters revealed 186 proteins differentially regulated between A549 and A549 treated with 5-FU of which 71 were identified.

Preparative gels for protein identification were prepared as described in sections 2.21-25. Differentially regulated proteins were identified using MALDI-ToF MS as described in section 2.27. Of the 296 proteins differentially regulated 56 proteins were identified. Identified differentially regulated proteins locations are indicated in figure

3.1.25 and figure 3.1.26 displays the number of differentially regulated proteins identified and ontological data on these proteins. The identity of these proteins can be seen in table 3.1.4. Proteins identification data from MALDI-ToF MS is included in the appendices.

Table 3.1.4: Ettan DIGE experimental design for the analysis of differential protein expression induced in A549 by exposure to 5-FU for 7 days.

Gel number	CY2 label	CY3 label	CY5 label
1	Pooled internal standard (50µg of protein)	A549, P.14 (50µg of protein)	A549, P. 14, 5-FU treated (50µg of protein)
2	Pooled internal standard (50µg of protein)	A549, P.14 (50µg of protein)	A549, P. 14, 5-FU treated (50µg of protein)
3	Pooled internal standard (50µg of protein)	A549, P. 15 (50µg of protein)	A549, P. 15, 5-FU treated (50µg of protein)
4	Pooled internal standard (50µg of protein)	A549, P. 15 (50µg of protein)	A549, P. 15, 5-FU treated (50µg of protein)
5	Pooled internal standard (50µg of protein)	A549, P. 16 (50µg of protein)	A549, P. 16, 5-FU treated (50µg of protein)
6	Pooled internal standard (50µg of protein)	A549, P. 16 (50µg of protein)	A549, P. 16, 5-FU treated (50µg of protein)

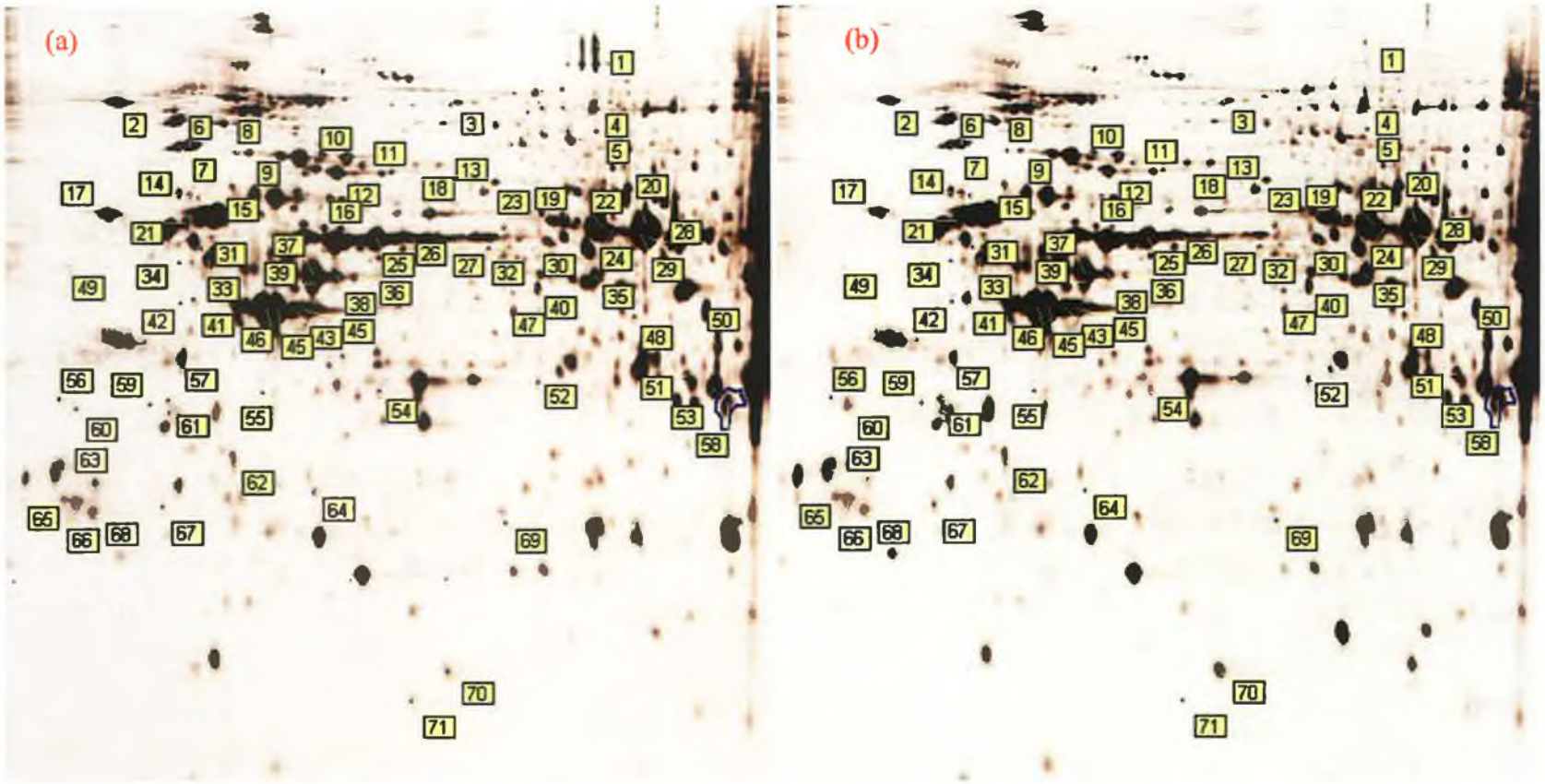

Figure 3.1.43: 2D-DIGE images of A549 (CY3) and A549 after 7 days treatment with 10μM 5-FU (CY5). Identified differentially regulated protein spots are encircled by blue lines and are given a protein number. Refer to table 3.1.13.1.2 for protein identification.

Figure 3.1.44: A pie chart demonstrating the number of differentially regulated proteins in each biological process identified in A549 treated with 5-FU. Individual proteins in each biological process are included in table 3.1.4. Biological process information obtained from the human protein reference database. Some well described proteins are represented in the database as unknown, there actual names are included.

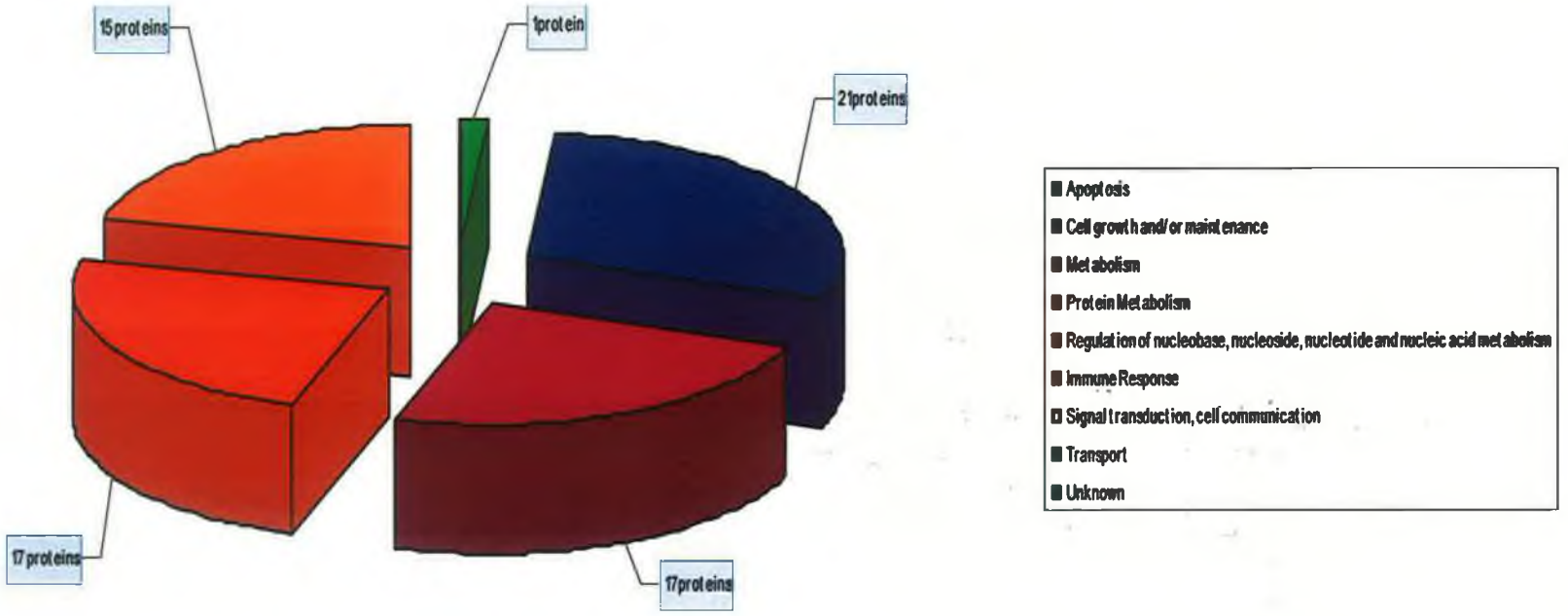

Table 3.1.4: List of differentially expressed proteins in A549 treated with 5-FU. Proteins names that are unknown were identified as described in section 2.16.13.3, names are included.

Protein location	GI accession Number	Gene symbol	Name	Fold Change	T-test	Molecular function
Apoptosis						
4	gi|30583573|	PDCD6IP	programmed cell death 6 interacting protein [Homo sapiens]	1.64	1.9x10-5	Unknown
Cell growth and/or maintainance						
32	gi|16924319|	ACTB	Unknown (protein for IMAGE:3538275) [Homo sapiens] β-actin	1.8	5.6 x10-5	structural molecule activity
46	gi|16924319|	ACTB	Unknown (protein for IMAGE:3538275) [Homo sapiens] β-actin	1.66	3.7 x10-4	structural molecule activity
44	gi|62897625|	ACTB	beta actin variant [Homo sapiens]	1.49	1.3 x10-3	structural molecule activity
43	gi|62897671|	ACTB	beta actin variant [Homo sapiens]	1.5	1.1 x10-4	structural molecule activity
45	gi|62897671|	ACTB	beta actin variant [Homo sapiens]	1.34	8.7 x10-4	structural molecule activity
38	gi|12653819|	KRT18	Keratin 18 [Homo sapiens]	-1.51	3.5 x10-4	structural molecule activity
33	gi|30311|	KRT18	cytokeratin 18 (424 AA) [Homo sapiens]	-1.58	1.5 x10-4	structural molecule activity
39	gi|30311|	KRT18	cytokeratin 18 (424 AA) [Homo sapiens]	-2.04	4.0 x10-5	structural molecule activity
37	gi|62897747|	KRT18	keratin 18 variant [Homo sapiens]	-1.56	1.5 x10-4	structural molecule activity
41	gi|24234699|	KRT19	keratin 19 [Homo sapiens]	3.22	7.2 x10-6	structural molecule activity
42	gi|24234699|	KRT19	keratin 19 [Homo sapiens]	2.55	1.9 x10-2	structural molecule activity
26	gi|33875698|	KRT8	KRT8 protein [Homo sapiens]	-2.16	4.1 x10-2	structural molecule activity
25	gi|62913980|	KRT8	KRT8 protein [Homo sapiens]	-2.15	3.4 x10-2	structural molecule activity
8	gi|5031877|	LMNB1	lamin B1 [Homo sapiens]	-1.74	6.6 x10-3	structural molecule activity
9	gi|50415798|	LMNB1	LMNB1 protein [Homo sapiens]	-2.17	1.2 x10-2	structural molecule activity
58	gi|41223219|	PCDH11X	protocadherin [Homo sapiens]	2.68	3.5 x10-3	Cell adhesion molecule activity
71	gi|5031851|	STMN1	stathmin 1 [Homo sapiens]	-5.07	1.5 x10-8	cytoskeletal protein binding
60	gi|88928|	TPM3	tropomyosin 3, fibroblast - human	2.29	6.6 x10-3	cytoskeletal protein binding
63	gi|4507651|	TPM4	tropomyosin 4 [Homo sapiens]	1.61	2.1 x10-3	cytoskeletal protein binding
15	gi|14389309|	TUBA6	tubulin alpha 6 [Homo sapiens]	1.64	3.2 x10-3	structural molecule activity
21	gi|62897639|	TUBB3	tubulin, beta, 4 variant [Homo sapiens]	1.51	4.2 x10-3	structural molecule activity
Metabolism; Energy pathway						
50	gi|62738430|	AKR1B1	Chain A, Apo R268a Human Aldose	2.38	6.7 x10-4	Oxidoreductase activity

			Reductase			
53	gi|62738430|	AKR1B1	Chain A, Apo R268a Human Aldose Reductase	2.52	4.0 x10-4	Oxidoreductase activity
24	gi|178400|	ALDH1A1	aldehyde dehydrogenase 1 (EC 1.2.1.3)	1.63	7.7 x10-3	Catalytic activity
20	gi|2183299|	ALDH1A1	aldehyde dehydrogenase 1 [Homo sapiens]	1.73	5.0 x10-2	Catalytic activity
30	gi|283971|	ALDH3A1	aldehyde dehydrogenase [NAD(P)] (EC 1.2.1.5) 3 - human	1.87	1.8 x10-5	Catalytic activity
22	gi|30583043|	ALDH3A1	aldehyde dehydrogenase 3 family, memberA1 [Homo sapiens]	2.55	1.4 x10-3	Catalytic activity
1	gi|219553|	CPS1	carbamyl phosphate synthetase I [Homo sapiens]	-6.38	1.3 x10-4	Ligase Activity
27	gi|643589|	DLST	dihydrolipoamide succinyltransferase [Homo sapiens]	-1.9	3.4 x10-2	Acetyltransferase activity
29	gi|30582259|	DARS	aspartyl-tRNA synthetase [Homo sapiens]	1.48	3.9 x10-2	ATPase activity
28	gi|26224874|	G6PD	glucose-6-phosphate dehydrogenase [Homo sapiens]	1.47	1.6 x10-2	Catalytic activity
3	gi|577295|	GANAB	KIAA0088 [Homo sapiens]	2.14	1.9 x10-5	Hydrolase activity
70	gi|29468184|	NME1	NM23-H1 [Homo sapiens]	2.14	5.3x10-9	Catalytic activity
18	gi|2245365|	PDIA3	ER-60 protein [Homo sapiens]	-1.56	4.9 x10-3	Carboxyl-lyase activity
31	gi|1710248|	PDIA6	protein disulfide isomerase-related protein 5 [Homo sapiens]	-1.92	1.7 x10-2	Carboxyl-lyase activity
34	gi|1710248|	PDIA6	protein disulfide isomerase-related protein 5 [Homo sapiens]	2	2.5x10-2	Carboxyl-lyase activity
19	gi|49168498|	TXNRD1	TXNRD1 [Homo sapiens]	1.76	3.4x10-4	Oxidoreductase activity
36	gi|1082896|	UQCRB	ubiquinol-cytochrome-c reductase (EC 1.10.2.2) core protein I - human	-1.51	1.4 x10-2	Catalytic activity
Protein Metabolism						
67	gi|54781355|	CAPNS1	calpain, small subunit 1 [Homo sapiens]	2.01	1.7 x10-9	Cysteine-type peptidase activity
57	gi|25453472|	EEF1BD	eukaryotic translation elongation factor 1 delta isoform 2 [Homo sapie	1.65	7.1 x10-4	Translation regulator activity
59	gi|25453472|	EEF1BD	eukaryotic translation elongation factor 1 delta isoform 2 [Homo sapie	2.05	2.5 x10-2	Translation regulator activity
35	gi|15530265|	EEF1BG	Eukaryotic translation elongation factor 1 gamma [Homo sapiens]	2.09	1.5 x10-6	Translation regulator activity
2	gi|61656607|	TRA1	tumor rejection antigen (gp96) 1 [Homo	-2.22	9.2 x10-3	Chaperone activity

			sapiens]			
12	gi|2119712|	HSPA1A	dnaK-type molecular chaperone HSPA1L - human	-1.82	5.4 x10-3	Chaperone activity
11	gi|13676857|	HSPA2	heat shock 70kDa protein 2 [Homo sapiens]	-2.38	4.7 x10-4	Chaperone activity
6	gi|16507237|	HSPA5	BiP protein [Homo sapiens]	-1.61	1.5 x10-2	Chaperone activity
10	gi|24234688|	HSPA9B	heat shock 70kDa protein 9B precursor [Homo sapiens]	-1.58	2.3 x10-2	Chaperone activity
64	gi|662841|	HSPB1	heat shock protein 27 [Homo sapiens]	-1.51	8.8 x10-4	Chaperone activity
69	gi|662841|	HSPB1	heat shock protein 27 [Homo sapiens]	1.7	9.9 x10-4	Chaperone activity
17	gi|20070125|	P4HB	prolyl 4-hydroxylase, beta subunit [Homo sapiens]	-1.61	3.3 x10-3	Isomerase activity
52	gi|42490917|	PSMD14	26S proteasome-associated pad1 homolog [Homo sapiens]	1.47	3.7 x10-3	Ubiquitin-specific protease activity
47	gi|47123412|	RPLP0	RPLP0 protein [Homo sapiens]	1.45	2.6 x10-2	ribosomal subunit
55	gi|62088696|	SFRS1	splicing factor, arginine/serine-rich 1	1.59	4.3 x10-5	RNA binding
13	gi|12653759|	CCT1	TCP1 protein [Homo sapiens]	1.46	2.8 x10-2	Chaperone activity
Regulation of nucleobase, nucleoside, nucleotide and nucleic acid metabolism						
48	gi|7448823|	ADK	adenosine kinase (EC 2.7.1.20) - human	1.6	6.4 x10-5	Catalytic activity
23	gi|12655001|	HNRPH1	HNRPH1 protein [Homo sapiens]	1.55	8.9 x10-4	Ribonucleoprotein
16	i|38197650|	HNRPK	Hnrpk protein [Rattus norvegicus]	-1.83	9.1 x10-5	Ribonucleoprotein
5	gi|51094603|	MCM7	MCM7 minichromosome maintenance deficient 7 (S. cerevisiae) [Homo sapien	-3.52	2.2 x10-4	
Signal transduction and cell communication						
54	gi|1421662|	ANXA1	Annexin Family Mol_id: 1; Molecule: Annexin Iii; Chain: Null; Engineered: Yes;	1.66	1.2 x10-5	Calcium ion binding
14	gi|57113993|	GDI1	GDP dissociation inhibitor 1 [Pan troglodytes]	2.01	2.9 x10-3	GTPase activator activity
56	gi|2914387|	PCNA	Chain E, Human Pcna	-1.87	2.2 x10-4	regulation of cell cycle
49	gi|34234|	RPSA	laminin-binding protein [Homo sapiens]	-1.36	6.4 x10-5	ribosomal subunit
68	gi|21328448|	YWHAB	tyrosine 3-monooxygenase/tryptophan 5-monooxygenase activation protein	1.38	1.6 x10-3	Receptor signalling complex scaffold activityactivity
65	gi|55930909|	YWHAQ	Tyrosine 3/tryptophan 5 -monooxygenase activation protein, theta polypep	1.6	2.8 x10-4	Receptor signalling complex scaffold activityactivity
66	gi|49119653|	YWHAZ	YWHAZ protein [Homo sapiens]	1.45	9.6 x10-3	Receptor signalling complex scaffold activityactivity

62	gi|55961619|	CLIC1	chloride intracellular channel 1 [Homo sapiens]	1.47	3.9 x10-2	intracellular ligand-gated ion channel activity
51	gi|1905874|	PDLIM1	carboxyl terminal LIM domain protein [Homo sapiens]	1.59	1.6 x10-3	Unknown
40	gi|12653109|	AHSA1	AHA1, activator of heat shock 90kDa protein ATPase homolog 1 [Homo sapie	1.57	8.0 x10-6	
61	gi|229691|		Chain D, Deoxyribonuclease I Complex With Actin	1.48	2.9 x10-2	

Protein modifications such as protein phosphorylation alter the pI of proteins and thus contribute to the various isoforms identified for apparently the same protein. MALDI-ToF MS is not capable of distinguishing between such modifications. Pro-Q diamond is a fluorescent dye that selectively binds to phosphorylated residues of serine, threonine and tyrosine. For analysis of proteins being differentially regulated in this experiment a pooled sample of both control and treated was separated by 2D electrophoresis and stained and matched to the BVA as described in section 2.25. Proteins that were deemed phosphorylated at serine/threonine/thyrosine residues as a result of staining with Pro-Q diamond. Locations on 2D gels are indicated in figure 3.1.27 and are summarised in Table 3.1.4. Modification data is listed in same table where available. Gene Symbol conversion and processing where applicable was carried as indicated in section 2.28.

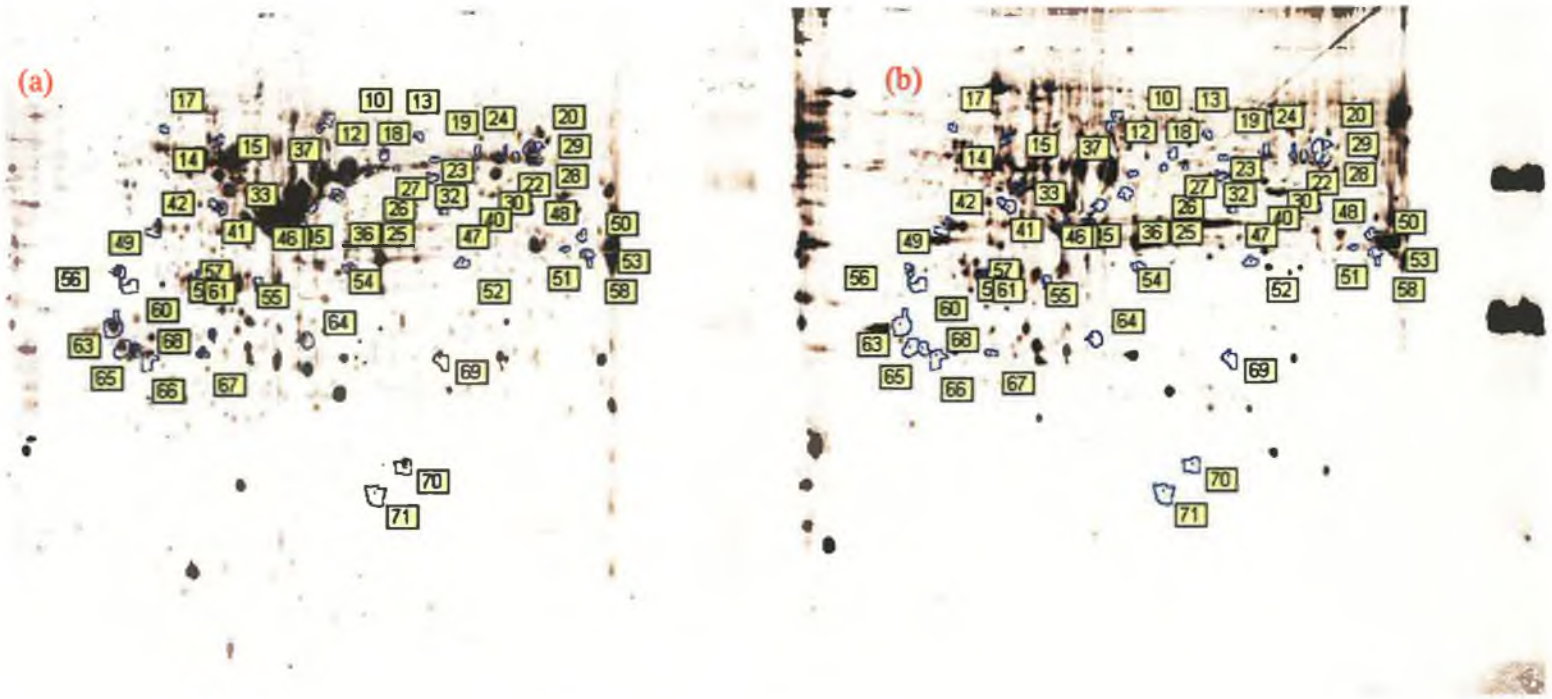

Figure 3.1.45: A pooled protein sample from A549 and A549 5-FU treated separated by 2D electrophoresis and stained with (a) RuPBS to visualise total cell lysate proteome and (b) Pro-Q diamond to visualise phosphorylated proteins. Molecular weight ladder run on right side of images contains a mixture of 2 phosphorylated and 4 non-phosphorylated proteins.

Table 3.1.5 list of proteins differentially expressed proteins from the A549 5-FU treatment DIGE experiment that were found to be phosphorylated by Pro-Q diamond staining.

Location on 2D gel	Gene Symbol	GI accession number	Protein Name	Fold change	Known phospho site	Kinases/ phosphorylase	Implication of phosphorylation
14	GDI1	gi|57113993|	GDP dissociation inhibitor 1 [Pan troglodytes]	2.01	?	?	?
32	ACTB	gi|16924319|	Unknown (protein for IMAGE:3538275) [Homo sapiens]	1.8	?	?	?
33	KRT18	gi|30311|	cytokeratin 18 (424 AA) [Homo sapiens]	-1.58	S21 S22 S24 S37 S43 S74 S432	 MAPK14 MAPK14 MAPK14 ERK2 P38 kinase	Association of 14-3-3 proteins during mitosis
42	KRT19	gi|24234699|	keratin 19 [Homo sapiens]	2.55	S10 S35 S46	? ? ?	
56	PCNA	gi|2914387|	Chain E, Human Pcna	-1.87	?	?	?
57	EEF1BD	gi|25453472|	eukaryotic translation elongation factor 1 delta isoform 2 [Homo sapie	1.65	S449	CDC2	?
59	EEF1BD	gi|25453472|	eukaryotic translation elongation factor 1 delta isoform 2 [Homo sapie	2.05	S449	CDC2	?
61		gi|229691|	Chain D, Deoxyribonuclease I Complex With Actin	1.48			

In order to identify the important proteins differentially regulated in A549 by 5-FU treatment the gene symbols of these proteins were imported into Pathway Assist Software in order to determine the direct interactions between these proteins.

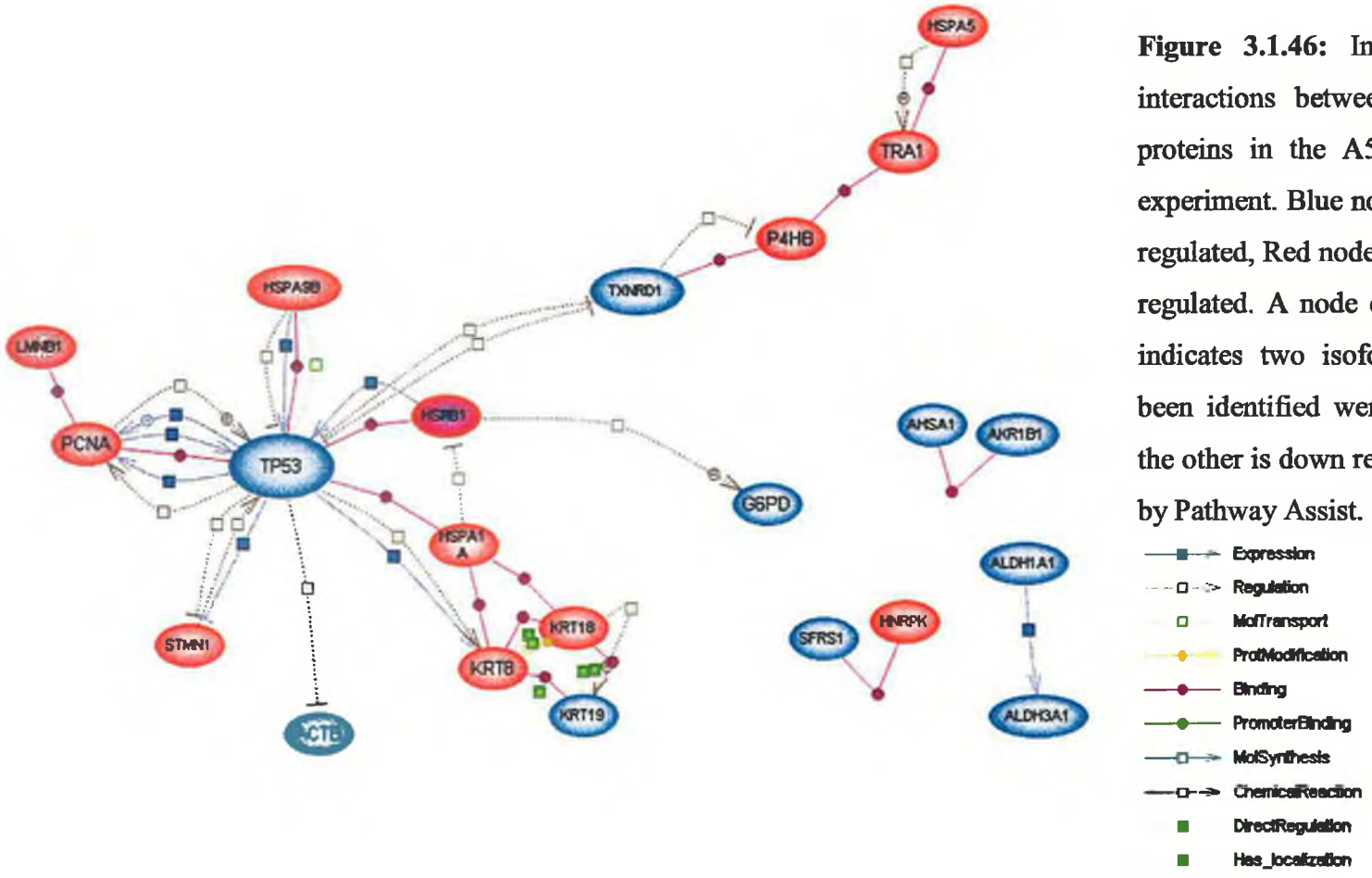

Figure 3.1.46: Image demonstrating direct interactions between differentially expressed proteins in the A549 5-FU treatment DIGE experiment. Blue nodes indicate a protein is up regulated, Red nodes indicate a protein is down regulated. A node coloured both red and blue indicates two isoforms of that protein have been identified were one is up regulated and the other is down regulated. Pathway generated by Pathway Assist.

Summary of proteomic alterations induced in A549 by treatment with 5-FU

Figure 3.1.46 was generated by pathway assist and shows the direct interactions between differentially regulated protein isoforms listed in figure 3.1.4. In summary, direct interactions were identified between 22 of the proteins listed. These proteins that are listed are involved in intermediate filament dynamics of Keratin, Lamins, Actin and tubulin and include LMNB1, STMN1, ACTB, KRT8, KRT18 and KRT19. The HSP70 proteins, HSPA1A and HSPA9B, form complexes with p53 and are involved in cytoplasm sequestering and stabalisation of p53, {*Selkirk, et al., 1994*}. The ER proteins TRA1, HSPA5, P4HB which form a multiprotein complex in the ER and this complex is important in the folding of secretory proteins (*Meunier et al. 2002*). AHSA1 and AKR1B1 play an important role in cell survival {Galvez, et al., 2003}.

3.1.8 Proteomic analysis of DLKP post 5-FU exposure

As already stated, investigation of the proteomic alterations induced by 5-FU treatment is poorly described in the literature and no studies have been performed on lung cell lines. Investigation of the proteomic alterations induced by 5-FU treatment of DLKP a NSCLC may indicate pathways and biological processes activated by 5-FU that would contribute to the understanding of the anti-metabolites mode of action. Furthermore, in conjunction with invasion data presented above an insight into the mechanisms that control alterations in invasion would be elucidated. Finally, identification of proteins involved in the inhibition of apoptosis would lead to the development of drugs that would target such pathways.

Cell culture of DLKP and DLKP treated with 5-FU was carried out as described in section 2.7.2. Total protein extractions were prepared as described in 2.17. These were prepared in biological triplicate. Each biological triplicate was run in technical duplicates. Sample labelling with Cy dyes is shown in table 3.1.6. Protein filters of greater than 1.2 or less than -1.2 with a t-test of 0.01 or a fold change of greater than 1.5 or less than -1.5 with a t-test of 0.05 were used to identify differentially regulated proteins.These filters identified 373 differentially regulated proteins of which 84 were identified.

Differentially regulated proteins were identified as statistically important using the following filters. A fold change less than minus 1.2 or greater than plus 1.2 with a t-test score less than 0.01 was deemed significant or a fold change less than minus 1.5 or greater than plus 1.5 with a t-test less than 0.05 was deemed significant. These filters revealed 373 proteins differentially regulated between DLKP and DLKP treated with 5-FU.

Preparative gels for protein identification were prepared as described in sections 2.21-2.25. Differentially regulated proteins were identified using MALDI-ToF MS as described in section 2.27. Identified differentially regulated proteins locations are indicated in figure 3.1.48 and figure 3.1.49 displays the number of differentially regulated proteins identified and ontological data on these proteins. The identity of

these proteins can be seen in table 3.1.6. Proteins identification data from MALDI-ToF MS is included in the appendices.

Table 3.1.6: Ettan DIGE experimental design for the analysis of differential protein expression induced in DLKP by exposure to 5-FU for 7 days.

Gel number	CY2 label	CY3 label	CY5 label
1	Pooled internal standard (50μg of protein)	DLKP, P.16 (50μg of protein)	DLKP, P. 16, 5-FU treated (50μg of protein)
2	Pooled internal standard (50μg of protein)	DLKP, P.16 (50μg of protein)	DLKP, P. 16, 5-FU treated (50μg of protein)
3	Pooled internal standard (50μg of protein)	DLKP, P. 17 (50μg of protein)	DLKP, P. 17, 5-FU treated (50μg of protein)
4	Pooled internal standard (50μg of protein)	DLKP, P. 17 (50μg of protein)	DLKP, P. 17, 5-FU treated (50μg of protein)
5	Pooled internal standard (50μg of protein)	DLKP, P. 18 (50μg of protein)	DLKP, P. 18, 5-FU treated (50μg of protein)
6	Pooled internal standard (50μg of protein)	DLKP, P. 18 (50μg of protein)	DLKP, P. 18, 5-FU treated (50μg of protein)

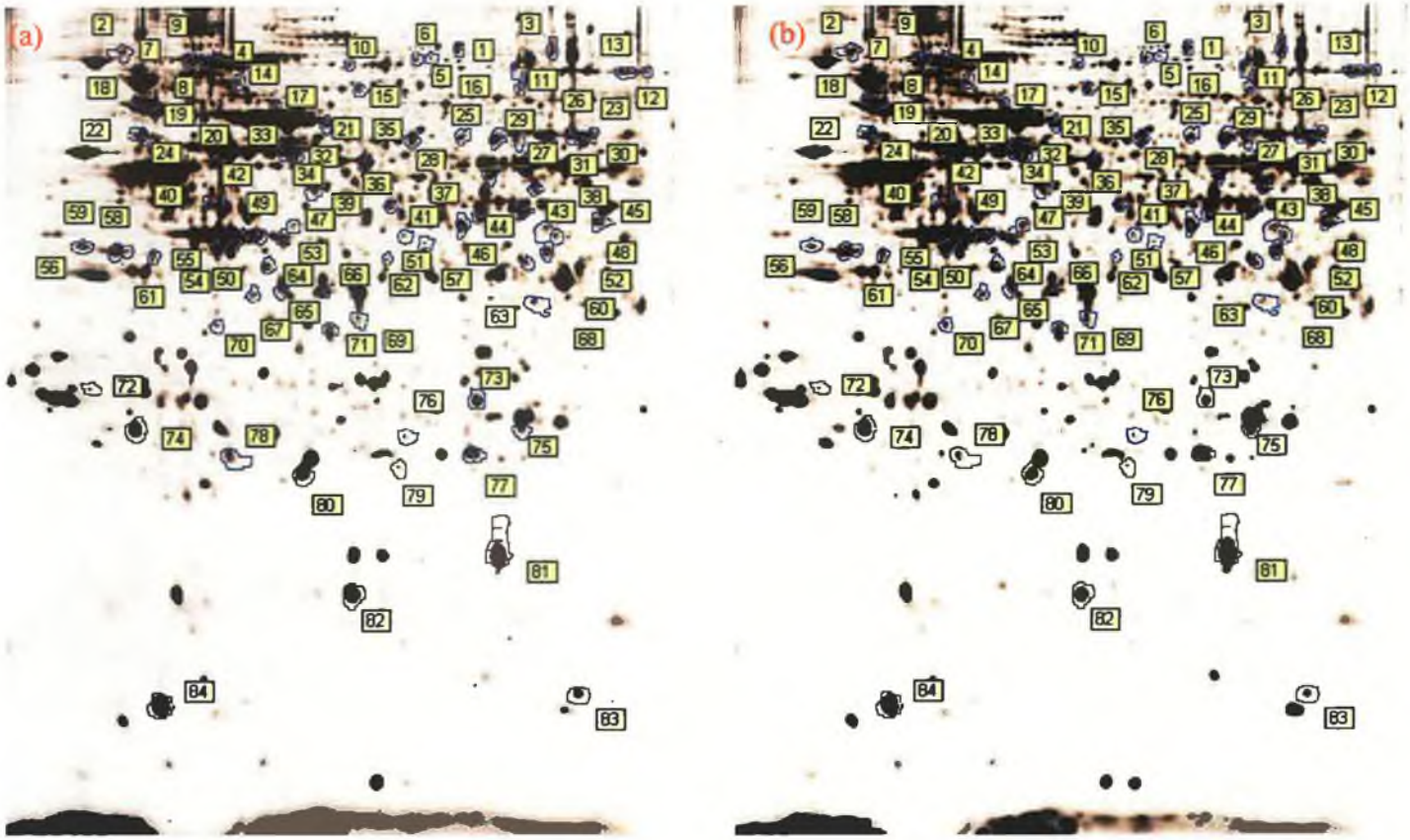

Figure 3.1.48: 2D-DIGE images of DLKP (CY3) and DLKP after 7 days treatment with 10μM 5-FU (CY5). Identified differentially regulated protein spots are encircled by blue lines and are given a protein number. Refer to table 3.1.7 for protein identification

Figure 3.1.49: A pie chart demonstrating the number of proteins in each biological process in DLKP affected by exposure to 5-FU. Individual proteins in each biological process are included in table 3.1.7. Biological process information obtained from the human protein reference database.

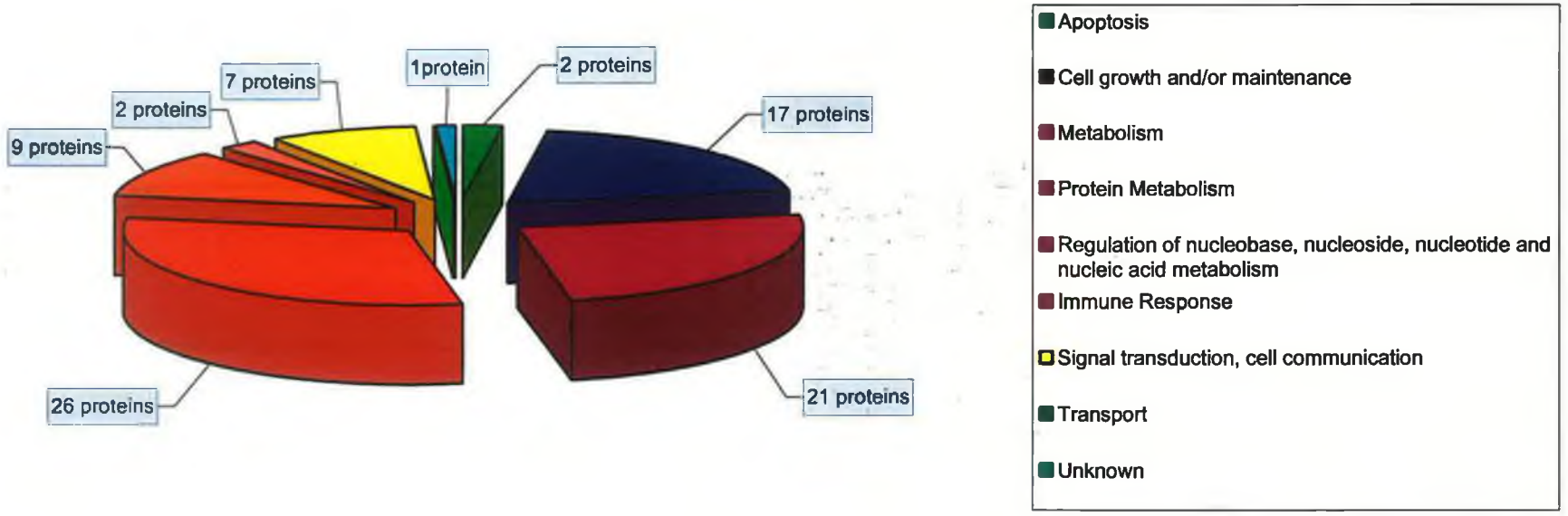

Table 3.1.7: Proteins identified from DLKP 5-FU treatment 2D-DIGE experiment. Position number refers to location in figure 3.1.48 for location on 2D gel. Proteins names that are unknown were identified as described in section 2.16.13.3, names are included.

Protein location on 2D DIGE gel	GI accession Number	Gene symbol	Name	Fold Change	T-test	Molecular function
Apoptosis						
3	PDCD6IP	gi|46249756|	gi|46249756|gb|AAH68454.1 - PDCD6IP protein [Homo sapiens]	1.34	0.0091	Unknown
11	PDCD6IP	gi|13375569|	HP95 [Homo sapiens]	1.69	0.00027	Unknown
Cell growth and/or maintainance						
49	ACTB	gi|16924319|	Unknown (protein for IMAGE:3538275) [Homo sapiens] β-actin	1.66	0.00096	structural molecule activity
54	ACTB	gi|16924319|	Unknown (protein for IMAGE:3538275) [Homo sapiens] β-actin	1.67	0.00031	structural molecule activity
55	ACTB	gi|15277503|	ACTB protein [Homo sapiens]	1.53	0.0019	structural molecule activity
50	ACTB	gi|16924319|	Unknown (protein for IMAGE:3538275) [Homo sapiens] β-actin	1.73	0.00024	structural molecule activity
48	ARP	gi|381964|	actin-related protein	1.28	5.4x10-6	Structural constituent of cytoskeleton
65	CAPZA1	gi|12652785|	CAPZA1 protein [Homo sapiens]	-1.38	0.0092	structural molecule activity
71	CAPZB	gi|55665442|	capping protein (actin filament) muscle Z-line, beta [Homo sapiens]	1.34	0.0028	cytoskeletal protein binding
81	CFL1	gi|30582531|	cofilin 1 (non-muscle) [Homo sapiens]	2.25	0.0002	cytoskeletal protein binding
14	CTTN	gi|477079|	mammary tumor/squamous cell carcinoma-associated protein EMS1 - human	1.5	0.0024	Cytoskeletal protein binding
15	GSN	gi|38044288|	gelsolin isoform b [Homo sapiens]	2.07	9.0x10-7	Structural constituent of cytoskeleton
57	gCAP39	gi|63252913|	gelsolin-like capping protein [Homo sapiens]	-1.52	0.0089	Structural constituent of cytoskeleton
68	LASP1	gi|2135552|	Lasp-1 protein - human	-1.4	0.00042	cytoskeletal protein binding
23	LMNA	gi|57014045|	lamin A/C transcript variant 1 [Homo sapiens]	1.3	0.0011	structural molecule activity
20	LMNB1	gi|15126742|	Lamin B1 [Homo sapiens]	-1.59	5.6x10-5	structural molecule activity
21	PLS3	gi|57162424|	plastin 3 (T isoform) [Homo sapiens]	1.73	0.0012	structural molecule activity
82	STMN1	gi|5031851|	stathmin 1 [Homo sapiens]	-2.1	0.00015	cytoskeletal protein binding

1	VCL	gi|24657579|	VCL protein [Homo sapiens]	1.48	0.0068	Cytoskeletal protein binding
Immune Response						
84	LGALS1	gi|4504981|	beta-galactosidase binding lectin precursor [Homo sapiens]	-1.3	0.00032	Receptor Binding
Metabolism; Energy pathway						
74	GLO1	gi|5729842|	glyoxalase I [Homo sapiens]	1.37	3.7x10-5	Gluthathione transferase activity
63	ACAT2	gi|19880019|	acetyl CoA transferase-like protein [Homo sapiens]	1.47	0.00062	Acetyl-transferase activity
46	AHCY	gi|178277|	S-adenosylhomocysteine hydrolase	1.56	2.1x10-5	Hydrolase activity
36	ALDH1A1	gi|21361176|	aldehyde dehydrogenase 1A1 [Homo sapiens]	1.86	0.00083	Catalytic activity
17	APEH	gi|7144648|	Acylpeptide hydrolase	1.6	0.0071	Hydrolase activity
26	ATIC	gi|14250818|	5-aminoimidazole-4-carboxamide ribonucleotide formyltransferase/IMP cycl	1.4	0.0027	Hydrolase activity
53	CKB	gi|180570|	creatine kinase [Homo sapiens]	-1.25	0.00047	Catalytic activity
6	GANAB	gi|577295|	KIAA0088 [Homo sapiens]	1.77	4.4x10-6	Hydrolase activity
8	GANAB	gi|577295|	KIAA0088 [Homo sapiens]	1.63	0.013	Hydrolase activity
78	GSTA1	gi|34811306|	Chain B, A Folding Mutant Of Human Class Pi Glutathione Transferase, Create	-1.53	0.0011	Gluthathione transferase activity
75	HPRT1	gi|47115227|	HPRT1 [Homo sapiens]	1.53	0.0033	Catalytic activity
45	IDH1	gi|3641398|	NADP-dependent isocitrate dehydrogenase [Homo sapiens]	1.8	0.001	Catalytic activity
66	LDHAL6B	gi|13786848|	Chain B, Human Heart L-Lactate Dehydrogenase H Chain, Ternary Complex With	-1.3	0.0042	Catalytic activity
69	MDH1	gi|49259212|	Chain D, Human B Lactate Dehydrogenase Complexed With Nad+ And 4- Hydroxy-1	1.27	0.004	Catalytic activity
35	PDIA3	gi|2245365|	ER-60 protein [Homo sapiens]	1.25	0.0069	Carboxyl-lyase activity
80	PRDX2	gi|33188452|	peroxiredoxin 2 isoform b [Homo sapiens]	-1.4	0.00039	Peroxidase activity
58	SMS	gi|791051|	spermine synthase [Homo sapiens]	1.51	0.00092	-
59	SMS	gi|55716035|	Spermine synthase [Homo sapiens]	1.44	0.0027	-
70	SRM	gi|56204109|	spermidine synthase [Homo sapiens]	1.41	0.0002	
64	TXNL1	gi|6840947|	PKCq-interacting protein PICOT [Homo sapiens]	1.81	4.4x10-6	Oxidoreductase activity
62	UROD	gi|18158958|	Uroporphyrinogen Decarboxylase	-1.56	0.004	Carboxyl-lyase activity

Protein metabolism						
28	CCT1	gi|12653759|	TCP1 protein [Homo sapiens]	1.77	0.00018	Chaperone activity
37	CCT2	gi|48146259|	CCT2 [Homo sapiens]	1.65	2.3x10-6	Chaperone activity
25	CCT3	gi|58761484|	chaperonin containing TCP1, subunit 3 isoform c [Homo sapiens]	1.41	0.0034	Chaperone activity
29	CCT3	gi|31542292|	chaperonin containing TCP1, subunit 3 (gamma) [Homo sapiens]	2.04	5.5x10-5	Chaperone activity
32	CCT5	gi|603955|	KIAA0098 protein [Homo sapiens]	1.64	0.00059	Chaperone activity
27	CCT6A	gi|62089036|	chaperonin containing TCP1, subunit 6A isoform a variant [Homo sapiens]	1.43	0.0021	Chaperone activity
31	CCT6A	gi|14517632|	acute morphine dependence related protein 2 [Homo sapiens]	1.98	0.0023	Chaperone activity
34	CCT8	gi|62896539|	chaperonin containing TCP1, subunit 8 (theta) variant [Homo sapiens]	1.64	0.0014	Chaperone activity
43	EEF1BG	gi|4503481|	eukaryotic translation elongation factor 1 gamma [Homo sapiens]	1.46	0.00075	Translation regulator activity
12	EEF2	gi|19353009|	Similar to Elongation factor 2b [Homo sapiens]	1.67	0.0013	Translation regulator activity
13	EEF2	gi|19353009|	Similar to Elongation factor 2b [Homo sapiens]	1.32	0.0061	Translation regulator activity
40	EIF3S5	gi|30582627|	eukaryotic translation initiation factor 3, subunit 5 epsilon, 47kDa [Ho	-1.57	0.00022	Translation regulator activity
73	ERP29	gi|5803013|	endoplasmic reticulum protein 29 precursor [Homo sapiens]	-1.63	8.5x10-7	Chaperone activity
7	HSPA4	gi|62087882|	heat shock 70kDa protein 4 isoform a variant [Homo sapiens]	1.54	0.015	Chaperone activity
9	HSPA4	gi|38327039|	heat shock 70kDa protein 4 isoform a [Homo sapiens]	1.77	0.003	Chaperone activity
18	HSPA5	gi|6470150|	BiP protein [Homo sapiens]	-1.42	0.0012	Chaperone activity
19	HSPA5	gi|6470150|	BiP protein [Homo sapiens]	-1.51	0.0015	Chaperone activity
4	HSPH1	gi|55957725|	heat shock 105kDa protein 1 [Homo sapiens]	1.69	0.0002	Heat Shock protein activity
41	PSMC2	gi|41472112|	unknown [Homo sapiens]	1.29	0.0037	Ubiquitin-specific protease activity
83	RPS12	gi|51468838|	similar to ribosomal protein S12 [Homo sapiens]	-1.36	0.00088	ribosomal subunit
67	SFRS1	gi|62088696|	splicing factor, arginine/serine-rich 1	1.24	0.0014	RNA binding

42	TXNDC5	gi|12654715|	TXNDC5 protein [Homo sapiens]	-1.38	2.7x10-5	Oxidoreductase activity
22	UBQLN1	gi|55958669|	ubiquilin 1 [Homo sapiens]	1.35	0.0072	Ubiquitin-specific protease activity
2	USP5	gi|1585128|	isopeptidase T	2.33	9.7x10-5	Ubiquitin-specific protease activity
79	VBP1	gi|54696078|	von Hippel-Lindau binding protein 1 [Homo sapiens]	-1.61	0.00018	Chaperone activity
regulation of nucleobase, nucleoside, nucleotide and nucleic acid metabolism						
52	ADK	gi|7448823|	adenosine kinase (EC 2.7.1.20) - human	1.2	0.0085	Catalytic activity
39	BAT1	gi|55742824|	HLA-B associated transcript 1 [Sus scrofa]	1.57	0.00057	RNA binding
5	HDAC1	gi|59016833|	hypothetical protein [Homo sapiens]	1.59	0.016	Transcription regulator activity
33	HNRPK	gi|59381084|	heterogeneous nuclear ribonucleoprotein K transcript variant [Homo sapie	-1.45	0.00014	Ribonucleoprotein
16	MCM7	gi|51094603|	MCM7 minichromosome maintenance deficient 7 (S. cerevisiae) [Homo sapien	1.49	0.007	
10	MSH2	gi|62898129|	mutS homolog 2 variant [Homo sapiens]	1.54	0.019	DNA repair protein
60	OLIG2	gi|1199657|	protein kinase C-binding protein RACK17 [Homo sapiens]	1.75	0.00017	Transcription regulator activity
38	RUVBL1	gi|62896709|	TATA binding protein interacting protein 49 kDa variant	2.17	2.5x10-5	DNA binding
Signal transduction, cell cummunication						
44	ANXA7	gi|62896663|	annexin VII isoform 1 variant [Homo sapiens]	-1.47	0.0013	Calcium ion binding
76	GRB2	gi|28876|	ash protein [Homo sapiens]	-1.49	0.0036	Receptor signalling complex scaffold activityactivity
24	PPP2R5A	gi|4558259|	Chain B, Crystal Structure Of Constant Regulatory Domain Of Human Pp2a, Pr65	1.92	0.0019	protein serine/threonine kinase activity
56	RPSA	gi|34234|	laminin-binding protein [Homo sapiens]	-2.02	7.3x10-5	ribosomal subunit
30	STIP1	gi|54696884|	stress-induced-phosphoprotein 1 (Hsp70/Hsp90-organizing protein) [Homo s	1.34	6.5x10-5	Receptor signalling complex scaffold activityactivity
61	STRAP	gi|4519417|	WD-40 repeat protein [Homo sapiens]	1.3	0.00042	Regulation of Cell cycle
72	YWHAZ	gi|49119653|	YWHAZ protein [Homo sapiens]	-1.47	2.6x10-5	Receptor signalling complex scaffold activityactivity
Not present in Database						
51	C6orf 55	gi|12052892|	hypothetical protein [Homo sapiens]	1.29	0.0035	
77	DJBP	gi|42543006|	Chain A, Crystal Structure Of Human Dj-1	1.29	0.00014	
47	hfl-B5	gi|62896687|	dendritic cell protein variant [Homo sapiens]	1.65	0.00064	

Protein modifications such as protein phosphorylation alter the pI of proteins and thus contribute to the various isoforms identified for apparently the same protein. MALDI-ToF MS is not capable of distinguishing between such modifications. Pro-Q diamond is a fluorescent dye that selectively binds to phosphorylated residues of serine, threonine and thyrosine. For analysis of proteins being differentially regulated in this experiment a pooled sample of both control and treated was separated by 2D electrophoresis and stained and matched to the BVA as described in section 2.25. Proteins that were deemed phosphorylated at serine/threonine/thyrosine are indicates in figure 3.1.50 and are summarised in Table 3.1.8. Phosphorylation data is listed in same table where available.

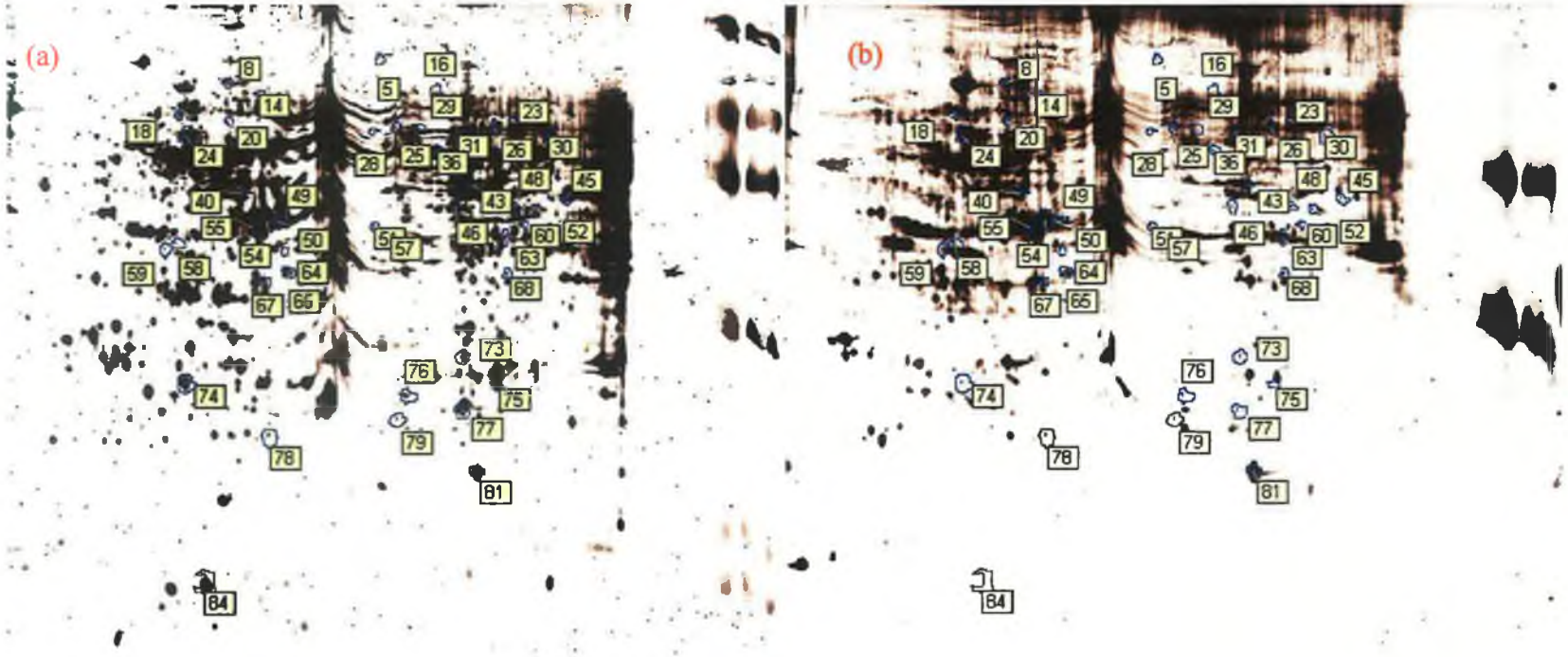

Figure 3.1.50: A pooled protein sample from DLKP and DLKP 5-FU treated separated by 2D electrophoresis and stained with (a) RuPBS to visualise total cell lysate proteome and (b) Pro-Q diamond to visualise phosphorylated proteins. Molecular weight ladder run on right side of images contains a mixture of 2 phosphorylated and 4 non-phosphorylated proteins.

Table 3.1.8: list of differentially expressed proteins from the DLKP 5-FU treatment DIGE experiment that were found to be phosphorylated by Pro-Q diamond staining.

Location on 2D gel	Gene Symbol	GI accession number	Protein Name	Fold change	Known phospho site	Kinases/ phosphorylase	Implication of phosphorylation
24	PPP2R5A	gi|4558259|	Chain B, Crystal Structure Of Constant Regulatory Domain Of Human Pp2a, Pr65	1.92	S28	Protein Kinase R	ER stress
40	EIF3S5	gi|30582627|	eukaryotic translation initiation factor 3, subunit 5 epsilon, 47kDa [Ho	-1.57	S46	Cyclin dependent kinase 11	Phosphorylation occurs during apoptosis
81	CFLN1	gi|30582531|	cofilin 1 (non-muscle) [Homo sapiens]	2.25	S3 S3 S3	PAK2 LIMK1/2 TESK1/2	Actin remodelling
63	ACAT2	gi|19880019|	acetyl CoA transferase-like protein [Homo sapiens]	1.47	?	?	?
65	CAPZA1	gi|12652785|	CAPZA1 protein [Homo sapiens]	-1.38	?	?	?

In order to determine what biological process was effected by the 5-FU treatment of DLKP the list of differentially regulated protein were converted to there gene symbols using the DAVID database conversion tool and imported into Pathway assist to determine direct interactions between these proteins and are summarised in figure 3.1.51.

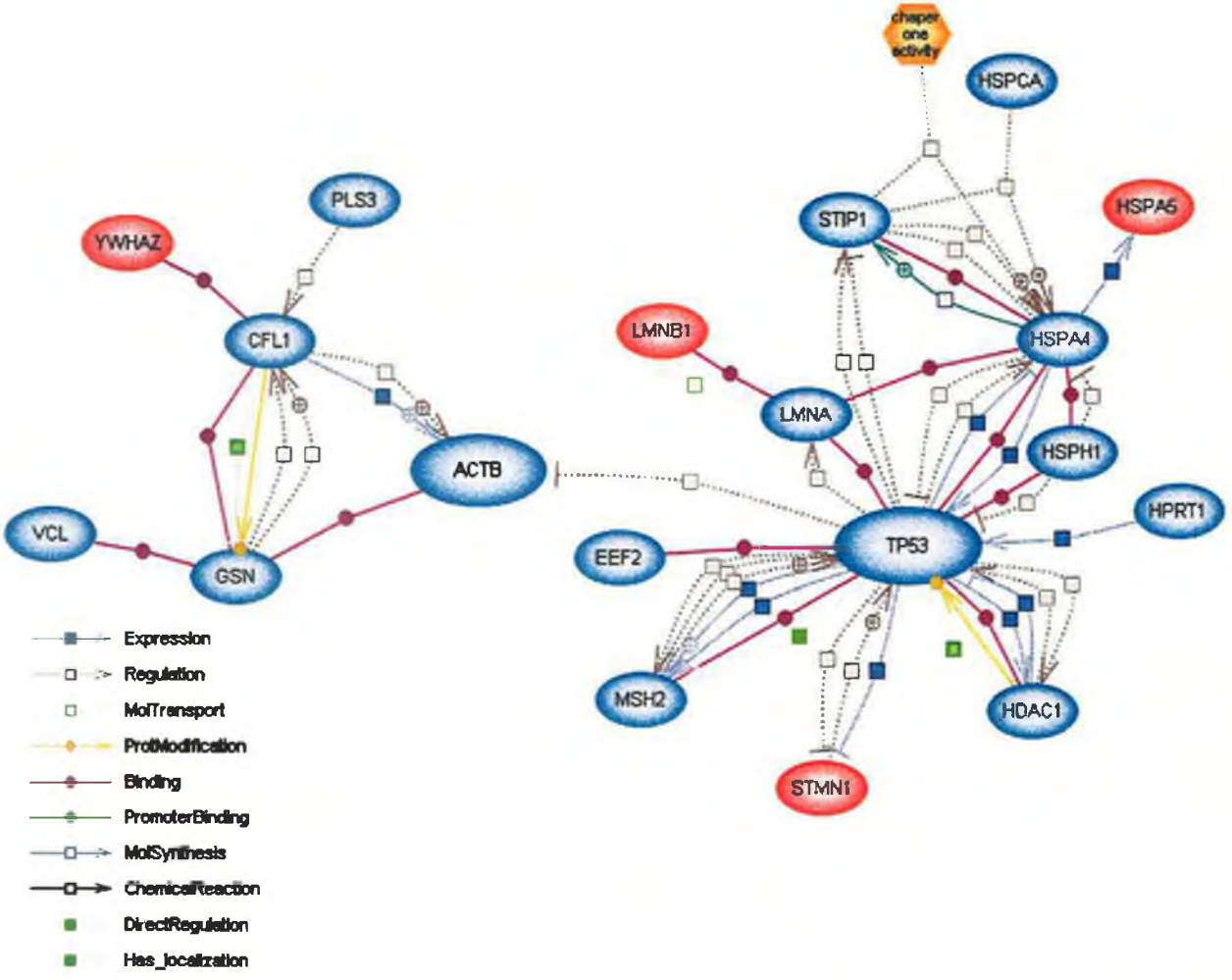

Figure 3.1.51: Image demonstrating direct interactions between differentially expressed proteins in the DLKP 5-FU treatment DIGE experiment. Blue nodes indicate a protein is up regulated, Red nodes indicate a protein is down regulated. A node coloured both red and blue indicates two isoforms of that protein have been identified were one is up regulated and the other is down regulated. Pathway generated by Pathway Assist.

Proteins found to interact include YWHAZ and cofilin, YWHAZ binds to phosphorylated cofilin. Gelsolin, cofilin and actin bind each other and are involved in F-actin depolymerisation. Gelsolin caps F-actin and binds to vinculin. The HSP70 proteins, HSPA1A and HSPA9B, form complexes with p53 and are involved in cytoplasm sequestering and stabalisation of p53, {Selkirk, et al., 1994}. EEF2 was found to bind p53 in polyribosomes and p53 has been implicated in regulation of its own translation rate (Yin et al., 2003). STMN1 has been shown to be directly down regulated by the accumulation of p53 and stalls cell cycle progression at G2/M phase of the cell cycle (Johnsen et al. 2000).

3.1.9 Proteomic analysis of NHBE post 5-FU exposure

As stated proteomic alteration induced by 5-FU treatment are poorly described in the literature and only two publications have been published to date. Data presented above demonstrates how two lung carcinomas respond to 5-FU treatment. Cancer contains mutations and as such it response to 5-FU will be properly regulated. To over come this treatment of the normal bronchial epithelial cells with 5-FU was carried out at two concentration 10 and 30 μM, equi-molar and equi-toxic concentrations. Thus this data should provide an isight into how normal cells respond to 5-FU treatment. Further more it should help identify a common response between normal and cancer cell line treated with 5-FU.

Cell culture of NHBE and NHBE treated with 5-FU (at 10 and 30μM) was carried out as described in section 2.7.2 and 2.7.3. Total cell lysate protein extractions were prepared as described in 2.16.2.1. These were prepared in biological triplicate. Each biological triplicate was run in technical duplicates. Sample labelling with Cy dyes is shown in table 3.1.9. Protein filters of greater than 1.2 or less than -1.2 with a t-test less than 0.01, or a fold change of less than -1.5 or greater than 1.5 with t-test less than 0.05 were used to identify differentially regulated proteins. This resulted in the identification of 399 differentially regulated proteins of which 60 have been identified by MALDI-ToF MS.

Preparative gels for protein identification were prepared as described in sections 2.16.5-2.16.11. Differentially regulated proteins were identified using MALDI-ToF MS as described in section 2.16.12. Identified differentially regulated proteins locations are indicated in figure 3.1.53 and figure 3.1.54 displays the number of differentially regulated proteins identified and ontological data on these proteins. The identity of these proteins can be seen in table 3.1.10. Proteins identification data from MALDI-ToF MS is included in the appendices.

Figure 3.1.56 was generated by pathway assist and shows the direct interactions between differentially regulated protein isoforms listed in table 3.1.10 and does not distinguish between drug concentration in these images as they are purely for visualisation purposes. In summary, direct interactions were identified between 18 of the proteins listed. These proteins that are listed are involved in intermediate filament dynamics of Keratin, Lamins, Actin and tubulin and include LMNA, STMN1, ACTB, YWHAZ, CFLN1, and GSN.

Table 3.1.9: Ettan DIGE experimental design for the analysis of differential protein expression induced in NHBE by exposure to 5-FU for 7 days.

Gel number	CY2 label	CY3 label	CY5 label
1	Pooled internal standard (50μg of protein)	NHBE, (50μg of protein)	NHBE, 10μM 5-FU, (50μg of protein)
2	Pooled internal standard (50μg of protein)	NHBE, (50μg of protein)	NHBE, 30μM 5-FU, (50μg of protein)
3	Pooled internal standard (50μg of protein)	NHBE, (50μg of protein)	NHBE, 10μM 5-FU, (50μg of protein)
4	Pooled internal standard (50μg of protein)	NHBE, 30μM 5-FU, (50μg of protein)	NHBE, (50μg of protein)
5	Pooled internal standard (50μg of protein)	NHBE, 10μM 5-FU, (50μg of protein)	NHBE, (50μg of protein)
6	Pooled internal standard (50μg of protein)	NHBE, 30μM 5-FU, (50μg of protein)	NHBE, (50μg of protein)
7	Pooled internal standard (50μg of protein)	NHBE, 10μM 5-FU, (50μg of protein)	NHBE, 30μM 5-FU, (50μg of protein)
8	Pooled internal standard (50μg of protein)	NHBE, 30μM 5-FU, (50μg of protein)	NHBE, 10μM 5-FU, (50μg of protein)
9	Pooled internal standard (50μg of protein)	NHBE, 10μM 5-FU, (50μg of protein)	NHBE, 30μM 5-FU, (50μg of protein)

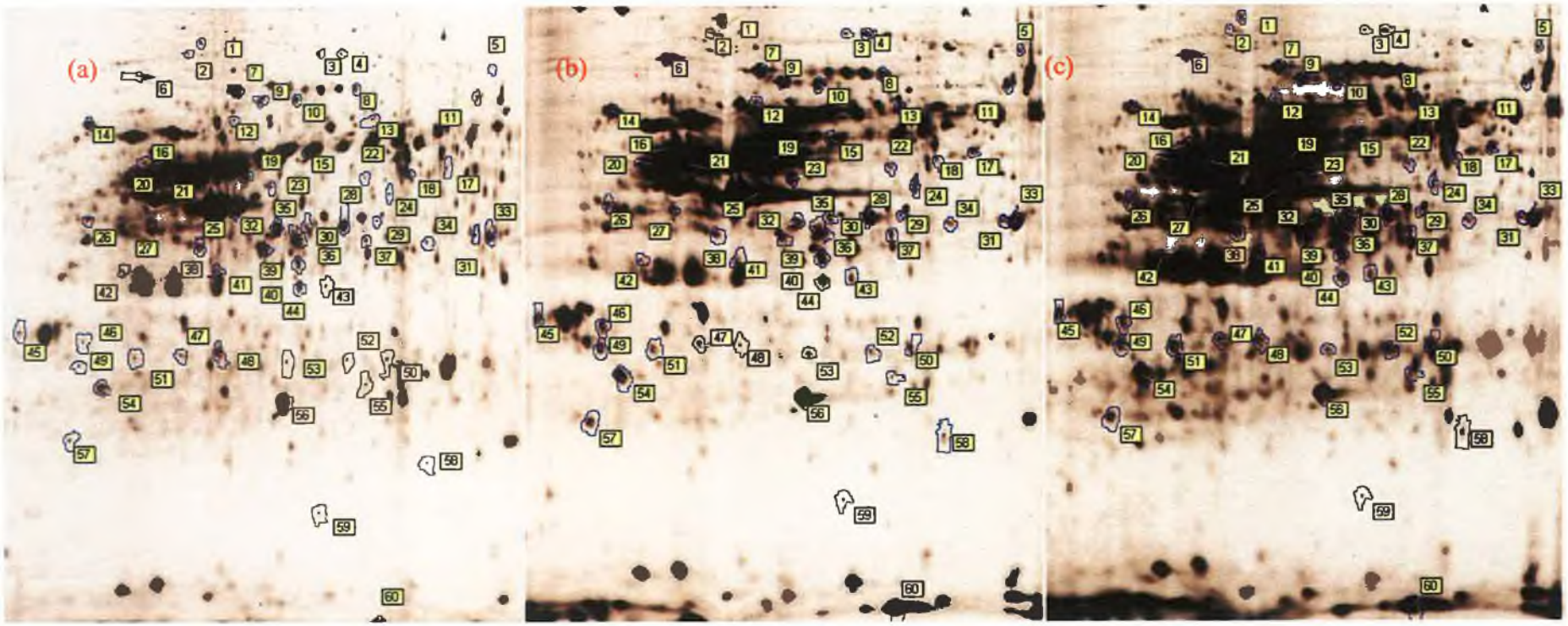

Figure 3.1.53: 2D-DIGE images of (a) NHBE (CY3) and (b) NHBE after 7 days treatment with 10μM 5-FU (CY5) (c) NHBE after 7 days treatment with 30μM 5-FU (CY-5). Identified differentially regulated protein spots are encircled by blue lines and are given a protein number. Refer to table 3.1.10 for protein identification

Figure 3.1.54: A pie chart demonstrating the number of proteins in each biological process in DLKP affected by exposure to 5-FU. Individual proteins in each biological process are included in table 3.1.10 Biological process information obtained from the human protein reference database.

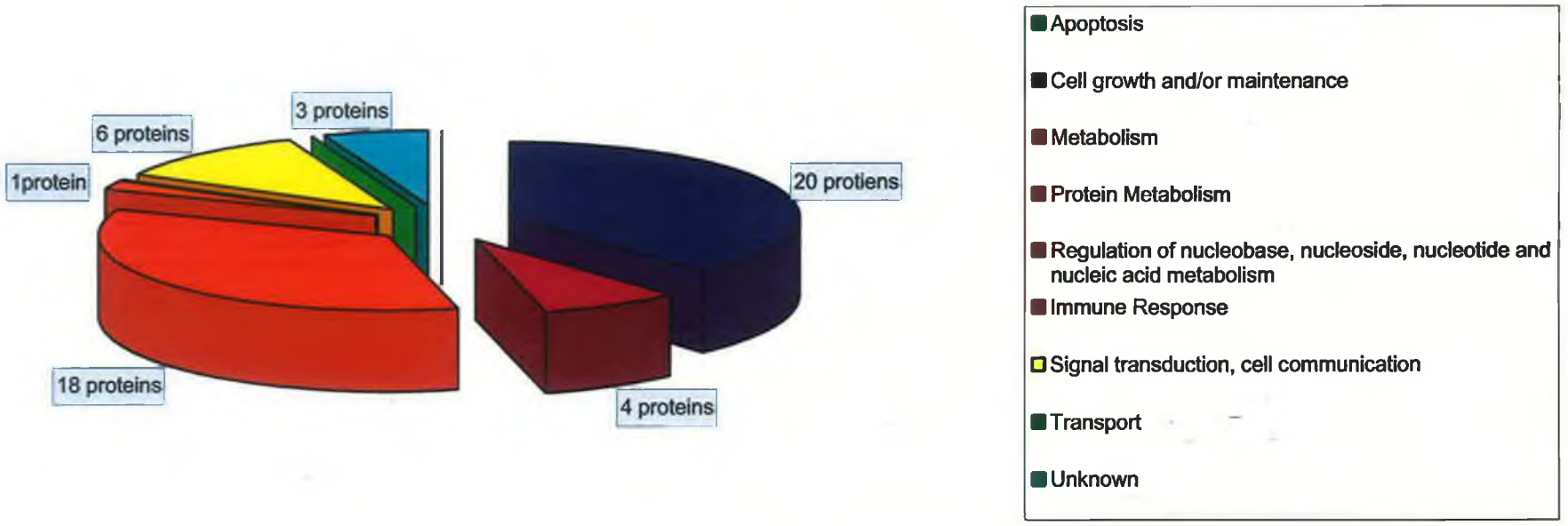

Table 3.1.10: Proteins identified from NHBE 5-FU treatment 2D-DIGE experiment. Position number refers to location in figure 3.1.53 for location on 2D gel. Information of fold changes in both 10μM and 30μM 5-FU treatments were included. Data from both treatments were included even where statistics indicated its expression is not significant in order to demonstrate that the proteins expression is dose dependent (in significant fold changes are shaded grey).Unknown or unnamed proteins were identified as described in section 2.16.13.3.

Protein Location on 2D-DIGE Gels	Gene Symbol	GI Accession	Protein Name	NHBE 10μM 5-FU		NHBE 30μM 5-FU		Molecular Function
				Fold Change	T-test	Fold Change	T-test	
Cell growth and/or maintainance								
25	ACTB	gi|62897625|	beta actin variant [Homo sapiens]	1.26	0.0017	1.23	0.0038	structural molecule activity
39	CAPZA1	gi|12652785|	CAPZA1 protein [Homo sapiens]	-3.53	0.036	-1.94	0.31	structural molecule activity
36	CAPZA2	gi|433308|	capping protein alpha [Homo sapiens]	-1.09	0.41	1.29	0.0014	structural molecule activity
44	CAPZB	gi|55665440|	capping protein (actin filament) muscle Z-line, beta [Homo sapiens]	1.3	0.0011	1.23	0.0098	structural molecule activity
58	CFL1	gi|30582531|	cofilin 1 (non-muscle) [Homo sapiens]	16.63	1.7x10-8	14.17	1.8x10-8	cytoskeletal protein binding
2	CTTN	gi|20357556|	cortactin isoform b [Homo sapiens]	-1.18	0.3	-1.82	0.0049	Cytoskeletal protein binding
3	GSN	gi|38044288|	gelsolin isoform b [Homo sapiens]	2.61	0.00053	1.77	0.027	Structural constituent of cytoskeleton
4	GSN	gi|38044288|	gelsolin isoform b [Homo sapiens]	2.5	0.0034	1.53	0.099	Structural constituent of cytoskeleton
21	KRT14	gi|27769301|	Keratin 14 [Homo sapiens]	4.56	0.00041	3.81	0.0005	structural molecule activity
16	KRT17	gi|21754583|	unnamed protein product [Homo sapiens]	5.18	2.9x10-7	3.31	9.6x10-6	structural molecule activity
20	KRT17	gi|21754583|	unnamed protein product [Homo sapiens]	2.07	0.0022	1.69	0.034	structural molecule activity
19	KRT18	gi|62897747|	keratin 18 variant [Homo sapiens]	2.33	0.00024	2.31	7.8x10-5	structural molecule activity
23	KRT19	gi|34039|	unnamed protein product [Homo sapiens]	2.78	0.00019	3.66	0.00021	structural molecule activity
13	KRT5	gi|47940601|	Keratin 5 [Homo sapiens]	2.13	0.0038	3	0.00067	structural molecule activity

15	KRT8	gi|33875698|	KRT8 protein [Homo sapiens]	-1.47	0.00044	-1.34	0.071	structural molecule activity
5	LMNA	gi|57014047|	lamin A/C transcript variant 1 [Homo sapiens]	1.92	0.00015	2.05	0.0035	structural molecule activity
10	PLS3	gi|57162424|	plastin 3 (T isoform) [Homo sapiens]	2.1	6.2x10-5	2.37	0.00013	structural molecule activity
59	STMN1	gi|5031851|	stathmin 1 [Homo sapiens]	-2.18	0.0002	-2.78	1.1x10-5	cytoskeletal protein binding
54	TPT1	gi|33285832|	TCTP [Homo sapiens]	1.39	0.00049	1.61	4.4x10-5	Calcium ion binding
11	WDR1	gi|62897353|	WD repeat-containing protein 1 isoform 1 variant [Homo sapiens]	2.29	0.0023	1.99	0.03	cytoskeletal protein binding
Metabolism; Energy pathway								
56	GSTA1	gi|23200509|	Chain B, A Folding Mutant Of Human Class Pi Glutathione Transferase, Create	1.45	0.00014	1.53	5.0x10-5	Gluthathione transferase activity
31	PRPS1	gi|35700|	unnamed protein product [Homo sapiens]	1.70	0.019	1.28	0.2	Ligase activity
41	SRM	gi|531202|	spermidine synthase	1.16	0.46	2.57	0.00028	
1	VCP	gi|55662798|	valosin-containing protein [Homo sapiens]	2.11	0.016	1.48	0.11	ATPase activity
Protein metabolism								
51	CAPNS1	gi|40674605|	CAPNS1 protein [Homo sapiens]	1.15	0.14	1.56	0.00048	Cysteine-type peptidase activity
42	EEF1BD	gi|38522|	human elongation factor-1-delta [Homo sapiens]	1.08	0.43	1.73	0.015	Translation regulator activity
17	EEF1BG	gi|39644794|	EEF1BG protein [Homo sapiens]	1.34	0.24	1.9	0.021	Translation regulator activity
32	EIF3S2	gi|56204149|	eukaryotic translation initiation factor 3, subunit 2 beta, 36kDa [Homo	-3.69	0.013	-1.65	0.36	Translation regulator activity
9	HSPA1B	gi|14424588|	HSPA1A protein [Homo sapiens]	1.75	0.0045	1.43	0.0077	Chaperone activity
6	HSPA5	gi|6470150|	BiP protein [Homo sapiens]	2.82	0.00098	2.42	0.0044	Chaperone activity
7	HSPA8	gi|62896815|	heat shock 70kDa protein 8 isoform 2 variant [Homo sapiens]	2.00	0.015	1.01	0.12	Chaperone activity
53	HSPB1	gi|15126735|	Heat shock 27kDa protein 1 [Homo sapiens]	2.63	6.5x10-6	2.69	3.7x10-6	Chaperone activity
50	HSPB1	gi|15928913|	Unknown (protein for IMAGE:3906970) [Homo sapiens]	1.74	6.0x10-5	2.1	2.1x10-5	Chaperone activity

52	HSPB1	gi|15928913|	Unknown (protein for IMAGE:3906970) [Homo sapiens]	2.1	1.0x10-6	2.9	5.0x10-8	Chaperone activity
48	HSPB1	gi|662841|	heat shock protein 27 [Homo sapiens]	-3.73	0.019	-1.76	0.39	Chaperone activity
14	P4HB	gi|48735337|	Prolyl 4-hydroxylase, beta subunit [Homo sapiens]	-1.27	0.019	-1.77	0.0014	Isomerase activity
47	PSMA3	gi|48145983|	PSMA3 [Homo sapiens]	-1.63	4.1x10-5	-1.24	0.048	Ubiquitin-specific protease activity
22	PSMC2	gi|41472112|	unknown [Homo sapiens]	1.57	0.044	1.58	0.0038	Ubiquitin-specific protease activity
35	RPLP0	gi|12654583|	Ribosomal protein P0 [Homo sapiens]	1.01	0.79	2.06	0.00047	ribosomal subunit
24	SERPINB1	gi|62898301|	serine (or cysteine) proteinase inhibitor, clade B (ovalbumin), member	2.53	0.0052	1.89	0.016	Protease inhibitor activity
29	SERPINB5	gi|56554673|	Chain A, 3.10 A Crystal Structure Of Maspin, Space Group I 4 2 2	1.78	0.00035	1.58	0.0067	Protease inhibitor activity
30	SERPINB5	gi|56554673|	Chain A, 3.10 A Crystal Structure Of Maspin, Space Group I 4 2 2	1.22	0.023	1.45	0.00071	Protease inhibitor activity
regulation of nucleobase, nucleoside, nucleotide and nucleic acid metabolism								
12	HNRPK	gi|55958547|	heterogeneous nuclear ribonucleoprotein K [Homo sapiens]	1.73	0.017	1.4	0.11	Ribonucleoprotein
Signal transduction, cell cummunication								
26	RPSA	gi|34234|	laminin-binding protein [Homo sapiens]	-1.66	0.00012	-1.93	4.8x10-5	ribosomal subunit
60	S100A11	gi|32880167|	S100 calcium binding protein A11 (calgizzarin) [Homo sapiens]	1.54	2.0x10-5	1.61	2.0x10-6	Calcium ion binding
45	SFN	gi|16306737|	SFN protein [Homo sapiens]	1.65	0.00043	1.97	9.4x10-5	Receptor signalling complex scaffold activityactivity
27	STRAP	gi|4519417|	WD-40 repeat protein [Homo sapiens]	-1.38	0.0023	-1.26	0.047	Regulation of Cell cycle
46	YWHAG	gi|82407958|	Chain F, Crystal Structure Of 14-3-3 Gamma In Complex With A Phosphoserine	1.37	0.0019	1.44	0.00056	Receptor signalling complex scaffold activityactivity
49	YWHAZ	gi|68085578|	Tyrosine 3/tryptophan 5 - monooxygenase activation protein, zeta polypeptide	1.34	0.0018	1.23	0.012	Receptor signalling complex scaffold activityactivity
Not present in database								
38	ATP5B	gi|16741373|	ATP synthase, H+ transporting, mitochondrial F1 complex	-1.53	0.0034	-1.2	0.21	

28		gi|62738526|	Chain B, The 2.8 A Structure Of A Tumour Suppressing Serpin	1.82	0.00017	1.38	0.031	
8		gi|6729803|	Heat-Shock 70kd Protein 42kd Atpase	1.17	0.4	2.63	4.8x10-6	

Protein modifications such as protein phosphorylation alter the pI of proteins and thus contribute to the various isoforms identified for apparently the same protein. MALDI-ToF MS is not capable of distinguishing between such modifications. Pro-Q diamond is a fluorescent dye that selectively binds to phosphorylated residues of serine, threonine and thyrosine. For analysis of proteins being differentially regulated in this experiment a pooled sample of both control and treated was separated by 2D electrophoresis and stained and matched to the BVA as described in section 2.25. Proteins that were deemed phosphorylated at serine/threonine/thyrosine are indicates in figure 3.1.56 and are summarised in Table 3.1.11. Phosphorylation data is listed in same table where available.

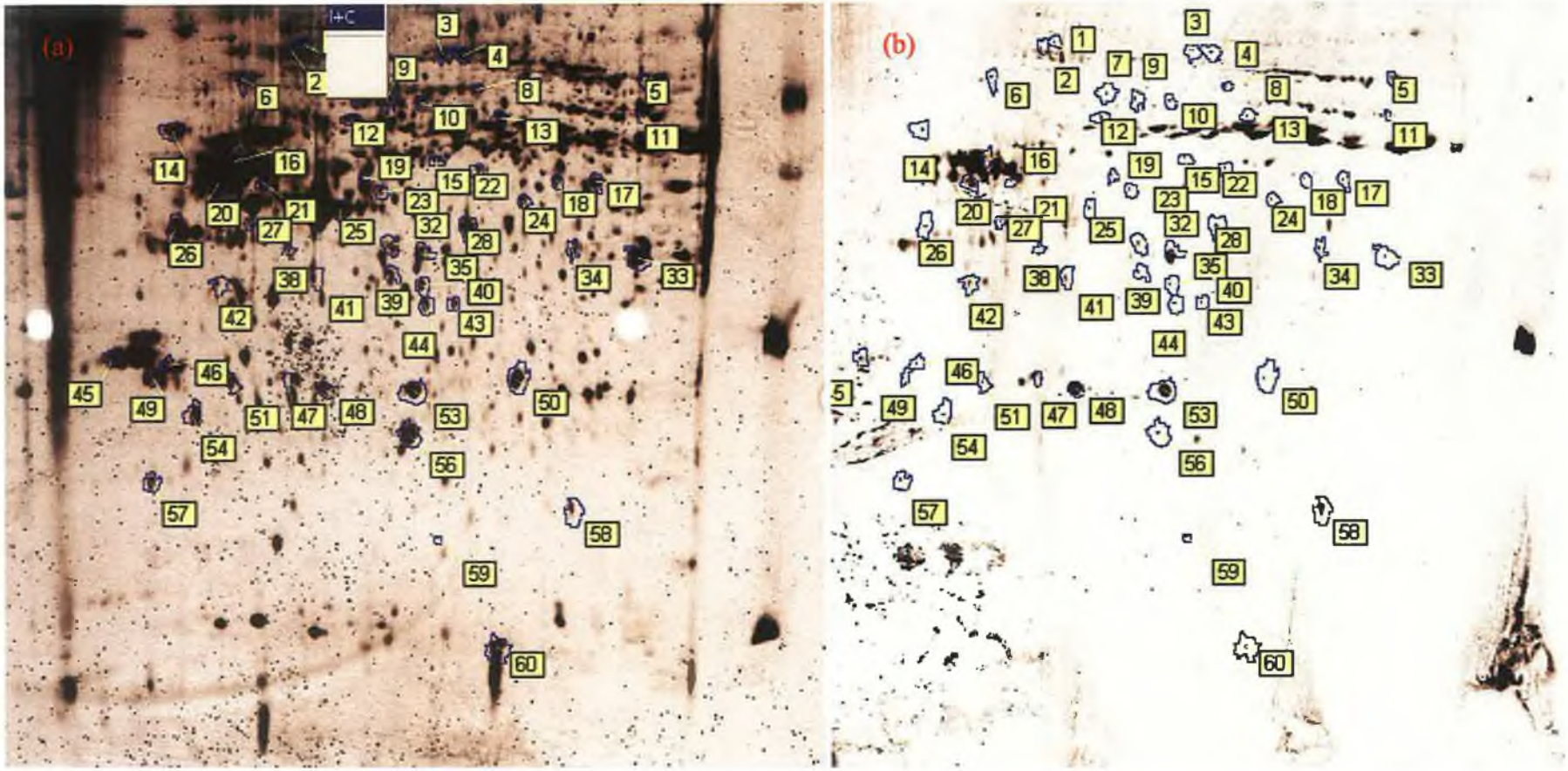

Figure 3.1.56: A pooled protein sample from NHBE and NHBE 5-FU treated separated by 2D electrophoresis and stained with (a) RuPBS to visualise total cell lysate proteome and (b) Pro-Q diamond to visualise phosphorylated proteins. Molecular weight ladder run on right side of images contains a mixture of 2 phosphorylated and 4 non-phosphorylated proteins..

Table 3.1.11: list of proteins differentially expressed proteins from the NHBE 5-FU treatment DIGE experiment that were found to be phosphorylated by Pro-Q diamond staining.

Location on 2D gel	Gene Symbol	GI accession number	Protein Name	Fold change	Known phospho site	Kinases/ phosphorylase	Implication of phosphorylation
5	LMNA	gi|57014047|	lamin A/C transcript variant 1 [Homo sapiens]	2.05	S5 T19 S22 T199 S390 S392 S403 S404/S406/S407 T409 T416 S423 T480 S525	PKC CDC2 CDC2 PKC CDC2 Protein kinase Cα Protein kinase Cα ?/?/? PKC ? PKC Protein kinase Cα ?	Lamin assembly
20	KRT17	gi|21754583|	unnamed protein product [Homo sapiens]	1.69	?	?	?
32	EIF3S2	gi|56204149|	eukaryotic translation initiation factor 3, subunit 2 beta, 36kDa [Homo	-1.65	?	TGFBR2	activation
35	RPLPO	gi|12654583|	Ribosomal protein P0 [Homo sapiens]	2.06	?	?	?
42	EEF1BD	gi|38522|	human elongation factor-1-delta [Homo sapiens]	1.73	S449	CDC2	?
53	HSPB1	gi|15126735|	Heat shock 27kDa protein 1 [Homo sapiens]	2.69	S15/S78/S82	MAPKAPK2	Cell survival
58	CFLN1	gi|30582531|	cofilin 1 (non-muscle) [Homo sapiens]	14.17	S3 S3 S3	PAK2 LIMK1/2 TESK1/2	Actin remodelling

In order to identify biological processes impacted by proteins differentially regulated by 5-FU treatment of NHBE protein identifications were converted to gene symbols using DAVID database ID conversion tool and imported into Pathway Assist to determine direct interactions between these proteins. Figure 3.1.51 was generated by Pathway Assist and shows the direct interactions between differentially regulated protein isoforms listed in table 3.1.6.

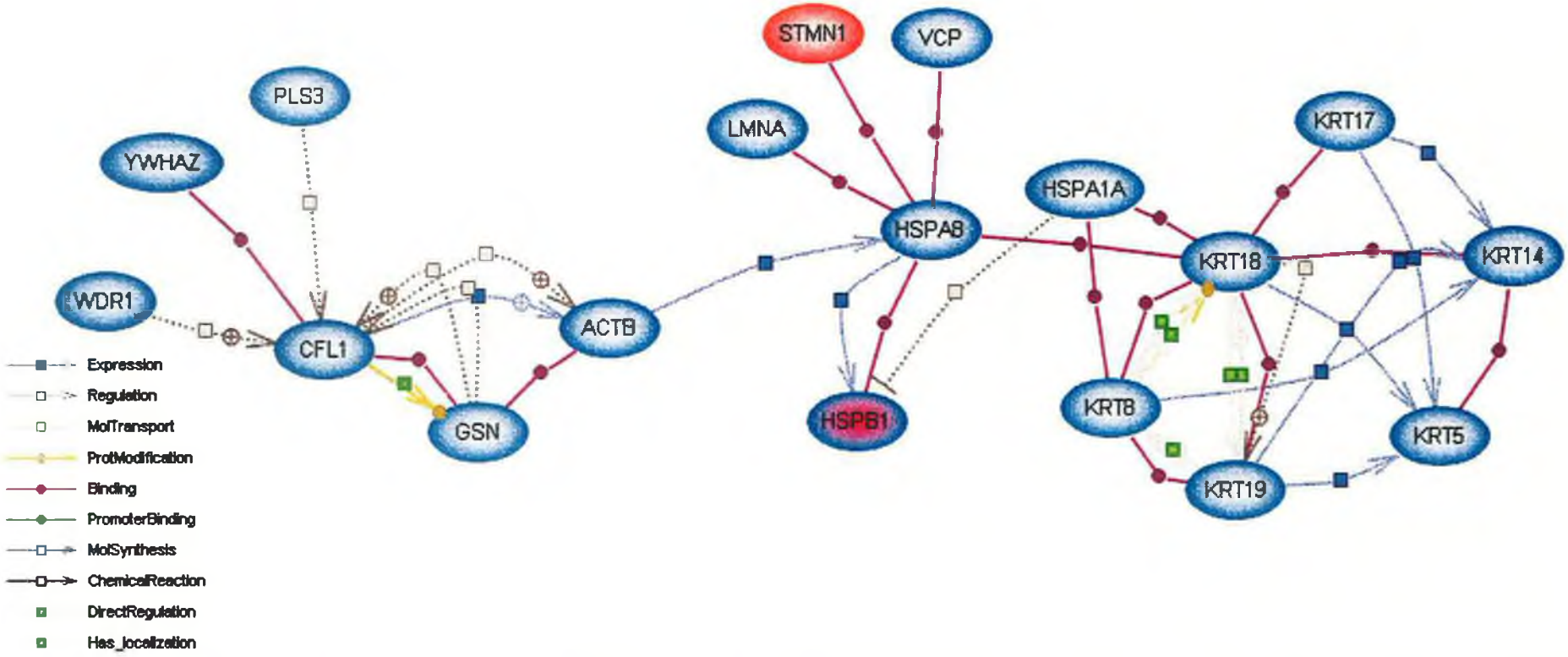

Figure 3.1.57: Image demonstrating direct interactions between differentially expressed proteins in the NHBE 5-FU treatment DIGE experiment. Blue nodes indicate a protein is up regulated, Red nodes indicate a protein is down regulated. A node coloured both red and blue indicates two isoforms of that protein have been identified were one is up regulated and the other is down regulated. Pathway generated by Pathway Assist.

In summary, direct interactions were identified between 20 of the proteins listed. These proteins that are listed are involved in intermediate filament dynamics of Keratin, Lamins, Actin and tubulin and include LMNA, STMN1, ACTB, YWHAZ, CFLN1, GSN, KRT 5, 8, 14, 17, and 18. WDR-1 enhances cofilin depolymerisation of F-actin (Rodal et al., 1999). YWHAZ binds p-cofilin and prevents its recycling during actin depolymerisation (Gohla, *et al.,* 2002; Berkenfeld, *et al.,* 2003). Gelsolin and cofilin depolymerise actin as already discussed. HSPA8 associates with the t-complex of protein chaperones and actin or tubulin and is responsible for actin or tubulin turnover. This complex transports actin in its native form where it ensures its correct incorporation into microfilaments (*Bourke et al., 2002*). Phosphorylated Stathmin binds HSP70 and plays a role in regulation of cell growth (Manceau, et al., 1999).

3.1.10 Proteomic analysis of MCF-7 post 5-FU exposure

DIGE analysis of protein expression in MCF-7 after 7 days exposure 5-FU at a concentration of 10μM

To date there have been several DNA microarray experiments performed on the breast adenocarcinoma cell line MCF-7 treated with 5-FU. However no proteomic experiments have performed on MCF-7 or any other cell line of breast origin. Investigation of proteomic alterations will identify differentially regulated proteins that contribute to increased invasion induced by 5-FU treatment of MCF-7. Furthermore, identified differentially expressed proteins may indicate anti-apoptopic mechanisms employed by MCF-7 to survive 5-FU treatment and could contribute to the development of drugs that overcome resistance to apoptosis during 5-FU treatments. Cell culture of MCF-7 and MCF-7 treated with 5-FU were carried out as described in section 2.7.3. Total protein extractions were prepared as described in section 2.16.2.1. These were prepared in biological triplicate. Each biological triplicate was run in technical duplicates. Sample labelling with Cy dyes is shown in table 3.1.12. Protein filters of less than minus 1.2 or grater than plus 1.2 with t-test of less than 0.01, and fold change of less than minus 1.5 or greater than plus 1.5 with a t-test of 0.05 were used to identify differentially regulated proteins. This resulted in the selection of 429 proteins of which 152 have been identified.

Preparative gels for protein identification were prepared as described in sections 2.21-2.25. Differentially regulated proteins were identified using MALDI-ToF MS as described in section 2.27. Identified differentially regulated proteins locations are indicated in figure 3.1.59 and figure 3.1.60 displays the number of differentially regulated proteins identified and ontological data on these proteins. The identity of these proteins can be seen in table 3.1.13. Proteins identification data from MALDI-ToF MS is included in the appendices.

Table 3.1.12: Ettan DIGE experimental design for the analysis of differential protein expression induced in MCF-7 by exposure to 5-FU for 7 days.

Gel number	CY2 label	CY3 label	CY5 label
1	Pooled internal standard (50µg of protein)	MCF-7, P.183 (50µg of protein)	MCF-7, P. 183, 5-FU treated (50µg of protein)
2	Pooled internal standard (50µg of protein)	MCF-7, P.183 (50µg of protein)	MCF-7, P. 183, 5-FU treated (50µg of protein)
3	Pooled internal standard (50µg of protein)	MCF-7, P. 185 (50µg of protein)	MCF-7, P. 185, 5-FU treated (50µg of protein)
4	Pooled internal standard (50µg of protein)	MCF-7, P. 185 (50µg of protein)	MCF-7, P. 185, 5-FU treated (50µg of protein)
5	Pooled internal standard (50µg of protein)	MCF-7, P. 186 (50µg of protein)	MCF-7, P. 186, 5-FU treated (50µg of protein)
6	Pooled internal standard (50µg of protein)	MCF-7, P. 186 (50µg of protein)	MCF-7, P. 186, 5-FU treated (50µg of protein)

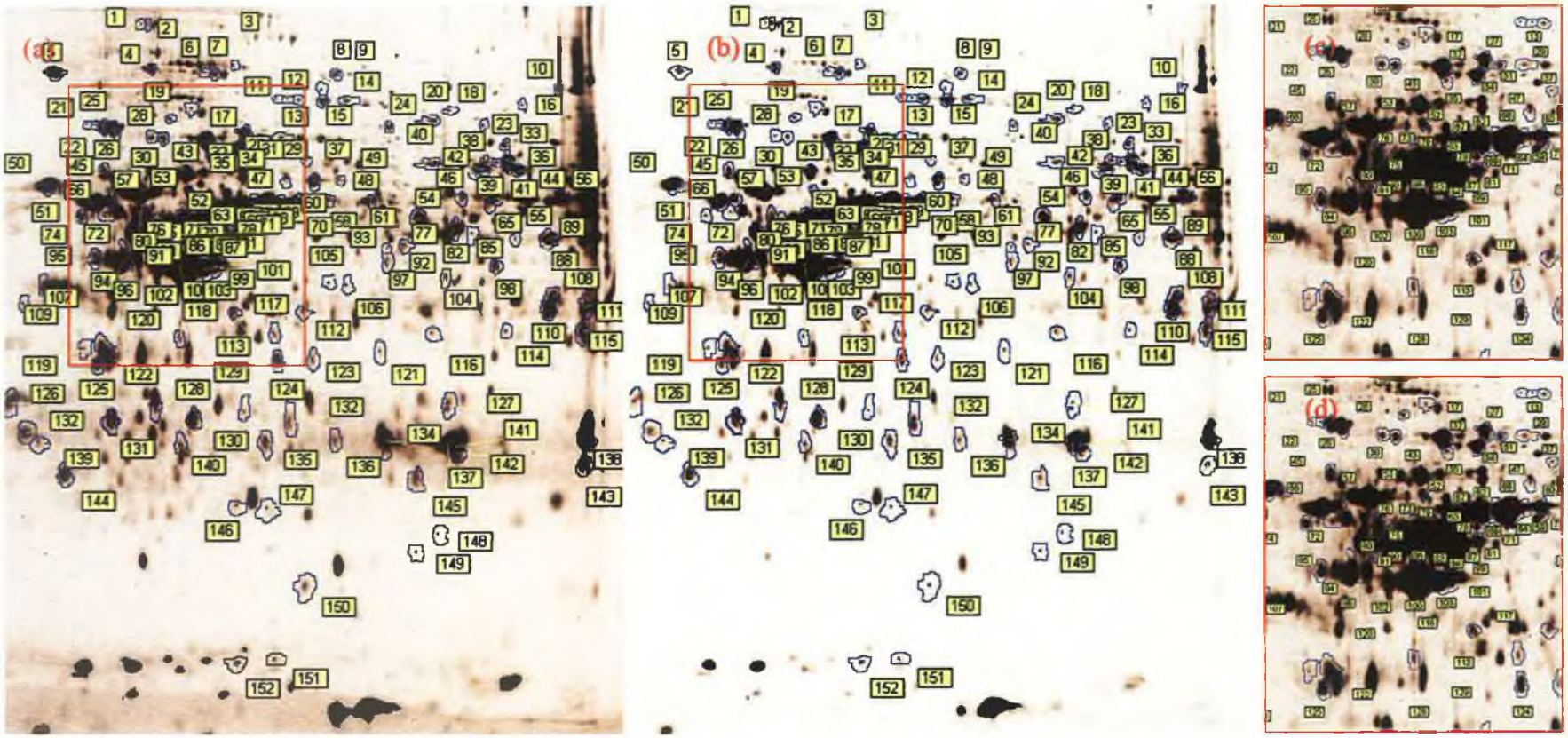

Figure 3.1.59: Images of representative DIGE gels from (a) MCF-7, (b) MCF-7 after 7 days treatment with 5-FU, (c) close up region highlighted in 'image (a)' and (d) close up of image highlighted in 'image (b)'. Identified differentially regulated protein spots are encircled by blue lines and are given a protein number. Refer to table 3.1.13 for protein identification.

Figure 3.1.60: A pie chart demonstrating the number of proteins in each biological process in MCF-7 effected by exposure to 5-FU. Individual proteins in each biological process are included in table 3.1.13. Biological process information obtained from the human protein reference database.

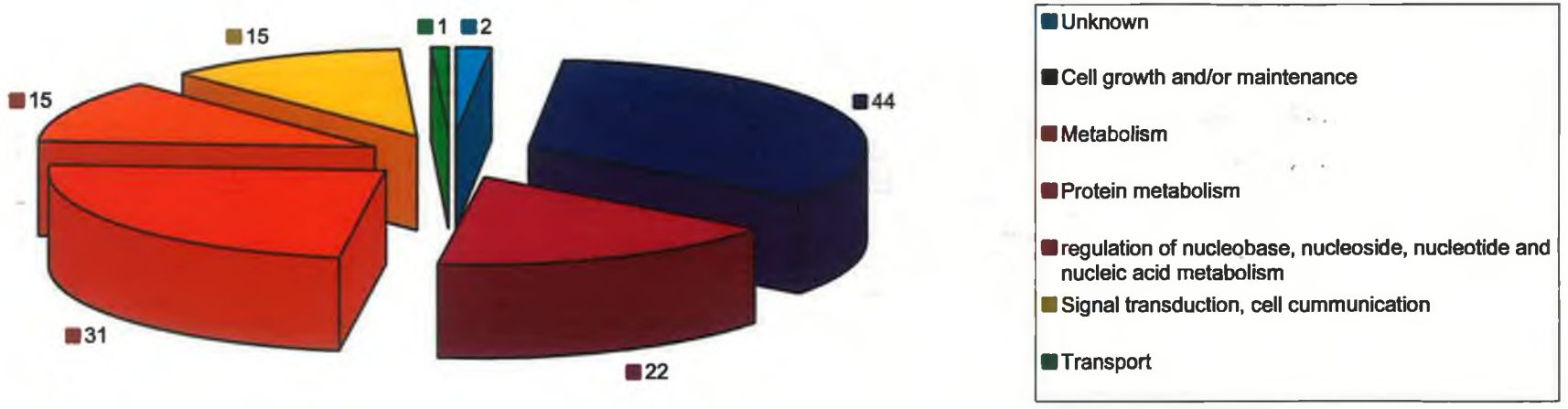

Table 3.1.13: Proteins identified by MALDI-ToF MS that were found to be differentially regulated in MCF-7 cells after 7 days exposure to 5-FU. Protein expression data is included in table (fold change and t-test) as well Protein location on 2D gels (see figure 3.1.13.4.1 for locations). GI accession number was obtained from MS data and protein name, Gene symbol was found from DAVID database, Human protein reference database or swissprot. Molecular and biological functions were obtained from the human protein reference database. Unknown/unnamed proteins (an artefact of poorly updated databases) names were determined as described in section 2.16.13.3.

Protein location	**GI accession Number**	**Gene symbol**	**Name**	**T-test**	**Fold change**	**Molecular function**
Biological Function: Unknown						
21	gi|21071030|	A1BG	alpha 1B-glycoprotein [Homo sapiens]	$2.4x10^{-4}$	1.9	
122	gi|20271412|	TBC1D16	TBC1 domain family, member 16 [Homo sapiens]	$2.4x10^{-3}$	1.79	
Biological Function: Cell growth and/or maintenance						
144	gi|61679634|	TPT1	Chain A, Solution Structure Of Human Translationally Controlled Tumor Prote	$2.4x10^{-8}$	1.91	Calcium ion binding
20	gi|46249758|	VIL2	Villin 2 [Homo sapiens]	$8.7x10^{-5}$	3.46	cytoskeletal anchoring activity
23	gi|28436809|	RDX	Radixin [Homo sapiens]	$5.6x10^{-4}$	2.27	cytoskeletal protein binding
114	gi|2135552|	LASP1	Lasp-1 protein - human	$1.6x10^{-4}$	1.64	cytoskeletal protein binding
148	gi|30582531|	CFL1	cofilin 1 (non-muscle) [Homo sapiens]	$6.3x10^{-4}$	5.08	cytoskeletal protein binding
150	gi|62088144|	STMN1	stathmin 1 variant [Homo sapiens]	$7.2x10^{-9}$	-3.43	cytoskeletal protein binding
14	gi|8131894|	IMMT	mitofilin [Homo sapiens]	$2.7x10^{-4}$	2.79	Motor activity
19	gi|55250201|	DYNC1I2	cytoplasmic dynein intermediate chain 2C [Homo sapiens]	$8.4x10^{-3}$	1.59	Motor activity
11	gi|38044288|	GSN	gelsolin isoform b [Homo sapiens]	$2x10^{-3}$	4.03	Structural constituent of cytoskeleton
12	gi|38044288|	GSN	gelsolin isoform b [Homo sapiens]	$1.9x10^{-4}$	3.03	Structural constituent of cytoskeleton
13	gi|38044288|	GSN	gelsolin isoform b [Homo sapiens]	$1.7x10^{-6}$	7.35	Structural constituent of cytoskeleton

15	gi|38044288|	GSN	gelsolin isoform b [Homo sapiens]	$3.4x10^{-6}$	5.86	Structural constituent of cytoskeleton
28	gi|5031877|	LMNB1	lamin B1 [Homo sapiens]	$7.7x10^{-2}$	-1.24	structural molecule activity
45	gi|27227551|	TUBB2A	class II beta tubulin isotype [Homo sapiens]	$4x10^{-3}$	1.49	structural molecule activity
59	gi|39645331|	KRT8	KRT8 protein [Homo sapiens]	$1.3x10^{-3}$	2.1	structural molecule activity
60	gi|30313|	KRT8	cytokeratin 8 (279 AA) [Homo sapiens]	$4.6x10^{-3}$	2.19	structural molecule activity
62	gi|181400|	KRT8	cytokeratin 8	$1.8x10^{-3}$	2.39	structural molecule activity
63	gi|181400|	KRT8	cytokeratin 8	$3.4x10^{-3}$	3.25	structural molecule activity
64	gi|30313|	KRT8	cytokeratin 8 (279 AA) [Homo sapiens]	$1.8 x10^{-2}$	2.47	structural molecule activity
67	gi|181400|	KRT8	cytokeratin 8	$8.2 x10^{-4}$	2.68	structural molecule activity
68	gi|39645331|	KRT8	KRT8 protein [Homo sapiens]	$92 x10^{-3}$	2.02	structural molecule activity
69	gi|39645331|	KRT8	KRT8 protein [Homo sapiens]	$2 x10^{-2}$	2.87	structural molecule activity
71	gi|39645331|	KRT8	KRT8 protein [Homo sapiens]	$4.7 x10^{-3}$	2.37	structural molecule activity
73	gi|30313|	KRT8	cytokeratin 8 (279 AA) [Homo sapiens]	$5.4 x10^{-3}$	1.88	structural molecule activity
75	gi|181400|	KRT8	cytokeratin 8	$9.8 x10^{-7}$	2.36	structural molecule activity
76	gi|62897747|	KRT18	keratin 18 variant [Homo sapiens]	$3.5 x10^{-2}$	1.55	structural molecule activity
81	gi|6330926|	KRT18	Keratin 18 [Homo sapiens]	$3.1 x10^{-4}$	2.68	structural molecule activity
83	gi|12653819|	KRT18	Keratin 18 [Homo sapiens]	$3.6 x10^{-4}$	4.01	structural molecule activity
84	gi|62897747|	KRT18	keratin 18 variant [Homo sapiens]	$1.4x10^{-3.}$	2.27	structural molecule activity
86	gi|12653819|	KRT18	Keratin 18 [Homo sapiens]	$7.7 x10^{-5}$	1.8	structural molecule activity
87	gi|30311|	KRT18	cytokeratin 18 (424 AA) [Homo sapiens]	$1.9 x10^{-2}$	1.9	structural molecule activity
90	gi|30311|	KRT18	cytokeratin 18 (424 AA) [Homo sapiens]	$3 x10^{-3}$	1.39	structural molecule activity
91	gi|34039|	KRT19	unnamed protein product [Homo sapiens] keratin 19	$4.9 x10^{-3}$	3.79	structural molecule activity
93	gi|453155|	KRT9	keratin 9 [Homo sapiens]	$2.1 x10^{-2}$	2.71	structural molecule activity
94	gi|14043271|	KRT19	Keratin 19 [Homo sapiens]	$1.1 x10^{-3}$	2.5	structural molecule activity
95	gi|24234699|	KRT19	keratin 19 [Homo sapiens]	$6.7 x10^{-4}$	2.33	structural molecule activity

96	gi|24234699|	KRT19	keratin 19 [Homo sapiens]	5×10^{-2}	1.82	structural molecule activity
99	gi|34039|	KRT19	unnamed protein product [Homo sapiens] keratin 19	5.9×10^{-3}	1.61	structural molecule activity
100	gi|15277503|	ACTB	ACTB protein [Homo sapiens]	3.2×10^{-2}	1.33	structural molecule activity
101	gi|62897625|	ACTB	beta actin variant [Homo sapiens]	6.3×10^{-3}	1.64	structural molecule activity
103	gi|15277503|	ACTB	ACTB protein [Homo sapiens]	1.5×10^{-2}	1.53	structural molecule activity
121	gi|30311|	KRT18	cytokeratin 18 (424 AA) [Homo sapiens]	2×10^{-4}	2.17	structural molecule activity
147	gi|33150590|	MTCBP1	submergence induced protein 2 [Homo sapiens]	8.1×10^{-4}	-1.65	
Biological Function: Metabolism; Energy Pathway						
58	gi|643589|	DLST	dihydrolipoamide succinyltransferase [Homo sapiens]	5.8×10^{-3}	1.82	Acetyltransferase activity
149	gi|251370|	ACP1	acid phosphatase isoenzyme Af [human, erythrocytes, Peptide, 157 aa]	3.2×10^{-4}	1.55	Acid phosphatase activity
65	gi|62896511|	DARS	aspartyl-tRNA synthetase variant [Homo sapiens]	4.5×10^{-2}	1.62	ATPase activity
105	gi|40889569|	hemE	Uroporphyrinogen Decarboxylase Single Mutant D86g In Complex With	1.3×10^{-2}	2.04	Carboxyl-lyase activity
113	gi|387010|	PDHB	pyruvate dehydrogenase E1-beta subunit precursor	1×10^{-3}	1.39	Carboxyl-lyase activity
33	gi|62988942|	GPD2	unknown [Homo sapiens]	3.9×10^{-2}	1.72	Catalytic activity
55	gi|7546530|	G6PD	Chain H, X-Ray Structure Of Human Glucose 6-Phosphate Dehydrogenase	3×10^{-3}	2.18	Catalytic activity
56	gi|338827|	PKM2	cytosolic thyroid hormone-binding protein (EC 2.7.1.40)	3.3×10^{-2}	2.05	Catalytic activity
85	gi|62896593|	ENO1	enolase 1 variant [Homo sapiens]	2.1×10^{-2}	1.97	Catalytic activity
142	gi|459815|	HPRT1	hypoxanthine phosphoribosyltransferase	1.8×10^{-3}	1.3	Catalytic activity

146	gi|71773201|	APRT	adenine phosphoribosyltransferase isoform b [Homo sapiens]	1.6×10^{-5}	1.77	Catalytic activity
41	gi|14250818|	ATIC	5-aminoimidazole-4-carboxamide ribonucleotide formyltransferase/IMP cycl	7.8×10^{-3}	1.57	Hydrolase activity
92	gi|10241525|	AHCY	AHCY [Homo sapiens]	5.2×10^{-3}	1.8	Hydrolase activity
110	gi|1311149|	FBP1	Chain D, Fructose-1,6-Bisphosphatase(D-Fructose-1,6-Bisphosphate, 1-Phosphoh	1.9×10^{-2}	1.53	Hydrolase activity
137	gi|56204402|	PRDX6	peroxiredoxin 6 [Homo sapiens]	1.3×10^{-3}	2.13	Peroxidase activity
116	gi|47168568|	NP	Chain E, Crystal Structure Of Human Pnp Complexed With Acyclovir	2.8×10^{-4}	2.93	phosphorylase activity
57	gi|32189394|	ATP5B	ATP synthase, H+ transporting, mitochondrial F1 complex, beta subunit	4×10^{-3}	1.67	Transporter activity
72	gi|28940|	ATP5B	unnamed protein product [Homo sapiens] ATP synthase	4×10^{-2}	1.5	Transporter activity
39	gi|23200451|	CBS	Chain F, Cystathionine-Beta Synthase: Reduced Vicinal Thiols	8.8×10^{-3}	2.74	
108	gi|8453156|	NANS	N-acetylneuraminic acid phosphate synthase [Homo sapiens]	1.4×10^{-3}	1.65	
Biological Function: Protein Metabolism						
29	gi|10933784|	RNPEP	aminopeptidase B [Homo sapiens]	2×10^{-3}	2.73	Aminopeptidase activity
129	gi|5822091|	CTSD	Chain H, Cathepsin D At Ph 7.5	1.8×10^{-5}	1.62	Aspartic-type signal peptidase activity
130	gi|30582659|	CTSD	cathepsin D (lysosomal aspartyl protease) [Homo sapiens]	6.5×10^{-7}	2.19	Aspartic-type signal peptidase activity
132	gi|30582659|	CTSD	cathepsin D (lysosomal aspartyl protease) [Homo sapiens]	5×10^{-6}	2.62	Aspartic-type signal peptidase activity
1	gi|1794219|	HYOU1	150 kDa oxygen-regulated protein ORP150 [Homo sapiens]	1.4×10^{-4}	3.49	Chaperone activity

2	gi|10720185|	HYOU1	150 kDa oxygen-regulated protein precursor (Orp150) (Hypoxia up-r	4.6×10^{-4}	3.97	Chaperone activity
4	gi|62087882|	HSPA4	heat shock 70kDa protein 4 isoform a variant [Homo sapiens]	6.5×10^{-3}	1.92	Chaperone activity
5	gi|62088648|	TRA1	tumor rejection antigen (gp96) 1 variant [Homo sapiens]	5×10^{-2}	1.81	Chaperone activity
6	gi|62897207|	AARS	alanyl-tRNA synthetase variant [Homo sapiens]	2×10^{-2}	2.31	Chaperone activity
7	gi|57209340|	ATG7	ubiquitin-activating enzyme E1 (A1S9T and BN75 temperature sensitivity	9.4×10^{-4}	3.77	Chaperone activity
9	gi|31077164|	HSPA4L	Heat shock 70 kDa protein 4L (Osmotic stress protein 94) (Heat s	2.7×10^{-3}	2.1	Chaperone activity
22	gi|1143492|	HSPA5	BiP [Homo sapiens]	2.5×10^{-2}	2.31	Chaperone activity
25	gi|1143492|	HSPA5	BiP [Homo sapiens]	1.2×10^{-3}	2.46	Chaperone activity
34	gi|5123454|	HSPA1B	heat shock 70kDa protein 1A [Homo sapiens]	2.3×10^{-2}	1.56	Chaperone activity
36	gi|58761484|	CCT3	chaperonin containing TCP1, subunit 3 isoform c [Homo sapiens]	5×10^{-2}	1.45	Chaperone activity
38	gi|62089036|	CCT6A	chaperonin containing TCP1, subunit 6A isoform a variant [Homo sapiens]	5.8×10^{-3}	1.92	Chaperone activity
40	gi|62087344|	CCT3	chaperonin containing TCP1, subunit 3 (gamma) variant [Homo sapiens]	3.8×10^{-3}	1.65	Chaperone activity
42	gi|62089036|	CCT6A	chaperonin containing TCP1, subunit 6A isoform a variant [Homo sapiens]	1.4×10^{-2}	1.91	Chaperone activity
134	gi|662841|	HSPB1	heat shock protein 27 [Homo sapiens]	4.1×10^{-4}	2.39	Chaperone activity
135	gi|662841|	HSPB1	heat shock protein 27 [Homo sapiens]	3.4×10^{-5}	2.47	Chaperone activity
43	gi|77702086|	HSPD1	heat shock protein 60 [Homo sapiens]	4.2×10^{-2}	-1.73	heat shock protein activity
52	gi|6996447|	HSPD1	chaperonin 60, Hsp60 [Homo sapiens]	3.2×10^{-2}	-1.84	heat shock protein activity
48	gi|1085373|	ER-60	protein disulfide-isomerase (EC 5.3.4.1)	5.8×10^{-3}	1.43	Isomerase activity

			ER60 precursor - human			
49	gi|2245365|	ER-60	ER-60 protein [Homo sapiens]	8.2×10^{-3}	1.55	Isomerase activity
50	gi|20070125|	P4HB	prolyl 4-hydroxylase, beta subunit [Homo sapiens]	3.3×10^{-3}	1.66	Isomerase activity
104	gi|13489087|	SERPINB1	serine (or cysteine) proteinase inhibitor, clade B (ovalbumin), member	3.3×10^{-2}	1.58	Protease inhibitor activity
118	gi|55646721|	SFRS1	splicing factor, arginine/serine-rich	2.7×10^{-3}	1.47	RNA binding
89	gi|2136315|	TUFM	translation elongation factor EF-Tu precursor - human	7.4×10^{-4}	1.83	Translation regulator activity
119	gi|25453474|	EEF1BD	eukaryotic translation elongation factor 1 delta isoform 1 [Homo sapie	3.5×10^{-4}	2.18	Translation regulator activity
120	gi|25453472|	EEF1BD	eukaryotic translation elongation factor 1 delta isoform 2 [Homo sapie	3.5×10^{-2}	1.58	Translation regulator activity
145	gi|15278174|	PSMB3	Proteasome beta 3 subunit [Homo sapiens]	3.1×10^{-4}	1.43	ubiquitin-specific protease activity
Biological function: Regulation of nucleobase, nucleoside, nucleotide and nucleic acid metabolism						
98	gi|30582415|	ADK	adenosine kinase [Homo sapiens]	7.6×10^{-3}	1.43	Catalytic activity
127	gi|55958718|	HMGB1	high-mobility group box 1 [Homo sapiens]	2.2×10^{-2}	1.54	DNA binding
51	gi|62898690|	RAD23B	UV excision repair protein RAD23 homolog B variant [Homo sapiens]	1.9×10^{-2}	1.76	DNA repair protein
136	gi|55650119|	LOC456359	PREDICTED: similar to DNA-directed RNA polymerase II 23 kDa polypeptid	1.5×10^{-5}	2.28	DNA-directed RNA polymerase
82	gi|40788956|	DDX48	KIAA0111 [Homo sapiens] eIF4AIII	1.1×10^{-3}	1.73	NMD of mRNA
35	gi|62896771|	G3BP	Ras-GTPase-activating protein SH3-domain-binding protein variant [Homo	3.7×10^{-2}	2.27	Ribonuclease activity
47	gi|55958547|	HNRPK	heterogeneous nuclear	2.4×10^{-2}	1.68	Ribonucleoprotein

			ribonucleoprotein K [Homo sapiens]			
61	gi|12655001|	HNRPH1	HNRPH1 protein [Homo sapiens]	4.3×10^{-3}	1.36	Ribonucleoprotein
79	gi|15990432|	HNRPF	HNRPF protein [Homo sapiens]	1.7×10^{-5}	2.34	Ribonucleoprotein
54	gi|46370086|	TCF12	transcription factor 12 isoform c [Homo sapiens]	2.9×10^{-3}	2.55	Transcription factor activity
109	gi|2564242|	NFYC	CCAAT transcription binding factor, gamma subunit [Homo sapiens]	1.5×10^{-3}	1.93	Transcription factor activity
74	gi|4506439|	RBBP7	retinoblastoma binding protein 7 [Homo sapiens]	5.8×10^{-3}	-1.62	Transcription regulator activity
151	gi|3318698|	Crabp2	Chain B, Apo-Cellular Retinoic Acid Binding Protein Ii	6.6×10^{-6}	2.12	Transcription regulator activity
152	gi|3318698|	Crabp2	Chain B, Apo-Cellular Retinoic Acid Binding Protein Ii	1.2×10^{-8}	2.48	Transcription regulator activity
18	gi|51094603|	MCM7	MCM7	3.7×10^{-2}	-1.97	
Biological Function: Signal transduction, cell communication						
31	gi|71773415|	ANXA6	annexin VI isoform 2 [Homo sapiens]	1.9×10^{-2}	2.1	Calcium ion binding
111	gi|56967119|	ANXA2	Chain B, Structure Of Human Annexin A2 In The Presence Of Calcium Ions	1.4×10^{-5}	1.68	Calcium ion binding
115	gi|56967119|	ANXA2	Chain B, Structure Of Human Annexin A2 In The Presence Of Calcium Ions	3.3×10^{-2}	1.29	Calcium ion binding
117	gi|1421662|	ANXA3	Annexin Family Mol_id: 1; Molecule: Annexin Iii; Chain: Null; Engineered: Yes;	1.3×10^{-5}	2.17	Calcium ion binding
123	gi|1703319|	ANXA4	Annexin A4 (Annexin IV) (Lipocortin IV) (Endonexin I) (Chromobind	2.2×10^{-2}	1.52	Calcium ion binding
124	gi|1421662|	ANXA3	Annexin Family Mol_id: 1; Molecule: Annexin Iii; Chain: Null; Engineered: Yes;	5×10^{-2}	1.43	Calcium ion binding

37	gi|32483399|	PAK2	p21-activated kinase 2 [Homo sapiens]	5.8×10^{-4}	2.58	protein serine/threonine kinase activity
112	gi|6537210|	PPP6C	serine/threonine protein phosphatase catalytic subunit [Homo sapiens]	2.3×10^{-3}	1.56	protein serine/threonine phophatase activity
44	gi|54696884|	STIP1	stress-induced-phosphoprotein 1 (Hsp70/Hsp90-organizing protein) [Homo s	1×10^{-2}	1.76	Receptor signalling complex scaffold activityactivity
46	gi|54696884|	STIP1	stress-induced-phosphoprotein 1 (Hsp70/Hsp90-organizing protein) [Homo s	3.4×10^{-3}	1.55	Receptor signalling complex scaffold activityactivity
131	gi|46015374|	ARHGDIB	Chain D, Crystal Structure Of Rhogdi K(199,200)r Double Mutant	2.5×10^{-5}	1.74	Receptor signalling complex scaffold activityactivity
132	gi|82407958|	YWHAG	Chain F, Crystal Structure Of 14-3-3 Gamma	3.3×10^{-2}	1.53	Receptor signalling complex scaffold activityactivity
139	gi|68085578|	YWHAZ	Tyrosine 3/tryptophan 5 - monooxygenase activation protein, zeta	1.4×10^{-3}	1.66	Receptor signalling complex scaffold activityactivity
107	gi|34234|	RPSA	laminin-binding protein [Homo sapiens]	1×10^{-2}	-1.33	ribosomal subunit
97	gi|16904374|	RIS1	Ras-induced senescence 1 [Homo sapiens]	1.8×10^{-2}	1.86	Unknown
Biological Function: Transport						
128	gi|4588526|	CLIC1	nuclear chloride channel [H. sapiens]	3.5×10^{-4}	1.86	intracellular ligand-gated ion channel

Protein modifications such as protein phosphorylation alter the pI of proteins and thus contribute to the various isoforms identified for apparently the same protein. MALDI-ToF MS is not capable of distinguishing between such modifications. Pro-Q diamond is a fluorescent dye that selectively binds to phosphorylated residues of serine, threonine and tyrosine. For analysis of proteins being differentially regulated in this experiment a pooled sample of both control and treated was separated by 2D electrophoresis and stained and matched to the BVA as described in section 2.16.10. Proteins that were deemed phosphorylated at serine/threonine/thyrosine are indicates in figure 3.1.61 and are summarised in Table 3.1.14. Phosphorylation data is listed in same table where available.

Figure 3.1.61: 2D-Gel images of (a) RuPBS stained and (b) Pro-Q diamond stained protein sample pool of MCF-7 and MCF-7 treated with 5-FU (c) close up view of region in red box in "image (a)", and (d) close up view of region in red box in "image (a)". Phosphorylated proteins are stained with Pro-Q diamond stain while all proteins are stained with RuPBS.

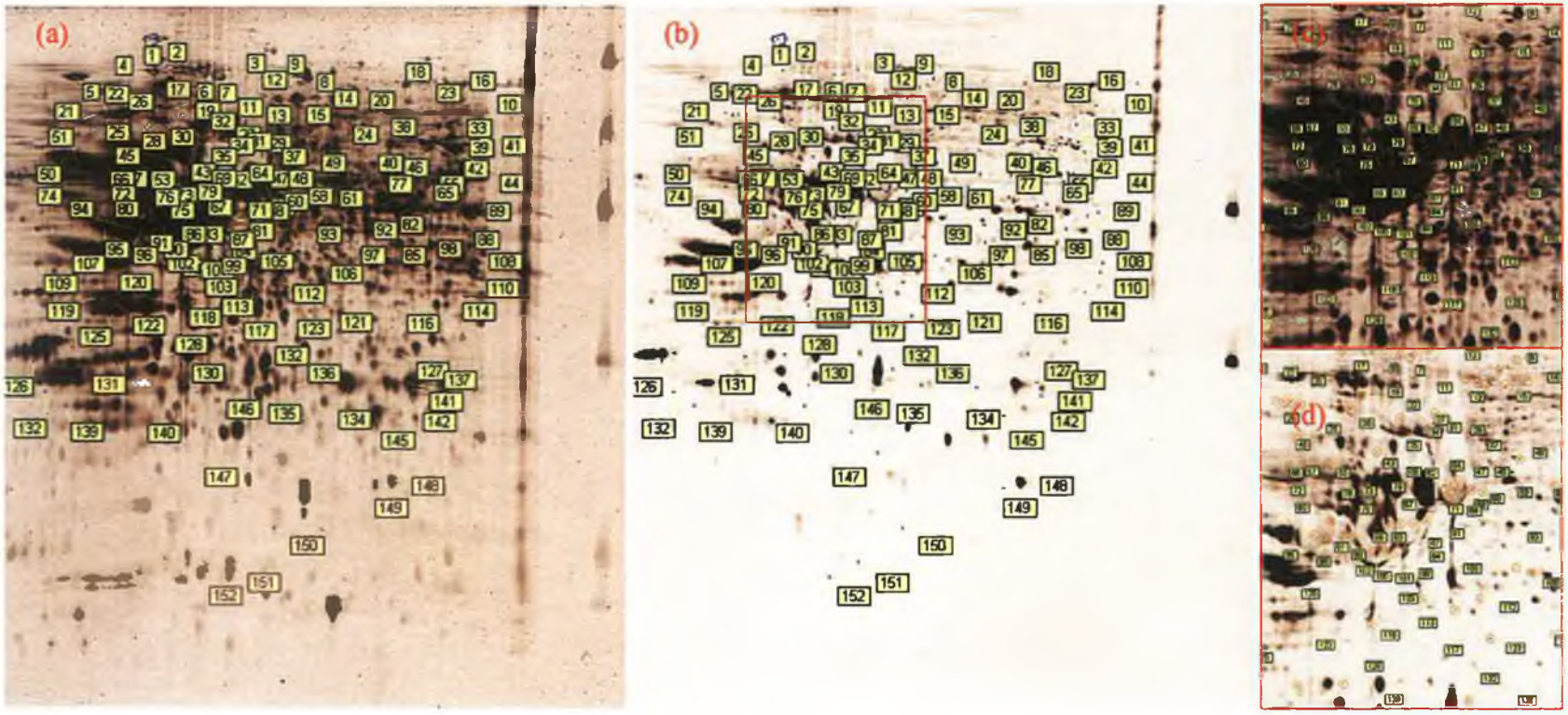

Table 3.1.14: list of proteins differentially expressed proteins from the MCF-7 5-FU treatment DIGE experiment that were found to be phosphorylated by Pro-Q diamond staining. Known phosphorylation sites are listed and protein kinases and phosphorylases.

Location on 2D gel	Gene Symbol	GI accession number	Protein Name	Fold change	Known phospho site	Kinases/ phosphorylase	Implication of phosphorylation
19		gi|55250201|	cytoplasmic dynein intermediate chain 2C [Homo sapiens]	1.59	?	?	?
35	G3BP	gi|62896771|	Ras-GTPase-activating protein SH3-domain-binding protein variant [Homo	2.27	S149 S231 S231 S232	? ? ? ?	Nuclear localisation ? ? ?
37	PAK2	gi|32483399|	p21-activated kinase 2 [Homo sapiens]	2.58	S19 S20 S55 Y130 S141 S192 S197 T403	PAK2 PAK2 PAK2 Src PAK2 PAK2 PAK2 PAK2	
67	KRT8	gi|181400|	cytokeratin 8	2.68	S21 S22 S24 S37 S43 S74 S432	 MAPK14 MAPK14 MAPK14 ERK2 P38 kinase	
69	KRT8	gi|39645331|	KRT8 protein [Homo sapiens]	2.87	S23 S74 S432	MAPK14 ERK2 P38 kinase	
75	KRT8	gi|181400|	cytokeratin 8	2.36	S23 S74 S432	MAPK14 ERK2 P38 kinase	
76	KRT18	gi|62897747|	keratin 18 variant [Homo sapiens]	1.55	S34 S53	CDC2 CAMK2A	

					S53 S53 S53	RPS6KA3 PRKCE PRKCA	
79	HNRPF	gi|15990432|	HNRPF protein	2.34	S310		
86	KRT18	gi|12653819|	Keratin 18 [Homo sapiens]	1.8	S34 S53 S53 S53 S53	CDC2 CAMK2A RPS6KA3 PRKCE PRKCA	
95	KRT19	gi|24234699|	keratin 19 [Homo sapiens]	2.33	S10 S35 S36	? ? ?	? ? ?
109	NFYC	gi|2564242|	CCAAT transcription binding factor, gamma subunit [Homo sapiens]	1.91	?	?	?
119	EEF1BD	gi|25453474|	eukaryotic translation elongation factor 1 delta isoform 1 [Homo sapie	2.18	S449	CDC2	?
120	EEF1BD	gi|25453474|	eukaryotic translation elongation factor 1 delta isoform 2 [Homo sapie	1.58	S449	CDC2	?
135	HSPB1	gi|662841|	heat shock protein 27 [Homo sapiens]	2.47	S15 S78 S82	MAPKAPK2 MAPKAPK2 MAPKAPK2	Clell survival (actin stability)
141	PSMA6	gi|8394076|	proteasome (prosome, macropain) subunit, alpha type 6 [Rattus norvegicu	1.68	?	?	?
148	CFLN1	gi|30582531|	cofilin 1 (non-muscle) [Homo sapiens]	5.08	S3 S3 S3	PAK2 LIMK1/2 TESK1/2	Actin remodelling

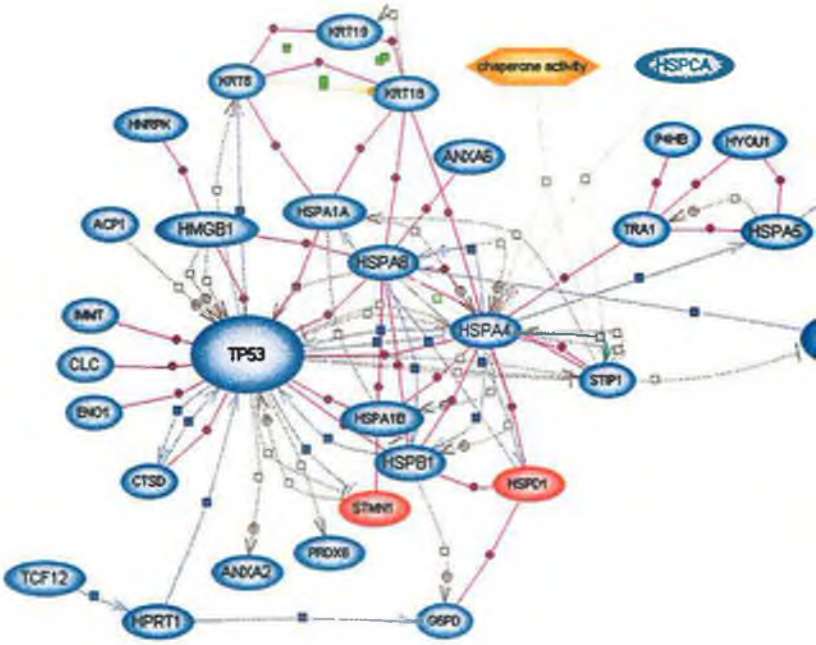
KRT19
KRT8
KRT18
chaperone activity
HSPCA
HNRNPK
ANXA5
PHB
HYOU1
ACP1
HMGB1
HSPA1A
TRA1
HSPA5
HSPA8
IMMT
TP53
HSPA4
CLC
STIP1
ENO1
HSPA1B
HSPB1
CTSD
HSPD1
STMN1
PRDX6
ANXA2
TCF12
HPRT1
G6PD

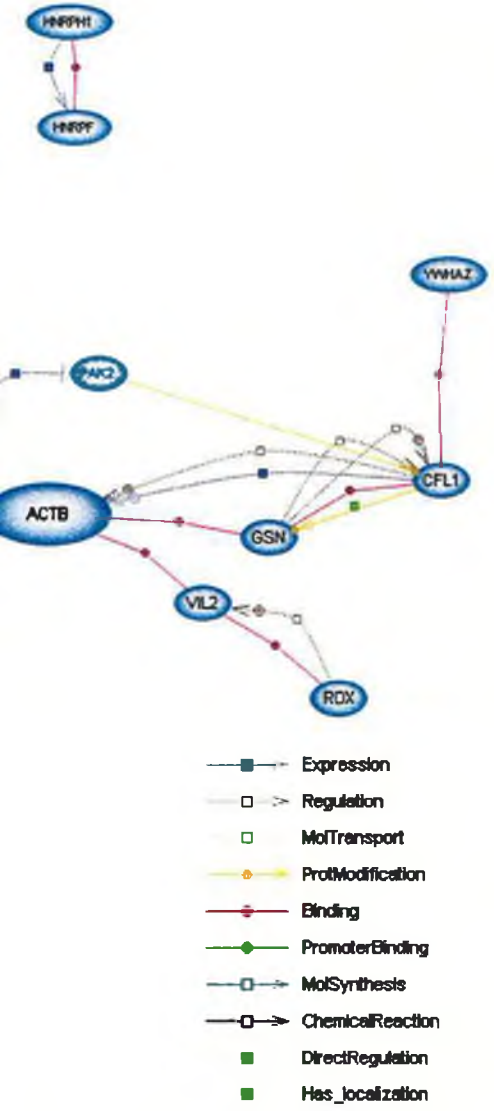

Figure 3.1.62: Figure shows direct interactions known between proteins found to be differentially regulated in the MCF-7 5-FU exposure 2D-DIGE experiment, the protein p53 was included in protein list as it was found to be up regulated by western blot. Proteins in blue are up regulated and those in red are down regulated. Blue arrows indicate positive regulation. Purple lines indicate binding partners, green arrows indicate protein modifies another protein and green arrows with green boxes indicate proteins localise a protein. Direct interaction pathway was generated using Pathway assist software.

Figure 3.1.62 was generated by pathway assist and shows the direct interactions between differentially regulated protein isoforms listed in table 3.1. In summary, direct interactions were identified between 42 of the proteins listed. These proteins that are listed are involved in intermediate filament dynamics of Keratin, Lamins, Actin and tubulin and include LMNA, STMN1, ACTB, YWHAZ, CFLN1, and GSN. The HSP protein, HSPA1A, HSPA8, STIP1 and HSPA4 are direct interactors with p53 and stabilise it in the cytoplasm {Manceau, et al., 1999; Fourie, et al.,1997; Scheufler, et al., 2000; Wang, et al., 2003; Peng, et al., 2001; Wadhwa, et al., 2002; Liao, et al., 1995; Selkirk, et al., 1994}. HSPB1 promotes cell survival through several mechanisms and is regulated by various stresses {Parcellier, et al., 2006}. TRA1 associates with HSPA5, P4HB and HSPA4 and is important in the folding of secretory proteins {Meunier, et al., 2002} PAK2 when activated by phosphorylation directly phosphorylates cofilin {Misra, et al., 2005}. Figure 3.1.48 shows both cofilin and PAK2 proteins are phosphorylated. p53 bound to DNA is stabilised by binding of HMGB1 and HNRPK and participate in transcription together . All proteins are up regulated and suggest there cooperation in transcription

3.1.11 Proteomic analysis of HMEC exposed to 5-FU for 7 days

As already stated, proteomic analysis of breast cell lines treated with 5-FU is not described in the literature and thus investigation of the proteomic alterations induced by 5-FU would substantially contribute to the understanding in the field. Characterisation of proteomic alterations induced in normal breast cells treated with 5-FU would expand the understanding of how normal breast cells respond to 5-FU exposure. In addition, data obtained from this experiment would contribute greatly to the understanding of how normal cells respond to 5-FU treatment and how generally cells respond to 5-FU treatment in conjunction with other experiments.

In order to compare the alterations induced in the proteome of HMEC after 7 days treatment with 5-FU protein samples were prepared from HMEC and HMEC after 7 days treatment with 5-FU at the concentrations of 10μM and 30μM(see materials and methods for conditions). These were prepared in biological triplicate. Each biological triplicate was run in technical duplicates. Sample labelling with Cy dyes is shown in table 3.1.15.

Table 3.1.15: Ettan DIGE experimental design for the analysis of differential protein expression induced in A549 by exposure to 5-FU for 7 days.

Gel number	CY2 label	CY3 label	CY5 label
1	Pooled internal standard (50μg of protein)	HMEC (50μg of protein)	HMEC 5-FU 10μM (50μg of protein)
2	Pooled internal standard (50μg of protein)	HMEC (50μg of protein)	HMEC 5-FU 30μM (50μg of protein)
3	Pooled internal standard (50μg of protein)	HMEC (50μg of protein)	HMEC 5-FU 10μM (50μg of protein)
4	Pooled internal standard (50μg of protein)	HMEC 5-FU 10μM (50μg of protein)	HMEC (50μg of protein)
5	Pooled internal standard (50μg of protein)	HMEC 5-FU 10μM (50μg of protein)	HMEC 5-FU 30μM (50μg of protein)
6	Pooled internal standard (50μg of protein)	HMEC 5-FU 10μM (50μg of protein)	HMEC 5-FU 30μM (50μg of protein)

7	Pooled internal standard (50µg of protein)	HMEC 5-FU 30µM (50µg of protein)	HMEC 5-FU 10µM (50µg of protein)
8	Pooled internal standard (50µg of protein)	HMEC 5-FU 30µM (50µg of protein)	HMEC (50µg of protein)
9	Pooled internal standard (50µg of protein)	HMEC 5-FU 30µM (50µg of protein)	HMEC (50µg of protein)

Images were scanned using the typhoon scanner and were processed and imported into Decyder (see materials and methods). Protein spots in gels were semi-automatically matched (i.e. matched automatically by the software and reviewed individually by user to ensure matching was correct, spots that were not matched properly were corrected) using Biological Variation Analysis (BVA), a software component of the Decyder software. Proteins with a fold change of greater than 1.2 and less than -1.2 with a t-test less than 0.01 were deemed significant. Proteins with a fold chane gretar than 1.5 and less than -1.5 with a t-test less than 0.05 were deemed significant. A total of 361 protein spots were found to have statistically significant fold changes were marked as "pick" and this list of proteins is referred to as "the pick list". Preparative gels were prepared as described in materials and methods and the pick list in the BVA was manually matched to each preparative gel. Identified proteins were imputed back into the BVA. A total of 29 proteins were identified by MALDI-ToF MS. Locations of Identified proteins from the pick list in this experiment can be seen in figure 3.1.64 and the identity of these proteins can be seen in table 3.1.16. Proteins were identified using MALDI-ToF MS and this data is included in the appendices.

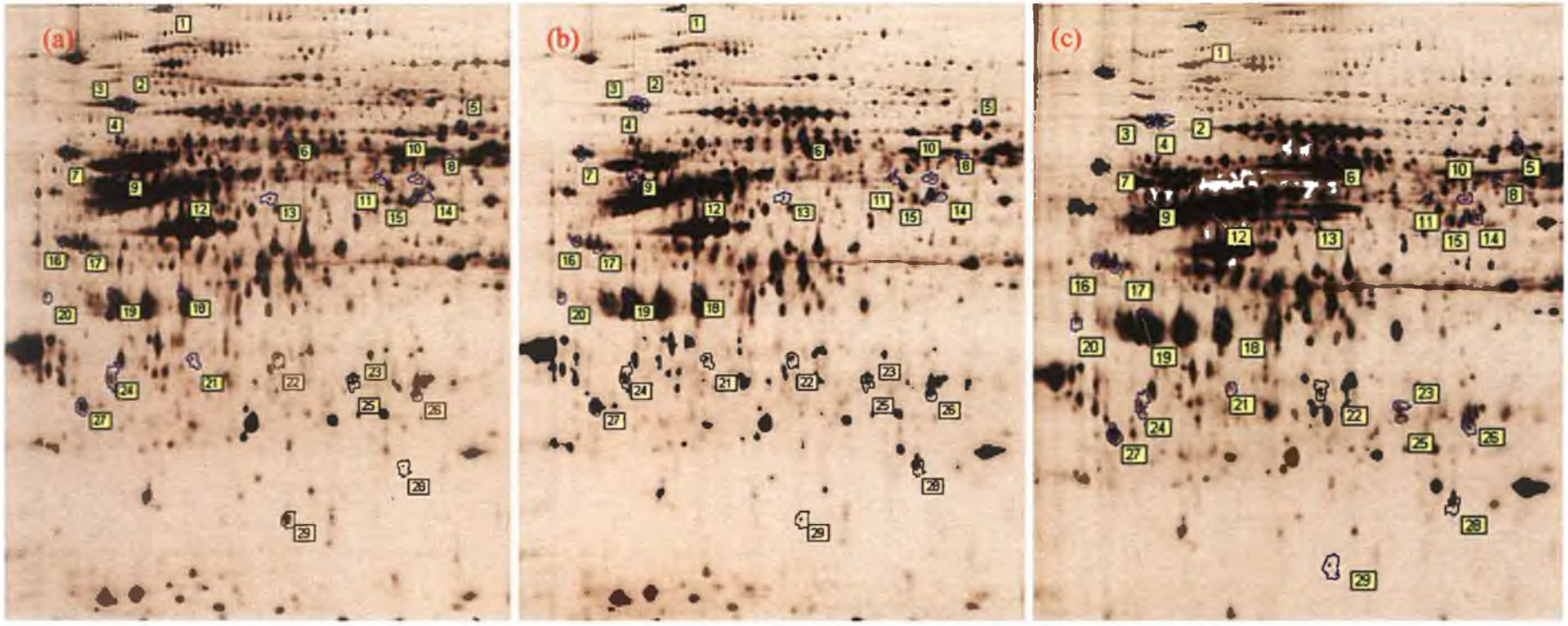

Figure 3.1.64: Images of representative DIGE gels from (a) HMEC, (b) HMEC after 7 days treatment with 10μM 5-FU, and (c) HMEC after 7 days treatment with 30μM 5-FU. Identified differentially regulated protein spots are encircled by blue lines and are given a protein number. Refer to table 3.1.14 for protein identification.

Figure 3.1.65: A pie-chart demonstrating the number of proteins in each biological process in HMEC affected by exposure to 5-FU. Individual proteins in each biological process are included in table 3.1.15. Biological process information obtained from the human protein reference database.

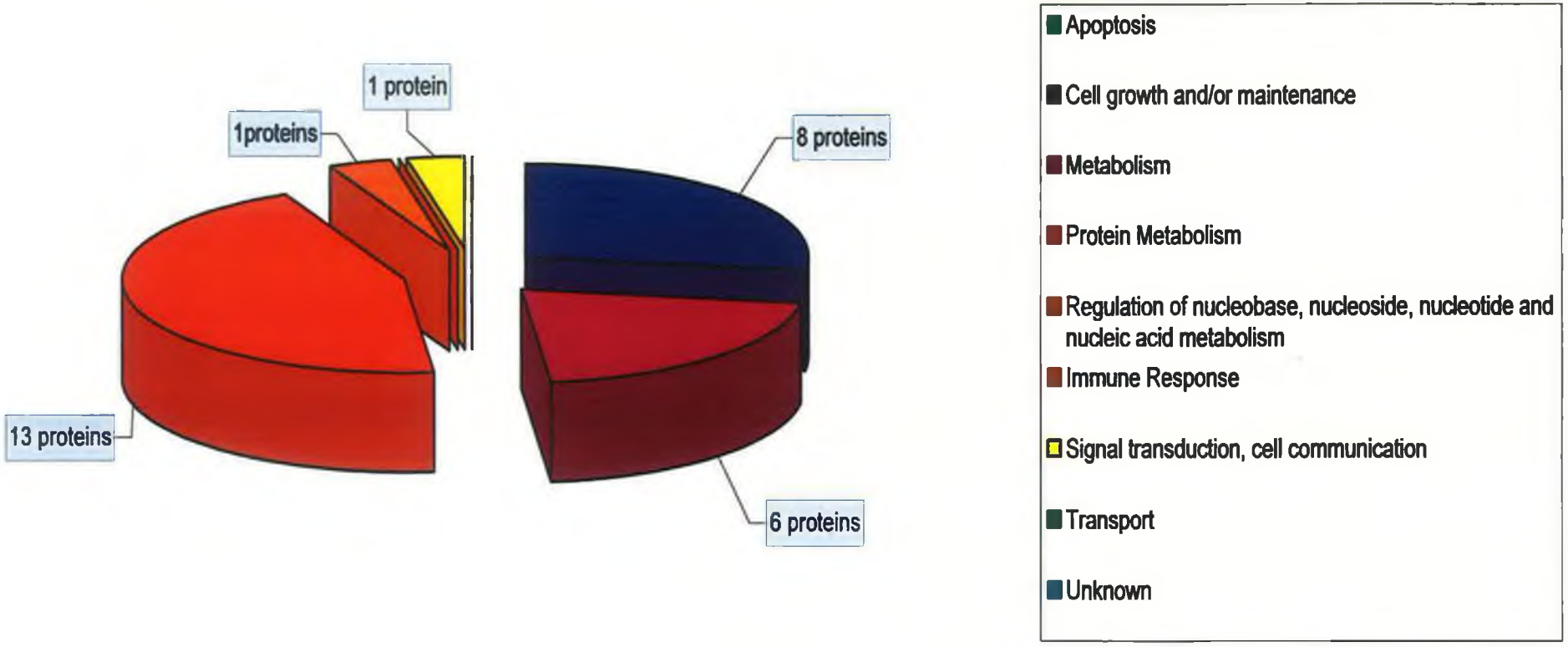

Table 3.1.16: Proteins identified by MALDI-ToF MS that were found to be differentially regulated in HMEC cells after 7 days exposure to 5-FU. Protein expression data is included in table (fold change and t-test) as well Protein location on 2D gels (see figure 3.1.13.4.1 for locations). GI accession number was obtained from MS data and protein name, Gene symbol was found from DAVID database, Human protein reference database or swissprot. Molecular and biological functions were obtained from the human protein reference database.

Location on 2D Gels	Gene Symbol	GI Accession	Protein Name	HMEC 10μM 5-FU		HMEC 30μM 5-FU		Molecular Function
				Fold Change	T-test	Fold Change	T-test	
Cell growth and/or maintainance								
27	TPT1	gi|33285832|	Translation controlled tumour protein TCTP [Homo sapiens]	2.14	$2.1x10^{-7}$	2.26	$2.5 x10^{-8}$	Calcium ion binding
28	CFL1	gi|30582531|	cofilin 1 (non-muscle) [Homo sapiens]	10.71	$5.7x10^{-11}$	7.85	$4.1 x10^{-8}$	cytoskeletal protein binding
29	STMN1	gi|5031851|	stathmin 1 [Homo sapiens]	-3.18	$1.1x10^{-8}$	-3.19	$1.1 x10^{-9}$	cytoskeletal protein binding
9	TUBB	gi|338695|	beta-tubulin	-2.34	$7.9x10^{-6}$	-2.36	$2.9 x10^{-5}$	cytoskeletal protein binding
6	WDR1	gi|3420181|	WDR1 protein [Homo sapiens]	2.47	$3.2x10^{-5}$	3.47	$2.1 x10^{-7}$	cytoskeletal protein binding
10	KRT6A	gi|15559584|	Keratin 6A [Homo sapiens]	2.01	$2.2x10^{-4}$	2.07	$3 x10^{-4}$	structural molecule activity
12	KRT14	gi|30583211|	keratin 14 (epidermolysis bullosa simplex, Dowling-Meara, Koebner) [Homo sapiens]	1.39	$3.7x10^{-2}$	1.56	$9.8 x10^{-4}$	structural molecule activity
13	KRT17	gi|21754583|	unnamed protein product [Homo sapiens]	2.04	$4.3x10^{-2}$	1.94	$1.9 x10^{-2}$	structural molecule activity
Metabolism; Energy pathway								
8	ALDH1A3	gi|46621670|	Aldehyde dehydrogenase 1A3 [Homo sapiens]	2.47	$5.9x10^{-5}$	2.7	$3.3 x10^{-6}$	Catalytic activity
24	CAPNS1	gi|18314496|	Calpain, small subunit 1 [Homo sapiens]	1.62	$7.0x10^{-5}$	1.75	$6.0 x10^{-5}$	Catalytic activity
17	SMS	gi|791051|	spermine synthase [Homo sapiens]	-1.22	$2.4x10^{-3}$	-1.33	$3.3 x10^{-4}$	
11	DARS	gi|78394948|	DARS protein [Homo sapiens]	1.71	$1.4x10^{-3}$	2.14	$1.8 x10^{-4}$	ATPase activity
5	GPD2	gi|62988942|	unknown [Homo sapiens]	1.68	$1.6x10^{-5}$	1.59	$2.9 x10^{-3}$	Catalytic activity
26	HPRT1	gi|459815|	hypoxanthine phosphoribosyltransferase	1.3	$9.6x10^{-3}$	1.47	$9.7 x10^{-5}$	Catalytic activity
Protein metabolism								

21	CTSD	gi|30582659|	cathepsin D (lysosomal aspartyl protease) [Homo sapiens]	2.42	$5.3x10^{-8}$	2.47	$2.9 x10^{-8}$	Aspartic-type signal peptidase activity
22	CTSD	gi|30582659|	cathepsin D (lysosomal aspartyl protease) [Homo sapiens]	1.92	$5.8x10^{-6}$	1.9	$3.0 x10^{-7}$	Aspartic-type signal peptidase activity
2	HSPA5	gi|6470150|	BiP protein [Homo sapiens]	-1.45	$3.5x10^{-7}$	-1.46	$2.3 x10^{-6}$	Chaperone activity
3	HSPA5	gi|6470150|	BiP protein [Homo sapiens]	-1.52	$6.7x10^{-7}$	-1.46	$6.6 x10^{-6}$	Chaperone activity
1	HYOU1	gi|47938913|	HYOU1 protein [Homo sapiens]	-1.82	$1.3x10^{-6}$	-2.12	$1.4 x10^{-7}$	Chaperone activity
23	HSPB1	gi|15928913|	Unknown (protein for IMAGE:3906970) [Homo sapiens]	1.52	$3.5x10^{-6}$	1.69	$3.3 x10^{-6}$	Chaperone activity
25	HSPB1	gi|15928913|	Unknown (protein for IMAGE:3906970) [Homo sapiens]	2.08	$3.3x10^{-4}$	2.75	$8.7 x10^{-5}$	Chaperone activity
4	HSPA5	gi|6470150|	BiP protein [Homo sapiens]	-1.45	$2.4x10^{-3}$	-1.51	$4 x10^{-4}$	Chaperone activity
7	P4HB	gi|48735337|	Prolyl 4-hydroxylase, beta subunit [Homo sapiens]	-1.47	$1.2x10^{-5}$	1.55	$2.4 x10^{-6}$	Isomerase activity
18	SFRS1	gi|55646721|	PREDICTED: similar to splicing factor, arginine/serine-rich 1 (ASF/SF2)	1.77	$1.0x10^{-2}$	2	$2 x10^{-3}$	RNA binding
15	EEF1BG	gi|15530265|	Eukaryotic translation elongation factor 1 gamma [Homo sapiens]	2.46	$3.7x10^{-6}$	2.49	$9.9 x10^{-6}$	Translation regulator activity
19	EEF1BD	gi|25453472|	eukaryotic translation elongation factor 1 delta isoform 2 [Homo sapiens]	2.25	$4.8x10^{-5}$	2.74	$4.6 x10^{-8}$	Translation regulator activity
20	TPM1	gi|825723|	tropomyosin (227 AA) [Homo sapiens]	3.26	$5.4x10^{-5}$	2.96	$6.1 x10^{-5}$	Translation regulator activity
regulation of nucleobase, nucleoside, nucleotide and nucleic acid metabolism								
14	DDX48	gi|60655857|	DEAD-box polypeptide 48 [synthetic construct]	2.07	$2.1x10^{-3}$	2.64	$1.4 x10^{-4}$	NMD of mRNA
Signal transduction, cell communication								
16	RPSA	gi|34234|	laminin-binding protein [Homo sapiens]	-1.46	$1.0x10^{-3}$	-1.56	$2.3 x10^{-6}$	ribosomal subunit

Proteins listed in table 3.1.15 were converted to their gene symbols using the DAVID database conversion tool and were imported into Pathway Assist. The gene list was processed to determine direct interactions between proteins. A summary image can be seen in figure 3.1.66.

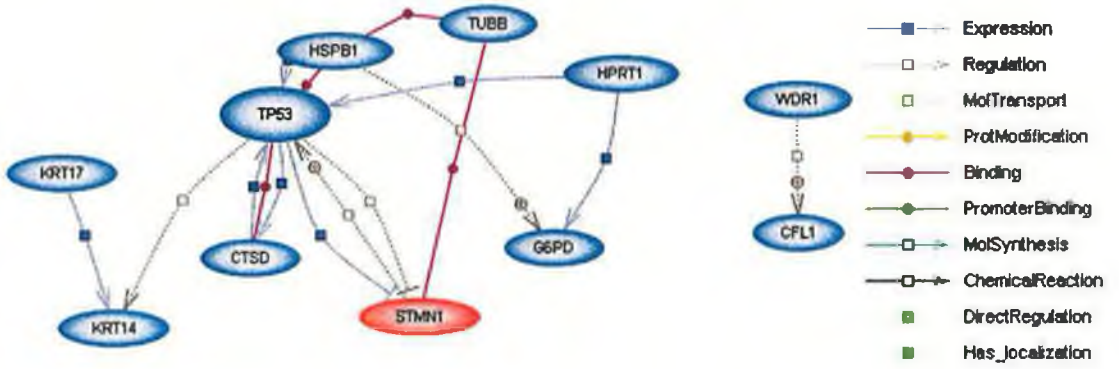

Figure 3.1.66: Figure shows direct interactions known between proteins found to be differentially regulated in the HMEC 5-FU exposure 2D-DIGE experiment, the protein p53 was included in protein list as it was found to be up regulated by western blot.

In summary 5-FU induces genotoxic stress which leads to DNA lesions and the generation of reactive oxygen species. This triggers Cathepsin D to induce cytochrome C release from the mitochondria. HSPB1 is upregulated and inhibits apoptosis at this point by sequestering cytochrome c, further more HSPB1 induces the upregulation of Glucose 6 phosphate dehydrogenase which generates NADPH and reduces the extent of ROS damage. Increased expression of the epithelial markers are observed, KRT 14 and 17, which promote cell survival.

3.1.12 Validation of proteomics data by western blot

In order to validate expression observed by 2D-DIGE and identifications by MALDI-ToF several western blots were carried out on protein lysates separated by SDS PAGE aswell as on 2DE-separated samples, respectively.

The expression BiP/HSPA5 and GSN were investigated to confirm expression trends.

Figure 3.1.67: Increased expression of BiP/HSPA5 in A549 and A549 after 7 days exposure to 5-FU (10µg of protein per lane) – confirmation of result

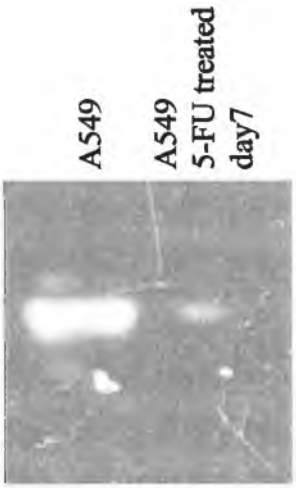

Figure 3.1.68: Decreased expression of BiP/HSPA5 in DLKP and DLKP after 7 days exposure to 5-FU (10µg of protein per lane) – confirmation of result

Figure 3.1.69: Increases expression of BiP/HSPA5 in NHBE and NHBE after 7 days exposure to 5-FU (10µg of protein per lane) – confirmation of result

Figure 3.1.70: Increase expression of BiP/HSPA5 in MCF-7 and MCF-7 after 7 days exposure to 5-FU (10µg of protein per lane) – confirmation of result

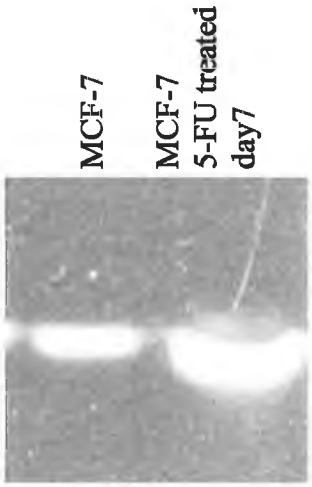

Figure 3.1.71: Decreased expression of BiP/HSPA5 in HMEC and HMEC after 7 days exposure to 5-FU (10µg of protein per lane) – confirmation of result

Summary of HSPA5 expression in all cell lines treated with 5-FU

The expression trend of HSPA5 follows that of the 2D-DIGE experiments. In summary HSPA5 is upregulate in NHBE and MCF-7 treated with 5-FU. This data in dicates a possible induction of ER stress in MCF-7 and NHBE.

Gelsolin expression confirmed by western blot in DLKP, MCF-7 and NHBE

Gelsolin is an important protein in invasion and stress. Thus confirmation of its expression will validate the fold changes observed in the 2D-DIGE experiment.

Figure 3.1.72: Increased expression of GSN in DLKP and DLKP after 7 days exposure to 5-FU (10μg of protein per lane) – confirmation of result

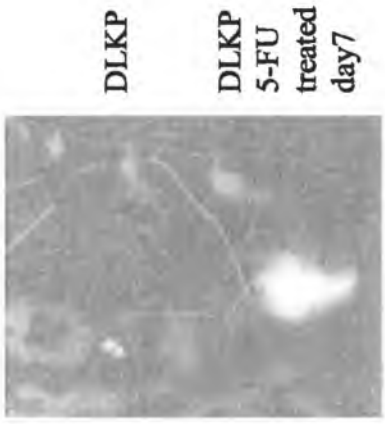

Figure 3.1.73: Increased expression of GSN in NHBE and NHBE after 7 days exposure to 5-FU (10μM) (10μg of protein per lane) – confirmation of result

Figure 3.1.74: Increased Expression of GSN in MCF-7 and MCF-7 after 7 days exposure to 5-FU (10μg of protein per lane) – confirmation of result

Summary of GSN expression in DLKP, MCF-7 and NHBE

Data reveals the accumulation of GSN in DLKP, MCF-7 and NHBE. All three cell lines showed increased invasion post 5-FU treatment and suggest a link with invasion. GSN is involved in F-actin dynamics a process important in regulating invasion.

3.1.13 Summary analysis of 5-FU's treatments on the lung and breast cancer and normal cells

As stated in sections 3.1.5-9 there remains a large proportion of the differentially regulated proteins that remain unidentified. However, sufficient numbers of proteins have been identified across experiments to identify common and different responses. Common and different responses between DLKP and A549 are listed in table 3.1.17, this would show how lung carcinomas respond to 5-FU. Common and different responses between A549 and NHBE are listed in table 3.1.18, this would show how a lung adenocarcinoma would respond differently to normal cells when exposed to 5-FU. Common and different responses between DLKP and NHBE are listed in table 3.1.19, this would show how DLKP, a NSCLC, would respond differently to normal lung cells in response to 5-FU. Common and different responses between A549, DLKP and NHBE are listed in table 3.1.20, this would show how lung cells regardless of disease state respond to 5-FU. Common and different responses between MCF-7 and HMEC are listed in table 3.1.21, this would show how a breast adenocarcinoma cell line, MCF-7, and normal breast cell line would respond to 5-FU exposure and how normal cells respond differently to cancer cells in response to 5-FU exposure. Common and different responses between HMEC and NHBE are listed in table 3.1.22, this would show how normal cells respond to 5-FU and how organ origin can alter the response to 5-FU. Common and different responses between HMEC and A549 are listed in table 3.1.23, this would show how cells that appear to become less invasive due to exposure to 5-FU respond at a protein level. Common and different responses between DLKP, MCF-7 and NHBE are listed in table 3.1.24, this would show how cells that appear to become more invasive in response to 5-FU exposure do so at a protein level. Common and different responses between MCF-7 and NHBE are listed in table 3.1.25, this would identify potential proteins involved in the progression

from non-invasive to invasive in response to 5-FU. Common response in all cell lines to 5-FU exposure is shown in table 3.1.26. A summary of protein identification success rate in the various cell lines is listed in table 3.1.28 and demonstrate that protein identification

Table 3.1.17: Common and different responses between DLKP and A549 in response to 5-FU exposure

Gene Symbol	**A549**	**DLKP**
Common trend		
ACTB	1.8	1.66
ADK	1.6	1.2
ALDH1A1	1.63	1.86
CCT1	1.46	1.77
EEF1BG	2.09	1.46
GANAB	2.14	1.77
HNRPK	-1.83	-1.45
HSPA5	-1.61	-1.42
HSPA5	-1.47	-1.51
LMNB1	-1.74	-1.59
PDCD6IP	1.64	1.34
RPSA	-1.36	-2.02
SFRS1	1.59	1.24
STMN1	-5.07	-2.1
Different trend		
YWHAZ	1.45	-1.47
MCM7	-3.52	1.49
PDIA3	-1.56	1.25

Table 3.1.18: Common and different responses between A549 and NHBE in response to 5-FU exposure. *Dose dependent similarities

Gene Symbol	**A549**	**NHBE 10μM**	**NHBE 30μM**
Common trend			
ACTB	1.8	1.26	1.23
CAPNS1	2.01	1.15	1.56
EEF1BD	1.65	1.08	1.73
EEF1BG	2.09	1.34	1.9
HSPB1	1.7	1.74	2.1
KRT19	3.22	2.78	3.66
KRT8	-2.16	-1.47	-1.34
P4HB	-1.61	-1.27	-1.77
RPLP0*	1.45	1.01	2.06
RPSA	-1.36	-1.66	-1.93
STMN1	-5.07	-2.18	-2.78
YWHAZ	1.45	1.34	1.23
Different Trend			
HNRPK	-1.83	1.73	1.4
HSPA5	-1.61	2.82	2.42
HSPB1	-1.51	2.63	2.69

Table 3.1.19 Common and different responses between DLKP and NHBE in response to 5-FU exposure

Gene Symbol	DLKP	NHBE 10μM	NHBE 30μM
Common trend			
ACTB	1.66	1.26	1.23
CAPZA1	-1.38	-3.53	-1.94
CAPZB	1.34	1.3	1.23
CFL1	2.25	16.63	14.17
EEF1BG	1.46	1.34	1.9
GSN	2.07	2.61	1.77
LMNA	1.3	1.92	2.05
PLS3	1.73	2.1	2.37
PSMC2	1.29	1.57	1.58
RPSA	-2.02	-1.66	-1.93
SRM	1.41	1.16	2.57
STMN1	-2.1	-2.18	-2.78
Different trend			
GSTA1	-1.53	1.45	1.53
HNRPK	-1.45	1.73	1.4
HSPA5	-1.42	2.82	2.42
STRAP	1.3	-1.38	-1.26
YWHAZ	-1.47	1.34	1.23

Table 3.1.20 Common and different responses between A549, DLKP and NHBE in response to 5-FU exposure

Gene Symbol	DLKP	A549	NHBE 10μM	NHBE 30μM
Common Trend				
ACTB	1.66	1.8	1.26	1.23
EEF1BG	1.46	2.09	1.34	1.9
RPSA	-2.02	-1.36	-1.66	-1.93
STMN1	-2.1	-5.07	-2.18	-2.78
NHBE different trend				
HNRPK	-1.45	-1.83	1.73	1.4
HSPA5	-1.42	-1.61	2.82	2.42
DLKP different trend				
YWHAZ	-1.47	1.45	1.34	1.23

Table 3.1.21: Common and different responses between MCF-7 and HMEC in response to 5-FU exposure.

Gene Symbol	MCF-7	HMEC 10μM	HMEC30μM
Common trend			
CFL1	5.08	10.71	7.85
CTSD	2.19	2.42	2.47
DARS	1.62	1.71	2.14
DDX48	1.73	2.07	2.64
EEF1BD	2.18	2.25	2.74
GPD2	1.72	1.68	1.59
HPRT1	1.3	1.3	1.47
HSPB1	2.39	1.52	1.69
RPSA	-1.33	-1.46	-1.56
SFRS1	1.47	1.77	2
STMN1	-3.43	-3.18	-3.19
TPT1	1.91	2.14	2.26
Different trend			
HSPA5	2.31	-1.45	-1.46
HYOU1	3.49	-1.82	-2.12
P4HB	1.66	-1.47	1.55

Table 3.1.22: Common and different responses between HMEC and NHBE in response to 5-FU exposure. * Dose dependent expression

Gene Symbol	NHBE 10μM	NHBE 30μM	HMEC 10μM	HMEC30μM
Common trend				
CAPNS1	1.15	1.56	1.62	1.75
CFL1	16.63	14.17	10.71	7.85
EEF1BD*	1.08	1.73	2.25	2.74
EEF1BG*	1.34	1.9	2.46	2.49
HSPB1	2.63	1.53	1.52	1.69
HSPB1	1.74	1.53	2.08	2.75
KRT14	4.56	2.42	1.39	1.56
KRT17	2.07	2.69	2.04	1.94
P4HB	-1.27	-1.77	-1.47	1.55
RPSA	-1.66	-1.93	-1.46	-1.56
STMN1	-2.18	-2.58	-3.18	-3.19
TPT1	1.39	1.58	2.14	2.26
Different trend				
HSPA5	2.82	2.42	-1.45	-1.51

Table 3.1.23: Common and different responses between HMEC and A549 in response to 5-FU exposure

Gene Symbol	**A549**	**HMEC 10μM**	**HMEC30μM**
Common trend			
CAPNS1	2.01	1.62	1.75
DARS	1.48	1.71	2.14
EEF1BD	2.05	2.25	2.74
EEF1BG	2.09	2.46	2.49
HSPA5	-1.61	-1.45	-1.46
HSPA5	-1.47	-1.52	-1.46
HSPB1	-1.51	1.52	1.69
HSPB1	1.7	2.08	2.75
P4HB	-1.61	-1.47	1.55
RPSA	-1.36	-1.46	-1.56
SFRS1	1.59	1.77	2

Table 3.1.24: Common and different responses between DLKP, MCF-7 and NHBE in response to 5-FU exposure

Gene Symbol	**MCF-7**	**DLKP**	**NHBE 10μM**	**NHBE 30μM**
Common trend				
ACTB	1.64	1.66	1.26	1.23
p-CFL1	5.08	2.25	16.63	14.17
GSN	7.35	2.07	2.61	1.77
RPSA	-1.33	-2.02	-1.66	-1.93
STMN1	-3.43	-2.1	-2.18	-2.78
Different trend				
HNRPK	1.68	-1.45	1.73	1.4
HSPA5	2.31	-1.42	2.82	2.42
YWHAZ	1.66	-1.47	1.34	1.23

Table 3.1.25: Common and different responses between MCF-7 and NHBE in response to exposure to 5-FU. * Dose dependent

Gene Symbol	NHBE 10μM	NHBE 30μM	MCF-7
Common trend			
ACTB	1.26	1.23	1.64
CFL1	16.63	14.17	5.08
EEF1BD*	1.08	1.73	2.18
GSN	2.61	1.77	7.35
GSN	2.5	1.53	5.86
HNRPK	1.73	1.4	1.68
HSPA1B	1.75	1.43	1.56
HSPA5	2.82	2.42	2.31
HSPB1	2.63	2.69	2.39
HSPB1	1.74	2.1	2.47
KRT18	2.33	2.31	4.01
KRT19	2.78	3.66	3.79
RPSA	-1.66	-1.93	-1.33
SERPINB1	2.53	1.89	1.58
STMN1	-2.18	-2.78	-3.43
TPT1	1.39	1.61	1.91
YWHAG	1.37	1.44	1.53
YWHAZ	1.34	1.23	1.66
Different trend			
ATP5B	-1.53	-1.2	1.5
KRT8	-1.47	-1.34	2.1
P4HB	-1.27	-1.77	1.66

Table 3.1.26: Common response to 5-FU exposure in all cell lines.

Gene symbol	A549 10μM	DLKP 10μM	NHBE 10μM	NHBE 30μM	MCF-7 10μM	HMEC 10μM	HMEC 30μM
RPSA	-1.36	-2.02	-1.66	-1.93	-1.33	-1.46	-1.56
STMN1	-5.07	-2.1	-2.18	-2.78	-3.43	-3.18	-3.19

3.1.14 Summary of differentially regulated protein identification success rates using MALDI-ToF MS.

As stated a large portion of proteins remain unidentified in the previously described experiments and are summarised in table 3.1.27. Assuming all preparative gels are equal, then factors that would influence the success rate of identification include protein abundance, protein purity (i.e. is spot a mixture of two or more proteins), protein modifications, ability to locate protein on preparative gel, the abundance of trypsin sites per protein, and ease of peptide ionisation during MALDI-ToF MS.

Table 3.1.27: Summary of differentially regulated proteins in all cell lines treated with 5-FU.

Cell line	Total regulated in experiment	Fold change		Phosphorylated	
		+/- 1.2	+/- 1.5	Total regulated	Up regulated
A549	187	124	179	20	18
DLKP	373	317	248	4	2
NHBE (10μM)	290	164	202	8	6
NHBE (30μM)	290	173	243	8	6
MCF-7	376	160	237	18	17
HMEC (10μM)	361	309	223	not available	not available
HMEC (30μM)	361	321	264	not available	not available

3.2 Analysis of the fluoropyrimidine treatments of DLKP

As stated in the introduction section 1.0, 5-FU is progressively being replaced in the clinic with third generation drugs such as capcitabine. Capcitabine is converted to 55FdU in the liver and at the site of the tumour 55FdU is converted into 5-FU. Thus to simulate capcitabine treatments *in vitro* cells should be treated with 55FdU. By comparing 5-FU to 55FdU treated DLKP the degree of over lap between the two experiments should indicate how the knowledge base of 5-FU treatments is transferable to the knowledge base on 55FdU treatments. Further more characterisation of 55FdU treatments may indicate how cells respond to treatment with the drug and how the capcitabine derivative 55FdU induces inhibition of cell growth.

Previous work performed in the laboratory found that 52FdU induced expression of KRT8 and 18 in the cell line DLKP - similar to 5-FU (McMorrow, Ph. D. thesis 2004). To characterise its differentiation effect treatments were carried out on DLKP and compared to 5-FU to determine if cell lines respond in a significantly diffent manner to 52FdU than 5-FU. Furthermore identification of differences between the drugs responces may indicate situation were treatment with 52fdU is preferable over treatment with 5-FU.

3.2.1 Determination of IC_{80} drug concentration for each fluoropyrimidine in the cell line DLKP

Determination of the drug concentration that would inhibit the growth of DLKP after 7 days culture in media supplemented with 52FdU and 55FdU was carried out as described in section 2.7.2. This was done in order to compare IC_{80} drug effects of the fluoropyrimidines and to determine unique differences between the drugs.

Figure: 3.2.1 Growth inhibition after 7days exposure to by 52FdU compared to 5-FU at concentration ranging from 0 to 10μM in the cell line DLKP.

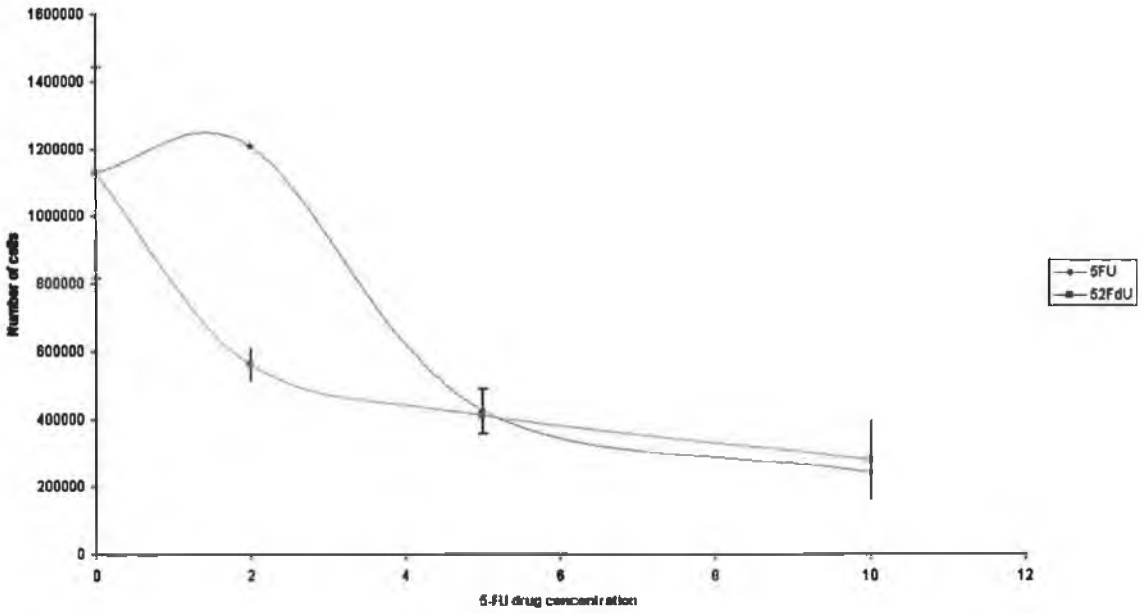

Figure: 3.2.2 Growth inhibition after 7days exposure to by 52FdU compared to 5-FU at concentration ranging from 0 to 10μM in the cell line DLKP.

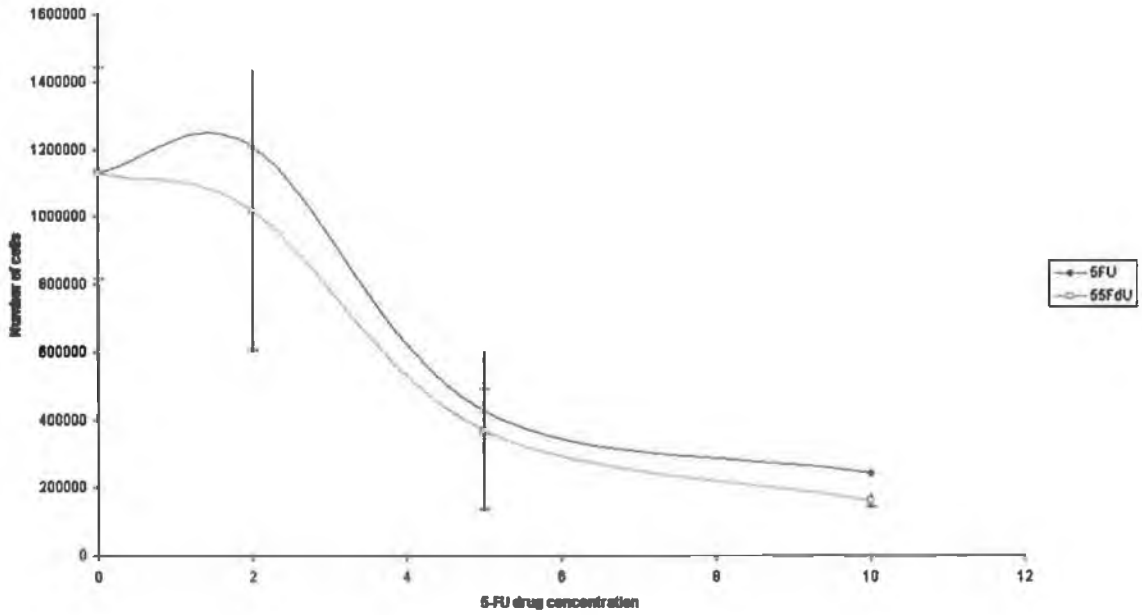

A similar IC_{80} growth inhibition of 10μM was found for all fluoropyrimidines however comparison between IC_{50}'s show 52FdU is more toxic.

3.2.2 Proteomic analysis of 5-fluoro-2'-deoxyuridine's treatment of DLKP

Cell culture of DLKP and DLKP treated with 5-FU were carried out as described in section 2.7.3. Total protein extractions were prepared as described in 2.16.2.1. These were prepared in biological triplicate. Each biological triplicate was run in technical duplicates. Sample labelling with Cy dyes is shown in table 3.2.1. Protein filters of greater than plus 1.2 or less than minus 1.2 fold with t-test of less than 0.01, and fold change of greater than plus 1.5 or less than minus 1.5 with t-test of 0.05 were used to identify differentially regulated proteins.

Table 3.2.1: Ettan DIGE experimental design for the analysis of differential protein expression induced in DLKP by exposure to 5-FU for 7 days.

Gel number	CY2 label	CY3 label	CY5 label
1	Pooled internal standard (50μg of protein)	DLKP, P.16 (50μg of protein)	DLKP, P. 16, 52FdU treated (50μg of protein)
2	Pooled internal standard (50μg of protein)	DLKP, P.16 (50μg of protein)	DLKP, P. 16, 52FdU treated (50μg of protein)
3	Pooled internal standard (50μg of protein)	DLKP, P. 17 (50μg of protein)	DLKP, P. 17, 52FdU treated (50μg of protein)
4	Pooled internal standard (50μg of protein)	DLKP, P. 17 (50μg of protein)	DLKP, P. 17, 52FdU treated (50μg of protein)
5	Pooled internal standard (50μg of protein)	DLKP, P. 18 (50μg of protein)	DLKP, P. 18, 52FdU treated (50μg of protein)
6	Pooled internal standard (50μg of protein)	DLKP, P. 18 (50μg of protein)	DLKP, P. 18, 52FdU treated (50μg of protein)

Preparative gels for protein identification were prepared as described in sections 2.21-25. Differentially regulated proteins were identified using MALDI-ToF MS as described in section 2.27. Identified differentially regulated proteins locations are indicated in figure 3.2.3. The identity of these proteins can be seen in table 3.2.2. Proteins identification data from MALDI-ToF MS is included in the appendices.

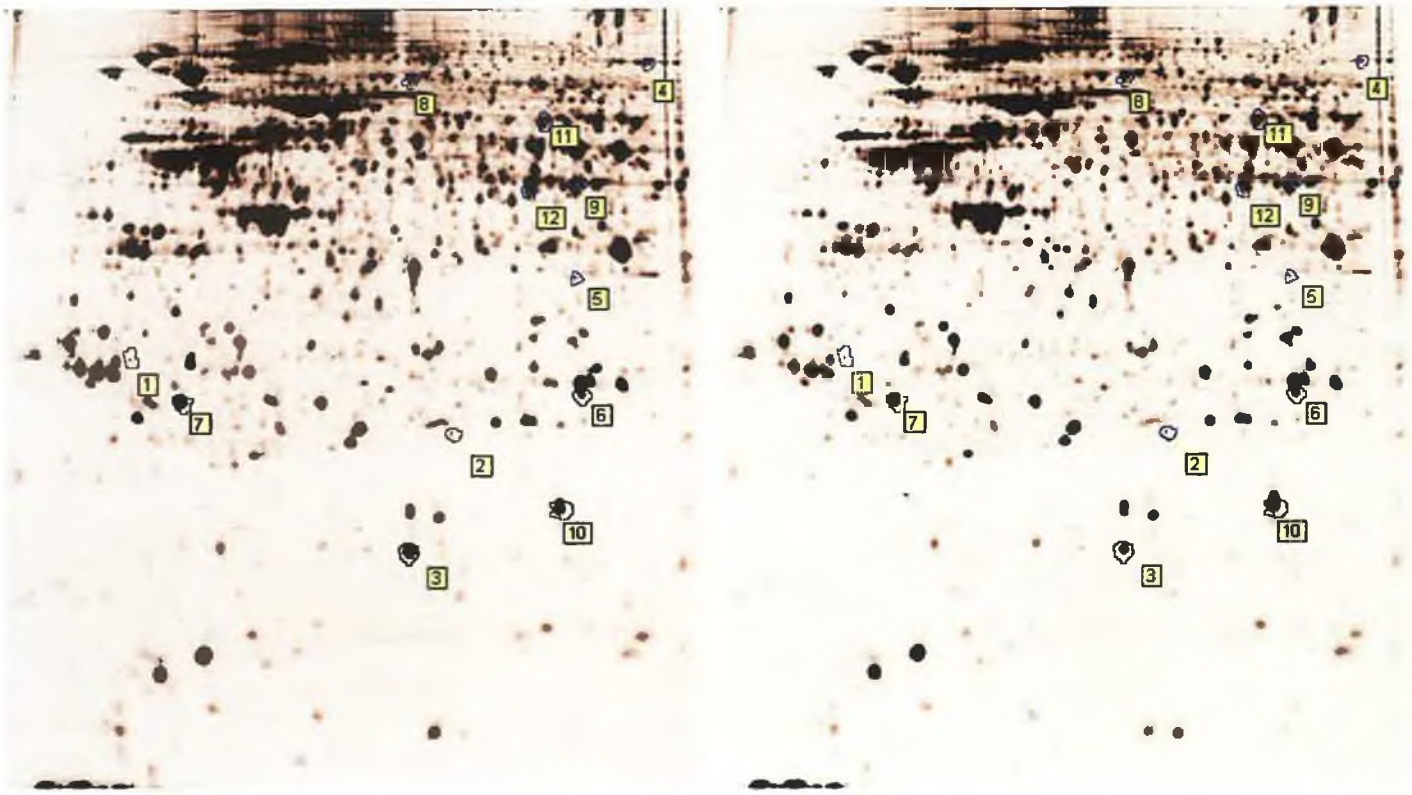

Figure 3.2.3: Images of representative DIGE gels from (a) DLKP, (b) DLKP after 7 days treatment with 10μM 55FdU. Identified differentially regulated protein spots are encircled by blue lines and are given a protein number. Refer to table 3.2.2 for protein identification.

Table 3.2.2: Proteins differentially regulated in DLKP treated with 52FdU that overlap with differentially regulated protein in DLKP treated with 5-FU.

Protein location on 2D-DIGE gel	GI accession Number	Gene symbol	Name	T-test	Fold change	Molecular function
Similar expression trend						
1	gi|49119653|	YWHAZ	YWHAZ protein [Homo sapiens]	-1.68	0.0027	
2	gi|54696078|	VBP1	von Hippel-Lindau binding protein 1 [Homo sapiens]	-1.41	0.0041	
3	gi|5031851|	STMN1	stathmin 1 [Homo sapiens]	-1.53	0.003	
6	gi|47115227|	HPRT1	HPRT1 [Homo sapiens]	1.35	0.0018	
7	gi|5729842|	GLO1	glyoxalase I [Homo sapiens]	1.29	0.00027	
8	gi|38044288|	GSN	gelsolin isoform b [Homo sapiens]	1.32	0.0001	
9	gi|4503481|	EEF1BG	eukaryotic translation elongation factor 1 gamma [Homo sapiens]	1.27	0.00018	
10	gi|30582531|	CFLN1	cofilin 1 (non-muscle) [Homo sapiens]	1.64	0.023	
11	gi|31542292|	CCT1	chaperonin containing TCP1, subunit 3 (gamma) [Homo sapiens]	1.23	1.8x10-5	
12	gi|62896663|	ANXA7	annexin VII isoform 1 variant [Homo sapiens]	-1.58	0.0036	
Opposite expression trend to 5-FU treatment						
4	gi|19353009|	EEF2	Similar to Elongation factor 2b [Homo sapiens]	-1.98	0.02	
5	gi|2135552|	LASP1	Lasp-1 protein - human	1.19	0.0037	

3.2.3 Proteomic analysis of 5-fluoro-5'-deoxyuridine's treatment of DLKP

Cell culture of DLKP and DLKP treated with 5-FU were carried out as described in section 2.7.3. Total protein extractions were prepared as described in 2.17. These were prepared in biological triplicate. Each biological triplicate was run in technical duplicates. Sample labelling with Cy dyes is shown in table 3.2.3. Protein filters of >+/<- 1.2 fold with t-test of 0.01, and fold change of >+/<- 1.5 with t-test of 0.01 were used to identify differentially regulated proteins.

Table 3.2.3: Ettan DIGE experimental design for the analysis of differential protein expression induced in DLKP by exposure to 5-FU for 7 days.

Gel number	CY2 label	CY3 label	CY5 label
1	Pooled internal standard (50µg of protein)	DLKP, P.16 (50µg of protein)	DLKP, P. 16, 55FdU treated (50µg of protein)
2	Pooled internal standard (50µg of protein)	DLKP, P.16 (50µg of protein)	DLKP, P. 16, 55FdU treated (50µg of protein)
3	Pooled internal standard (50µg of protein)	DLKP, P. 17 (50µg of protein)	DLKP, P. 17, 55FdU treated (50µg of protein)
4	Pooled internal standard (50µg of protein)	DLKP, P. 17 (50µg of protein)	DLKP, P. 17, 55FdU treated (50µg of protein)
5	Pooled internal standard (50µg of protein)	DLKP, P. 18 (50µg of protein)	DLKP, P. 18, 55FdU treated (50µg of protein)
6	Pooled internal standard (50µg of protein)	DLKP, P. 18 (50µg of protein)	DLKP, P. 18, 55FdU treated (50µg of protein)

Preparative gels for protein identification were prepared as described in sections 2.21-25. Differentially regulated proteins were identified using MALDI-ToF MS as described in section 2.27. Identified differentially regulated proteins locations are indicated in figure 3.2.4. The identity of these proteins can be seen in table 3.2.4. Proteins identification data from MALDI-ToF MS is included in the appendices.

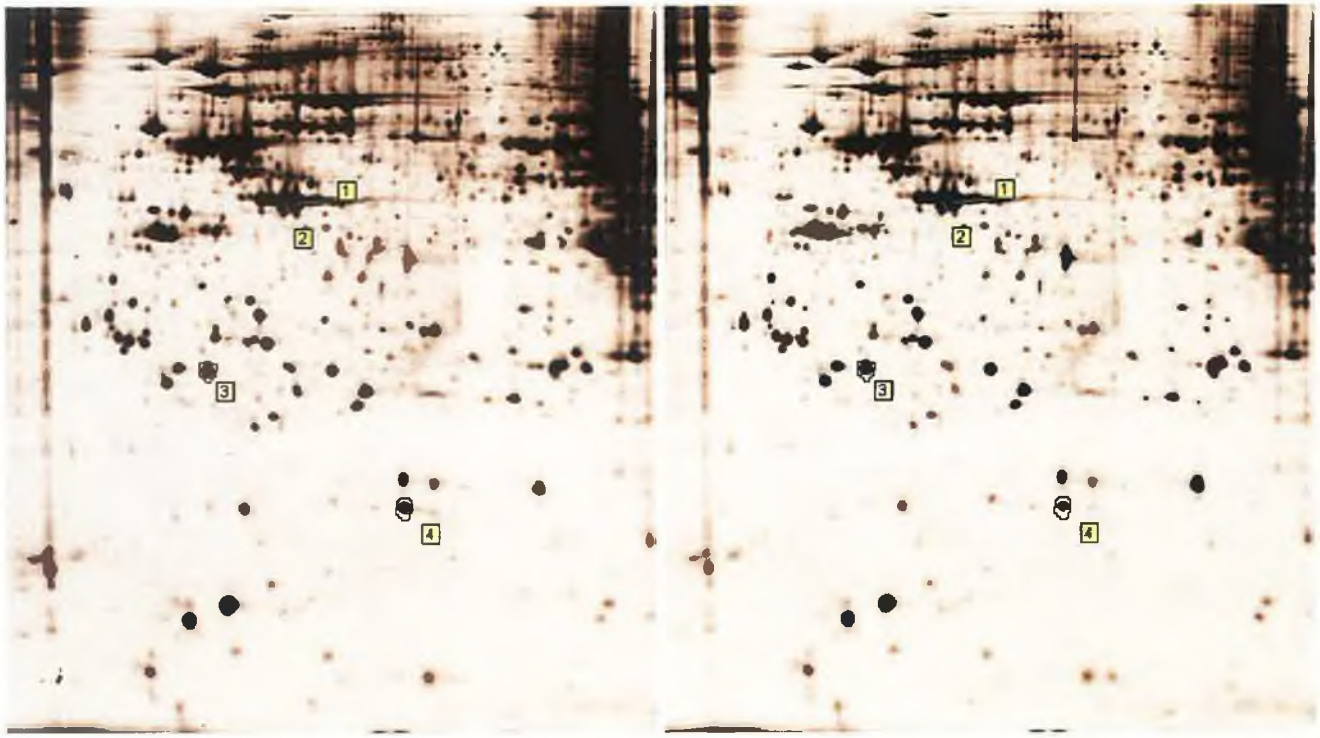

Figure 3.2.4: Images of representative 2D-DIGE gels from (a) DLKP, (b) DLKP after 7 days treatment with 10μM 55FdU. Identified differentially regulated protein spots are encircled by blue lines and are given a protein number. Refer to table 3.4.2.2 for protein identification.

Table 3.2.4: Proteins differentially regulated in DLKP treated with 55FdU that overlap with differentially regulated protein in DLKP treated with 5-FU..

Protein location	GI accession Number	Gene symbol	Name	Fold change	T-Test	Molecular function
1	gi|15277503|	ACTB	ACTB protein [Homo sapiens]	1.27	0.0015	
2	gi|15277503|	ACTB	ACTB protein [Homo sapiens]	1.34	0.00038	
3	gi|5729842|	GLO1	glyoxalase I [Homo sapiens]	1.38	3.9x10-5	
4	gi|5031851|	STMN1	stathmin 1 [Homo sapiens]	-1.23	0.0095	

3.2.4 Summary

Fluoropyrimidine exposure of DLKP causes similar inhibition of cell growth at 10μM. However, examination of the proliferation curve shows that 52FdU is far more toxic than 5-FU. Proteomic analysis of DLKP treated with 52FdU showed more in common with 5-FU than 55FdU. None of the heat shock proteins that were differentially regulated in the 5-FU DIGE experiment showed differential expression in the other fluoropyrimidine treatment DIGE experiments. A total of 12 proteins showed overlap between DLKP 5-FU treatment and DLKP 52FdU treatment, 4 proteins showed over lap between DLKP 5-FU treatment and DLKP 55FdU treatment. STMN1 and GLO1 are the only proteins that appear to be differentially expressed in all 3 fluoropyrimidine experiments.

3.3 Analysis of DLKP-55, a 5-FU resistant cell line

Resistance to 5-FU is a major obstacle in the treatment of cancer. 5-FU resistance is mediated by over expression of a combination of or individual over expression of TS TP or DHPD. Development of 5-FU resistant are described in this section and the identification of a stable resistant variant of DLKP, DLKP-55, is described. Few proteomic based investigation of 5-FU resistance have been published in the literature. Thus to address this and discover potential new mechanisms of 5-FU resistance and alternative drug targets during therapy of 5-FU resistant cell lines protein preps from DLKP and DLKP-55 were prepared and analysed.

3.3.1 Pulse selection process

The cell lines DLKP and A549 were pulse selected for 10 4-hour pulses with three fluoropyrimidine anti-metabolite drugs. These drugs were 5-Fluorouracil (5-FU), 5-Fluoro-2-deoxyuridine (52FdU), a metabolic derivative of 5-FU, and 5-fluoro-5-deoxyuridine (55FdU), a 5-FU prodrug. The interval between pulsing ranged from 1 week to 8 weeks and timing of subsequent pulses was determined by two factors. These factors are (a) cells appear to be proliferating and (b) cells are at a confluency of between 50-80%. See figure 3.2.1 drug concentrations at each pulse, see section 2.10 for further details on pulse selection methodology.

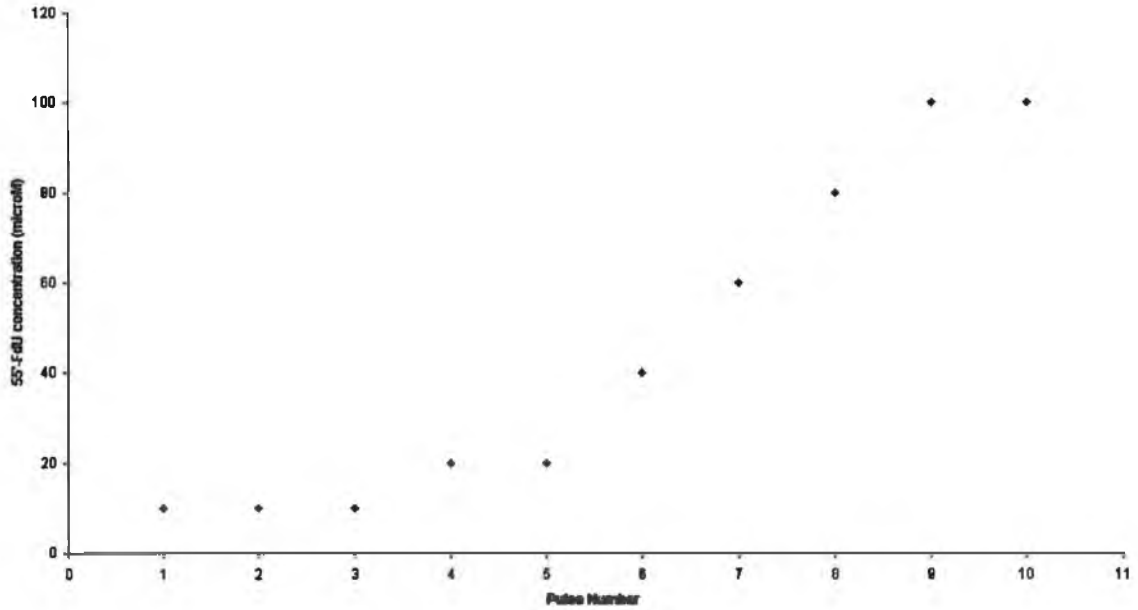

Figure 3.3.1: The concentration of 55FdU for each pulse used in the generation of the 5-FU resistant cell line DLKP-55

3.3.2 Fluoropyrimidine drug resistance model, DLKP versus DLKP-55

Drug resistance generated in pulse selection with the fluoropyrimidines on the cell lines DLKP and A549. A549 displayed no stable resistance to any drug, DLKP selected with 52FdU did not survive 10 pulses and DLKP selected with 5-FU failed to show stable resistance. Only DLKP selected with 55FdU showed a stable resistance to any of the fluoropyrimidines and was given the name DLKP-55.

Toxicity assays performed on DLKP-55 compared to DLKP (Passage 18-25) showed that DLKP-55 showed resistance to 5-FU and 55FdU, and showed cross-resistance to Adriamycin (Adr), see figures 3.3.1, 3.3.2 and 3.3.3. Resistance was assessed to Bromodeoxyuridine (BrdU) and taxol (Txl) as it was hoped that resistance would not be shown to one of these drugs and thus would act as a control for the toxicity assay. The bromopyrimidine, BrdU, was selected as 5-FU resistance has been linked to Thymidylate Synthetase (TS) over expression. The bromo- metabolic derivatives of BrdU are not processed in the same manner as fluoro- derivatives. Specifically the literature shows that bromouracil can not irreversibly bind to TS and thus can not cause inhibition of its activity. Thus 5-FU resistance mediated by TS over expression would not cause BrdU resistance. Taxol was also used as a control as its mechanism of action inhibits microtubule polymerisation thus inducing apoptosis, while 5-FU's anti-proliferative effect induces apoptosis by incorporation into RNA and DNA inducing apoptosis through the genotoxic response. Thus resistance to Txl would be unexpected. Toxicity assays showed no resistance to these drugs, see figures 3.3.4 and 3.3.5. Summary of resistance can be seen in figure 3.3.6.

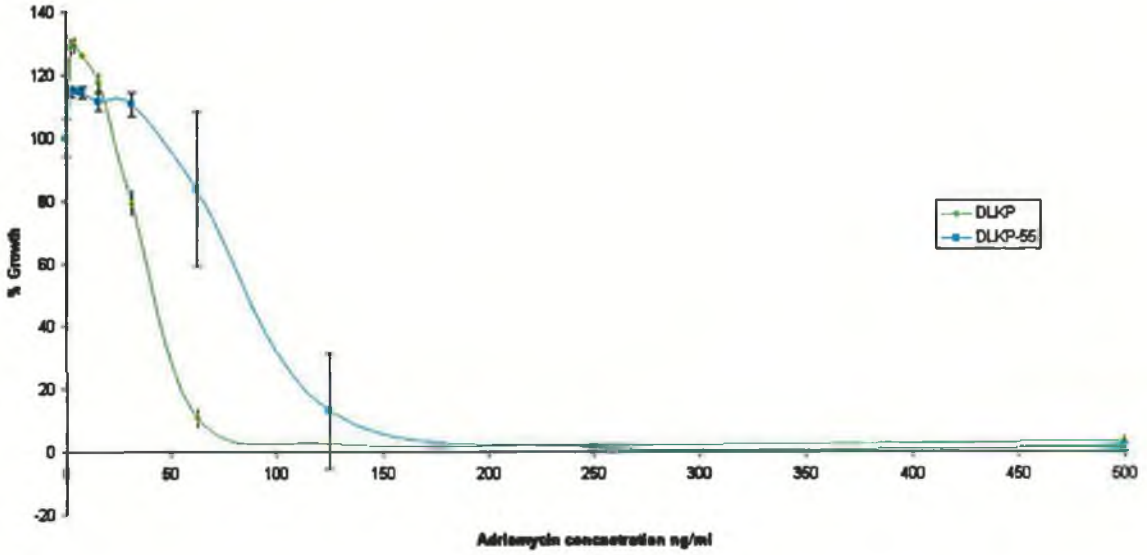

Figure 3.3.1: Toxicity assays of DLKP and DLKP-55 to adriamycin demonstrating DLKP-55 is approximately 2 fold more resistant to DLKP (n=3).

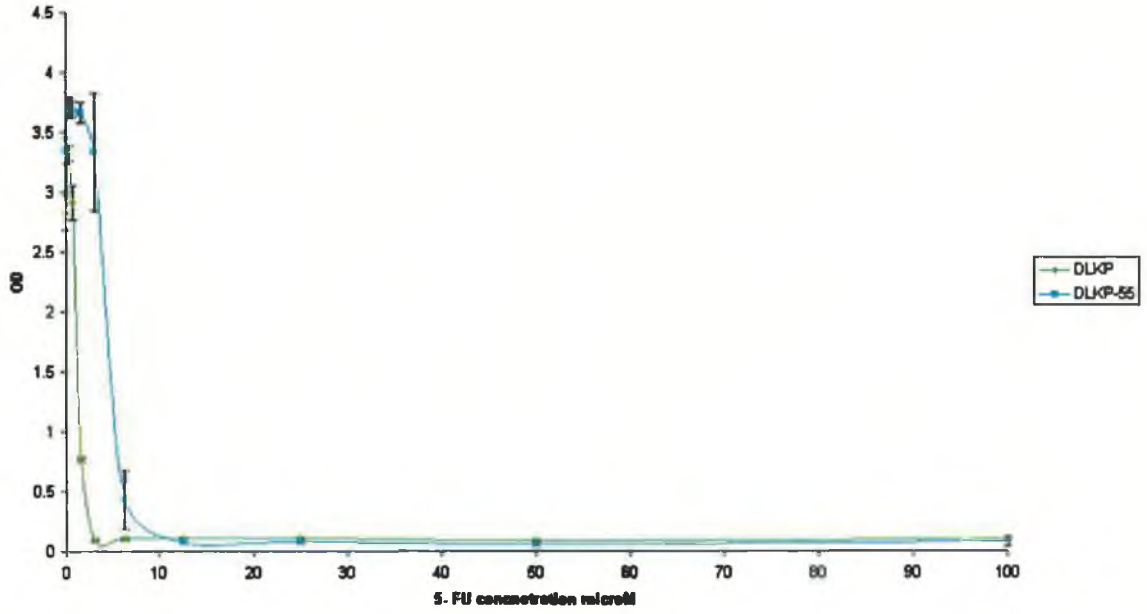

Figure 3.3.2: Toxicity assays of DLKP and DLKP-55 to 5-FU demonstrating DLKP-55 is approximately 4 fold more resistant to DLKP (n=3).

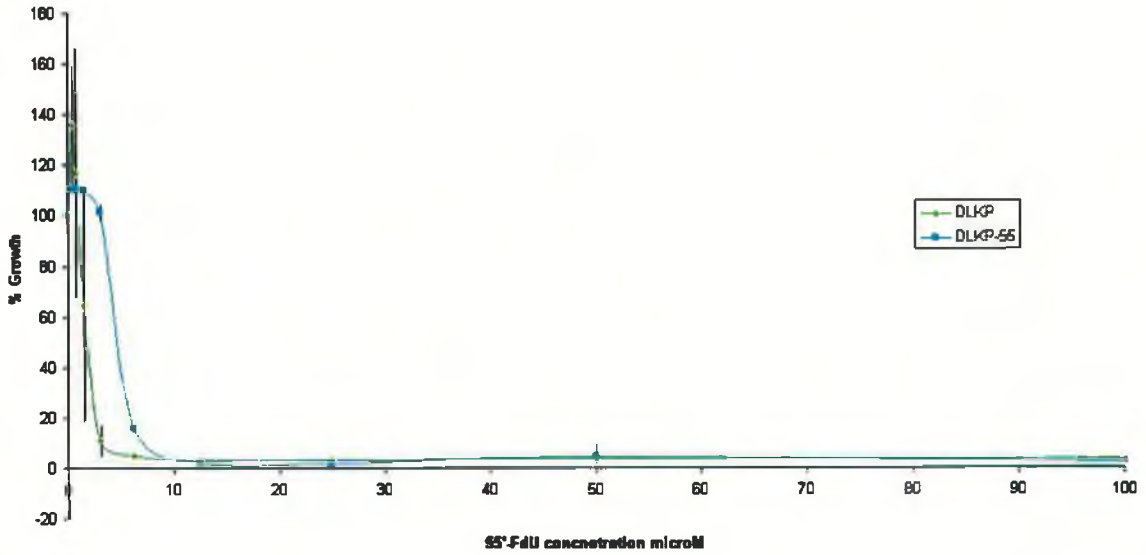

Figure 3.3.3: Toxicity assays of DLKP and DLKP-55 to 55-FdU demonstrating DLKP-55 is approximately 4 fold more resistant to DLKP (n=3).

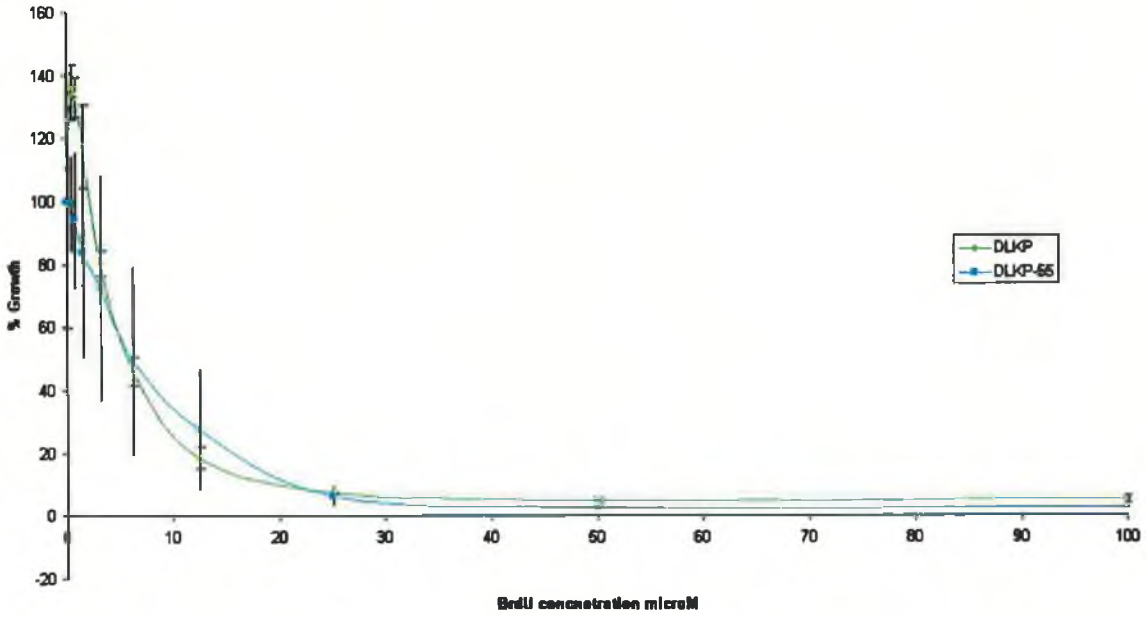

Figure 3.3.4: Toxicity assays of DLKP and DLKP-55 to BrdU demonstrating DLKP-55 and DLKP share equal resistance to BrdU (n=3).

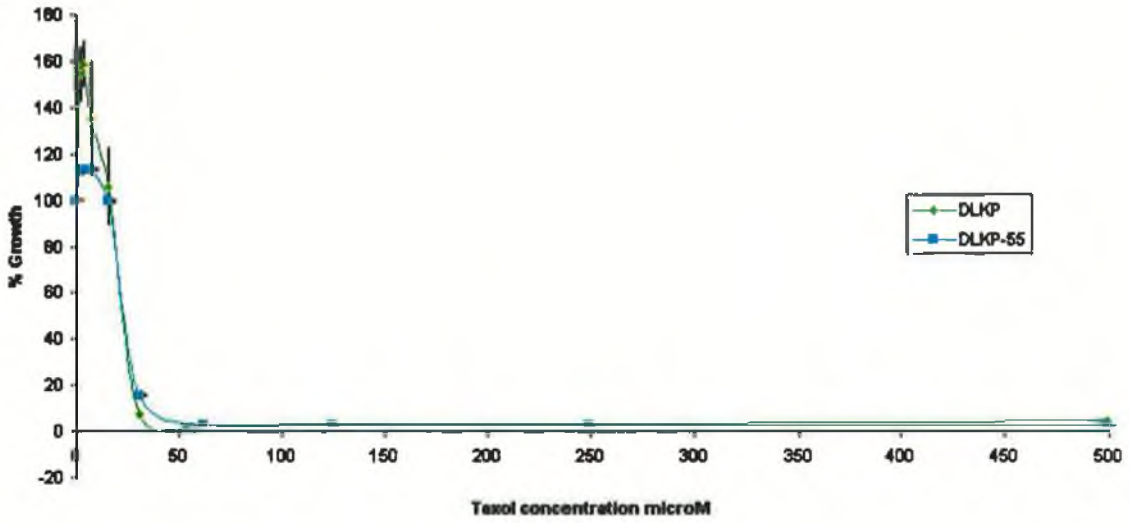

Figure 3.3.5: Toxicity assays of DLKP and DLKP-55 to Taxol demonstrating DLKP-55 and DLKP share equal resistance to taxol (n=3).

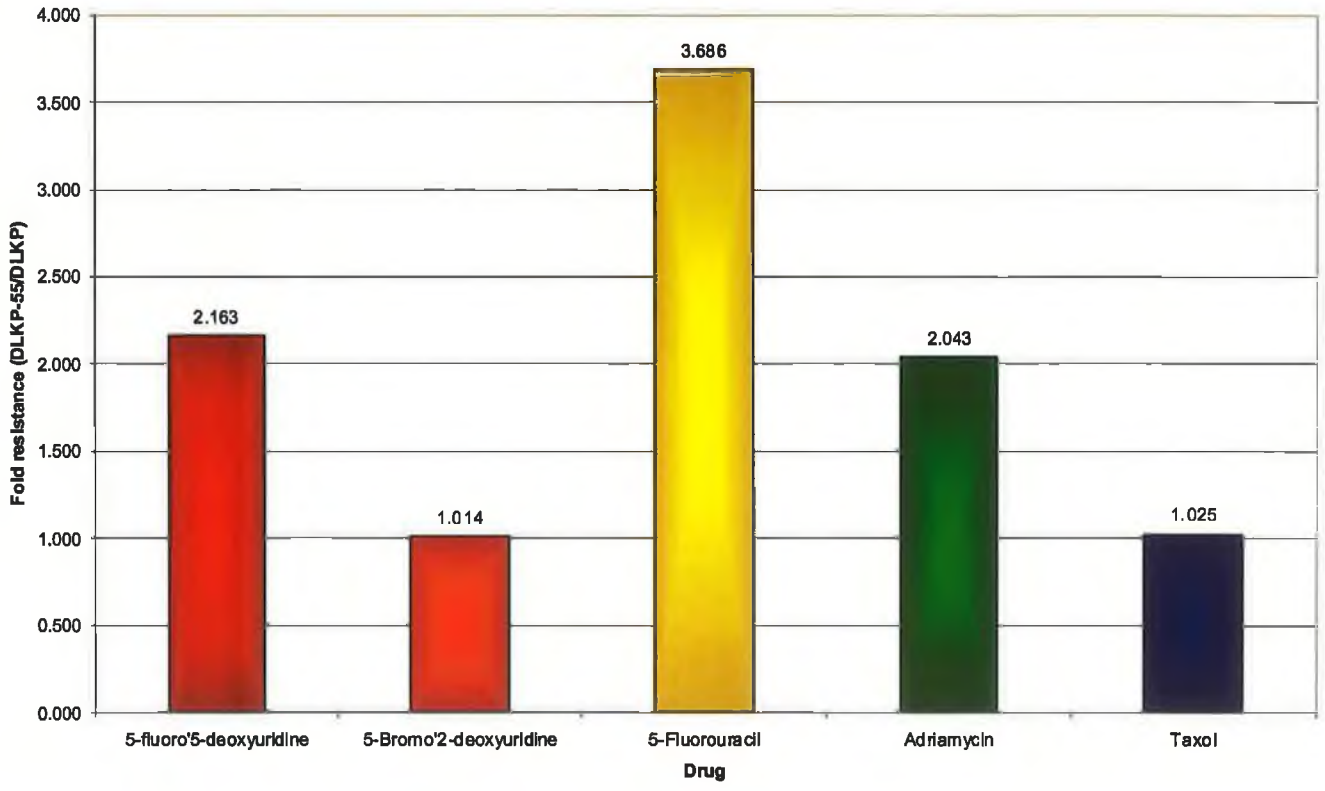

Figure 3.3.6: Summary of fold change resistance between DLKP-55 and DLKP between the chemotherapeutic and anti-metabolite drugs in figures 3.3.1 to 3.3.5.

3.3.3 Western blots on protein extracts from DLKP versus DLKP-55

Western blots were performed on DLKP versus DLKP-55 to investigate proteins found regulated as a result of 5-FU treatment of DLKP. This includes the investigation of integrin subunit β_1, BiP, Gelsolin, and Rho. Thymidylate synthetase (TS) was investigated as it is reported to correlate with 5-FU resistance. TS is only protein that showed up regulation by western blot.

Figure 3.3.7: Western blot for the integrin subunit β_1 on protein extracts from DLKP and DLKP-55 (10μg of protein per lane).

The integrin subunit β_1 does not show a difference in expression between DLKP and DLKP-55. This may rule out signal transduction from the β_1 integrin protein been involved in 5-FU resistance (see figure 3.3.7).

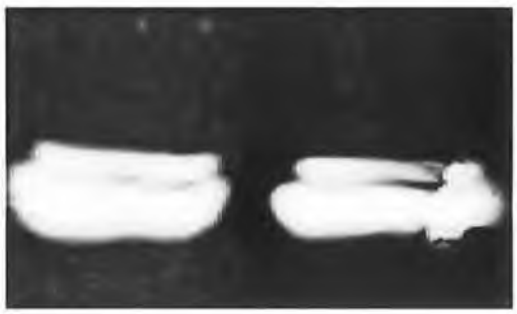

Figure 3.3.8: Western blot for HSPA5 on protein extracts from DLKP and DLKP-55 (10μg of protein per lane).

Western blot revealed no expression difference between DLKP and DLKP-55 for the ER protein – HSPA5. Data confirms 2D-DIGE data (see figure 3.3.8).

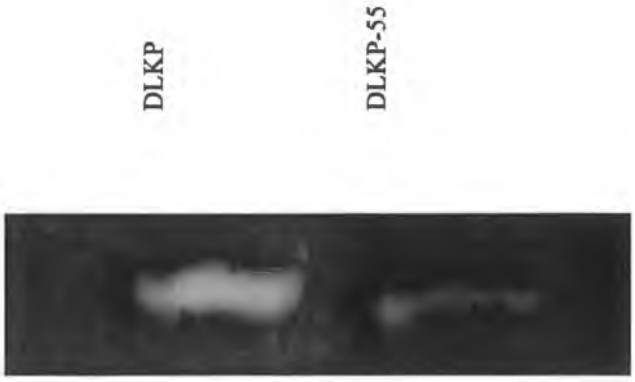

Figure 3.3.9: Western blot for Gelsolin on protein extracts from DLKP and DLKP-55 (10µg of protein per lane).

Western blot revealed no expression difference between DLKP and DLKP-55 for the actin binding protein gelsolin. Data confirms 2D-DIGE data (see figure 3.3.9).

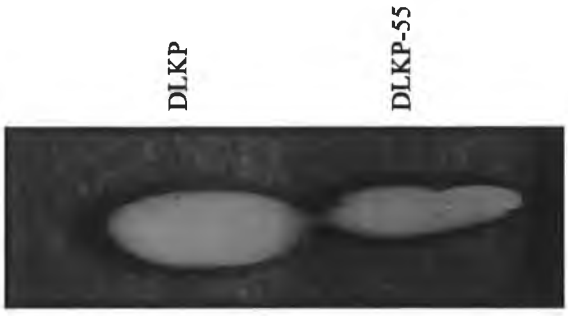

Figure 3.3.10: Western blot for Rho on protein extracts from DLKP and DLKP-55 (10µg of protein per lane).

Indicates a decreased expression of Rho and suggested decreased invasion rates in DLKP-55 (see figure 3.3.10).

Figure 3.3.11: Western blot for TS on protein extracts from DLKP and DLKP-55 (10µg of protein per lane).

DLKP-55 shows over expression of TS a protein shown to be the major cause of 5-FU resistance (see figure 3.3.11)

3.3.4 Proteomic analysis of DLKP versus DLKP-55

In order to compare the proteomes of DLKP and DLKP-55 – the 5-FU/55FdU resistant variant of DLKP - protein samples were prepared for 2D-DIGE as described in section 2.16.2.1. These samples were prepared in biological triplicate. Each biological triplicate was run in technical duplicates. Proteomic samples were prepared from cells used to set up toxicity assays in section 3.2.2. Sample labelling with Cy dyes is shown in table 3.3.1. Protein filters of greater than 1.2 or less than -1.2 fold with t-test of less than 0.01, or a fold change of greater than 1.5 or less than -1.5 fold with t-test of less than 0.05 were used to identify differentially regulated proteins.

Table 3.3.1: Ettan DIGE experimental design for the analysis of differential protein differential expression between DLKP and DLKP-55.

Gel number	CY2 label	CY3 label	CY5 label
1	Pooled internal standard (50µg of protein)	DLKP, P.20 (50µg of protein)	DLKP-55, P.53 (50µg of protein)
2	Pooled internal standard (50µg of protein)	DLKP-55, P.53 (50µg of protein)	DLKP, P.20 (50µg of protein)
3	Pooled internal standard (50µg of protein)	DLKP, P.21 (50µg of protein)	DLKP-55, P.54 (50µg of protein)
4	Pooled internal standard (50µg of protein)	DLKP-55, P.54 (50µg of protein)	DLKP, P.21 (50µg of protein)
5	Pooled internal standard (50µg of protein)	DLKP, P.22 (50µg of protein)	DLKP-55, P.55 (50µg of protein)
6	Pooled internal standard (50µg of protein)	DLKP-55, P.55 (50µg of protein)	DLKP, P.22 (50µg of protein)

Representative DIGE images of Cy labelled protein lysates separated by 2DE can be seen in figure 3.3.7. Differentaillay regulated proteins were identified by MALDI-ToF MS as described in section 2.27. Locations of identified proteins from the pick list in this experiment can be seen in figure 3.3.7 and the identity of these proteins can be seen in table 3.3.2. The distribution of differentially regulated proteins amongst ontologies can be seen figure 3.3.8.

Metabolism is an important aspect of 5-FU resistance. The locations of upregulated enzymes in each respective pathway can be seen in figures 3.3.9 to 3.3.12.

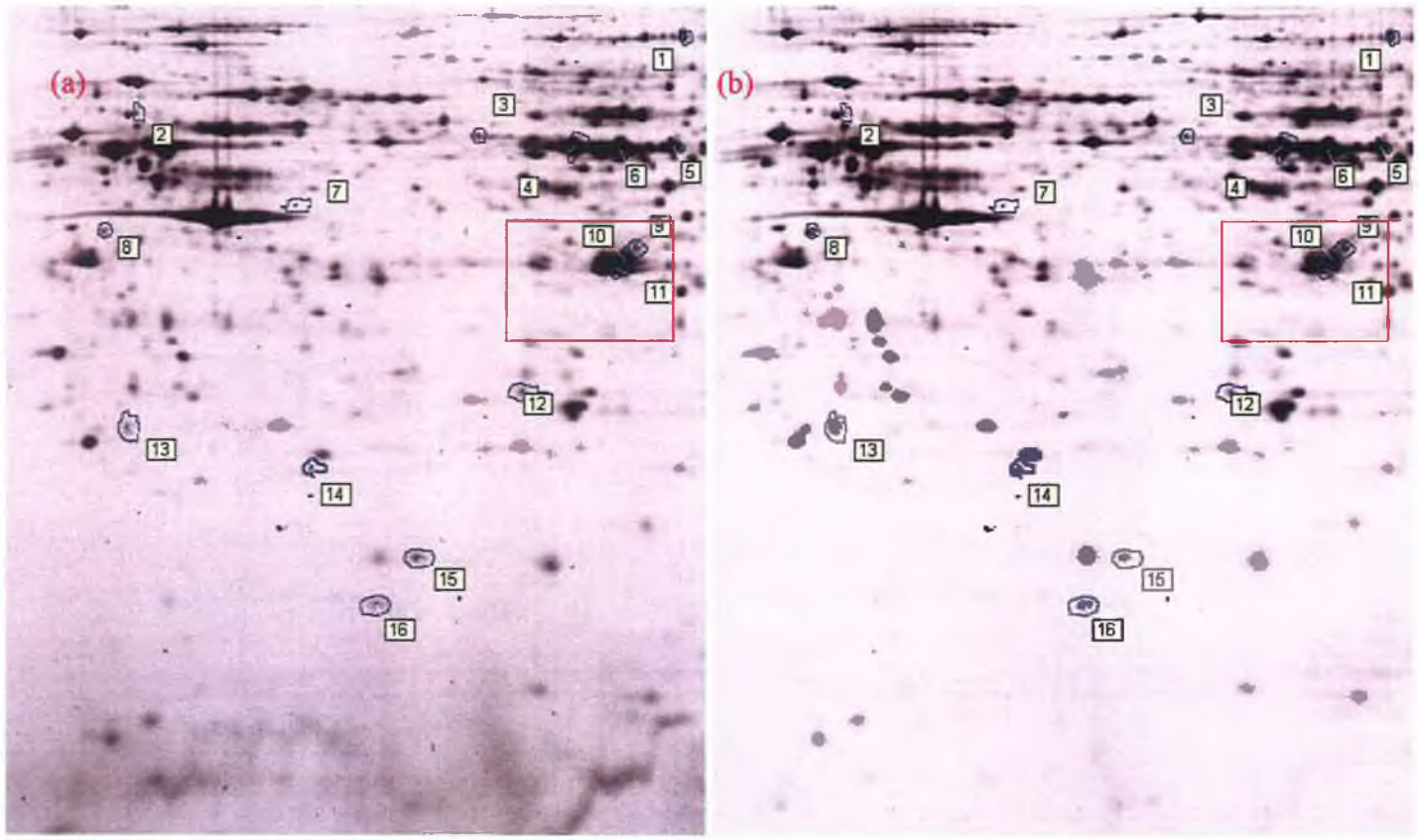

Figure 3.3.7: Images of representative DIGE gels from (a) DLKP, (b) DLKP-55. Differentially regulated proteins that have been identified are encircled by a blue line and are marked by number. The number refers to the protein identity, and the identity, statistical data and molecular and biological functions of the protein can be found in table 3.3.2. Red box indicates the predicted region in which TS occurs on 2D-gels.

Figure **3.3.8**: Pie chart demonstrating the number of proteins in each biological process differentially expressed between DLKP and DLKP-55. Identity of proteins can be found in table 3.3.2.

Table 3.3.2: Proteins identified by MALDI-ToF MS that were found to be differentially regulated between DLKP and DLKP-55 cells. Protein expression data is included in table (fold change and t-test) as well Protein location on 2D gels (see fig. 3.3.7 for locations). Stathmin included as its expression is shown to correlate with resistance to Taxol and indicates that there is no difference in resistance to taxol as data toxicity assays suggest (see fig. 3.3.5).Three unidentified upregulated protein are shown in table and there location falls in the predicted locations of TS.

Protein location	GI accession Number	Gene symbol	Name	T-test	Fold change	Molecular function	Enzyme Code
Cell growth and/or maintenance							
16	STMN1	gi|5031851|	stathmin 1 [Homo sapiens]	0.58	-1.05	-	-
Metabolism; Energy pathway							
4	G6PD	gi|7546530|	gi|7546530|pdb|1QKI|H - Chain H, X-Ray Structure Of Human Glucose 6-Phosphate Dehydrogenase (Variant	$9.6x10^{-4}$	1.34	Catalytic activity	EC:1.1.1.49
5	PKLR	gi|338827|	cytosolic thyroid hormone-binding protein (EC 2.7.1.40) (Pyruvate Kinase)	$2.2 x10^{-6}$	2.01	Catalytic activity	EC 2.7.1.40
6	ALDH1A1	gi|21361176|	aldehyde dehydrogenase 1A1 [Homo sapiens]	$3.3 x10^{-8}$	2.43	Catalytic activity	EC:1.2.1.36
8	SMS	gi|791051|	spermine synthase [Homo sapiens]	$9.9 x10^{-4}$	-2.02	-	EC:2.5.1.16
13	GLO1	gi|5729842|	glyoxalase I [Homo sapiens]	$3.4 x10^{-5}$	-1.59	Gluthathione transferase activity	EC:4.4.1.5
14	PRDX2	gi|33188452|	peroxiredoxin 2 isoform b [Homo sapiens]	$5.2 x10^{-4}$	-1.35	Peroxidase activity	EC:1.11.1.15
15	NME1	gi|29468184|	NM23-H1 [Homo sapiens]	$1.4 x10^{-4}$	1.76	Catalytic activity	EC:2.7.4.6
Protein Metabolism							
1	EEF2	gi|19353009|	Similar to Elongation factor 2b [Homo sapiens]	$1.1x10^{-3}$	1.49	Translation regulatory activity	-
3	CCT3	gi|58761484|	chaperonin containing TCP1, subunit 3 isoform c [Homo sapiens]	$3.8 x10^{-3}$	1.41	Chaperone activity	-
12	ERP29	gi|5803013|	endoplasmic reticulum protein 29 precursor [Homo sapiens]	$4.1 x10^{-3}$	1.25	Chaperone activity	-
2	PPP2CB	gi|4558259|	Chain B, Crystal Structure Of Constant Regulatory Domain Of Human Pp2a, Pr65	$5.9 x10^{-3}$	-1.56	Protein serine/threonine phosphatase activity	-
Signal transduction							
7	-	gi|62896687|	dendritic cell protein variant [Homo sapiens]	$2 x10^{-3}$	-1.35	-	-
Unidentified							
9	-	-	Possibly TS	$8.3 x10^{-3}$	2.00	-	-
10	-	-	Possibly TS	$1.30 x10^{-7}$	3.51	-	-
11	-	-	Possibly TS	$1.6 x10^{-4}$	2.39	-	-

Analysis of Proteomic implication in metabolism

5-FU is an anti-metabolite as stated earlier and thus metabolism is important in 5-FU resistance. Seven proteins listed in table 3.3.2 are involved in metabolism four of which are up regulated. These four proteins location in various metabolic pathways are shown in figures 3.3.9-12 and there location in

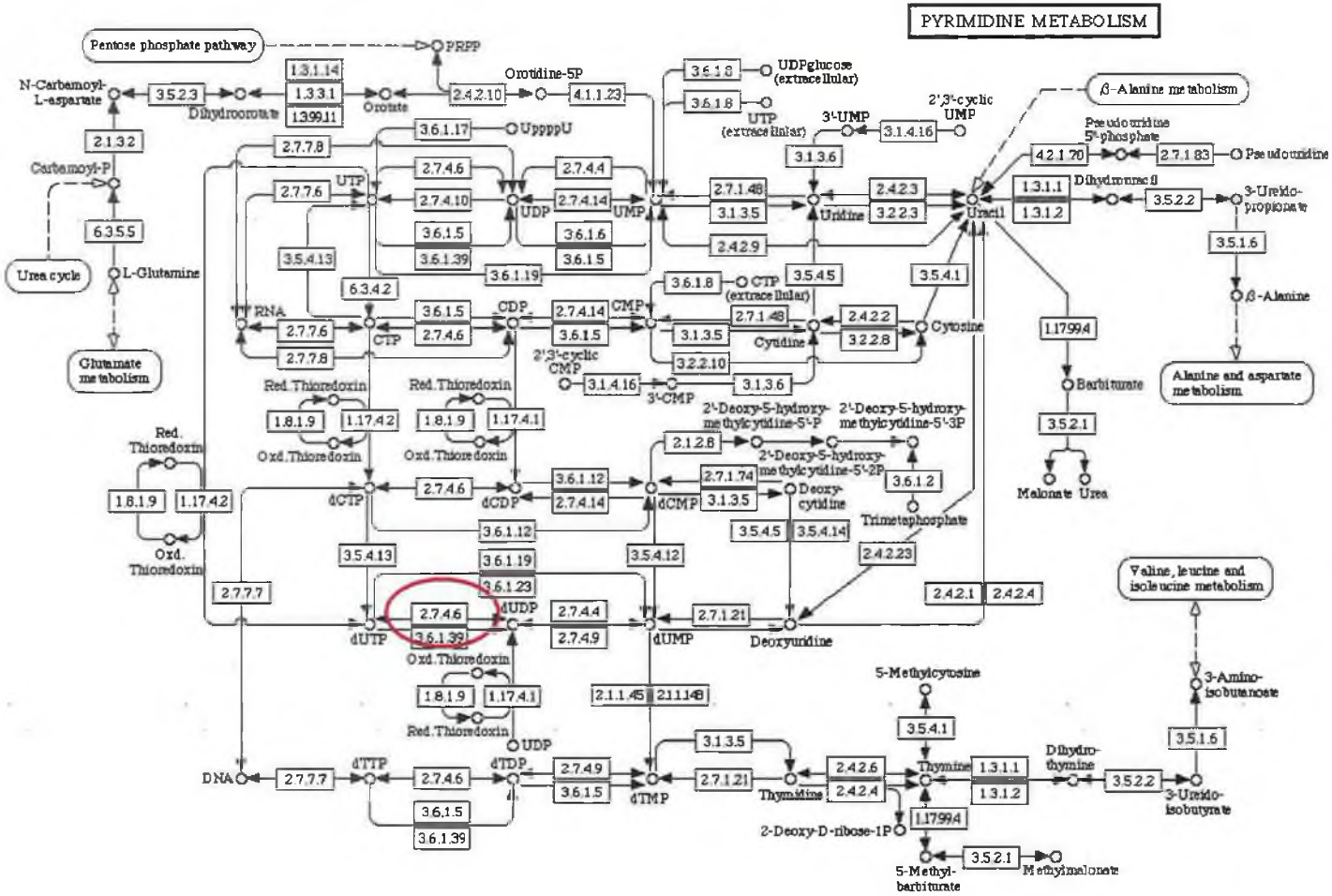

Figure 3.2.9: Figure displaying the pyrimidine metabolism pathway. Location of NME1 in the pyrimidine metabolism pathway is shown. It is responsible for the reversible conversion of dUTP to dUDP. Image downloaded from the KEGG web site.

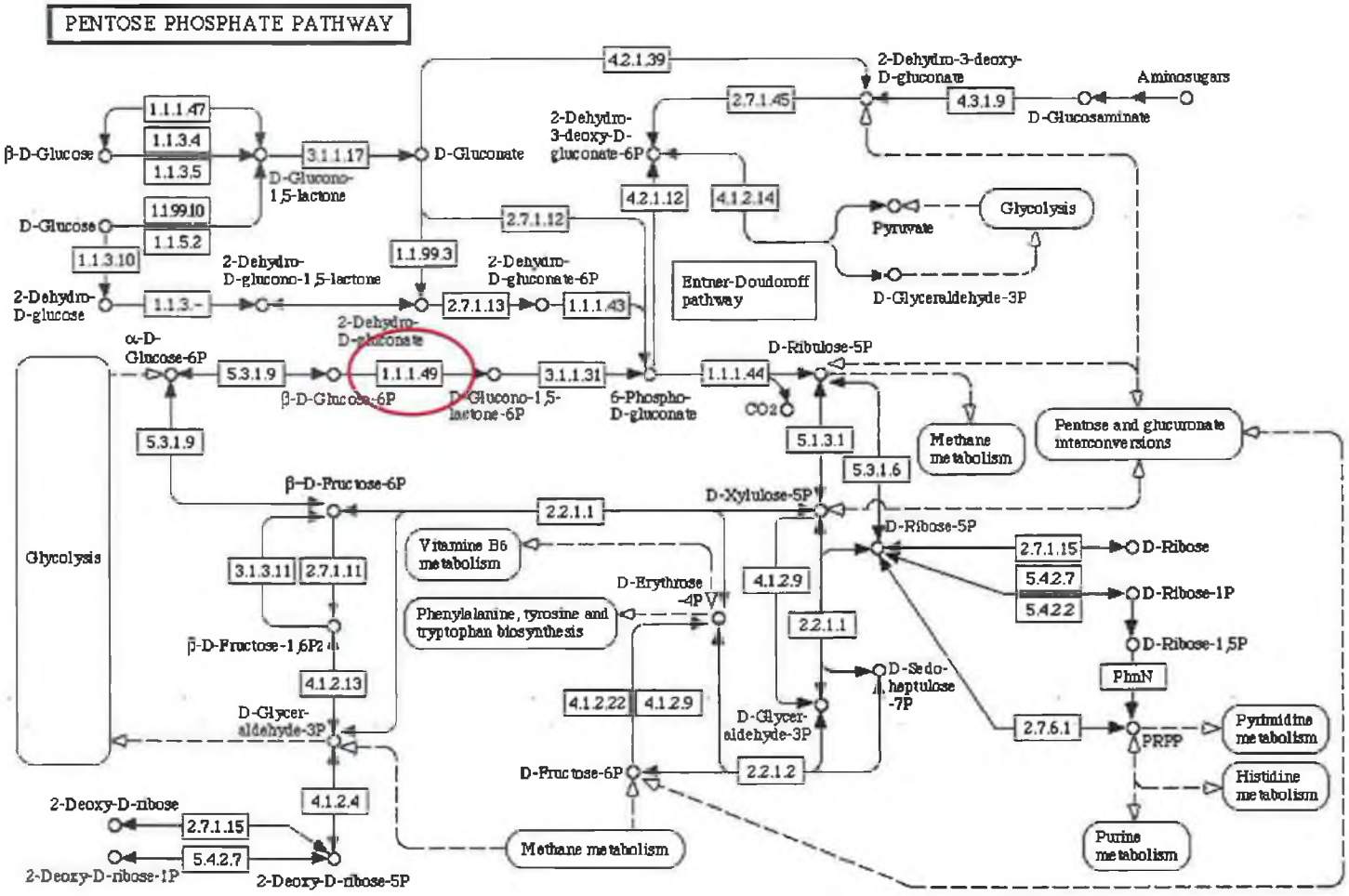

Figure 3.2.10 Figure displaying the pentose phosphate metabolism pathway. Location of G6PD in the pentose phosphate pathway is shown. It is a rate limiting step in and it is responsible for the production of D-Glucono-1,5-lactone-6P. Image downloaded from the KEGG web site.

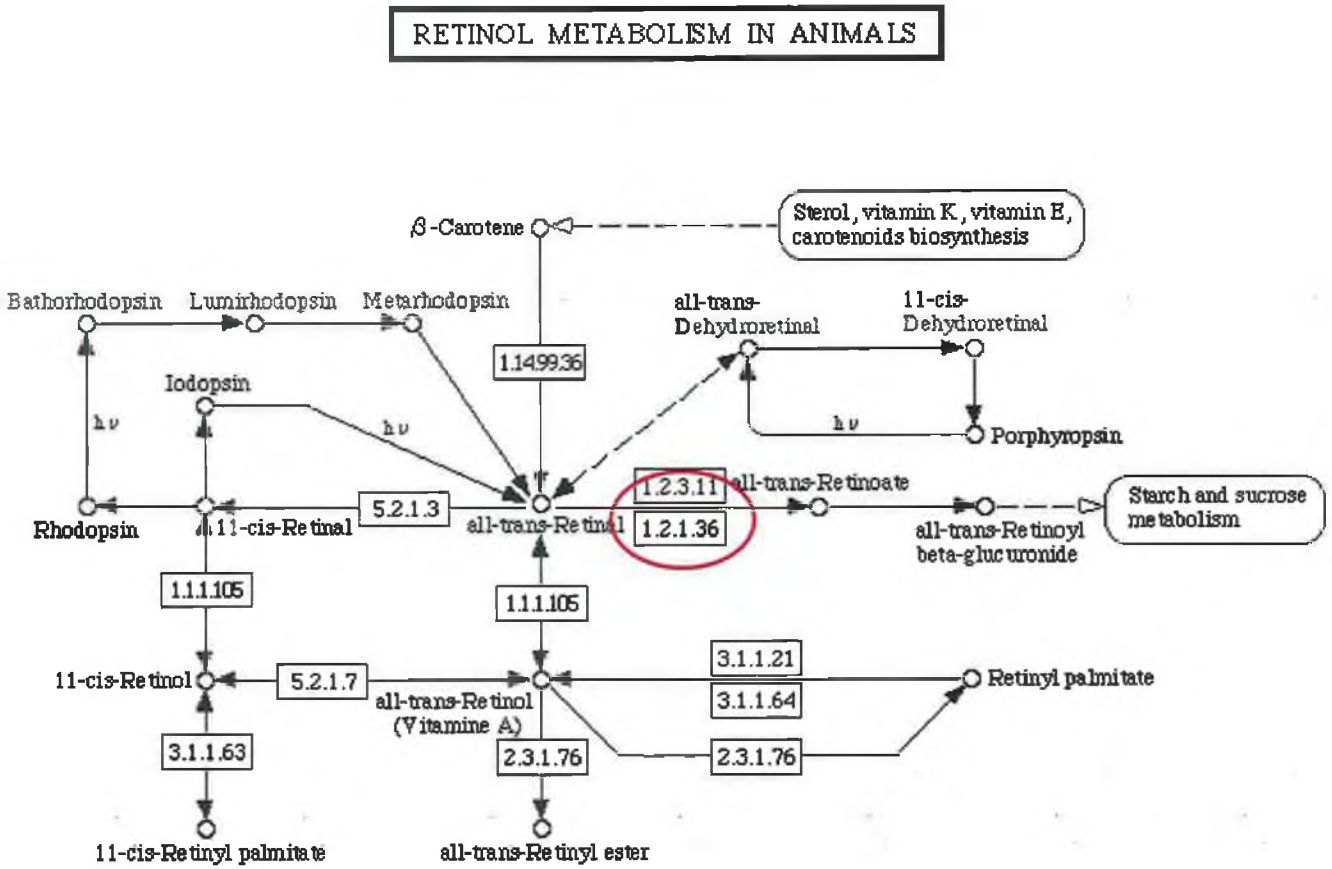

Figure 3.2.11: Figure displaying the Retinol metabolism pathway. Location of ALDH1A1 in the Retinol metabolism pathway is shown. It is responsible for the conversion of all-trans-Retinal to all-trans-Retinoate. Image downloaded from the KEGG web site.

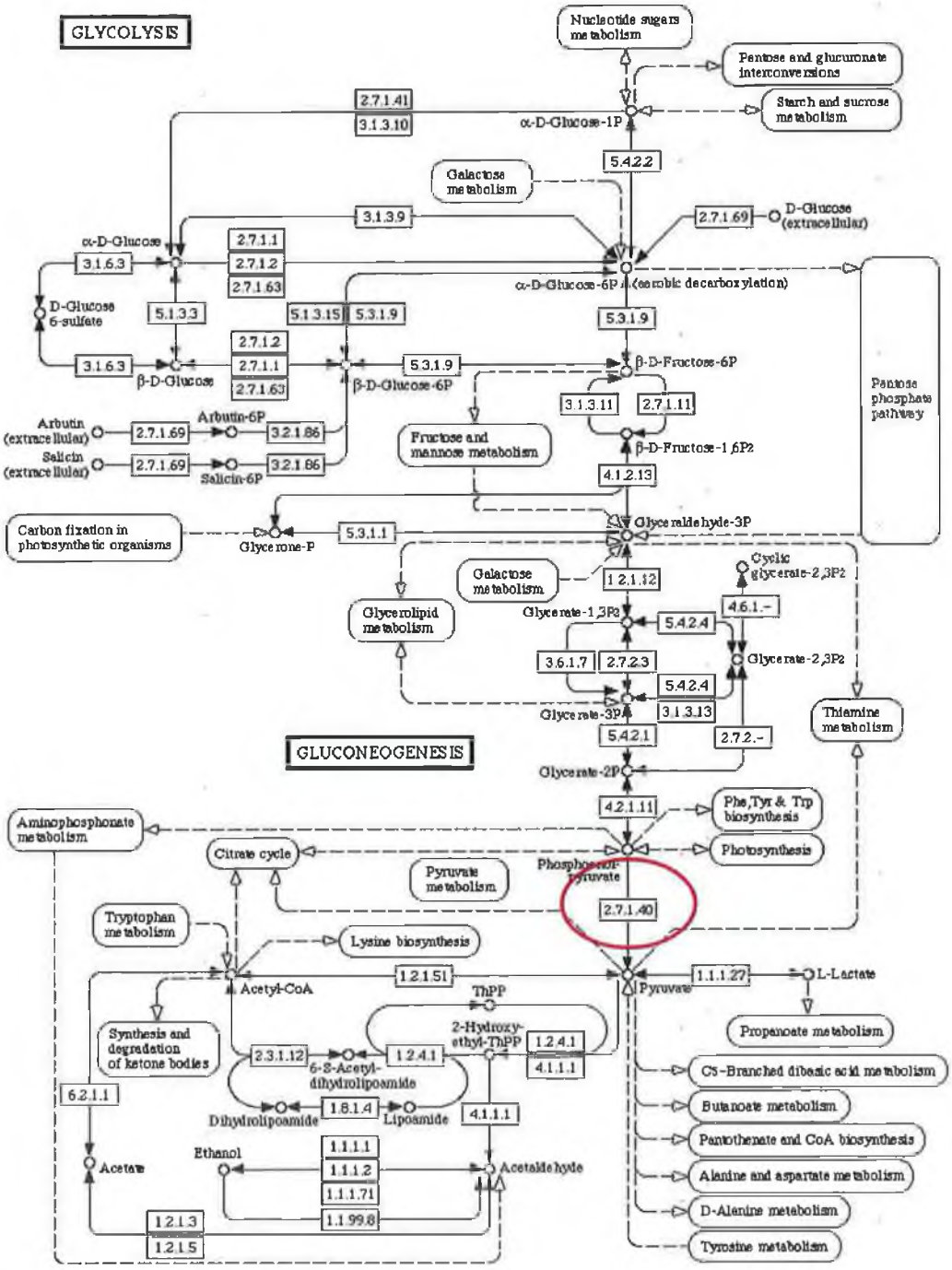

Figure 3.2.12: Figure displaying the Glycolysis pathway. Location of PKLR in this pathway is shown. PKLR is responsible for the conversion of phosphoenolpyruvate to pyruvate. Image downloaded from the KEGG web site.

3.3.5 Summary of analysis of DLKP-55 versus DLKP

The 5-FU/55FdU resistant variant of DLKP was generated by selection with the 5-FU prodrug 55FdU. It displayed an approximate 4-fold resistance to 5-FU and an approximate 2-fold resistance to 55FdU and Adr. No resistance to BrdU or taxol was observed.

Proteomic analysis of DLKP-55 versus DLKP resulted in the successful identification of 11 proteins differentially expressed between the groups – 7 of which were enzymes. Those proteins upregulated includes G6PD, PKLR, ALDH1A1 and NME1 and are involved in the Pentose Phosphate Pathway, Gluconeogenesis, Retinol Metabolism and Pyrimidine Metabolism, respectively.

Comparison to 5-FU treatments

Comparison between 5-FU treatment and 5-FU resistant variant may indicate a mechanism responsible for 5-FU resistance induced by 5-FU treatment. The data identified 7 proteins differentially regulated in both experiments 3 of which showed the same expression trend. These are PRDX2, EEF2, and CCT3. This may implicate EEF2 expression as a factor in 5-FU resistance.

3.4 Analysis of DLKP and its subpopulations; DLKP-SQ, DLKP-I and DLKP-M.

As stated NSCLC are often heterogeneous in nature and characterisation of these subpopulations is important in determining the nature of cancer biology. DLKP is described as being composed of at least 3 distinct subpopulation; DLKP-SQ, DLKP-I and DLKP-M and named based on morphological differences. Previous characterisations of these cell lines observed that DLKP-M displayed decreased growth rates compared to other populations and increased adherence rate to fibronectin. No differences were observed in drug resistance (McBride S., Ph. D. thesis, 1996). Characterisation of invasion and motility rates has not been described in these populations and here data is presented on invasion and motility differences between the clones and parent. Proteomic analysis was undertaken to investigate mechanisms controlling the differentiation processes governing the interconversion process in DLKP and to add to knowledge base of motility and invasion in NSCLC. Proteomic investigation was targeted at the total protein and the hydrophobic and hydrophobic associated protein complexes. Motility and invasion require cytoskeletal to membrane connection, thus analysis of this fraction between the clones will indicate what proteins are important in regulating motility/invasion in the DLKP clonal subpopulations.

3.4.1 Analysis of motility and invasion in DLKP and its subpopulations

Analysis of motility and invasion rates in DLKP and its subpopulations; DLKP-SQ, DLKP-I and DLKP-M was performed by Helena Joyce. Invasion rates are a result of two factors, motility and the ability to degrade ECM. Thus for thorough analysis of invasion both motility and invasion rates need to be determined.

Data revealed that DLKP-I and DLKP-M display apparent higher invasion rates than DLKP and DLKP-SQ (see figure 3.4.1). However analysis of motility showed that this trend was the same in the subpopulations (see figure 3.4.2). Motility assays presented here are saturated for DLKP-M and DLKP-I and are only included to demonstrate that the trend observed in invasion assays is present in motility assays.

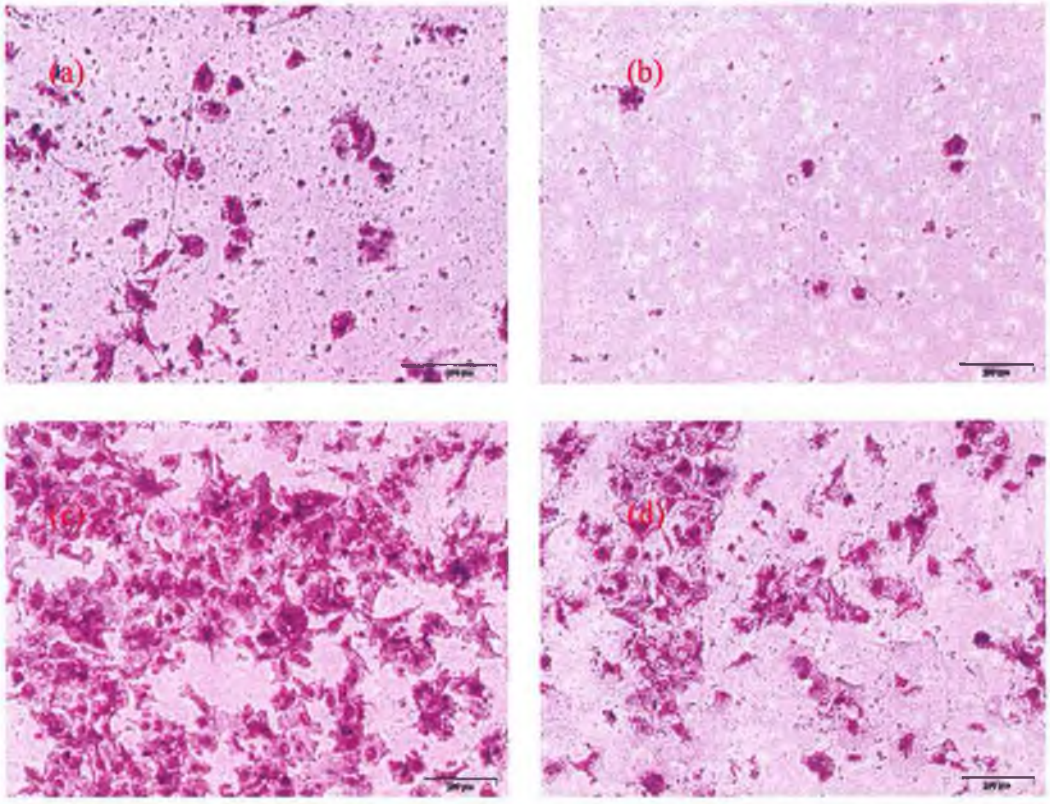

(e)

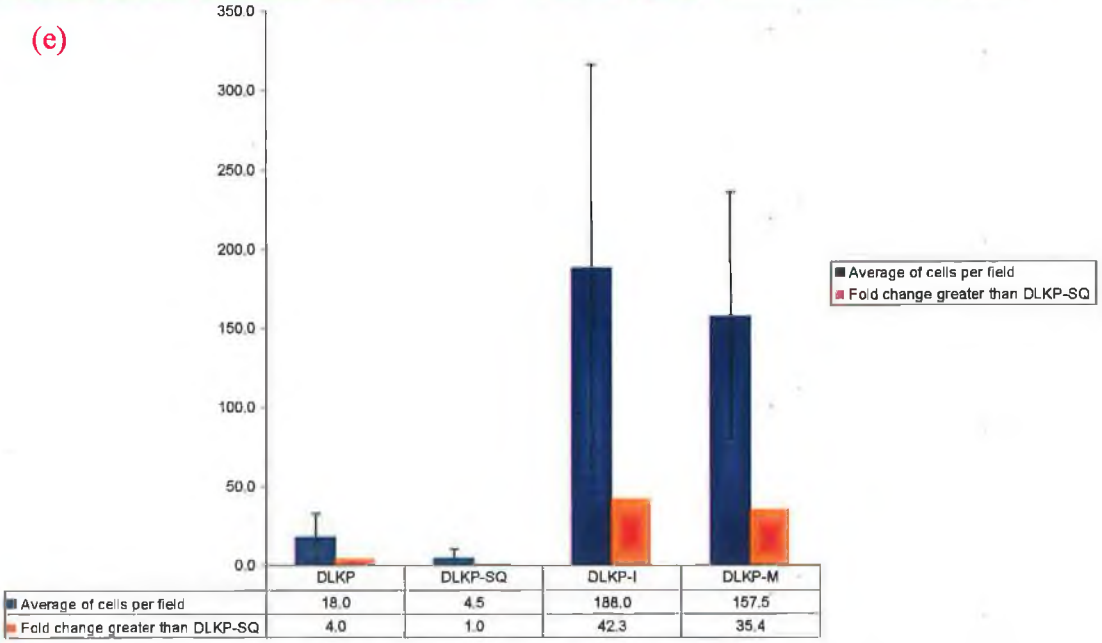

	DLKP	DLKP-SQ	DLKP-I	DLKP-M
Average of cells per field	18.0	4.5	188.0	157.5
Fold change greater than DLKP-SQ	4.0	1.0	42.3	35.4

Figure 3.4.1: Analysis of invasion rates in DLKP and it sub populations. (a) DLKP 48 hour invasion assay, (b) DLKP-SQ 48 hour invasion assay, (c) DLKP-I 48 hour invasion assay, and (d) DLKP-M 48 hour invasion assay (e) summary of statistics and fold changes between populations. Data indicates that DLKP-I and DLKP-M are more invasion then DLKP or DLKP-SQ or the other populations.

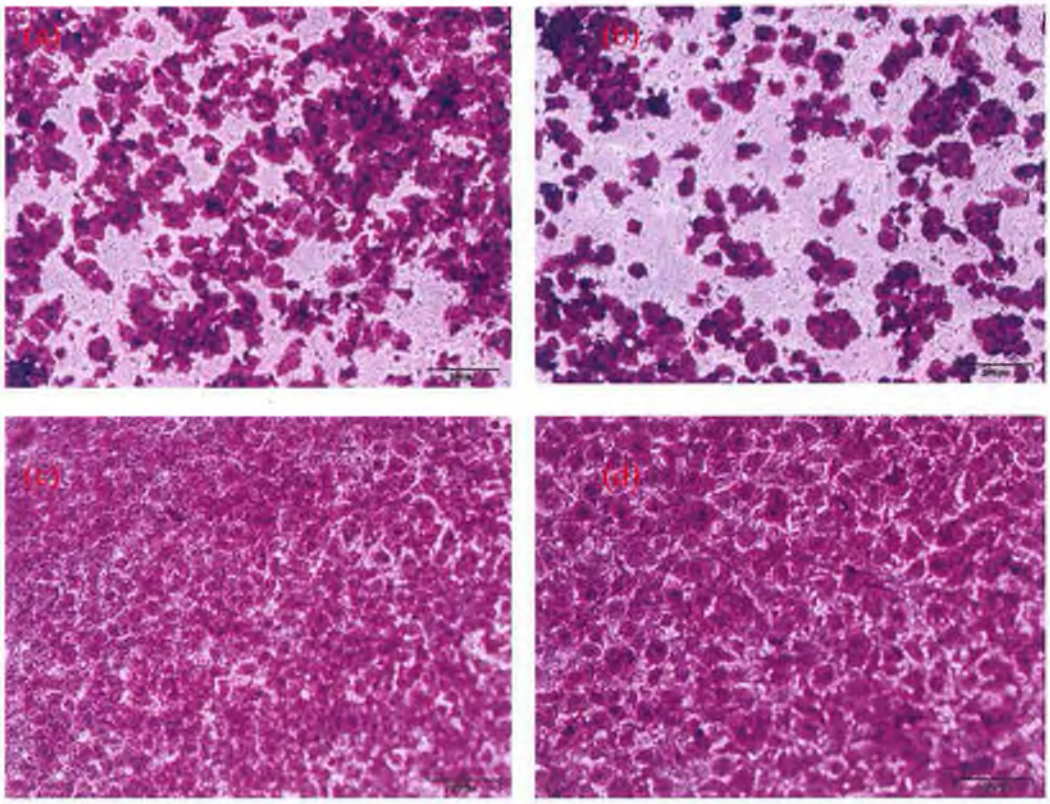

(e)

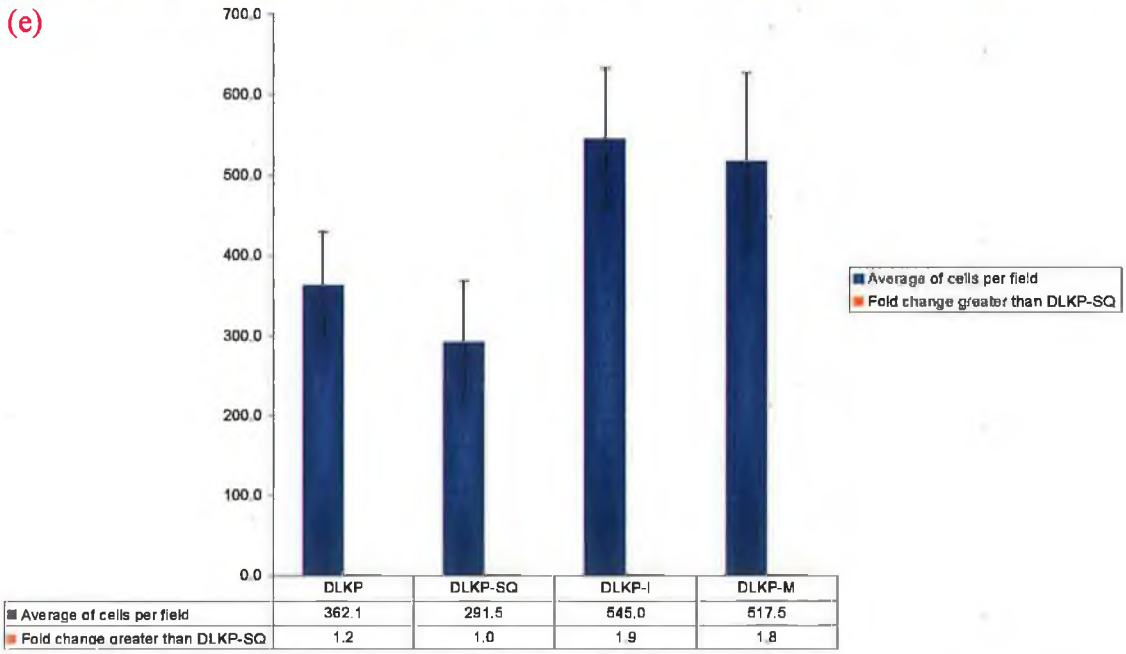

	DLKP	DLKP-SQ	DLKP-I	DLKP-M
Average of cells per field	362.1	291.5	545.0	517.5
Fold change greater than DLKP-SQ	1.2	1.0	1.9	1.8

Figure 3.4.2: Analysis of motility rates in DLKP and it sub populations. **(a)** DLKP 48 hour Motility assay, **(b)** DLKP-SQ 48 hour Motility assay, **(c)** DLKP-I 48 hour Motility assay, **(d)** DLKP-M 48 hour motility assay. Data indicates that DLKP-I and DLKP-M are apparently more motile than DLKP and DLKP-SQ and **(e)** Bar chart summarising of motility and fold changes.

3.4.2 Total proteomic analysis in DLKP and its subpopulations

In order to compare the alterations induced in the proteome of DLKP and its subpopulations, and for determination of the underlying mechanism that governs the interconversion between DLKP-SQ, DLKP-I and DLKP-M protein samples were prepared from each population. Total protein extracts were prepared as described in section 2.17. These were prepared in biological triplicate. Each biological triplicate was run in technical duplicates. Sample labelling with Cy dyes is shown in table 3.4.1. Differentially regulated proteins were based on a fold change of greater than 3 or less than -3 fold change between two of the populations and a t-test less than 0.01. A summary of protein trends is highlighted in table 3.4.2.

Table 3.4.1: Ettan DIGE experimental design for the analysis of differential protein expression induced in MCF-7 by exposure to 5-FU for 7 days.

Gel number	CY2 label	CY3 label	CY5 label
1	Pooled internal standard (50µg of protein)	DLKP, P.30, (50µg of protein)	DLKP-M, P.30, (50µg of protein)
2	Pooled internal standard (50µg of protein)	DLKP, P.30, (50µg of protein)	DLKP-M, P.30, (50µg of protein)
3	Pooled internal standard (50µg of protein)	DLKP, P.32, (50µg of protein)	DLKP-M, P.32, (50µg of protein)
4	Pooled internal standard (50µg of protein)	DLKP, P.32, (50µg of protein)	DLKP-M, P.32, (50µg of protein)
5	Pooled internal standard (50µg of protein)	DLKP, P.34, (50µg of protein)	DLKP-M, P.34, (50µg of protein)
6	Pooled internal standard (50µg of protein)	DLKP, P.34, (50µg of protein)	DLKP, P.34, (50µg of protein)
7	Pooled internal standard (50µg of protein)	DLKP-SQ, P.30, (50µg of protein)	DLKP-I, P.30, (50µg of protein)
8	Pooled internal standard (50µg of protein)	DLKP-SQ, P.30, (50µg of protein)	DLKP-I, P.30, (50µg of protein)
9	Pooled internal standard (50µg of protein)	DLKP-SQ, P.32, (50µg of protein)	DLKP-I, P.32, (50µg of protein)
10	Pooled internal standard (50µg of protein)	DLKP-SQ, P.32, (50µg of protein)	DLKP-I, P.32, (50µg of protein)
11	Pooled internal standard (50µg of protein)	DLKP-SQ, P.34, (50µg of protein)	DLKP-I, P.34, (50µg of protein)
12	Pooled internal standard (50µg of protein)	DLKP-SQ, P.34, (50µg of protein)	DLKP-I, P.34, (50µg of protein)

Table 3.4.2: Summary table of protein fold changes between each population. Only 15 of the proteins regulated between the sub populations have been identified and are summarised in table 3.4.3

Statistical filters		**Population comparison**					
Fold change filter	Fold change t-test	DLKP / DLKP-SQ	DLKP / DLKP-I	DLKP / DLKP-M	DLKP-SQ / DLKP-M	DLKP-I / DLKP-M	DLKP-SQ / DLKP-I
+/-1.2	<0.01	880	891	847	639	492	628
+/-1.5	<0.01	726	256	448	484	330	487
+/-3	<0.01	120	27	51	63	38	67

DLKP-I shows the least differences between the subpopulations and the parental population appears to be the most similar however DLKP-I and DLKP-M appear to more similar than DLKP-I and DLKP-SQ.

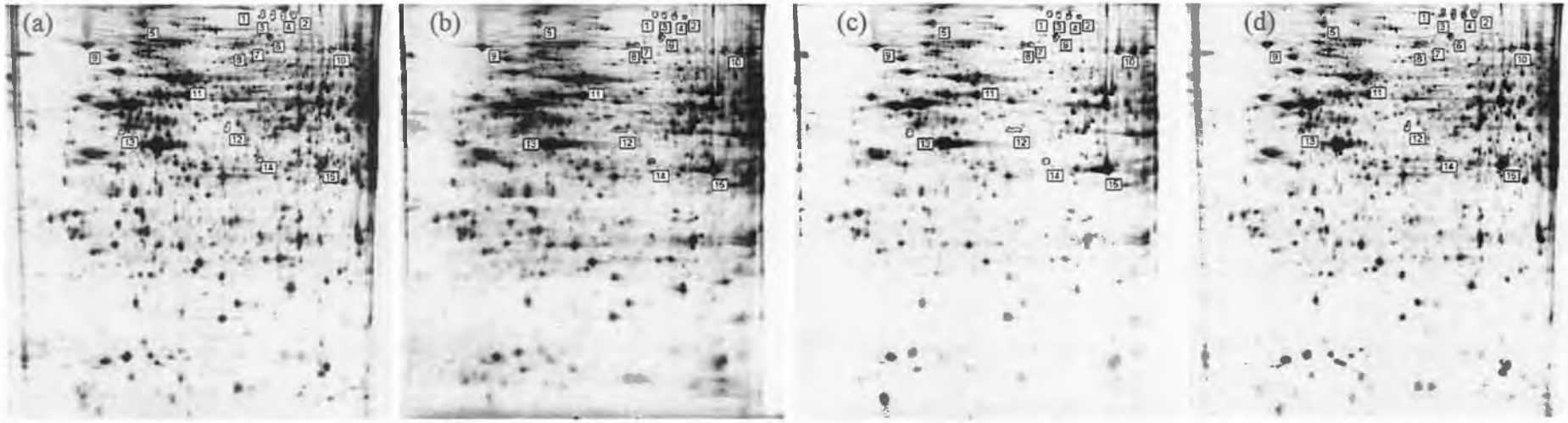

Figure 3.4.3: Images protein extracts labelled with CY dyes and separated by 2D-electrophoresis over a pH gradient of 4-7 from **(a)** DLKP, **(b)** DLKP-SQ, **(c)** DLKP-I, and **(d)** DLKP-M.

Table 3.4.2: Proteins identified by MALDI-ToF MS that were differentially regulated between DLKP and its subpopulation in the total proteomes. Protein expression data is included in table (fold change and t-test) as well Protein location on 2D gels (see figure 3.1.10.4.1 for locations).Proteins that correlate with invasion are highlighted in yellow and those abundant in DLKP are highlighted in blue. Proteins expression data was included between all clones to show that expression of protein between some of the population is not significant and indicates similar expression trend. *standardised log abundatace for each clone is shown in a graph form in figure3.4.4

Location on 2D Gel	Protein Name	Accession Number	Gene Name	Molecular Function	Proteins negative in all three fields indicate the protein has a higher expression in DLKP than the clonal subpopulations						Protein with fold positive fold changes in all three fields become enriched from DLKP-SQ->DLKP-I->->DLKP-M					
					DLKP-M / DLKP		DLKP-I / DLKP		DLKP-SQ / DLKP		DLKP-I / DLKP-SQ		DLKP-M / DLKP-SQ		DLKP-M / DLKP-I	
					Av. Ratio	T-test	Av. Ratio	T-test	Av. Ratio	T-test	Av. Ratio	T-test	Av. Ratio	T-test	Av. Ratio	T-test
Biological Function: Cell growth and/or maintenance																
1	type III preprocollagen alpha 1 chain [Homo sapiens]	gi|16197601|	COL3A1	ECM protein	23.35	3.9×10^{-12}	2.65	0.22	-2.08	3.3×10^{-3}	5.52	0.059	48.65	1.4×10^{-8}	8.82	3.7×10^{-4}
2	type III preprocollagen alpha 1 chain [Homo sapiens]	gi|16197601|	COL3A1	ECM protein	3.63	6.4×10^{-5}	2.28	0.051	1.11	0.94	2.06	0.09	3.28	6.9×10^{-4}	1.59	6.3×10^{-2}
3*	type III preprocollagen alpha 1 chain [Homo sapiens]	gi|16197601|	COL3A1	ECM protein	39.36	8.9×10^{-8}	3.97	0.3	1.25	0.05	3.17	0.45	31.43	7.2×10^{-9}	9.92	0.0062
4	type III preprocollagen alpha 1 chain [Homo sapiens]	gi|16197601|	COL3A1	ECM protein	22.27	3.20E-11	2.98	3.4x10-1	1.1	5.1x10-1	2.72	0.42	20.27	3.1×10^{-11}	7.47	1.3×10^{-3}
6*	VCL protein [Homo sapiens]	gi|24657579|	VCL	Cytoskeletal protein binding	-1.41	1.6×10^{-6}	-1.58	0.11	-5.21	6.9×10^{-4}	3.29	0.31	3.7	0.0025	1.13	0.25
13*	Tubulin, beta polypeptide [Homo sapiens]	gi|18088719|	TUBB2A	Structural molecule avtivity	7.48	1.5×10^{-8}	2.72	2.8×10^{-5}	6.64	2.8×10^{-8}	-2.44	2.8×10^{-7}	1.13	0.0067	2.75	8.0×10^{-8}
Biological Function: histone deacetylation																
7*	hypothetical protein [Homo sapiens]	gi|59016833|	HDAC1	histone deacetylase activity	-1.38	3.5×10^{-7}	-1.83	0.0072	-3.06	8.6×10^{-6}	1.67	0.09	2.22	0.00013	1.33	0.098
Biological Process: Protein metabolism																
8*	GANAB protein [Homo sapiens]	gi|40807091|	GANAB	Hydrolase activity	-1.39	6.3×10^{-6}	-1.92	0.0038	-3.84	1.0×10^{-7}	2	1.6×10^{-2}	2.77	1.8×10^{-6}	1.39	0.066
5*	HYOU1 protein [Homo sapiens]	gi|47938913|	HYOU1	Chaperone activity	-2.76	1.6×10^{-10}	-2.29	0.0033	-4.83	1.3×10^{-5}	2.1	0.052	1.75	1.0×10^{-2}	-1.2	0.83
9	Tumour rejection antigen (gp96) 1 [Homo sapiens]	gi|61656607|	TRA1	Heat Shock protein activity	-1.27	3.2×10^{-4}	-1.66	0.014	-3.26	1.2×10^{-5}	1.97	2.9×10^{-2}	2.57	8.5×10^{-5}	1.3	0.11
10*	Similar to Elongation factor	gi|19353009|	EEF2	translation	5.55	1.3	5.25	0.00022	1.17	0.26	4.5	0.00066	4.76	5.9	1.06	0.48

	2b [Homo sapiens]			regulator activity		$x10^{-10}$								x10-8		
11*	HSPA1A protein [Homo sapiens]	gi|14424588|	HSPA1A	Chaperone activity	-3.65	2 $x10^{-10}$	-1.5	0.064	-1.98	7.6 $x10^{-3}$	1.33	0.48	-1.84	7.5 $x10^{-2}$	-2.44	0.017
12	Chain A, The Crystal Structure Of The Human Hsp70 Atpase Domain	gi|42543698|	HSPA1A	Chaperone activity	7.43	5.0 $x10^{-6}$	2.6	0.0059	19.41	3.7 $x10^{-7}$	-7.46	4.2 $x10^{-6}$	-2.61	2.4 $x10^{-4}$	2.86	0.00028
Biological Process: Signal transduction ; Cell communication																
14	regulator of G protein signaling 6 beta [Homo sapiens]	gi|19908833|	RGS6	GTPase activator activity	5.38	2.0 $x10^{-6}$	1.95	0.0026	4.1	1.0 $x10^{-5}$	-2.1	1.6 $x10^{-6}$	1.31	0.0017	2.76	4.3 $x10^{-8}$
15*	Annexin I	gi|442631|	ANXA1	Calcium ion binding	2.08	0.0007	4.83	1.5 $x10^{-5}$	1.6	0.027	3.01	0.00051	1.3	0.14	-2.32	0.0021

In summary comparison between the subpopulations shows the accumulation of extracellular matrix protein type III preprocollagen alpha 1 chain in DLKP-M. An accumulation of ER proteins is also seem in DLKP-M and include GANAB (responsible for processing secreted and membrane proteins), VCL (responsible for connecting F-actin to the cell membrane), HYOU1 (involved in hypoxic response and tissue repair), HSPA1A, EEF2 (translation elongation factor), and HDAC1 (responsible for altering chromatin structure and regulating transcription) and the role of these proteins are discussed in section 4.4.1.

Figure 3.4.4: Standardised log abundance for each of the protein spots (a) Col3A1, (b) TUBB2A, (c) HDAC1, (d) GANAB, (e) HYOU1, (f) EEF2, (g) HSPA1A and (h) ANXA1.

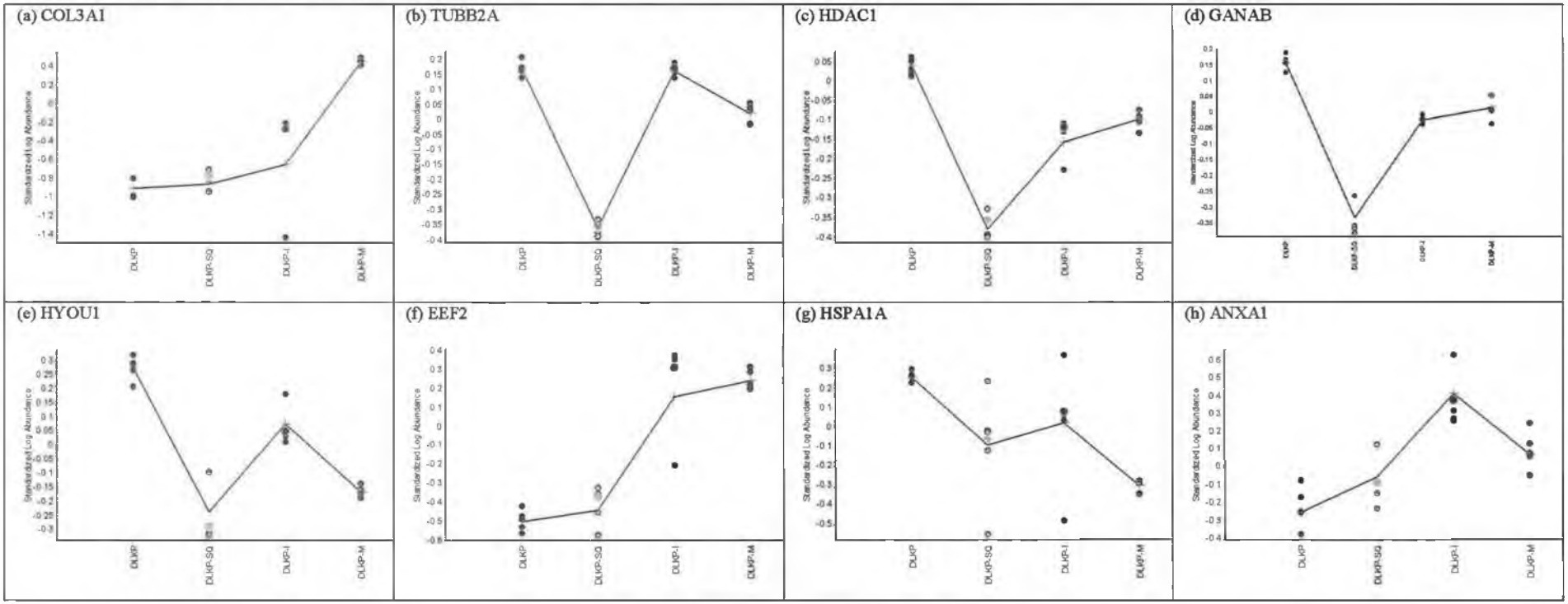

In summary the data shows an increased accumulation of Col3a1 suggesting DLKP-M produces extracellular matrix. Col3a1, and EEF2 correlate with invasion. Amongst the clonal populations HDAC1, GANAB and TUBB2A correlate with invasion.

3.4.3 Membrane and membrane associated proteomic analysis in DLKP and its subpopulations

In order to compare the alterations induced in the proteome of DLKP and its subpopulations, and for determination of the underlying mechanism that governs the interconversion and altered motility rates between DLKP-SQ, DLKP-I and DLKP-M, protein samples were prepared from each population using a fractionation process that selectively isolates proteins of the membrane and proteins associated to the membrane These hydrophobic protein and protein complexes were prepared as described in section 2.17. These were prepared in biological triplicate. Each biological triplicate was run in technical duplicates. Sample labelling with Cy dyes is shown in table 3.4.4. Fractionation process resulted in a low recovery of protein and this is due to the nature of the fractionation process. Previous 2D-DIGE experiments required 50μg of protein from each sample however due to the low level of protein recovery 25μg of protein was used for each sample in the DIGE experiment. This did not present a problem as fractionated samples contain fewer protein species and thus there individual abundance are enriched.

Differentially regulated proteins were selected based on a fold change of >+/<-3 fold change between two populations.

Representative DIGE images of Cy labelled protein lysates separated by 2DE can be seen in figure 3.4.5. Differentially regulated proteins were identified by MALDI-ToF MS as described in section 2.27. Locations of identified proteins from the pick list in this experiment can be seen in figure 3.4.4 and the identity of these proteins can be seen in table 3.4.4. The distribution of differentially regulated proteins amongst biological processes can be seen in figure 3.4.5.

Table 3.4.4: Ettan DIGE experimental design for the analysis of differential protein expression induced in MCF-7 by exposure to 5-FU for 7 days.

Gel number	CY2 label	CY3 label	CY5 label
1	Pooled internal standard (25μg of protein)	DLKP, P.30, (25μg of protein)	DLKP-M, P.30, (25μg of protein)
2	Pooled internal standard (25μg of protein)	DLKP, P.30, (25μg of protein)	DLKP-M, P.30, (25μg of protein)
3	Pooled internal standard (25μg of protein)	DLKP, P.32, (25μg of protein)	DLKP-M, P.32, (25μg of protein)
4	Pooled internal standard (25μg of protein)	DLKP, P.32, (25μg of protein)	DLKP-M, P.32, (25μg of protein)
5	Pooled internal standard (25μg of protein)	DLKP, P.34, (25μg of protein)	DLKP-M, P.34, (25μg of protein)
6	Pooled internal standard (25μg of protein)	DLKP-SQ, P.34, (25μg of protein)	DLKP-I, P.34, (25μg of protein)
7	Pooled internal standard (25μg of protein)	DLKP-SQ, P.30, (25μg of protein)	DLKP-I, P.30, (25μg of protein)
8	Pooled internal standard (25μg of protein)	DLKP-SQ, P.30, (25μg of protein)	DLKP-I, P.30, (25μg of protein)
9	Pooled internal standard (25μg of protein)	DLKP-SQ, P.32, (25μg of protein)	DLKP-I, P.32, (25μg of protein)
10	Pooled internal standard (25μg of protein)	DLKP-SQ, P.32, (25μg of protein)	DLKP-I, P.32, (25μg of protein)
11	Pooled internal standard (25μg of protein)	DLKP-SQ, P.34, (25μg of protein)	DLKP-I, P.34, (25μg of protein)
12	Pooled internal standard (25μg of protein)	DLKP-SQ, P.34, (25μg of protein)	DLKP-I, P.34, (25μg of protein)

Table 3.4.5: Summary of nuubers of differentially regulated proteins between each of the sub populations

Statistical filters		**Population comparison**					
Fold change filter	Fold change t-test	DLKP / DLKP-SQ	DLKP / DLKP-I	DLKP / DLKP-M	DLKP-SQ / DLKP-M	DLKP-I / DLKP-M	DLKP-SQ / DLKP-I
+/-1.2	<0.01	43	506	545	554	93	524
+/-1.5	<0.01	43	505	541	553	87	522
+/-3	<0.01	8	304	346	367	24	318

Analysis of the hydrophobic proteome and associated complexes reveal a remarkable similarity between lowly invasive populations (DLKP and DLKP-SQ, 8 proteins differentially regulated above 3 fold). The highly invasive population also show a remarkable similarity to each other (DLKP-I and DLKP-M only 24 protein differentially regulated between each clone). At least 300 proteins show regulation between each other comparison and each of these comparisons contains a highly and a

lowly invasive population. Thus this data contains an enormous amount of proteins that are potentially highly important in motility and invasion.

Figure 3.4.5: Images of hydrophobic proteins and associated protein extracts labelled with CY dyes and separated by 2D-electrophoresis over a pH gradient of 4-7 from (a) DLKP, (b) DLKP-SQ, (c) DLKP-I, and (d) DLKP-M.

Table 3.4.6: Proteins identified by MALDI-ToF MS that were differentially regulated between DLKP and its subpopulation in the hydrophobic proteomes. Protein expression data is included in table (fold change and t-test) as well Protein location on 2D gels (see figure 3.1.10.4.1 for locations). GI accession number was obtained from MS data. Protein name, Gene symbol were found from DAVID database, Human protein reference database or swissprot. Molecular and biological functions were obtained from the human protein reference database. Proteins that correlate with invasion are highlighted in Yellow those that are enriched in DLKP are highlighted in Blue. Proteins expression data was included between all clones to show that expression of protein between some of the population is not significant and indicates similar expression trend.

Position	Protein Name	Accession Number	Gene Symbol	Molecular Function	DLKP-M / DLKP		DLKP-I / DLKP		DLKP-SQ / DLKP		DLKP-I / DLKP -SQ		DLKP-M / DLKP-SQ		DLKP-M / DLKP-I	
					Av. Ratio	T-test	Av. Ratio	T-test	Av. Ratio	T-test	Av. Ratio	T-test	Av. Ratio	T-test	Av. Ratio	T-test
Biological Function: **Cell growth and/or maintenance**																
5	alpha-tubulin [Homo sapiens]	gi|37492|	TUBA3	Structural constituent of cytoskeleton	111.13	6.0x10^{-6}	69.15	7.7x10^{-7}	-2.39	1.8x10^{-1}	9.24	2.2x10^{-6}	-1.91	8.2x10^{-4}	-1.01	8.0x10^{-1}
6	alpha-tubulin [Homo sapiens]	gi|37492|	TUBA3	Structural constituent of cytoskeleton	26.40	5.3x10^{-5}	13.85	1.9x10^{-4}	-1.03	9.6x10^{-1}	3.07	1.0x10^{-3}	-1.61	2.0x10^{-1}	-1.24	5.5x10^{-1}
7	Tubulin, beta polypeptide [Homo sapiens]	gi|18088719|	TUBB2A	Structural constituent of cytoskeleton	24.67	7.3x10^{-7}	51.36	2.3x10^{-7}	2.27	8.6x10^{-1}	19.52	2.4x10^{-5}	-1.54	5.1x10^{-2}	-1.19	5.0x10^{-1}
8	Tubulin, beta polypeptide [Homo sapiens]	gi|18088719|	TUBB2A	Structural constituent of cytoskeleton	93.38	2.8x10^{-4}	16.05	3.8x10^{-7}	1.06	9.6x10^{-1}	2.57	1.3x10^{-3}	-1.82	6.2x10^{-1}	-1.47	7.3x10^{-1}
12	beta actin variant [Homo sapiens]	gi|62897625|	ACTB	Structural constituent of cytoskeleton	45.25	1.4x10^{-6}	43.88	4.8x10^{-7}	-1.15	3.0x10^{-1}	-5.13	4.7x10^{-4}	-1.03	9.7x10^{-1}	-1.08	9.8x10^{-1}
13	Beta Actin	AAH17450.1	ACTB	Structural constituent of cytoskeleton	33.39	3.7x10^{-6}	28.17	4.9x10^{-6}	1.44	9.8x10^{-1}	22.60	1.1x10^{-4}	-1.19	5.0x10^{-1}	-1.82	6.2x10^{-1}
14	ACTB protein [Homo sapiens]	gi|15277503|	ACTB	Structural constituent of cytoskeleton	28.15	5.2x10^{-7}	34.37	3.5x10^{-7}	-1.43	1.5x10^{-1}	5.87	7.7x10^{-5}	1.22	3.1x10^{-1}	1.17	3.5x10^{-1}
15	ACTB protein [Homo sapiens]	gi|15277503|	ACTB	Structural constituent of cytoskeleton	80.71	9.9x10^{-8}	50.01	3.3x10^{-7}	-1.93	1.5x10^{-2}	1.97	3.4x10^{-2}	-1.61	9.7x10^{-3}	-1.51	5.1x10^{-2}
21	gamma-actin	gi|178045|	ACTG1	Structural constituent of cytoskeleton	-2.75	1.4x10^{-2}	1.87	3.9x10^{-2}	-1.14	5.7x10^{-1}	-2.86	5.0x10^{-2}	5.14	5.2x10^{-4}	-1.21	8.0x10^{-1}
9	ATP synthase, H+ transporting,	gi|16741373|	ATP5B	Transporter activity	3.40	8.4x10^{-2}	2.31	2.6x10^{-2}	-1.11	8.4x10^{-1}	15.13	3.1x10^{-7}	-1.47	7.3x10^{-1}	-1.54	5.1x10^{-2}

	mitochondrial F1 complex, beta polypeptide [Homo sapiens]															
10	ATP synthase, H+ transporting, mitochondrial F1 complex, beta polypeptide [Homo sapiens]	gi|16741373|	ATP5B	Transporter activity	-5.69	3.2x10^{-3}	-10.15	3.9x10^{-3}	1.07	8.6x10^{-1}	2.13	9.1x10^{-3}	2.20	3.6x10^{-1}	5.14	5.2x10^{-4}
11	ATP synthase beta subunit	gi|179279|gb|	ATP5B	Transporter activity	-8.37	6.8x10^{-3}	-2.59	4.1x10^{-2}	1.10	8.8x10^{-1}	-3.49	4.6x10^{-3}	-1.21	8.0x10^{-1}	1.80	2.4x10^{-1}
1	heat shock 70kDa protein 8 isoform 2 variant [Homo sapiens]	gi|62896815|	HSPA8	ATP binding	3.52	1.9x10^{-2}	3.49	3.4x10^{-3}	1.20	4.9x10^{-1}	33.15	1.9x10^{-9}	-1.01	8.6x10^{-1}	-1.91	8.2x10^{-4}
2	heat shock 70kDa protein 8 isoform 2 variant [Homo sapiens]	gi|62896815|	HSPA8	ATP binding	12.89	1.2x10^{-4}	12.71	1.8x10^{-6}	1.37	3.3x10^{-1}	71.11	3.6x10^{-9}	-1.01	8.0x10^{-1}	-1.61	2.0x10^{-1}
3	Ubiquilin 1, isoform 1 [Homo sapiens]	gi|24659706|	UBQLN1	Ubiquitin-specific protease activity	8.07	2.0x10^{-4}	5.35	6.6x10^{-4}	2.71	1.0x10^{-1}	57.72	3.4x10^{-6}	-1.51	5.1x10^{-2}	-1.03	9.7x10^{-1}
4	MTHSP75	gi|292059|	HSPA9B	Chaperone activity	-4.92	1.5x10^{-2}	-5.32	3.6x10^{-3}	-1.04	9.3x10^{-1}	84.90	5.7x10^{-10}	-1.08	9.8x10^{-1}	-1.61	9.7x10^{-3}
20	elongation factor 2	gi|181969|	EEF2	Translation regulator activity	-11.50	1.1x10^{-3}	-6.39	8.7x10^{-3}	-1.83	2.9x10^{-1}	-10.81	5.7x10^{-4}	1.80	2.4x10^{-1}	2.20	3.6x10^{-1}
17	Annexin I	gi|442631|	ANXA1	Calcium ion binding	1.44	4.2x10^{-1}	3.78	1.0x10^{-3}	1.22	3.9x10^{-1}	1.80	2.7x10^{-3}	2.30	2.4x10^{-2}	-1.40	1.3x10^{-2}
18	annexin A1 [Homo sapiens]	gi|55959292|	ANXA1	Calcium ion binding	1.64	2.2x10^{-1}	3.50	7.4x10^{-4}	1.40	2.2x10^{-1}	2.92	2.1x10^{-3}	2.43	1.5x10^{-2}	-1.01	8.6x10^{-1}
19	guanine nucleotide binding protein (G protein), beta polypeptide 1 [Homo sapiens]	gi|30583449|	GNB1	Heterotrimeric G-protein GTPase activity	4.43	2.8x10^{-4}	3.16	1.1x10^{-3}	1.76	3.8x10^{-2}	3.10	7.9x10^{-4}	-1.40	1.3x10^{-2}	2.43	1.5x10^{-2}
16	HSPC108 [Homo sapiens]	gi|6841440|	STOML2	Auxiliary transport protein activity	12.89	1.2x10^{-4}	12.71	1.8x10^{-6}	1.37	3.3x10^{-1}	71.11	3.6x10^{-9}	-1.01	8.0x10^{-1}	-1.61	2.0x10^{-1}
22	Chain A, X-Ray Structure Of The Small G Protein Rab11a In Complex With Gdp	gi|60593433|	Rab11a	Signal transduction	4.90	1.7x10^{-3}	5.73	5.4x10^{-4}	-1.02	9.8x10^{-1}	49.30	1.4x10^{-6}	1.17	3.5x10^{-1}	1.22	3.1x10^{-1}

Association of f-actin and microtubules to cell membrane are required for movement of cell by causing membrane ruffles. The upregulation of proteins in the hydrophobic and hydrophobic associated caomplexes indicates an increased association of these proteins with the membrane and suggests a functional link with motility. Annexin A1 is involved in regulation attachment of F-actin to membrane although little is understood about its role. G proteins associate with activated integrins and their increase association to the hydrophobic fraction would suggest integrin activation and signal transduction. EEF2 associates with F-actin, the isoform identified is a low molecular weight complex comparison of this protein with the total protein for expression of EEF2 shows an inverse relation ship between the two isoforms and is highly suggestive that EEF2 regulation is important in the regulation of invasion and motility The implication of the regulation of these proteins is discussed in section 4.4.2.

Interesting proteins indicated by * in table 3.4.6 are represented in figure 3.4.6. This figure shows plots of proteins relative standard log abundance for each protein in comparison to each of the populations of DLKP.

Figure 3.4.6: Standardised log abundance for each of the protein spots (a) TUBA3, (b) TUB2A, (c) ACTB (d) ATP5B(e) EEF2, (f) ANXA1, (g) GNB1, (h) STOML2 and (h) Rab11a.

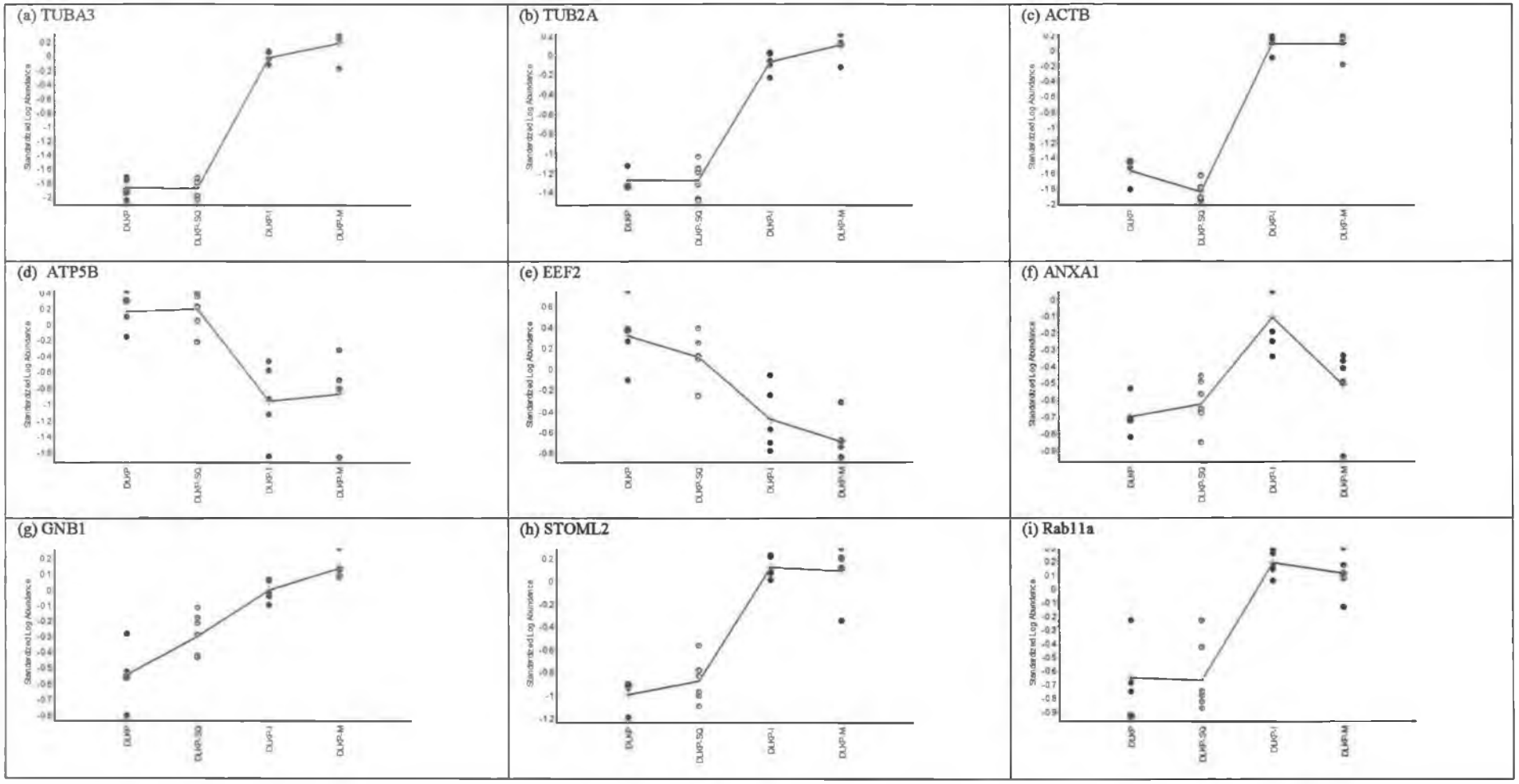

3.4.4 Unidentifed protein enriched in DLKP

The detection of proteins present in the parental population of DLKP that are much lower in the mixed population

Locations of three unidentified protein that are enriched in the mixed population of DLKP and may indicate cell-cell communication or the presence of an additional subpopulation

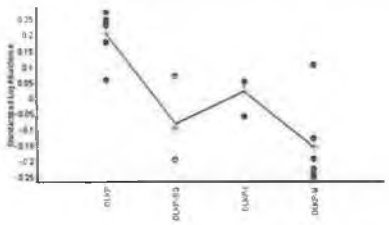

Unidentified Protein 1

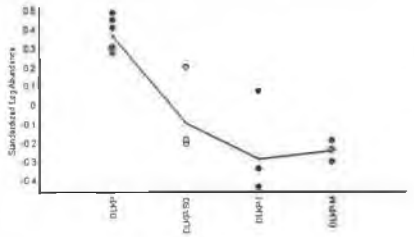

Unidentified Protein 2

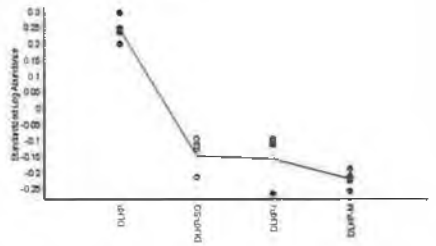

Unidentified Protein 13

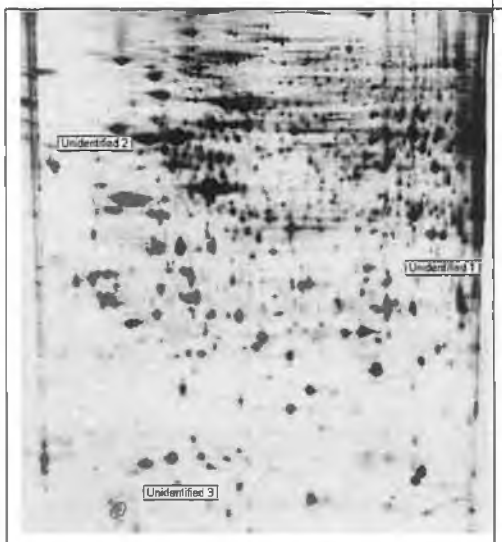

DLKP

DLKP-SQ

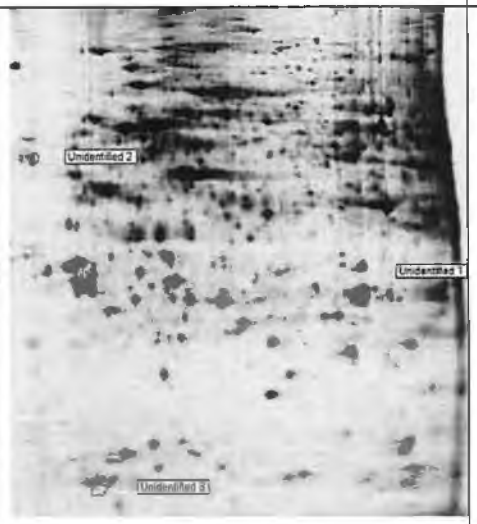

DLKP-I

DLKP-M

3.4.5 Summary analysis of DLKP and its clonal subpopulations

Invasion and motility assays reveal that DLKP and its subpopulations display altered invasion and motility rates. DLKP-I and DLKP-M were found to have high motility and invasion rates while DLKP-SQ and DLKP were found to have low motility and invasion rates.

Analysis of proteomic data in both total cell lysate proteome and hydrophobic proteome revealed a selection of proteins that correlate with the motility and invasion trends and are highlighted in table 3.4.2 and table 3.4.6 and are plotted in figures 3.4.4 and 3.4.6. Analysis of the hydrophobic proteome suggests increased association of actin filaments and tubulin filaments to the membrane and as stated previously microfilament connection to the membrane are important in the formation of membrane ruffles required for motility/invasion.

A potential marker protein was identified for the DLKP-M/DLKP-I population and this is Col3A1.

Finally, a selection of proteins highlighted in blue in tables 3.4.2 and 3.4.4 are more highly abundant in DLKP and figure 3.4.7 shows the location of 3 unidentified proteins that are more highly expressed in DLKP than any of the clonal subpopulations. This may be a result of cell-cell interactions or evidence of additional unidentified subpopulations and is discussed in section 4.4.3.

4.0 Discussion

Overview

Treatment of normal and cancer cells of the lung and breast with the anti-metabolite 5-FU at an IC80 concentration resulted in altered invasion status (see section 3.1.4), alteration in adherence profiles (see section 3.1.2), and a temporary inhibition of growth (see section 3.1.1) were cells appear to be halted in S-phase of the cell cycle as indicated by accumulation of p53 a marker of stalled DNA replication (see section 3.1.6) and alter keratin 8 and 18 expression in the cell lines A549, DLKP, and MCF-7 (see section 3.1.6) and the normal cell lines NHBE and HMEC (keratin expression not assessed in normal cell lines by western although in NHBE were found upregulated by 2D-DIGE). Proteomic analysis of 5-FU treated cells was undertaken (see sections 3.1.9, 10, 11, 12, and 13) and this data is discussed in **section 4.1.**

In order to investigate differences in the proteomic alterations induced by the fluoropyrimidines, 52FdU and 55FdU, DLKP was treated with both anti-metabolites under similar IC80 conditions (see section 3.2.1). Proteomic alterations induced by the treatment with these fluoropyrimidines that overlapped with DLKP treated with 5-FU are presented in section 3.2.2 and 3.2.3 and are discussed in **section 4.2**.

A 5-FU resistant (~4 fold) variant of DLKP was developed by pulse selection with the fluoropyrimidine 55FdU (see section 3.3.1) and resistance was characterised (see section 3.3.2). A proteomic comparison between DLKP and the resistant variant DLKP-55 was performed (see section 3.3.3) and potential mechanisms of resistance to 5-FU are discussed in **section 4.3**.

DLKP is a poorly differentiated NSCLC cell line consisting of at least 3 subpopulations that are shown to interconvert with each other. Invasion and motility

were investigated in DLKP and its subpopulations (see section 3.4.1) and analysis of its proteome (total cell extract see section 3.4.2) and hydrophobic proteome (see section 3.4.3) revealed a large selection of proteins that showed similar expression trends to motility/invasion phenotypes of these populations. These data are discussed in **section 4.4**.

4.1 *Overview of 5-FU treatments of normal and cancer cells*

Clinically 5-FU is used in the treatment of Breast and Lung carcinomas amongst others. In order to investigate the effect 5-FU would have on the proteome an *in vitro* approach was taken to investigate the effect of 5-FU treatment on the lung carcinoma cell lines DLKP (NSCLC) and A549 (adenocarcinoma) and the breast cell line MCF-7 (adenocarcinoma). In addition to this normal cells of epithelial origin of the lung and breast were treated with 5-FU to determine how normal cells respond to 5-FU treatment and if normal cell proteomic response is distinct or similar to cancer cell response.

All cell lines were treated at concentration of 5-FU that induced an approximate IC80 to IC90 inhibition of cell growth and was found to be 10μM, analysis of normal cell line inhibition of growth revealed a a equal or higher tolerance to 5-FU than cancer cell lines of similar tissue origin. An additional concentration of 30μM inhibition of cell growth was included in the analysis of the normal cell lines for this reason and as the literature was would suggest that normal cells would have lower incorporation frequencies of 5-FU into DNA and RNA (although incorporation rates were not investigated in our experiments) {*Rutman, et al., 1954*}. A common response to 5-FU treatment was observed including the down regulation of non-phosphorylated Stathmin and the Ribosomal protein SA (RPSA). Non-phosphorylated Stathmin depolymerises tubulin and the implications of its regulation are discussed in terms of microtubule polymerisation and the chemotherapeutic drugs the taxanes in section **4.1.1**.

Down regulation of RPSA is also a common response to 5-FU. Its role in ribosome dynamics, translation elongation and the role of other proteins involved in translation regulation are discussed in section **4.1.2**.

Previous work in the laboratory showed that the fluoropyrimidines, in common with the halogenated pyrimidines, induced the accumulation of the simple epithelial markers keratin 8 and 18 (*O' Sullivan, Ph.D. thesis 1999; McMorrow, Ph.D. thesis 2004; Mc Bride et al. 2000; Walsh et al., 2002*). Keratin 8/18 transfection into keratin 8/18 null cells has been shown to induce invasion 2-3 fold and induced focal adherence formation, and the upregulation of β_1 integrin. However keratin 8/18's precise role in the regulation of invasion is not known (Chu et al., 1996; and Izawa et al., 2006). Work performed here in this thesis sought to investigate if 5-FU could alter invasion status and adherence profiles of the cell lines DLKP, A549 and MCF-7 and the normal epithelial cell lines HMEC and NHBE (cultured without retinoic acid - retinoic acid induces epithelial differentiation in NHBE and would be expected to promote migration/invasion). The data shows that 5-FU treatment promoted invasion in low level invasive cell lines (DLKP, MCF-7 and NHBE) and induction of the epithelial markers, Keratin 8/18, was observed (see section 3.1.4 figures 3.1.12-16). This suggests that 5-FU treatment has the capacity to promote invasion through promotion of simple epithelial differentiation. In contrast A549 was shown to reduce expression of keratin8/18 protein (not determined in HMEC) and invasion of A549 was reduced following 5-FU treatment. Investigation of proteomic alterations was investigated and regulation of actin dynamics is discussed in section **4.1.3**.

A model for Keratin dynamics in the regulation of actin dynamics is discussed and presented in section **4.1.4**.

Growth rates post-treatment were assessed in A549, DLKP, and MCF-7 (see figures 3.1.6-9), but not in the normal cell lines due to a limited supply of cells and unstable phenotype associated with high cellular doublings, which can lead to cell death and or immortalisation with altered phenotype (>15 doublings (supplier guide lines see website www.cambrex.com)). The data indicates that the majority of cells survived the 5-FU treatment and a mechanism by which apoptosis may be inhibited in these cell lines is proposed and a possible link with the regulation of invasion and adherence (section 3.1.3-4) is discussed in section **4.1.5**.

Several transcription factors and mRNA processing proteins were found to be regulated in the proteomics data presented in tables 3.1.4, 7, 10, 13 and 16 and their involvement with proposed 5-FU related transcription models are discussed in section **4.1.6**.

4.1.1 Stathmin and microtubule filament stability – implications in taxol/vinca alkaloid/5-FU combinations

In all cell lines investigated stathmin (STMN1) was down regulated by 5-FU treatment (A549, DLKP, NHBE, MCF-7 and HMEC at all 5-FU concentrations). Stathmin is reported to be down regulated directly by p53 accumulation in cells {*Johnsen, et al. 2000*}. 5-FU is well known to induce p53 accumulation (*Gilkes, et al., 2006*), however p53 did not accumulate in NHBE cells as a result of 5-FU exposure (data only on 10 and not 30μM 5-FU treatment see section 3.1.4). This suggests that Stathmin down-regulation may be regulated by an additional mechanism or possibly the down-regulation is a result of isoform conversion - depleting one isoform and enriching another. Stathmin is an important protein in tubulin dynamics and 12 isoforms of this protein are known to exist. All stathmin isoforms phosphorylated at either Ser16 or Ser63 displayed a significantly reduced tubulin-binding affinity {*Steinmetz, 2006*}. Down-regulation of Stathmin by siRNA causes accumulation of cells in the G2/M phase of the cell cycle and the formation of atypical microtubules (Rubin et al., 2004). The stathmin isoform observed to be down-regulated is non-phosphorylated (although the phosphorylation status in HMEC has not been determined by comparison to other cell lines 2D images it is likely to be non-phophorylated due to its location). This may indicate that 5-FU prevents cells from progressing past G2/M phase of the cell cycle and p53 accumulation would indicate that cells are in S phase (p53 accumulates in response to DNA damage, 5-FU causes DNA damage only during S-phase – DNA synthesis stage of the cell cycle). The down regulation of non-phosphorylated stathmin may suggest phosphorylation of stathmin and would promote mitotic spindle formation at the G2/M phase of the cell and the formation of mitotic spindles required for mitosis (reviewed by Rubin and Atweh, 2004). The mechanism of tubulin depolymerisation and the role of stathmin are outlined in figure 4.1.

The Vinca alkoloids such as vincristine inhibits tubulin polymerisation and taxanes such as taxol stabilises microtubule filaments (*Mollinedo et al., 2004*). Deactivation of stathmin by phosphorylation or decreased expression of non-phosphorylated stathmin is required for the formation of mitotic spindles (Rubin and Atweh 2004). As stated

non-phosphorylated stathmin is down regulated and this may suggest that cells are producing or are about to produce mitotic spindles. Thus application of taxol or the vinca alkoloids may reveal that one of these drugs may interfere with mitotic spindle formation or function. Based on 5-FU down-regulation of non-phosphorylated stathmin this may indicate that mitotic spindles are being polymerised or are polymerised and are playing an active role in the cellular functions. Thus if tubulin is being polymerised into mitotic spindles treatment with vinca alkaloids would inhibit their formation and lead to cell death. Alternatively taxane treatment may lead to the stabilisation of taxanes and may prevent the separation of chromosomes by mitotic spindles at this stage of the cell cycle. However as 5-FU inhibits DNA synthesis it is likely that the nucleus is intact and that microtubulae are being polymerised. Thus it is more likely that vinca alkoliods would have a more effective role in combination with 5-FU treatments. Thus, this may indicate a potential synergistic mode of activity between 5-FU and microtubule interfering drugs in producing apoptosis. Further more experimental data here suggests that if taxol is used in combination with 5-FU it should be applied immediately post 5-FU treatment. As application with 5-FU would inhibit cell cycle progression past S-phase. However application of 5-FU with the vinca alkaloids may allow cell cycle at S/G1 phase of the cell cycle and may produce a synergistic activation of apoptosis.

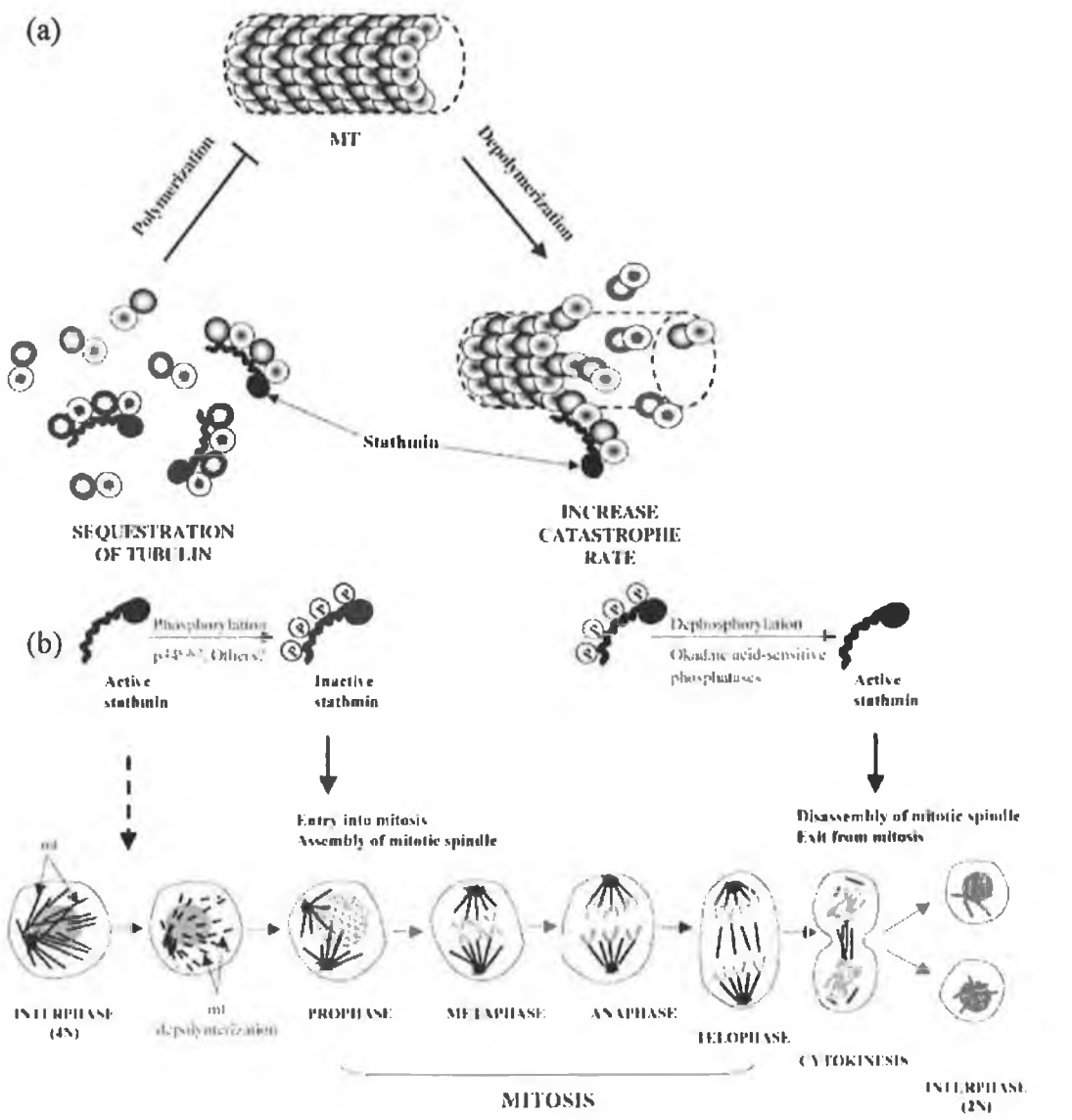

Figure 4.1: (a) Current model for the role of stathmin in the regulation of microtubule dynamics. Microtubule (MT) filaments continuously switch between phases of polymerization and depolymerization. Stathmin sequesters unpolymerized tubulin by binding two α/β-tubulin heterodimers (represented by light and dark shaded circles), thus reducing the pool of tubulin heterodimers available for polymerization. Stathmin can also bind to the end of polymerized microtubules and increase the rate of catastrophe (process leading to tubulin depolymerisation) by inducing a conformational change that promotes microtubule depolymerization. (b) Current model for the role of stathmin in the mitotic phase of the cell cycle. Chromosomes (represented in grey) condense and segregate during the mitosis (4 phases - prophase, metaphase, anaphase, and telophase) while cytoplasmic division occurs by cytokinesis. At the onset of mitosis, interphase microtubules (mt) depolymerize (illustrated by the interrupted lines) then repolymerize to assemble the mitotic spindle. The inactivation of stathmin by phosphorylation allows mitotic spindle assembly and entry into mitosis. Stathmins reactivation by dephosphorylation promotes mitotic spindle disassembly and exit from mitosis (Rubin and Atweh 2004).

4.1.2 Regulation of translation elongation in 5-FU treatments

Several ribosomal proteins and proteins involved in translation initiation and elongation were found regulated in the 5-FU treatments and are summarised in table 4.1. Their role in translation and their relationship to the cell cycle are discussed in the following subsections.

Table 4.1: Summary of translation elongation related proteins in All cell lines treated with 5-FU

Cell line	EEF1BG	p-EEF1BD	RPSA	RPLPO	TCTP	DARS
A549	↑	↑	↓	↑	?	↑
DLKP	↑	?	↓	?	?	?
NHBE	↑*	↑*	↓	↑*	?	?
MCF-7	?	↑	↓	?	↑	↑
HMEC	↑	↑	↓	?	↑	↑

*In a dose dependent manner (only at 30μM); ↑ increased accumulation; ↓ decreased expression; ? unknown.

4.1.2.1 Ribosomal protein SA (RPSA) and 5-FU treatments

The laminin binding protein Laminin receptor 1 binds to the extracellular matrix protein Laminin α 2. However the ribosomal protein SA (RPSA) is a product of the processing of this laminin receptor and generates the 40KDa protein observed regulated in these experiments and thus its regulation is to do with ribosome regulation and not adherence regulation (Sato et al., 1999). RPSA was observed to associate polyribosomes to the cytoskeleton (polyribosome - mRNA with numerous ribosomes attached indicating mRNA with high translation efficiency) (Auth D., 1992). Thus its down regulation would suggest a loss of cytoskeletal localisation of polyribosomes. Very little is known about the implication of RPSA expression, however RPSA may play a role in translation control and regulate association of polyribosomes to the cytoskeleton during 5-FU treatments.

4.1.2.2 The elongation factor 1 complex and 5-FU treatments

The translation elongation factor EEF1 is composed of two subunits, EEF1A and EEF1B. EEF1A (eukaryotic elongation factor 1 alpha) complex binds aminoacyl-tRNA to the ribosome with the hydrolysis of GTP. The EEF1B complex is composed of three subunits in mammals and these are EEF1B Beta, EEF1B Gamma and EEF1B Delta. The beta-gamma-delta complex facilitates the exchange of GDP for GTP in order to initiate another round of peptide elongation during translation (Sheu, et al., 1999). Phosphorylation of the Gamma and Delta subunits of EEF1BD was found to promote association of Valine tRNA synthetase and promote translation of Valine rich proteins. The EEF1B complex plays an important role in progression from the S-phase to G2/M-phase of the cell cycle and it relocalises from the endoplasmic reticulum to the nucleus prior to nuclear membrane breakdown where EEF1B complexes form a ring around the nucleus where it specifically facilitates the formation of mitotic spindles (*Boulben et al. 2003*). The subunits of EEF1B, EEF1B-gamma and EEF1B-delta, were found to be generally up-regulated in response to 5-FU exposure. Specifically, EEF1B gamma was found upregulated in A549, DLKP, NHBE and HMEC in response to 5-FU treatment. Phosphorylated-EEF1B delta was found up-regulated in A549, MCF-7, NHBE and HMEC in response to 5-FU treatment. In NHBE cells the response was dose dependent (accumulated at 30 μM and not 10μM 5-FU) and suggests a link with toxicity and not cell cycle progression and as Stathmin was downregulated at both concentrations it would suggest that its accumulation cannot be attributed to cell cycle stalling alone.

The expression of EEF1B delta was found to be enhanced by ionising radiation that caused oxidation and double strand breaks of DNA (*Jung et al., 1994*). This suggests a role for translation elongation in the genotoxic response. Taking this data with the data presented above it would support a stronger role for the elongation factors in a general DNA damage response.

The translationally controlled tumour protein, TPT1, has been shown to inhibit GDP-GTP exchange function of EEF1B-Beta, but not the gamma or delta subunits – and additionally stabilises the EEF1BG-EEF1BD translation elongation complex {*Cans, C. et al. 2003*}. This data would further support a role for the translation elongation factor 1B complex in the genotoxic response and may rule out the requirement for the EEF1B-beta subunit. This data would suggest an important role for the elongation

factors in both cell cycle and genotoxic response and is a novel finding in regards to 5-FU treatment.

The combination of stathmin downregulation, EEF1 subunit regulation may indicate that mitotic spindles are been formed and adds weight to the argument in section 4.1.1.1. The downregulation of RPSA may be important in the cell cycle. As stated in section 4.1.2.1 RPSA associates polyribosomes to the cytoskeleton and its common downregulation may facilitate the relocalisation of ribosomes to the nucleus and may facilitate the translation of proteins involved in the formation of mitotic spindles.

4.1.2.3 5-FU may induce selective translation by incorporation of amino acids during translation

Aminoacyl-tRNA synthetases ligate amino acids to their cognate tRNAs (*Sang Lee, et al., 2002*). The increased association of valine tRNA synthetase to EEF1B promoted increased expression of mRNA whose protein products contained high levels of valine (Le Sourde et al., 2006). The asparatate tRNA lygase - DARS - is responsible for the efficient channelling of aspartyl residues to the ribosome and binds to the EEF1 complex through EEF1BG (*Sang Lee, et al., 2002*). DARS shows a common up regulation between A549, MCF-7 and HMEC treated with 5-FU. Its expression together with data presented above may suggest a role in genotoxicity response or cell cycle. This may indicate that 5-FU treatment promotes increased expression of proteins that contain high levels of aspartyl residues.

Furthermore EEF1BD contains a phosphorylation site at serine 133 and is a substrate of CDC2 and controls translation efficiencies {*Kawaguchi, Y. et al. 2003*}. Phosphorylation of EEF1BD was found to increase selective incorporation rates of amino acid residues into synthesised proteins and caused the selective accumulation of protein enriched with Valine {*Monnier, A. et al. 2001*}. The EEF1BD isoform up-regulated by 5-FU treatment in all cell lines bar DLKP was found to be phosphorylated. This suggests a selective preference for amino acid incorporation during translation. Thus this data further supports the idea that 5-FU may alter translation efficiencies through regulation of EEF1 activity and translation elongation

efficiency. This data may indicate that phosphorylation of EEF1BD is important in production of proteins enriched in aspartyl residues and is important during 5-FU treatments.

The ribosomal phosphoprotein PO (RPLPO) forms a complex with ribosomal phosphoprotein 1/2 (RPLP1/2) and plays a role in selection of the translation elongation factors EEF1A and EEF2 during translation elongation (Uchiumi, et al. 2002). RPLPO showed accumulation in A549 treated with 5-FU and in NHBE treated with 30μM 5-FU but not 10μM 5-FU. Its expression trend was similar to that of translation elongation factor EEF1BD. These data indicates a role for RPLPO in the 5-FU genotoxic response and its increased expression is not just a product of cell cycle stalling.

4.1.2.4 eIF3 subunits may regulate translation during 5-FU treatments

The translation initiation factor eIF3S5 is down regulated in over 30% of NSCLC and breast cancers. It plays an important role in cap-dependent translation initiation and its down-regulation was found to promote cap independent translation through IRES mediated translation (*LeFebvre et al., 2006*). The translation initiation factor eIF3S5 was found down-regulated in DLKP cells treated with 5-FU, suggesting that 5-FU promotes a decrease in cap dependent translation initiation.

The identification of eIF3S5 protein in other cell lines investigated in this thesis by 2D-DIGE is highly challenging as is occurs in a region where keratin spots focus by 2D electrophoresis and thus keratin proteins will mask eIF3S5. DLKP is a keratin-negative cell line and as such allows for the identification of eIF3S5.

eIF3S2 is an important protein in the eIF3 complex and is involved in the recruitment of the translation canonical factors eIF2 (complexed in the translation pre-initiation complex), eIF5 during cap dependent translation initiation (*Valasek et al., 2002*). eIF3S2 was downregulated in NHBE treated with 10μM 5-FU. Down regulation of eIF3S2 would suggest that 5-FU promotes a reduction in cap dependent translation in NHBE. However its expression recovered at the higher 5-FU treatment in NHBE and suggests that its expression is important in the translation events regulated by the EEF1 protein as discussed above and may implicate it in translation regulation during genotoxicity.

eIF3S3 was reported down-regulated in Hela cells treated with 5-FU (*Yim et al., 2006*). Thus this combined with data presented above may indicate that 5-FU generally causes a down regulation of eIF3 activity and may promote selective translation or global repression of translation through down regulation of the eIF3 subunits.

A possible inhibition of cap dependent translation initiation is apparent but not conclusive by the common down regulation of eIF3 subunits. Cap-independent translation initiation of viruses requires the recruitment EEF1A and EEF2 (Pestova et al., 2003). Internal ribosome entry site-mediated translation or IRES-mediated translation is an important mechanism during cellular stresses, and its exact mechanism of translation is poorly described. Viral models are often used as a basis for the understanding of cellular driven IRES (*Jackson, 2005*). Thus the accumulation of the EEF1 proteins generally seen in all cell lines treated with 5-FU and accumulation of EEF2 in DLKP treated with 5-FU, may indicate that 5-FU promotes cap independent translation through regulation of the eIF3 subunits and upregulation of the elongation factors. Furthermore the selectivity of translation may be enhanced by the up regulation of DARS and may indicate selective translation of aspartyl rich proteins in an IRES driven translation regulated system.

4.1.3 Actin dynamics during 5-FU treatment and its potential role in regulation invasion in 5-FU treatments

Proteomic analysis of normal and cancer cell lines of the lung and breast identified a list of proteins involved in actin architecture and actin regulation to be differentially expressed as a result of 5-FU treatment (see tables 3.1.4, 7, 10, 13 and 16). Invasion status was found altered in all cell lines as a result of 5-FU treatment and adherence was found to be altered in A549 but not DLKP and MCF-7 (not investigated in normal cell lines due to limited number of cells), see sections 3.1.3, and 3.1.4. This data is briefly summarised in table 4.2 but refer to specific sections for more detailed data.

Table 4.2: A summary of invasion trends in cell lines post 5-FU treatment and the regulation of actin binding and regulating proteins identified by proteomic analysis.

Phenotype change or protein trend	A549 treated with 5-FU	DLKP treated with 5-FU	NHBE treated with 5-FU	MCF-7 treated with 5-FU	HMEC treated with 5-FU
Invasion trend	↓	↑	↑	↑	↓
Adherence to fibronectin and collagen	↑	-	-		
Actin	↑	↑	↑	↑	-
ARP		↑			
CAPZA1		↓	↓		
CAPZB		↑	↑		
p-CFL1		↑	↑	↑	↑
GSN		↑	↑	↑	
PLS3		↑	↑		
LASP-1		↓			↑
g-CAP39		↓			
CTTN		↑	↑		
VCL		↑			
WDR-1			↑		↑
PPP2CB		↑			
TPM1					↑
TPM3	↑				
TPM4	↑				
NME1	↑				
CAPNS1	↑				↑
VIL2				↑	
RDX				↑	
YWHAZ	↑	↓	↑	↑	↑
YWHAG	↑		↑	↑	↑
KRT8	↓	↑	↑	↑	
KRT18	↓	↑	↑	↑	

4.1.3.1 Actin accumulation and potential regulators of actin dynamics

The protein β-actin (ACTB) showed accumulation in all cell lines bar HMEC treated with 5-FU. Four isoforms in both DLKP and A549 cell lines showed accumulation. Matching of proteins between A549 and DLKP show that protein positions 46, 44, 43 and 45 on the A549 2DE DIGE images (figure 3.1.43) correspond with 55, 54, 50 and 49 on the DLKP 2D DIGE images (figure 3.1.48), respectively. DLKP shows about 1.5-1.7 fold change in all ACTB isoforms with position 50 (1.73 fold) showing the greatest accumulation. DLKP position 50 corresponds with the actin up-regulated in the NHBE experiment. A549 shows the greatest accumulation at position 46 (1.66) and least at position 45 (1.34). This may indicate that ACTB dynamics are altered by treatment with 5-FU. The alteration in ACTB dynamics that result in the accumulation of the ACTB most highly abundant in DLKP and NHBE may be important in the promotion of invasion while the alteration that promote the formation of ACTB isoform preferentially enriched in A549 result in decreased invasion. As ACTB is an important component of the actin threadmilling process (see section 1.4.8) in cellular motility and may explain in part why A549 shows decreased invasion post 5-FU exposure. In MCF-7 cells treated with 5-FU ACTB was found to be upregulated. A total of 3 isoforms were upregulated and isoform at position 101 corresponds with the most highly upregulated actin isoform in NHBE and DLKP treated with 5-FU (see figure 3.1.53 and 3.1.58). No actin isoforms showed upregulation in HMEC treated with 5-FU.

The cytoskeletal protein ACTB can be modified by various post transcriptional modifications and these include acetylation, metylation and ADP-ribosylation at D2, Y53 and V96, H73, and R177, respectively (*Gavaert, et al., 2002; Schuler et al., 2000; and Nyman et al., 2002*). ADP-Ribosylation of ACTB prevents ADP ATP exchange and prevent actin recycling (*Schuler et al., 2000*). These modifications could contribute to the various isoforms identified on the 2D gels. Further identification of the modifications present in the differentially regulated isoforms of ACTB may indicate a tentative role for these post translational modifications in the processes of motility and invasion.

This data suggests preferential accumulation of ACTB isoforms are associated with increased invasion. This data suggests that 5-FU treatments may promote and decrease invasion through altered actin dynamics.

As described in section 1.4.6-1.4.12, actin architecture is highly regulated and actin threadmilling is an essential component of migration and invasion (*dos Remedios, et al. 2003*). As can be seen from table 4.2 a selection of proteins are regulated by 5-FU treatment that influence actin architecture and are discussed in the following sections.

4.1.3.2 Regulation of actin dynamics by 5-FU treatment

No actin binding proteins were commonly regulated between NHBE, DLKP and A549 or DLKP and A549. However, between DLKP and NHBE five actin binding proteins were commonly regulated. These include CAPZA1, CAPZB, CFL1, GSN and PLS3. Table 3.1.7 subsection cell growth and/or maintenance lists 11 actin binding proteins regulated in DLKP treated with 5-FU. Those found upregulated include CAPZB, phosphorylated CFL1, CTTN, GSN, PLS3 and VCL and those down regulated include CAPZA1, LASP1 and gCAP 39. The actin binding proteins CAPZB, CFL1, PLS3 and GSN play important roles in actin dynamics and are thus important in motility and invasion (*dos Remedios, C.G. et al. 2003*).

CAPZB and CAPZA1 are up and down regulated, respectively. CAPZ proteins play an important role in nucleation of actin assembly, capture of pre-existing actin filaments, regulation of actin assembly at the barbed ends of filaments and elimination of annealing at the barbed ends of filaments (*Sept D, et al 1999*). CAPZB, CAPZA1 and CAPZA2 form a complex at the barbed end of actin filaments and prevent severing of actin, while CAPZB binds monomeric actin and stimulates its elongation (*Cassella et al., 1986; and Sept, et al., 1999*). The regulation of this CAPZ proteins in DLKP and NHBE treated with 5-FU may indicate increased actin nucleation and severing of F-actin.

Cofilin can nucleate actin in the presence of CAPZ and plays an important role in motility. Cofilin is diffusely distributed in the cytoplasm of quiescent cells. However,

in active cells, it translocates to cortical regions where the actin cytoskeleton is highly dynamic and drives the ruffling of membranes of motile cells. Cofilin depolymerises actin filaments. It removes actin-ADP from the pointed end of F-actin in the form of an actin-ADP-Cofilin complex which exists freely in the cytosol. Phosphorylation of cofilin releases actin and ADP from cofilin (dos Remedios, et al. 2003). Thus the observed increase in phosphorylated cofilin would increase the free actin monomers in solution available for F-actin elongation. Non-phophorylated cofilin was not detected on the 2D gels and it is not expected to as the pI of cofilin is greater than pH 7. Thus it is difficult to determine from this data if 5-FU induces accumulation of just phosphorylated cofilin or promotes the upregulation of both isoforms suggesting cofilin recycling and increased expression of cofilin. Clearly 5-FU treatment caused phosphorylation of cofilin which overall would contribute to increased levels of monomeric actin available for F-actin nucleation and elongation. Thus 5-FU promotes increased accumulation of phosphorylated cofilin. Taking into account the functions of cofilin and the high degree of cofilin accumulation in 5-FU treatment experiments it would suggest that its expression is highly important in promoting invasion in response to 5-FU treatment.

Cortactin (CTTN) is a *c-src* substrate associated with sites of dynamic actin assembly at the leading edge of migrating cells. CTTN binds to Arp2/3 complex, the essential molecular machine for nucleating actin filament assembly. CTTN potently inhibits the debranching of the filament networks. CTTN is necessary for direct activation of the Arp2/3 complex and stabilization of newly generated actin filament branch points. Thus, CTTN may promote the formation and stabilization of the actin network that drives protrusion at the leading edge of migrating cells (*Weave. et al., 2001*). CTTN was found to accumulate in DLKP and NHBE treated with 5-FU and would suggest a role in promoting F-actin elongation.

Gelsolin (GSN) is an actin binding protein and binding of gelsolin initiates the F-actin severing from the pointed end, but while binding to filaments is rapid, its severing action is slow (*dos Remedios, et al. 2003*). GSN acts more as a Ca^{2+}-regulated capping protein. Depolymerization is mainly caused by dissociation of actin subunits from the pointed ends of actin filaments and that inhibition of polymerization was achieved by gelsolin binding at the barbed ends. The rate of capping at the barbed end

was directly proportional to the free Ca^{2+} concentration and high calcium levels activate gelsolins F-actin severing functions (Gremm D and Wegner A, 2000). Gelsolin forms a complex with talin – the integrin binding protein –has been shown to attach of F-actin to the cell membrane via integrin intercellular domain and F-actin membrane connections are important in cell migration (Fischer et al., 1998; Chen H. et al. 2006). The mRNA expression of Gelsolin was reported to be up-regulatid by 5-FU treatment in MCF-7, however this altered expression could not be confirmed by Northern blotting (Maxwell *et al.,* 2003). The increased expression of gelsolin in DLKP, NHBE and MCF-7 by 5-FU treatment is shown here and the combination of its expression in these cell lines and the data presented above on its activity would suggest a highly important role for Gelsolin in promoting invasion during treatment with 5-FU.

Thus increased expression of Gelsolin shown here in MCF-7 seems important in promoting invasion in these systems. Furthermore this data also implicates a degree of similarity between the MCF-7 5-FU microarray experiments published by Maxwell et al., 2003 and the MCF-7 5-FU treatment data presented here. Maxwell et al., (2003) found that Gelsolin mRNA was up-regulated 7.3 in their DNA microarray experiments although northern blots failed to validate this result. The fold change for gelsolin in these 5-FU treated MCF-7 proteomic experiment found four Gelsolin isoforms were upregulated by 4-7.35 fold. (Additional data showing overlaps; Annexin II, and Annexin IV expression; on DNA microarray were 12.3, and 9.3, (Maxwell et al., 2003) and proteomic data 1.7, and 1.6, respectively) Down loading of this microarray data and analysis of both data sets (proteomic and DNA-microarray) may reveal further insights into the regulation of invasion and 5-FU treatment response in MCF-7 by 5-FU treatment and identify possible targets that are translationally regulated in 5-FU treatments.

The gelsolin like capping protein gCAP39 was down-regulated by 5-FU treatment of DLKP. It plays a role in invasion and caps F-actin however unlike gelsolin it does not have severing activity (*Yu et al. 1991*) Taken together with CAPZ protein expression and GSN expression it would suggest alteration in F-actin capping proteins and a preference for gelsolin capping of F-actin during 5-FU treatments in cell lines that become more invasive post 5-FU treatment.

Plastins are actin binding proteins which form parallel actin filaments known as actin bundles. At least in vitro, actin bundling through plastin-3 is inhibited if the concentration of calcium is increased and allows severing of F-actin filaments. Calcium gradients are important during migration and thus as an actin filament enters regions of high calcium plastin-3 would dissociate and in theory allow Gelsolin and cofilin to depolymerise F-actin filaments (*Pacaud et al., 1983*). Plastin-3, or T-Plastin, (PLS3) was found to inhibit depolymerisation of actin by cofilin, and is expressed predominantly in mesenchymal and epithelial cells. L-plastin disassociates from F-actin in high calcium gradients which are formed in F-actin depolymerising regions during migration and thus L-plastin would contribute to organised actin polymerisation and depolymerisation. Like L-plastin, T-plastin contains a calcium binding domain and calcium binding to L-Plastin induces disassociation from F-actin and T-plastin is probably similarly regulated (Arpin, *et al.*, 1994). Plastin-3 also promotes branching through association of the ARP2/3 complex and thus is vital during migration (Giganti, et al., 2005). Plastin-3 accumulates in both DLKP and NHBE in response to 5-FU treatment and this would suggest formation of actin bundles important in migration.

Vinculin (VCL) as stated above plays an important role in connecting gelsolin capped F-actin to the membrane and plays and important role in the formation of focal contacts (Fischer et al., 1998; Chen H. et al. 2006). VCL expression is increased in DLKP treated with 5-FU.

WDR-1 (AIP1 – actin interacting protein 1) cooperates with ADP/cofilin in its severing activity of F-actin (Ono S. et al., 2004). WDR-1 accumulated in both HMEC and NHBE treated with 5-FU. Its increased expression in NHBE and HMEC would promote actin depolymerisation.

PPP2CB phosphorylates and activates calpains responsible for breaking of actin-focal adherence contacts and is reported to promote invasion. Breaking of the talin contacts is important in the disassociation of integrins from ECM contacts {*Xu, L. et al. 2006*}. Increased expression of PPP2CB is observed in DLKP treated with 5-FU and suggests increased calpain activity.

Villin 2 (VIL2) also known as ezrin, anchors the F- actin to radixin and FAK and activates autophosphorylation of FAK (Shuster et al. 1995) and Radixin (RDX) binds ezrin (*Bharthur et al., 1998*). Both Vil2 and RDX are ERM proteins and require binding to moesin to regulate the activity of G-proteins. Protein kinase C activates ERM proteins by phosphorylation of Villin 2 and this forms a link between the membrane and F-actin (*Larsson C., 2006*) and activation is important in wound healing and invasion (*Jensen et al., 2004*). The ERM proteins were also found to bind syndecan-2 (*Granes et al., 2004*) and this would be consistent with a role in wound healing as syndecan-2 is required for ECM assembly. The accumulation of non-phosphorylated ezrin and radixin may suggest deactivation of the ERM proteins as suggested by the accumulation of non- phosphorylated isoforms. Villin is also a calcium dependent actin bundling and actin depolymerising protein. At high calcium levels it depolymerises and at low calcium levels it forms actin bundles (Molitoris et al., 1997). RDX and Vil2 were not found to be phosphorylated but were upregulated which suggests accumulation of the inactivated form of the ERM proteins (Larsson 2006). Further investigation is required to determine if phosphorylated forms are regulated on 2D gels. However this data would indicate a decreased association of ERM proteins to integrins and in combination with gelsolin expression may indicate an alteration in proteins present in the focal contacts. This may further indicate a transformation from a fibroblast like behaviour to epithelial like behaviour. Syndecan-2 is highly expressed in fibroblast and is important in the assembly of ECM proteins and promotes increased adherence to ECM proteins and decreased invasion (Villena et al., 2003). Although expression of syndecan-2 was not assessed in MCF-7 the data presented above may indicate a role for Syndecan-2 in invasion in MCF-7 5-FU treatments. Further more Syndecan-2 expression was found to accumulate in A549 and decrease in DLKP (see table 3.1.3) further suggesting a role for syndecan-2 expression in regulation of invasion during 5-FU treatment.

These proteins work synergistically together and it would be expected that small changes in these proteins expression would have large changes in phenotypic behaviour. Taking these data in context of NHBE MCF-7 and DLKP it would suggest that invasion is promoted by altered actin dynamics in regards to actin nucleation and

elongation, F-actin depolymerisation, F-actin bundling and F-actin attachment to membrane all processes important in migration.

In contrast A549 treated with 5-FU increased expression of the actin binding proteins tropomyosin-3 (TPM-3) and TPM4 in response to 5-FU exposure. In HMEC increase d expression of TPM 1 was observed. TPM proteins stabilise actin filament. TPM3 has been shown to inhibit the branching activity of ARP2/3 and ARP2/3 is an important protein in promoting motility (*Blanchoin et a.l 2001*). TPM-1 mRNA expression has been shown to correlate with decreased motility in a DNA microarray experiment (Okubo et al., 2002). Thus tropomyosin family member expression appears to inhibit invasion by possible inhibition of actin branching and stabilisation if actin filaments.

NME1 expression has also been shown to inversely correlate with invasion and its up regulation is suggested to interfere with PKC signalling pathway (Nie Q. et al., 2006). NME1 is upregulated in A549 treated with 5-FU and indicates a possible role in the inhibition PKC signalling.

Calpain 1 (CAPNS1) is a protease whose substrates include phosphorylated CTTN, GSN, talin, Plastin-3 and VCL. These proteins are important in maintaining cell cytoskeletal contacts with focal contacts. Calpains have been implicated in migration and have been shown to be important in breaking actin-focal contacts complexes through proteolytic cleavage of talin {Lebart, M.C. 2006}. Increased phosphorylation of CAPNS1 is linked with increased invasion and phosphorylation is enhanced by MEK, ERK1/2 and PKC signalling pathways. Dephosphorylation of CAPNS1 is associated with decreased cell migration and metastasis in the lung {Xu, L. et al. 2006}. There is an accumulation of non-phosphorylated CAPNS1 in A549 and accumulation of non-phosphorylated CAPNS1 may indicate decreased phosphorylation rates. Furthermore in NHBE a statistically significant increase in non-phosphorylated CAPNS1 was observed at the higher 30μM concentration of 5-FU and may indicate that high toxic doses of 5-FU pushes cells into a non-invasive state through down regulation PKC signalling pathway.

Tropomyosin 1 and HSPB1 were observed up regulated in HMEC and they contribute to actin stabilisation and decreased motility rates (Gunning et al., 1997; Concannon, 2003). This may explain how invasion is inhibited in HMEC. Less than 10% of proteins regulated in HMEC have been identified and further work needs to be done to explain the inhibition of invasion observed.

Cofilin and its regulation

The up-regulated Cofilin isoform is phosphorylated in MCF-7, DLKP and NHBE (indicated by pro-diamond staining) and probably in HMEC (as shares same location as phosphorylated cofilin in all other cell lines) and only one phosphorylation site is known to exist oncofilin. Cofilin is a substrate of phosphorylated LIMK which is phosphorylated by PAK2. Phosphorylated PAK2 accumulated in MCF-7 treated with 5-FU. The p-21 activated kinase PAK2 is activated by G-proteins such as CDC42, Rac or p21 and PAK2 activity was shown to be essential for the activation of metastasis by increased secretion of proteases and increased migration in macrophages (Misra *et al.* 2005). Transcription of p21 is well known to be activated by p53 accumulation and this indicates that 5-FU genotoxic stress leads to p53 accumulation, leading to transcriptional up-regulation of p21 (Schumm *et al.* 2006) leading to PAK2 activation and phosphorylation of LIMK which subsequently phosphorylates cofilin and promotes of invasion (Misra *et al.* 2005). PAK2 increased expression and activation are worth investigation in all other cell lines treated with 5-FU. PAK2 activation is an important observation in MCF-7 5-FU treatments and provides a functional link between 5-FU genotoxicity and migration in the carcinoma cell line MCF-7.

Activated PAK2 phosphorylates eIF4G and inhibits its role in cap dependent translation (Ling *et al.*, 2005). This data further supports the possibility that 5-FU treatments cause an inhibition of translation.

4.1.4 The role of Keratin intermediate filaments and 14-3-3 protein in regulation of actin dynamics during 5-FU treatment

The 14-3-3 proteins YWHAZ and YWHAG binds to keratin 18 phosphorylated at serine 33 and is important in regulating keratin dynamics (Ku *et al.*. 1998; Ku *et al.*, 2002). The 14-3-3 proteins bind to phosphorylated cofilin, and to slingshot a protein

responsible for dephosphorylating cofilin and allowing it to continue depolymerising F-actin (Pan S. *et al.,* 2006; Soosairajah *J. et al.* 2004*)*. Competition between phosphorylated keratin 18, p-cofilin and slingshot can be predicted from these regulations.

2D-DIGE data presented in tables 3.1.4, 7, 10, 13 and 16 shows that several 14-3-3 proteins accumulate in A549, NHBE, MCF-7 and HMEC. Members of the 14-3-3 protein family were observed up regulated; in A549 5-FU treatments include

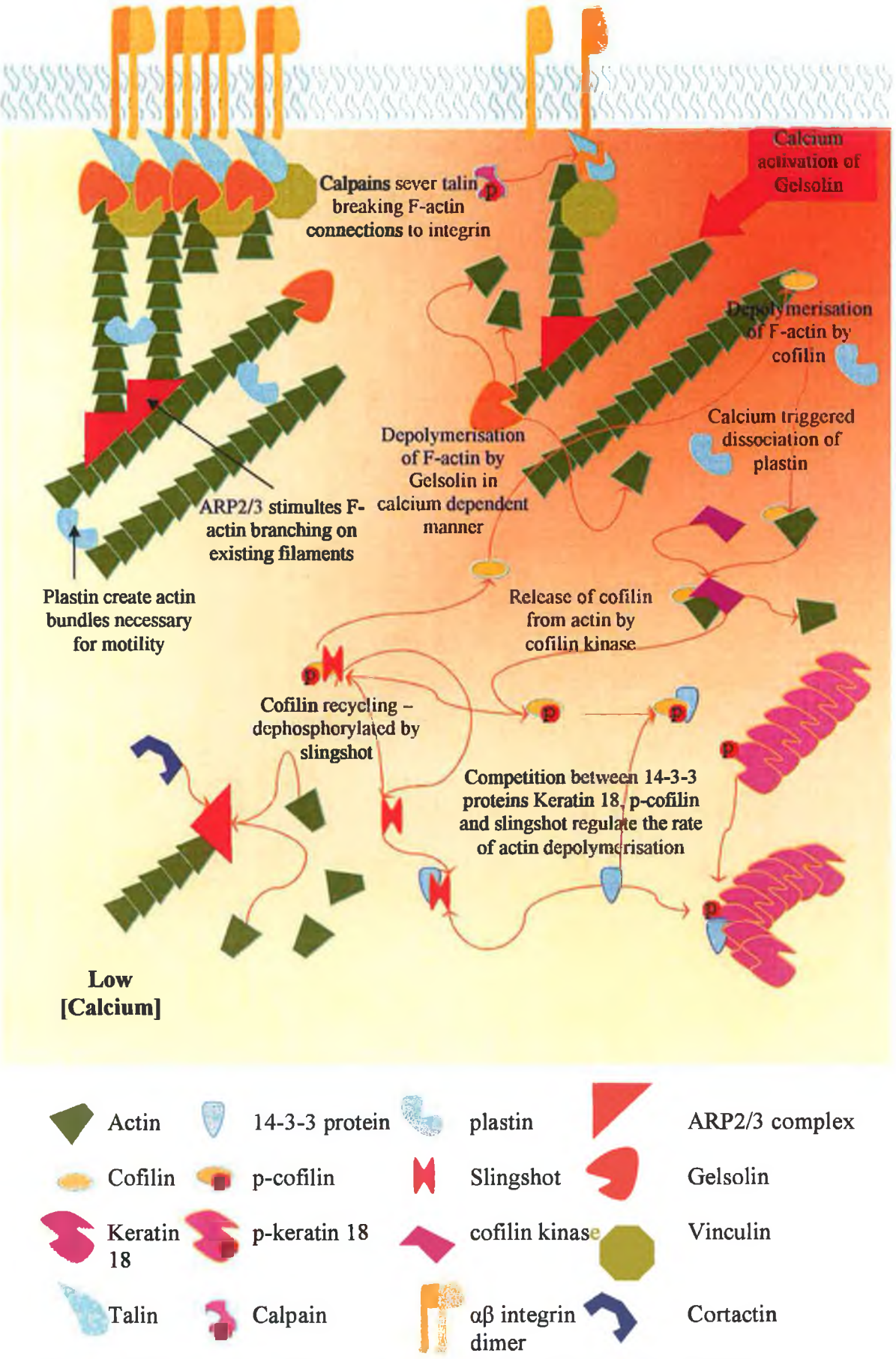

Figure 4.2: Potential role of phosphorylated keratin 18 and 14-3-3 proteins in the regulation of actin dynamics

YWHAZ, YWHAB and YWHAQ; in NHBE 5-FU treatments SFN and YWHAG; in MCF-7 5-FU treatments YWHAZ and YWHAG; in HMEC 5-FU treatments non were observed regulated; in DLKP YWHAZ was down regulated. Expression of keratin 18 was observed upregulated in DLKP, MCF-7 and NHBE while decreased expression of phosphorylated keratin 18 was observed in A549 and no alterations were observed in HMEC. Based on this expression data and known competition between 14-3-3 proteins and phosphorylated Keratin 18, phosphorylated cofilin and slingshot it is likely in DLKP, NHBE and MCF-7 14-3-3 proteins would accumulate in keratin filaments preventing sequestering of cofilin and promoting invasion by allowing cofilin recycling. In A549 the downregulation of p-keratin 18 would free 14-3-3 proteins into the cytoplasm and allow it to sequester p-cofilin and slingshot inhibiting invasion. In HMEC no regulation was observed however this may be a result of limited data from this experiment.

Thus a proposed model of regulation of cofilin recycling by 5-FU treatment is as follows. 14-3-3 protein are sequestered in the cytokeratin filaments thus promoting cofilin recycling by (1) releasing increased levels of slingshot proteins to regenerate cofilin (2) prevent the formation of 14-3-3 protein complex with phosphorylated cofilin.

BrdU treatments were found to upregulate keratin 18 expression in A549 (McBride et al., 1999). This data would suggest that 5-FU acts on A549 in a uniquely different manner than BrdU. However, retinoic acid treatment of A549 cells was shown to down-regulate keratin 18 expression in A549 and inhibit invasion – very similar to 5-FU data presented here- and cause an upregulation of the cellular retinoic acid binding protein Crabp (Fazely *et al.*, 1990). Also, 5-FU was found to induce an upregulation of the epithelial markers keratin 18, 14 and 17 amongst others in NHBE and Crabp2 was found upregulated in NHBE. This data may indicate that 5-FU functions in a similar manner to all-trans retinoic acid in inducing differentiation.

4.1.5 Inhibition of apoptosis during 5-FU treatments

The heat shock protein 27, HSPB1, has been shown to play an important role in cell survival as indicated by section 1.1.9. Over expression of HSPB1 increases resistance to various forms of apoptotic signaling and includes sequestering of cytochrome c in the cytoplasm preventing binding to APAF-1 and apoptosome formation {Gorman, A.M. *et al.* 2005}. Specifically phosphorylation of HSPB1 sequesters cytochrome-c in the cytoplasm preventing apoptosome formation (see figure 1.3). Furthermore HSPB1 over expression increases expression of Glucose-6-phosphate dehydrogenase causing resistance to ROS, and non-phosphorylated and non-oligomerised HSPB1 contribute to F-actin stabilization while phosphorylated and oligomerised isoforms do not {Concannon, C.G. 2003}.

NHBE and MCF-7 2D-DIGE experiments show the accumulation of phosphorylated HSPB1 (see tables 3.1.10, 11, 13 and 14) While in A549 and HMEC HSPB1 accumulated but was not phosphorylated. The upregulation of phosphorylated HSPB1 would suggest that HSPB1 sequesters released cytochrome c from the mitochondria. The accumulation of non-phosphorylated HSPB1 promotes actin stabilisation and seems probable by the data discussed in section 4.1.3. In DLKP HSPB1 was not regulated, however HSP70 appears up-regulated and as shown in figure 1.1.3 HSP70 can sequester APAF-1 and prevent apoptosome formation (Concannon, 2003).

Taking this data in context of 5-FU treatment it seems that cells may inhibit apopotosis by three potential mechanisms; (1) sequestering of cytochrome c by phophorylated HSPB1 preventing apoptosome formation, (2) sequestering of APAF-1 by HSP70, again preventing apoptosome formation and (3) HSPB1 promotion of F-actin stability.

Very little work to date has investigated the role HSPB1 in 5-FU treatments, and the importance of these observations is highlighted by work performed by Miyazaki, T. *et al.* (2005). Who demonstrated that HSPB1 negative expression was a predictor of a favourable outcome of patients suffering with oesophageal squamous carcinoma

treated with 5-FU in combination with other drugs. Thus Miyazaki, *et al.* (2005) data in combination with work here indicates that targeting of HSPB1 anti-apoptopic function may be crucial in improving clinical outcome of 5-FU based therapies. DLKP did not show alteration in HSPB1 expression.

Cathepsin D (CTSD), a protein involved in proteolytic remodelling of ECM is upregulated in HMEC and MCF-7 treated with 5-FU. Its expression does not correlate with invasion however CTSD activity is not limited to invasion and plays a functional role in ECM architecture (Sis *et al.*, 2004). Thus CTSD increased expression may suggest that 5-FU induces altered interactions with the ECM and CTSD expression is a component of but not a determinant of phenotypic alterations. An alternative role of CTSD is in apoptosis. During pre-induction of apoptosis CTSD is up-regulated in the lysosome and released from the lysosome into the cytosol where it stimulates the release of cytochrome c from the mitochondria (Zuzarte-luis *et al.*, 2006). 5-FU has been shown previously to induce cytochrome c release (Emert-Sedlak *et al.*, 2005). Cytochrome c participates in the formation of the apoptosome (Gorman, *et al.* 2005}. However, proliferation data demonstrated that MCF-7 survives treatment with 5-FU in this experiment. If CTSD is stimulating the release of cytochrome c from the mitochondria in to the cytosol in these cell lines the increased expression of HSPB1 would inhibit its role in apoptosis. Thus this data would further suggest that HSPB1 expression is crucial in inhibiting apoptosis and promoting cell survival during 5-FU treatment.

The apoptosis related protein Programmed Cell Death 6 Interacting Protein, (PDCD6IP also known as ALIX, HP95 and AIP1; should not be confused with WDR-1 also caused AIP1) was identified up regulated in both A549 and DLKP treated with 5-FU. PDCD6IP has been linked to promoting detachment-induced apoptosis (anoikis), inhibited detachment of viable cells from substratum and reduced tumorigenicity. PDCD6IP overexpression promoted flat cell morphology and decreased cell proliferation, whereas PDCD6IP down regulation had opposite effects. This data suggests that mammalian PDCD6IP is a positive regulator in apoptotic signalling and a negative regulator in cell transformation. They also suggest that PDCD6IP has roles in regulating cell adhesion and morphology (Wu *et al.* 2002). These findings are consistent with observed alterations in morphology and may

indicate that 5-FU promotes cell survival in an attachment dependent manner. However, DLKP and A549 adherence and invasion profiles suggest different interactions with ECM and may indicate that PDCD6IP influenced interactions with ECM may ultimately be decided by an additional factor. PDCD6IP expression is required for maintaining typical fibroblast morphology, associates with F-actin and F-actin based structures in lamellipodia and stress fibers. PDCD6IP binds CTTN, an activator of the ARP2/3 complex-mediated initiation of actin polymerization. PDCD6IP is required for lamellipodial localization of CTTN (CTTN expression is discussed in section 4.1.3). The C-terminal half of the middle region of PDCD6IP interacts with a-actinin, a key factor that bundles F-actin in stress fibers (Pan S. *et al.*, 2006).

In addition to this the integrin subunit β_1 was commonly found up regulated in A549 and DLKP in response to 5-FU treatment. Its binding partners α_2 and α_5 integrin were up regulated in A549 and DLKP, respectively, and syndecan-2 was up-regulated in A549 and down-regulated in DLKP. $\beta_1\alpha_5$ integrin and sdc-2 form a complex in focal contacts and promote adherence to fibronectin (Kusuno *et al.*, 2004) and there expression profiles would explain the adherence assays profiles in A549. DLKP showed decreased expression of sdc-2, and decreased expression has been shown to correlate with increased invasion rates and $\beta_1\alpha_5$ integrin was shown to correlate with increased invasion and signalling from this integrin complex was shown to stimulate MMP-9 expression - a potent collagenase – through PKC signalling (Hans *et al.*, 2006). This data indicates alteration in cell matrix interactions in both cell lines and is supported by invasion and adherence assays.

The upregulation of α_5 and β_1 integrin subunits in both A549 and DLKP may indicate its expression is crucial in cell survival during 5-FU treatment. Work performed by Stoeltzing, *et al.*, (2003) showed that the use of the α_5 β_1 antagonist, ATN-161, when used in combination with 5-FU infusion reduced liver metastases formation and improved survival in this colon cancer model when compared to 5-FU alone.

These data suggests an important role for $\alpha_5\beta_1$ integrin dimer in cell survival and Syndecan-2-$\alpha_5\beta_1$ integrin trimer in invasion during 5-FU treatment.

4.1.6 Regulation of mRNA metabolism during 5-FU treatments

Data presented in tables 1.1.4,710,13,16 show the regulation of numerous proteins involved in nucleoside, nucleotide and nucleobase regulation and are discussed in the following sections.

4.1.6.1 HSPA5 and HNRPK and p53 and HNRPK in translation and transcription regulation

HNRPK and p53 interact with each other stabilize the promoter/p53/HNRPK complex and facilitating additional steps of transcription-complex assembly together with transcriptional initiation itself. Several factors that interact with p53 and stimulate its DNA binding ability have also been reported to bind HNRPK; these include HMBG1, YB-1, and TBP (Moumen A., *et al.* 2005; Dinthilak *et al.*, 2002). HNRPK is down regulated in DLKP and A549. Further more in NHBE p53 does not accumulate and HNRPK accumulates. The HNRPK regulated isoforms are non-phosphorylated. Phosphorylation of HNRPK by c-Src drives translational activation of silenced mRNA's. HNRPK specifically binds and activates c-Src. c-Src mediates tyrosine phosphorylation of HNRPK and inhibition of its DICE (mRNA sequence) binding activity and translation repression. c-Src kinase specifically regulates HNRPK function as a translational silencer *in vivo* (Ostareck lederer *et al.*, 2002). This may indicate that during stress were p53 accumulates HNRPK suppression of silenced mRNAs is reduced. The role of phosphorylated HNRPK in its interaction with p53 has not been investigated. However in light of this data it may be speculated that phosphorylation of HNRPK leads to activation of translationally repressed mRNA's that may be involved in stress response. The phosphorylation of HNRPK would free it from mRNA silencing complex and this may allow it to participate with p53 in transcription.

Interestingly HNRPK and the Endoplasmic Reticulum protein HSPA5 show accumulation in NHBE while in A549 and DLKP it decreases. Also the genotoxic stress related protein p53 shows accumulation in DLKP and A549 and not in NHBE.

This data suggests a regulatory link. In deed there is, HSPA5 accumulation has been linked to ER stress and under such conditions GSKβ3 phosphorylates nuclear p53 causing it to be relocalised to the cytoplasm for degradation. However, p53 accumulation, nuclear localisation and nuclear deportation, and degradation rates have not been investigated and are worth further investigation in light of this data. Research on HNRPK has implicated it in processes including chromatin remodelling and transcription as well as mRNA splicing, export, and translation {Moumen, A. 2005}. Endoplasmic Reticulum resident chaperone HSPA5 shows down regulation in both DLKP and A549, and in NHBE it is upregulated as previously stated. HSPA5 upregulation indicates ER stress and suggests that NHBE cells are not responding to 5-FU exposure in a similar manner to the lung cancer cell lines. As DLKP and A549 show p53 accumulation and this indicates genotoxic response. This is not an entirely novel observation as 5-FU treatment of luminal cells was found to induce the expression of XBP1, a gene involved in activation of the ER stress response (Troester *et al.* 2005). Taking this together with the observed accumulation of HSPA5 (ER protein that is upregulated during the ER stress response) show that 5-FU can induce either ER-stress or genotoxic response. Cells experiencing ER stress have been shown to inhibit the genotoxic stress by GSKβ3 phosphorylation of p53 causing p53 relocalisation to the cytoplasm and degradation preventing genotoxic stress response. It has been suggested that this mechanism may inhibit the induction of p53-mediated apoptosis thus promoting cell survival.

In MCF-7 treated with 5-FU HSPA5 accumulates, non phosphorylated HNRPK accumulates and p53 accumulates and this would contradict the above argument. The expression of HNRPK seems to follow HSPA5 trends alone and suggests a link between there expression. HNRPK plays a role in stabilising transcription with HMBG1 (Moumen, *et al.*, 2005; Dinthilak *et al.*, 2002) and HMGB1 shows an upregulation in MCF-7 treated with 5-FU.

Further investigation is warranted to elucidate the role of HNRPK in the regulation of translation of these repressed mRNAs.

4.1.6.2 mRNA splicing during 5-FU treatment

The splicing factor SFRS1 was shown during heat shock in Hela cells to be necessary and sufficient for the recruitment of mRNA to nuclear stress bodies and generation of splice variants {Chiodi, I. *et al.*, 2004}. SFRS1 is up regulated in DLKP, A549, MCF-7 and HMEC in response to 5-FU treatment and may indicate that SFRS1 is regulated by p53 accumulation and may be an important component of the stress response. Proteomic analysis of the nuclear stress bodies during 5-FU genotoxicity would reveal interesting insights into possible regulation of alternative splicing during 5-FU treatment.

In combination with data discussed in section 4.1.2 a potential mechanism for the regulation of alternative protein products during 5-FU treatment may be evident. This further supports a role for further investigation into translation regulation occurring during 5-FU treatment.

4.1.6.3 mRNA decay during 5-FU treatments

Phosphorylated Ras-GTPase-activating protein (G3BP) is upregulated in MCF-7 treated with 5-FU (see table 3.1.13). Barnes *et al.*, 2002 showed that activation of the human epidermal growth factor receptor induced increased expression of HER2 in breast cell lines and over expression of HER2 induced over expression of G3BP (Barnes *et al.*, 2002). Phosphorylation of G3BP leads to binding to RasGAP and localisation to the nucleus. There, G3BP mediates mRNA decay of a specific subset of mRNAs including c-Myc (Tourriere, *et al.*, 2001). This data may indicate alteration in mRNA processing. Further more it may indicate increased expression of Her 2 as a result of 5-FU treatment. The translation initiation factor 4A isoform 3, DDX48, was found upregulated in both MCF-7 and HMEC after 5-FU exposure. DDX48 has been implicated in non-sense mediated mRNA decay a process that destroys non-sense RNA {Palacios, *et al.* 2004}. Incorporation of FUTP into RNA would lead to increased levels of fluorinated mRNA. As already discussed 5-FU alters a wide variety of mRNA functions (see section 1.1) and it is not surprising that increased expression of DDX48 is observed. Thus this data suggests that 5-FU treatment of both normal and cancer breast cell lines can lead to increased non-sense

mediated mRNA decay and may additionally indicate shorter half-lives of mRNA in general.

4.1.6.4. Transcription regulation during 5-FU treatment

The transcription factor E-Box binding protein (TCF-12) has been shown to directly bind to the transcription factors, inhibitors of DNA binding 1/2/3 (ID1, ID2, and ID3) (Langlands, *et al.*, 1997) and these proteins have been established to be regulated by 5-FU treatment of MCF-7 (Hernandez-Vargas *et al.*, 2006). Data presented in McMorrow Ph. D. thesis (2004) predicted the involvement of ID1, ID2 and ID3 in transcription during haogenpyrimidine treatment of DLKP and showed the upregulation of there transcripts and proteins. This data suggests a potential role for the E-box binding protein during 5-FU treatment.

NYF transcription factor complex requires redox potential for their activation (Nakshatri *et al.*, 1996). Oxidative stress in MCF-7 cells exposed to 5-FU would thus result in the activation of these transcription factors and NYFC was found 2 fold upregulated. Oxidative stress induced by 5-FU exposure may result in the activation of these transcription factors.

Crabp2 participates in transcription with RARα and releases retinoic acid from this receptor during transcription contributing to its stability allowing recruitment of RNA polymerase II and initiation of transcription (Despouy, *et al.*, 2003). RARα transcription has been shown to be a potent inducer of epithelial differentiation and may explain how 5-FU induces the upregulation of Keratin 8 and 18. As epithelial cells are often invasive this may implicate RARα transcription activation as an important inducer of the epithelial markers in MCF-7 and the invasive characteristics observed after 5-FU treatment. If Crabp2 is an important factor in inducing keratin expression in MCF-7 it may suggest that inhibition of its activity may enhance 5-FU toxicity. All-trans retinoic acid analogues in combination with 5-FU may inhibit activity of the transcription complex, prevent keratin accumulation and enhance the toxicity of 5-FU.

RUVBL1 was found to be up-regulated by 2 fold in DLKP treated with 5-FU. RUVBL1 plays important roles in essential signalling pathways such as the c-Myc and Wnt pathways, in chromatin remodelling, in transcriptional and developmental regulation, and in DNA repair and apoptosis (Matias *et al.*, 2006). Thus may indicate an additional mechanism of DNA repair activated in DLKP treated with 5-FU.

4.2 Fluoropyrimidine treatment of DLKP

Treatment of DLKP with various concentrations of the fluoropyrimidines 5-FU, 52FdU and 55FdU demonstrate that 52FdU is the most toxic of these drugs and 5-FU and 55FdU induce similar toxicities (see figures 3.2.1 and 3.2.2). Proteomic analysis revealed that 5-FU and 52FdU display 12 similarly regulated proteins 2 oppositely regulated proteins (see tables 3.2.2 and 3.2.4).

The commonly regulated proteins include GLO1 and STMN1. STMN1 is already discussed in the previous section (see section 4.1.1).

Glyoxyase 1 (GLO1) suppresses nucleotide glycation and over expression of GLO1 is responsible for, in many instances, drug resistance. During oxidative stress many products are formed that result in the glycation of DNA and its down regulation would lead to sensitisation to oxidising agents {Thornalley, P.J. 2003}. GLO1 was found up regulated in both 5-FU, 52FdU and 55FdU treatment. This data suggests that the fluoropyrimidines induce oxidative damage to DNA in DLKP.

52FdU was found to promote accumulation of EEF1BG, p-CFL1, CCT1 and GSN and there potential role in fluoropyrimidine treatments are discussed in section 4.1 Interestingly EEF2 shows a down regulation by 52FdU treatment while in 5-FU it showed an upregulation and the implications of EEF2 regulation are discussed in section 4.4.2.

In summary these data clearly indicate that the fluoropyrimidines induce disctinct proteomic responces in DLKP as indicated by the poor overlap with identified protein from DLKP treated with 5-FU and as such should not be considered as the same drug.

4.3 5-FU resistant variant of DLKP – DLKP-55 and comparison to fluoroyrimidine treatments.

The cell line DLKP-55 was developed by pulse selection with the 5-FU prodrug 55FdU. As can be seen from the previous section 5-FU and 55FdU effect the proteome in distinctly different manners and this may help understand why pulse selection with 5-FU failed to generate a 5-FU resistant variant while pulse selection with 55FdU did. Analysis of this variant revealed it was resistant to 5-FU, 55FdU, Adr but not BrdU or Taxol. Western blots revealed an over expression of TS. Analysis of proteome using 2D-DIGE identified 65 differentially regulated proteins between DLKP and DLKP-55. Of those regulated proteins 13 were identified by MALDI-ToF MS; 7 involved in metabolism, 4 involved in protein metabolism and 1 involved in signal transduction

The drugs 5-FU, 55FdU and Adr exert their anti-neoplastic effects by inducing DNA damage leading to p53 accumulation and generation of reactive oxygen species and apoptosis. While Taxol induces apoptosis by inhibiting microtubule depolymerisation in dividing cells leading apoptosis (Mollinedo *et al.*, 2004).. A key difference between apoptosis induced by Taxol and Adr/5-FU/55FdU is the amount of reactive oxygen species produced during induction of apoptosis and thus resistance may be linked with resistance to oxidative stress (Chen *et al.*, 2003). Resistance to 5-FU/55FdU may also be linked to pyrimidine metabolism. Several component of pyrimidine metabolism have been linked to 5-FU resistance (Longley *et al.*, 2003). DLKP-55 showed equal tolerance to BrdU as did DLKP. BrdU has not been shown to irreversibly bind to TS as does 5-FU (Shwartz *et al.*, 1994) and may indicate resistance is directly linked to TS over expression.

Resistance is summarised in figure 4.2.1 and shows that DLKP is ~4 resistant to 5-FU, 2 fold resistant to 55FdU and Adriamycin, and shows no resistance to BrdU or Taxol.

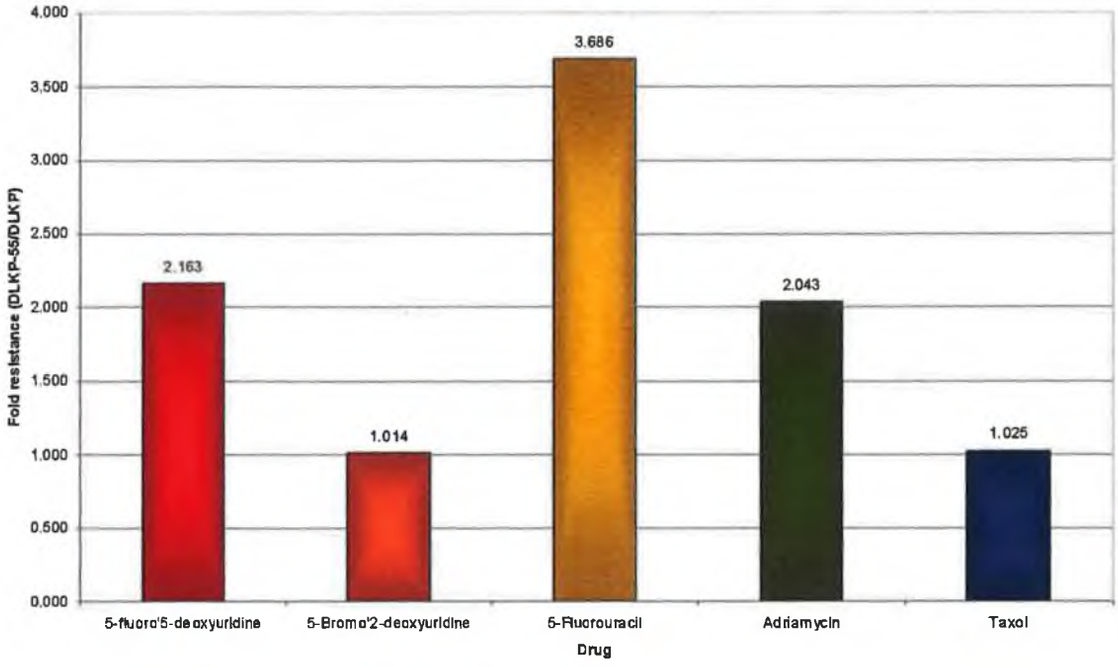

Figure 4.2.1: Summary of fold resistance in of DLKP-55 compared to DLKP. Data shows DLKP-55 are resistant to 5-FU, 55fdU and Adriamycin. No resistance was observed to BrdU or Taxol.

4.3.1 Pyrimidine and Purine metabolism

The nucleoside kinase NME1 was found to be upregulated by 2 fold in DLKP-55 compared to DLKP. The enzyme NME1 or nucleoside diphosphate kinase is responsible for the reversible conversion of dUTP to dUDP. dUDP is two metabolic steps from conversion to thymidine monophosphate, the substrate of TS (Gilles *et al.*, 1991). Higher expression of NME1 may cause increased metabolism of pyrimidines and purines and would allow for a generation of a larger pool dUDP or dUTP. As the reaction is reversible and equilibrium altered by TS inhibition by 5-FU may force increased conversion of FdUDP to FdUTP and may result in higher incorporation rates into DNA. Its role in metabolism is inferred from the KEGG database and is highlighted in red in figure 4.3.1.

However this may relieve inhibition of TS at a quicker rate and allow for recovery of thymidine pool and correct DNA repair. Further more, TS also showed increased expression in the resistant variant by western blot. TS is associated with 5-FU resistance. 5-FU inhibits TS activity by irreversibly binding to it (Longley *et al.*, 2003). Thus TS inhibition can be overcome by over expression of TS thus inhibition would require higher amounts of 5-FU.

Spermine synthase (SMS) converts Spermidine to Spermine producing 5'-Methylthioadenine which is converted to adenine, then to adenosine and then adenosine mono-, di- and tri- phosphate derivatives (Wiest *et al.*, 1998). SMS was found down-regulated by 2 fold and thus decreases the amount of adenine available for synthesis of adenosine triphosphate and thus DNA synthesis. The imbalance in purine and pyrimidine metabolism is suggested by increased expression of NME1 and TS and decreased expression of SMS may cause adenosine availability to be the rate limiting step during DNA synthesis in DLKP-55. Potentially this would alleviate pressure on thymidine synthesis and requirements of thymidine for DNA synthesis and thus allow cells to tolerate TS inhibition.

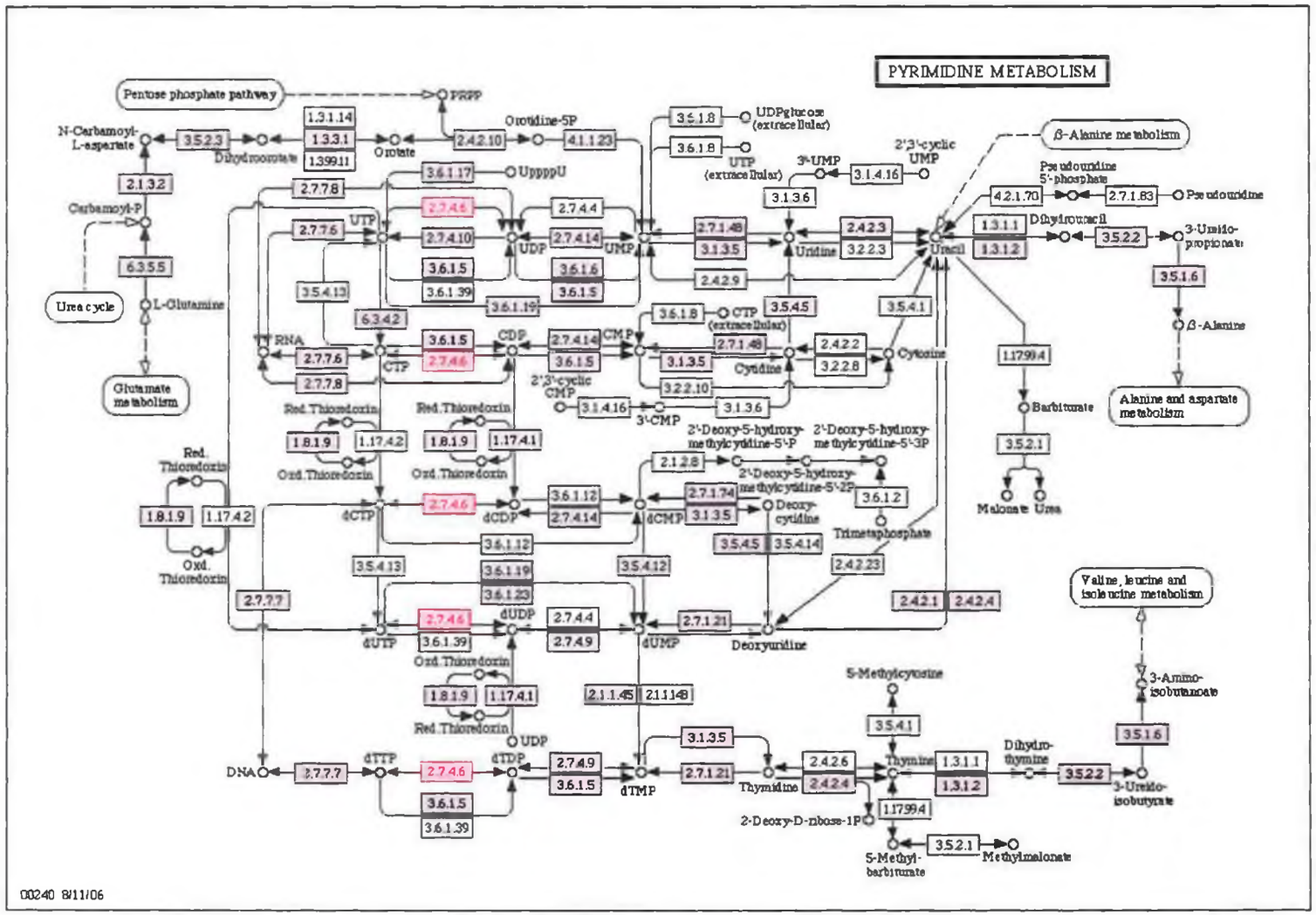

Figure 4.3.1: Shows the location of NME1 (EC2.7.46) in the various steps of pyrimidines metabolism indicate a highly efficient Metabolism in DLKP-55. Image downloaded from the KEGG database. TS (EC2.1.1.45)

GLO1 was down-regulated in the 5-FU resistant variant of DLKP and was specifically found to be responsible for the repair of glycated DNA during oxidative stress (Sakamoto *et al.*,2000). Its expression trend would suggest that DLKP-55 would be sensitised to oxidative stress. GLO1 is upregulated by both 5-FU and 55FdU treatments. Thus this data would suggest that GLO1 expression is not a determinant factor in resistance to 5-FU or 55FdU and that resistance is brought about by prevention of oxidative stress.

4.3.2 Oxidative Metabolism

Glucose-6-phosphate dehydrogenase was found to be upregulated by 1.4 fold in the 5-FU resistant variant of DLKP, DLKP-55, and it catalyzes the first step in the pentose phosphate pathway and provides reductive potential in the form of NADPH. As such it provides protection against oxidative stress {Pandolfi, *et al.* 1995} and as suggested above resistance to 5-FU may be a result of prevention of oxidative stress. This would be supported by over expression of NADPH.

Increased expression of G6PD would provide increased reserves of NADPH available for metabolism and as NADPH is required for pyrimidine synthesis it may result in an expanded pool. An end product of the pentose pyrimidine pathway is the production of PRPP that is an essential component required for the synthesis of UMP (see figures 3.2.8 and 3.2.9).

Pyruvate kinase, PKLR, converts phosphoenolpyruvate to pyruvate and is an essential substrate for a wide variety of metabolic processes and includes D-alanine metabolism amongst others. Alanine metabolism is important in the degradation of 5-FU

Aldehyde dehydrogenase 1A1 (ALDH1A1) or retinaldehyde is responsible for the conversion of all-trans-Retinal to all-trans-retinoate. All-trans retinoate and its derivates are subsequently metabolised in the sucrose metabolism. All-trans-retinal is the produced by the oxididation of Iodopsin, Porphyropsin and Rhodopsin (see figure 3.2.11). Sources of oxidation of Iodopsin, Porphyropsin and Rhodopsin include ionising radiation, and free radicals produced during oxidative stress. This may indicate that DLKP-55 is more efficient at dealing with oxidised retinol derivatives.

Data presented in section 3.1 and discussed in 4.1 indicate that 5-FU induces oxidative stress in DLKP and as DLKP-55 has higher ambient expression of G6PD and ALDH1A1 it would facilitate resistance to 5-FU induced oxidative stress.

4.3.3 DLKP and DLKP-55 compared to A549 treated with 5-FU

Comparison between DLKP treated with 5-FU and FLKP-55 revealed very few similar trends. DLKP treated with 5-FU becomes sensitised to 5-FU and this may explain why so few proteins overlap. Comparison between A549 treated with 5-FU and DLKP v DLKP-55 lists revealed an overlap with at least three proteins discussed above.

A parallel can be drawn between A549 treated with 5-FU and DLKP-55/DLKP proteomic analysis. Both models show resistance to 5-FU and both show an over expression of G6PD, ALDH1A1 and NME1. This data further strengthens the possibility that these proteins are involved in resistance to 5-FU.

4.3.4 Protein metabolism

ERP29 is expressed in most mammalian tissues and was thought to be involved in the production of secreted proteins but recent data suggests a role in production of endomembrane proteins. However a role in 5-FU resistance is not clear.

The translation elongation factor EEF2 is upregulated in DLKP-55 and would suggest higher protein turnover rates. Its role in resistance is not clear but it may provide larger pool of proteins and may promote cell survival. Indees the over expression translation elongation factor has been linked to oncogenic transformation and thus the increased expression of EEF2 may promote oncogenesis in DLKP-55.

CCT3 is involved in turn over of actin and tubulin, however none of these proteins were upregulated in DLKP-55 compared to DLKP. The implication of CCT3 in resistance to 5-FU is not clear.

4.3.5 Possible decrease in motility/invasion in DLKP-55 compared to DLKP

PPP2CB phosphorylates and activates calpains responsible for breaking of actin-focal adherence contacts and is reported to promote invasion {Xu, L. *et al.* 2006}. Phosphorylated PPP2CB is down regulated in DLKP- 55 and in contrast to this it is upregulated in DLKP treated with 5-FU. This may indicate a decreased invasion rate in DLKP-55. Increased expression of NME1 correlates with decreased invasion {Leary, J.A. *et al.* 1995} and is also upregulated in DLKP-55 suggesting decreased invasion.

4.4 Analysis of DLKP and its clonal subpopulations

As already stated, NSCLC are typically heterogeneous in nature. DLKP is a poorly differentiated NSCLC of lung epithelial origin, but lacks markers of epithelial origin. It was characterised as being composed of three subpopulation distinguishable by obvious morphological differences. And they were named according to there morphological characteristics. DLKP-squamous like or DLKP-SQ, DLKP-Mesenchymal like or DLKP-M and a third population which the other two populations interconverted with referred to DLKP-Intermediate or DLKP-I. Little differences could be determined between these subpopulations apart from DLKP-M having a slower growth rate and higher adherence rate to fibronectin. No differences in drug resistance were observed between the clonal population and parent (McBride, Ph. D. thesis 1995, McBride *et al.*, 2000). In order to further characterise these cell lines motility and invasion assays were performed in order to accurately determine how these cell lines behaved. The results of these assays can be seen in figures 3.4.2 and 3.4.3. the data revealed DLKP-SQ and DLKP were poorly invasive while DLKP-I and DLKP-M displayed highly invasive phenotype (10-40 times greater than DLKP and DLKP-SQ). Differences in motility were found to be less extreme however assays appear saturated and should be repeated at a lower incubation time. Proteomic analysis was preformed on the total proteome of DLKP and its subpopulations and this data can be found in section 3.4.2. An overview of total cell lysate proteome expression trends revealed that DLKP-I and DLKP-M appeared equally different to DLKP-SQ. DLKP-I and DLKP-M showed the least differences and DLKP-I appeared to be the most similar to the parent cell line (see table 3.4.2 and figure 3.4.3 for images of proteomes). Identification of these proteins resulted in a list of 15 proteins. Several isoforms of type III preprocollagen A1 were identifedand these were highly abundant iin DLKP-M. this wouold be consistent with it observed morphology as Mesenchymal cells are typically associated with stromagenesis, the process of ECM generation. In terms of cancer mesenchymal like cells are generally more invasive as seem here. Several of the proteins identified were found to be highly expressed in DLKP. These include TUBB2A, HDAC1, HYOU1 and HSPA1A and these proteins tended to be less abundant in DLKP-SQ than any of the other clonal subpopulations (see figure 3.4.4 and table 3.4.2). Amongst the clones TUBB2, HDAC1, GANAB, EEF2, and COL3A1, correlated with invasion.

4.4.1 Analysis of the DLKP and subpopulation total proteome

Only two proteins correlated with enrichment in DLKP-M and these include type 3 preprocollagen A1 (COL3A1), and eukaryotic elongation factor 2 (EEF2).
Proteomic data indicates that DLKP is more than the sum of its clones. Many proteins were found more highly expressed in DLKP than in the sub populations and suggest their accumulation is a result of either cell-cell communication or the presence of an unidentified fourth population. DLKP-M and DLKP-I to a lesser extent express the extracellular matric protein COL3A1 and suggest a role in stromagenesis. Understanding of how stromogenesis effect tumour progression is poorly understood and this is due to the lack of suitable cellular models (Amatangelo, 2005). Data presented here may suggest that DLKP and its subpopulations may have the capacity to address this issue.

The expression of EEF2 was found to 20 times higher in mammary tissue than in liver tissue and 50 times higher in mammary tissue than skeletal tissue in bovine models. This suggests a role for EEF2 in the production of secreted protein in mammals (Christophersen *et al.* 2002). The production of insulin in pancreatic beta cells is regulated by phosphorylation of EEF-2. Phosphorylation inhibits EEF2 activity and dephophorylation promotes its activity, and is closely regulated by glucose and insulin levels. Thus EEF2 appears to important in the production of secreted proteins (Yan *et al.*, 2003).

Glucosidase II (GANAB) was found to be at least 3 times more highly expressed in DLKP-I or DLKP-M than DLKP-SQ and suggests a role in the synthesis of collagen. GANAB was shown to be important in the production of collagen type I and IV and metastasis as its suppression was found to reduce collagen synthesis and metastasis (Atsumi *et al.*, 1993). A quality control system for monitoring the folding state of glycoproteins is located principally in the ER and is composed of the ER lectins calnexin and calreticulin, glucosidase II, UDP-glucose: glycoprotein glucosyltransferase

and various chaperones. Improperly folded glycoproteins will be retained in the ER prior to further transport by the concerted action of UDP-glucose: glycoprotein glucosyltransferase which reglucosylates improperly folded glycoproteins, calnexin and calreticulin which interact with the reglucosylated glycoproteins and glucosidase II which by glucose removal results in release of calnexin/calreticulin-bound glycoproteins. Monoglucosylated oligosaccharides play a key role in the control of glycoprotein folding. Since such oligosaccharides represent substrates for binding to both calnexin and calreticulin, they will be retarded in the ER through this interaction. Calnexin/calreticulin-glycoprotein complexes will be eventually dissociated by the action of glucosidase II and this represents an important aspect in the quality control performed by glucosidase II (Roth *et al.*, 2003). GANAB is an ER protein important in the production glycosylated secreted and membrane proteins. EEF2 is a translation elongation factor responsible for production of secreted proteins. Thus the increased expression of both these proteins may be important in production of the glycoprotein COL3A1 and the maintenance of the DLKP-M population.

GANAB is more highly expressed in DLKP than in the clonal population and suggests its expression is regulated by cell-cell communication. It was found to accumulate in response to 5-FU treatment. Further more GANAB and EEF2 were found to accumulate in DLKP treated with 5-FU. This suggests a potential link with invasion in DLKP biology.

Other proteins regulated in this experiment include α2 tubulin (TUB2A) and histone deacetylase 1 (HDAC1). Both proteins have a higher expression in DLKP than in any of the clonal subpopulations. A protein that is more abundant in DLKP than in any of the clones suggest its regulation is a result of cell-cell interaction/communication or its abundance is a result of cell-ECM interaction. Due to the small number of proteins identified enriched in DLKP it is difficult to determine a regulatory pathway that would influence there accumulation. However HDAC1 and TUB2A correlate with invasion in the subpopulations. TUB2A is component of the microtubule filaments and is important in invasion. The matrix metalloproteinases - MMP-2 and MMP-9 – are stored in vesicles aligned and attached to microtubules. MMP's vesicles are moved to the cell membrane in a microtubule dependent manner MMP's are excreted (Schnaeker *et al.*, 2004). Further more microtubule filaments have also been shown to be important in cell

migration and are responsible for retraction the tailing end of the cell as it migrates and microtubule polymerisation is regulated by stathmin and p27 (Baldassarre *et al.* 2005).
The hypoxia-upregulated protein HYOU1 and annexin A1 are more highly expressed in DLKP-I. However there is no statistically significant difference in expression between DLKP-I and DLKP-M for both proteins and they seem to correlate with invasion. HYOU1 forms a complex with TRA1, HSPA5, ERp72 in the ER and play an important role in the folding and maturation of secreted proteins (Kosnetsov *et al.*, 1997). It is likely that DLKP-I secretes different protein than the other populations.
Annexin A1 is a calcium dependent binding protein that is bound to the cell membrane. Inhibition of Annexin 1 using anti-serum was found to inhibit invasion (Babbin *et al.*, 2006), and suggests an important role in regulation of invasion. Vinculin (VCL) in a complex with talin – the integrin binding protein –has been shown to attach of F-actin to the cell membrane via integrin intercellular domain and F-actin membrane connections and is important in cell migration (Fischer *et al.*, 1998; Chen H. *et al.* 2006) Its accumulated expression in DLKP-I and DKP-M over DLKP-SQ suggests vinculin may play a role in regulating invasion in the clonal populations. It s increased expression in DLKP suggests its upregulation is stimulated by cell-cell interaction or cell-Mitogen interactions and its expression accumulated as a result of 5-FU treatment of DLKP which again supports a role for vinculin in the promotion of invasion.

HDAC1 is involved ERK activation of invasion. Upon ERK activation (as described in Figure 1.4) phosphorylates Sp-1 and recruits HDAC1 to the Reck 1 promoter and inhibits it transcription. Reck inhibits the activity of MMP's thus HDAC1 recruitment to the Reck promoter promotes invasion (Hsu *et al.*, 2006). It was also found more abundant in DLKP than the clonal populations and was found up-regulated by 5-FU treatment of DLKP. Thus this data may indicate that ERK signalling may be important in regulating invasion in the clonal population. ERK may inhibit transcription of Reck through HDAC1 as stated above thus promoting invasion.

The upregulation of TUBB2A may promote excretion of MMP vesicles and promote motility. The increased expression of GANAB and EEF2 may play an important role in processing Col3A1 and MMP's thus promoting invasion. The presence of COL3A1 production in smaller population may drastically alter the proteome of DLKP-SQ when

in the mixed population and thus this may severly alter expression levels of protein involved in integrin signalling.

4.4.2 Analysis of the hydrophobic proteome in DLKP and the subpopulations

DLKP and DLKP-SQ were found to be 10-40 times less invasive than DLKP-M and DLKP-I. If the degree of invasion in DLKP was directly proportional to the distribution of its subpopulations than the difference in invasion would by about 3-4 fold (as DLKP-I and DLKP-M constitute 35% of DLKP). However the difference in 10 fold and this suggests the presence of a component that inhibits invasion by 2-3 fold. As DLKP lacks cell-cell junctions (McBride *et al.*, 1999) communication between DLKP-SQ and DLKP-I and DLKP-M must be regulated by either membrane proteins such as integrins or soluble factors such as growth factors. Analysis of conditioned media would help identify growth factors that may be regulating invasion in DLKP.

Analysis of the hydrophobic proteome will identify proteins important in the regulation of motility/invasion. Initial characterisation of the the trends between the DLKP parental population and the subpopulations revealed that DLKP and DLKP-SQ are highly similar and DLKP-I and DLKP-M are also highly similar as suggested by invasion and motility assays (see table 3.4.5). An estimated **300-500 protein** are present in this experiment that show a similar expression trend as the invasion trend and due to the relevance of the fractionation process it is not surprising. The fractionation process was selected to isolate membrane protein and complexes associated with them. This would include any microfilaments involved in migration as they must continuously make contact and break contact with the cell membrane in order to achieve migration A list of identified differentially regulated proteins are present in table 3.4.6 and proteins of interest are highlighted in figure 3.4.6. In this list there is an over lap of 3 proteins with those discussed above and these are TUBB2A, EEF2, ANXA1.

The expression trend of ANXA1 is exactly the same as that in the total proteome as in the hydrophobic proteome and may indicate it is only located in the membrane. TUB2A shows a similar expression level in DLKP and DLKP-SQ and similarly expressed in DLKP-I and DLKP-M. Its expression alters slightly between DLKP and its subpopulations in the total proteome and this data highlights the importance of fractionation for the identification of proteins involved in various biological functions. This suggests that there is protein expressed in DLKP-I/-M that associates tubulin to the

membrane that is not expressed in DLKP or DLKP-SQ. The role of TUB2A and TUBA3 in invasion is discussed above. B-actin forms F-actin filaments important in cell migration and are discussed in section 1.4.7. The association of F-actin to cell membrane would suggest activation of talin, and vinculin and other actin binding proteins as discussed previously. ATP5B is a mitochondrial protein responsible for the production of ATP (Izquierdo *et al.*, 2006). Its expression has not been shown to correlate with invasion, although it inversely correlates with invasion the correlation is more than likely an artefact. Inversely correlating data in these experiment are enriched in fractionations by lack of the proteins that correlate with invasion and there link with invasion while arguable plausible is probably less likely. Stomatin like protein-2 (HSPC108 or STOML2) is expressed in many tissues but its function is entirely unknown (John *et al.* 2006). This data suggests a functional role for this protein in invasion.

The G-protein GNB1 is involved in regulating K^+ and Ca^+ channels in neurons of the heart and brain (Agler *et al.*, 2005). DLKP expresses neuroendocrine markers and the expression of neuronal protein is not surprising. The expression trend indicates that in DLKP its expression is lowest and it linearly increases from to DLKP-SQ, to DLKP-I and finally to DLKP-M its expression does not seem to correlate with invasion.

Finally the G-protein Rab11a correlates with invasion. Rab11a is not well studied in cancer, but has been shown to regulate the recycling of internalized cell surface proteins and receptors from the early endosome through the trans-Golgi network. It has been shown to modulate Epidermal growth factor receptor and has been shown to decrease invasion (Palmieri *et al.*, 2006). Here this data provides coutradictory data on Rab11a being an inhibitor of invasion and it localisation in a fraction may suggest it exists as a complex. Further investigation of these G-proteins are warranted as they will elucidate new interactions important in invasion.

Finally, numerous proteins appear to be more highly expressed in DLKP than in any of the clonal populations. Three proteins were highlighted in figure 3.4.4 and show there expression is almost exclusive to DLKP. This data shows that DLKP is more than the sum of the clones. These proteins could only be expressed at a higher level in DLKP due to cell-cell communication or the presence of a fourth sub population.

5.0 Conclusions

- 5-Fluorouracil (5-FU) treatments of both normal and cancer cell lines of epithelial origin of the lung and breast were found to alter invasive phenotype of these cell lines. This data suggests that 5-FU is capable of inducing a differentiation effect. Proteomics investigation of these cell lines treated with 5-FU identified a group of proteins involved in actin dynamics to be differentially regulated. The most important of these appear to Gelsolin and p-Cofilin which play important roles in both migraton/invasion and apoptosis. The data suggests 5-FU induces increased threadmilling of F-actin in the cell lines DLKP, MCF-7 and NHBE (three cells which showed an increased invasion post treatment) and play a role in cell survival.

- Expression of the 14-3-3 proteins and the simple epithelia marker p-Keratin 18 expression during 5-FU treatment are hypotosised to play a role in the regulation of cofilin phosphorylation and dephosphorylation. Specifically by sequestering of slingshot and p-cofilin, thus inhibiting F-actin threadmilling.

- Components of the elongation factor EEF1B were found regulated in all cell lines and in the normal cell line were found to accumulate at the higher concentration of 5-FU of 30μM and not 10μM. The expression of this did not correlate with Stathmin expression suggesting that its expression is not specifically linked to cell cycle progression. However its expression appears to correlate with p53 expression suggesting it may play a role in genotoxicity or apoptosis. The aspartyl tRNA Synthetase (DARS) was found to be up-regulated by 5-FU treatment and this may suggest a role in translation control. Specifically increased expression of amino acid tRNA synthetases have been shown to promote selective translation of protein with higher requirements for the specific cognate amino acid of the amino acid tRNA Synthetase up-regulated. This data may indicate the preferential translation of proteins with a high occurrence of the aspartyl residue.

- Growth inhibition curves by 5-FU treatment reveal that the normal cell lines have equal or higher tolerance to cancer cell lines of similar tissue origin. Proteomic comparison between normal and tumour cell lines treated with 5-FU

revealed an increased expression of specific keratins indicative of a more differentiated state in the normal cell lines. Keratins play specific roles in inhibition of apoptosis and this may suggest a role in the promotion of cell survival.

- Analysis of the phosphorylated proteomes of the cancer and normal cell lines show that the cancer cell lines express a high level of phosphorylated proteins where as the normal cell line NHBE expressed very few phosphorylated proteins. Investigation of these phosphorylated protein upregulated in the cancer cell lines may reveal signal transduction pathways active in cancer cell lines and indicate specific receptor signal kinases active in cancer cell lines.

- The resistant variant DLKP-55 shows specific up-regulation of few proteins when compared to DLKP, however data revealed specific up-regulation of proteins involved in pyrimidine metabolism and suggests a role in 5-FU resistance.

- Characterisation of the invasive phenotypes of DLKP and its subpopulations reveal that DLKP-I and DLKP-M have a highly invasive phenotype and that DLKP-SQ has a low invasive phenotype. DLKP shows a low invasive characteristic. Its invasive was lower than the expected degree of invasiveness – based purely on its composition of clonal populations. This data suggests that DLKP-SQ inhibit invasion through cell-cell communication

- Proteomic analysis of total cell lysates of DLKP and its subpopulations reveal a specific higher abundance of protein in DLKP compared to the clonal subpopulations. Protein expression values in DLKP would be expected to be an average of the subpopulations and thus the higher expression in DLKP suggests cell-cell communication.

- DLKP-I and DLKP-M express type III preprocollagen type 1A and increased migration/invasion which are characteristics of mesenchymal-like cells. Thus this may indicate that DLKP is a novel model for the study of cancer biology

and may allow for future study of stromatogenesis and cancer stroma interactions.

- Analysis of the hydrophobic proteomes of DLKP and its subpopulations found 300-500 proteins whose expression or inverse expression closely followed invasion trends. Identification of some of these proteins found higher abundance of actin and tubulin monomers in the hydrophobic proteome which may suggest increased association of these cytoskeletal proteins with the cell membrane a process important in cell migration/invasion. Thus this suggests this data set is a good model for identification of proteins involved in migration/invasion. A group of 3 poorly described proteins were identified whose expression follows the invasion trend thus suggesting a role in invasion.

6.0 Future Work

There are many future avenues of research from this work however only the more important points are discussed here. These include in regards to 5-FU treatments; actin dynamics, translation elongation, phosphorylated proteomes; and in regards to the clonal populations of DLKP; investigation of cell-cell interactions, identification of the hydrophobic proteome, and functional validation proteins suspected of being involved in invasion.

- Future work on these treatments described above would include the investigation of actin threadmilling during 5-FU treatment. Data suggests the increased formation of actin branching in the cell lines that show a higher invasive phenotype post treatment and thus staining of actin filaments by immunofluorescence based techniques would allow for confirmation of hypotosis. During invasion actin monomers need to be severed from F-actin and this is proposed to be accomplished by Gelsolin and cofilin. Thus, their role in this process needs to be confirmed. To this end immunofluorescent based techniques need to show the localisation of these proteins to the actin filaments. Construction of green fluorescent protein tagged plasmid constructs of actin, gelsolin and cofilin would allow for the study of actin dynamics over time and would allow for observations of actin polymerisation and severing. Alternatively microinjection of fluorescently labelled actin monomers, gelsolin and cofilin would show if actin polymerisation and severing were increased by 5-FU treatment and if these proteins played an important role in invasion progression. Confirmation of these proteins roles in actin threadmilling could be confirmed using siRNA knockdown. If this work proved promising it could potentially lead to the inclusion of F-actin inhibitors in future combinations with 5-FU treatments and development of more effective future chemotherapeutic therapies.

- The up-regulation of the elongation factors appears to correlate with p53 accumulation and suggests a role in genotoxicity or apoptosis. Their role in apoptosis and genotoxicity require investigation. A role in genotoxic response could be determined using siRNA knockout or partial knockdown and

investigation of induction of apoptosis by various genotoxic agents. If involved in DNA repair then genotoxic agents should be capable of inducing apoptosis more readily than non-DNA damage agents. If the elongation factors are important in triggering apoptosis than knock down of these elongation factors would promote cell survival. Again this could lead to the inclusion of translation inhibitors, such as a rapamycin, in future 5-FU therapies.

- Proteomic data also suggests the increased production of proteins rich in aspartyl. This hypotosis may be investigated by investigation of proteins up-regulated in parallel to the DARS protein and the elongation factors during 5-FU treatment. If this hypotosis was valid than up-regulated proteins would have a higher occurrence of aspartyl in their sequences. The hypotosis can then be confirmed by siRNA knockdown of DARS during 5-FU treatments and investigation of protein expression during knockdown by western blot of the protein DARS and suspected proteins regulated by increased expression of DARS. The role of such regulated proteins in terms of induction of cell survival or DNA repair need to be determined. If they were found to be inhibitors of apoptosis or important in DNA repair then this could lead to the development of aspartyl based drugs to be used in combination with 5-FU therapy.

- Investigation of the phosphorylated protein present in carcinoma cell lines and not present in normal cells may lead to the identification of signal transduction pathways active in carcinoma cell line and not active in normal cell lines. Data presented above show that normal cell lines express relatively few phosphoproteins while carcinoma cell lines express many phosphorylated proteins. This may lead to the identification of receptor signal kinases active in cancer cell lines that are not active in normal cell lines. Such signals can promote cell survival and thus inhibition of their signalling may promote apoptosis. These proteins should be identified using liquid chromatography Mass spectrometry/ Mass spectrometry or MALDI-ToF MS/MS which would allow for identification specific phosphorylated residues. This would allow for identification of a specific list of kinases and phosphorylases potentially active in cancer. Expression of such kinases can be determined by western blotting and validation of a role in phosphorylation of proteins can be determined by siRNA

knockout and decreased phosphorylation of target proteins can be confirmaed by western blotting thus confirming the role of the kinase in signalling. This should potentially lead to identification of a receptor and its expression should be examined a selection of cell lines. If it appears to be expressed in many cancer cell lines than its expression in clinical samples should be investigated. If it appears to be highly expressed in cancer patients than a humanised antibody should be developed to inhibit its activity. Thus this may lead to improved future therapies.

- DLKP and its subpopulation invasion experiments suggests DLKP-SQ inhibits invasion in DLKP-I and DLKP-M. Thus exchanging of conditioned media between cell lines during invasion assays may indicate if there is a soluble factor responsible for inhibiting invasion secreted by DLKP-SQ. If the conditioned media was found to be an inhibitor of invasion than it should be investigated by 2D-DIGE. Proteins should be identified by MALDI-ToF MS and purified using ion exchange columns and High Performance Liquid Chromatography. The role of such proteins as inhibitors of invasion should be investigated in by siRNA knockout. If these proteins inhibited invasion then they should be screened using animal models to determine if they could inhibit the spread of metastasis. If the results showed to be interesting than the protein should be developed as a drug for the suppression of metastasis.

- Analysis of the hydrophobic proteome in DLKP and its subpopulations revealed a list of 300-500 proteins potentially involved in invasion. Identification by MALDI-ToF MS and knockout by siRNA could reveal important roles in invasion that may lead to the development of future drug combinations that target such proteins either by localisation or expression inhibition.

- DLKP-M expressed high levels Col3a1 and may represent a novel in vitro source of the protein. Thus purification of this protein may allow for the development of an alternative source of Col3a1 for research and may have commercial value as an alternative source of collagen. Secretion of collagen needs to be determined from conditioned media experiments. Cultivation of DLKP-M with either DLKP-I or DLKP-SQ and compared to DLKP-I cultured

with DLKP-SQ may allow for the identification of proteins whose expression is altered by interaction with Col3a1. This would give insights into tumour behaviour and expand the understanding of tumour biology. This work in combination with conditioned media from these cell line mixes and the conditioned media of each individual population may allow for an understanding of how cancer cells communicate. This could lead to identification of signals important in promotion of cell survival, migration, invasion, and stromatogenesis.

7.0 Bibliography

Adjei, A.A., Reid, J.M., Diasio, R.B., Sloan, J.A., Smith, D.A., Rubin, J., Pitot, H.C., Alberts, S.R., Goldberg, R.M., Hanson, L.J., Atherton, P., Ames, M.M. & Erlichman, C. (2002) Comparative pharmacokinetic study of continuous venous infusion fluorouracil and oral fluorouracil with eniluracil in patients with advanced solid tumors. *Journal of Clinical Oncology : Official Journal of the American Society of Clinical Oncology,* **20**, 1683-1691.

Agler, H.L., Evans, J., Tay, L.H., Anderson, M.J., Colecraft, H.M. & Yue, D.T. (2005) G protein-gated inhibitory module of N-type (ca(v)2.2) ca2+ channels. *Neuron,* **46**, 891-904.

Alban, A., David, S.O., Bjorkesten, L., Andersson, C., Sloge, E., Lewis, S. & Currie, I. (2003) A novel experimental design for comparative two-dimensional gel analysis: Two-dimensional difference gel electrophoresis incorporating a pooled internal standard. *Proteomics,* **3**, 36-44.

Alexandre, J., Batteux, F., Nicco, C., Chereau, C., Laurent, A., Guillevin, L., Weill, B. & Goldwasser, F. (2006) Accumulation of hydrogen peroxide is an early and crucial step for paclitaxel-induced cancer cell death both *in vitro* and in vivo. *International Journal of Cancer.Journal International Du Cancer,* **119**, 41-48.

Amatangelo, M.D., Bassi, D.E., Klein-Szanto, A.J. & Cukierman, E. (2005) Stroma-derived three-dimensional matrices are necessary and sufficient to promote desmoplastic differentiation of normal fibroblasts. *American Journal of Pathology; the American Journal of Pathology,* **167**, 475-488.

Anderson, D.H. (2006) Role of lipids in the MAPK signaling pathway. *Progress in Lipid Research,* **45**, 102-119.

Anton, I.M. & Jones, G.E. (2006) WIP: A multifunctional protein involved in actin cytoskeleton regulation. *European Journal of Cell Biology,* **85**, 295-304.

Arioka, H. & Saijo, N. (1994) Microtubules and antineoplastic drugs. *Gan to Kagaku Ryoho.Cancer & Chemotherapy,* **21**, 583-590.

Arpin, M., Friederich, E., Algrain, M., Vernel, F. & Louvard, D. (1994) Functional differences between L- and T-plastin isoforms. *The Journal of Cell Biology,* **127**, 1995-2008.

Atsumi, S., Nosaka, C., Ochi, Y., Iinuma, H. & Umezawa, K. (1993) Inhibition of experimental metastasis by an alpha-glucosidase inhibitor, 1,6-epi-cyclophellitol. *Cancer Research,* **53**, 4896-4899.

Auth, D. & Brawerman, G. (1992) A 33-kDa polypeptide with homology to the laminin receptor: Component of translation machinery. *Proceedings of the National Academy of Sciences of the United States of America,* **89**, 4368-4372.

Aymerich, I., Duflot, S., Fernandez-Veledo, S., Guillen-Gomez, E., Huber-Ruano, I., Casado, F.J. & Pastor-Anglada, M. (2005) The concentrative nucleoside transporter family (SLC28): New roles beyond salvage? *Biochemical Society Transactions,* **33**, 216-219.

Babbin, B.A., Lee, W.Y., Parkos, C.A., Winfree, L.M., Akyildiz, A., Perretti, M. & Nusrat, A. (2006) Annexin I regulates SKCO-15 cell invasion by signaling through formyl peptide receptors. *The Journal of Biological Chemistry,* **281**, 19588-19599.

Bakin, A.V., Safina, A., Rinehart, C., Daroqui, C., Darbary, H. & Helfman, D.M. (2004) A critical role of tropomyosins in TGF-beta regulation of the actin cytoskeleton and cell motility in epithelial cells. *Molecular Biology of the Cell,* **15**, 4682-4694.

Baldassarre, G., Belletti, B., Nicoloso, M.S., Schiappacassi, M., Vecchione, A., Spessotto, P., Morrione, A., Canzonieri, V. & Colombatti, A. (2005) p27(Kip1)-stathmin interaction influences sarcoma cell migration and invasion. *Cancer Cell,* **7**, 51-63.

Barbieri, C.E., Tang, L.J., Brown, K.A. & Pietenpol, J.A. (2006) Loss of p63 leads to increased cell migration and up-regulation of genes involved in invasion and metastasis. *Cancer Research; Cancer Research,* **66**, 7589-7597.

Barnes, C.J., Li, F., Mandal, M., Yang, Z., Sahin, A.A. & Kumar, R. (2002) Heregulin induces expression, ATPase activity, and nuclear localization of G3BP, a ras signaling component, in human breast tumors. *Cancer Research,* **62**, 1251-1255.

Beere, H.M., Wolf, B.B., Cain, K., Mosser, D.D., Mahboubi, A., Kuwana, T., Tailor, P., Morimoto, R.I., Cohen, G.M. & Green, D.R. (2000) Heat-shock protein 70 inhibits apoptosis by preventing recruitment of procaspase-9 to the apaf-1 apoptosome. *Nature Cell Biology,* **2**, 469-475.

Birkenfeld, J., Betz, H. & Roth, D. (2003) Identification of cofilin and LIM-domain-containing protein kinase 1 as novel interaction partners of 14-3-3 zeta. *The Biochemical Journal,* **369**, 45-54.

Birkenfeld, J., Betz, H. & Roth, D. (2003) Identification of cofilin and LIM-domain-containing protein kinase 1 as novel interaction partners of 14-3-3 zeta. *The Biochemical Journal,* **369**, 45-54.

Blanchoin, L., Pollard, T.D. & Hitchcock-DeGregori, S.E. (2001) Inhibition of the Arp2/3 complex-nucleated actin polymerization and branch formation by tropomyosin. *Current Biology : CB,* **11**, 1300-1304.

Boulben, S., Monnier, A., Le Breton, M., Morales, J., Cormier, P., Belle, R. & Mulner-Lorillon, O. (2003) Sea urchin elongation factor 1delta (EF1delta) and evidence for cell cycle-directed localization changes of a sub-fraction of the protein at M phase. *Cellular and Molecular Life Sciences : CMLS,* **60**, 2178-2188.

Bourke, G.J., El Alami, W., Wilson, S.J., Yuan, A., Roobol, A. & Carden, M.J. (2002) Slow axonal transport of the cytosolic chaperonin CCT with Hsc73 and actin in motor neurons. *Journal of Neuroscience Research,* **68**, 29-35.

Brzoska, E. & Grabowska, I. (2005) Syndecans in cell adhesion and differentiation. *Postepy Biochemii; Postepy Biochemii,* **51**, 52-59.

Buttery, R.C., Rintoul, R.C. & Sethi, T. (2004) Small cell lung cancer: The importance of the extracellular matrix. *The International Journal of*

Biochemistry & Cell Biology; the International Journal of Biochemistry & Cell Biology, **36**, 1154-1160.

Cans, C., Passer, B.J., Shalak, V., Nancy-Portebois, V., Crible, V., Amzallag, N., Allanic, D., Tufino, R., Argentini, M., Moras, D., Fiucci, G., Goud, B., Mirande, M., Amson, R. & Telerman, A. (2003) Translationally controlled tumor protein acts as a guanine nucleotide dissociation inhibitor on the translation elongation factor eEF1A. *Proceedings of the National Academy of Sciences of the United States of America,* **100**, 13892-13897.

CANTAROW, A., PASCHKIS, K.E. & RUTMAN, R.J. (1955) Utilization of uracil by acetylaminofluorene-treated rats. *Journal of the National Cancer Institute; Journal of the National Cancer Institute,* **15**, 1615-1616.

Casella, J.F., Maack, D.J. & Lin, S. (1986) Purification and initial characterization of a protein from skeletal muscle that caps the barbed ends of actin filaments. *The Journal of Biological Chemistry,* **261**, 10915-10921.

Chen, H., Choudhury, D.M. & Craig, S.W. (2006) Coincidence of actin filaments and talin is required to activate vinculin. *Journal of Biological Chemistry,* .

Chen, Q., Crosby, M. & Almasan, A. (2003) Redox regulation of apoptosis before and after cytochrome C release. **7**, 1-9.

Chen, Q., Crosby, M. & Almasan, A. (2003) Redox regulation of apoptosis before and after cytochrome C release. **7**, 1-9.

Chiodi, I., Corioni, M., Giordano, M., Valgardsdottir, R., Ghigna, C., Cobianchi, F., Xu, R.M., Riva, S. & Biamonti, G. (2004) RNA recognition motif 2 directs the recruitment of SF2/ASF to nuclear stress bodies. *Nucleic Acids Research,* **32**, 4127-4136.

Chu, Y.W., Seftor, E.A., Romer, L.H. & Hendrix, M.J. (1996) Experimental coexpression of vimentin and keratin intermediate filaments in human melanoma cells augments motility. *The American Journal of Pathology,* **148**, 63-69.

Clark, E.A., Golub, T.R., Lander, E.S. & Hynes, R.O. (2000) Genomic analysis of metastasis reveals an essential role for RhoC. *Nature,* **406**, 532-535.

Concannon, C.G., Gorman, A.M. & Samali, A. (2003) On the role of Hsp27 in regulating apoptosis. *Apoptosis : An International Journal on Programmed Cell Death,* **8**, 61-70.

Damsky, C.H. & Ilic, D. (2002) Integrin signaling: It's where the action is. *Current Opinion in Cell Biology,* **14**, 594-602.

DesMarais, V., Ghosh, M., Eddy, R. & Condeelis, J. (2005) Cofilin takes the lead. *Journal of Cell Science,* **118**, 19-26.

Despouy, G., Bastie, J.N., Deshaies, S., Balitrand, N., Mazharian, A., Rochette-Egly, C., Chomienne, C. & Delva, L. (2003) Cyclin D3 is a cofactor of retinoic acid receptors, modulating their activity in the presence of cellular retinoic acid-binding protein II. *The Journal of Biological Chemistry,* **278**, 6355-6362.

Diasio, R.B. & Harris, B.E. (1989) Clinical pharmacology of 5-fluorouracil. *Clinical Pharmacokinetics,* **16**, 215-237.

Dintilhac, A. & Bernues, J. (2002) HMGB1 interacts with many apparently unrelated proteins by recognizing short amino acid sequences. *The Journal of Biological Chemistry,* **277**, 7021-7028.

dos Remedios, C.G., Chhabra, D., Kekic, M., Dedova, I.V., Tsubakihara, M., Berry, D.A. & Nosworthy, N.J. (2003) Actin binding proteins: Regulation of cytoskeletal microfilaments. *Physiological Reviews; Physiological Reviews,* **83**, 433-473.

Emert-Sedlak, L., Shangary, S., Rabinovitz, A., Miranda, M.B., Delach, S.M. & Johnson, D.E. (2005) Involvement of cathepsin D in chemotherapy-induced cytochrome c release, caspase activation, and cell death. *Molecular Cancer Therapeutics,* **4**, 733-742.

Erlichman, C., Fine, S., Wong, A. & Elhakim, T. (1988) A randomized trial of fluorouracil and folinic acid in patients with metastatic colorectal carcinoma. *Journal of Clinical Oncology : Official Journal of the American Society of Clinical Oncology,* **6**, 469-475.

Fang, F., Hoskins, J. & Butler, J.S. (2004) 5-fluorouracil enhances exosome-dependent accumulation of polyadenylated rRNAs. *Molecular and Cellular Biology; Molecular and Cellular Biology,* **24**, 10766-10776.

Fischer, C., Sanchez-Ruderisch, H., Welzel, M., Wiedenmann, B., Sakai, T., Andre, S., Gabius, H.J., Khachigian, L., Detjen, K.M. & Rosewicz, S. (2005) Galectin-1 interacts with the {alpha}5{beta}1 fibronectin receptor to restrict carcinoma cell growth via induction of p21 and p27. *The Journal of Biological Chemistry,* **280**, 37266-37277.

Fischer, K.D., Tedford, K. & Penninger, J.M. (1998) Vav links antigen-receptor signaling to the actin cytoskeleton. *Seminars in Immunology,* **10**, 317-327.

Fourie, A.M., Hupp, T.R., Lane, D.P., Sang, B.C., Barbosa, M.S., Sambrook, J.F. & Gething, M.J. (1997) HSP70 binding sites in the tumor suppressor protein p53. *Journal of Biological Chemistry; the Journal of Biological Chemistry,* **272**, 19471-19479.

Gabellini, C., Del Bufalo, D. & Zupi, G. (2006) Involvement of RB gene family in tumor angiogenesis. *Oncogene,* **25**, 5326-5332.

Galvez, A.S., Ulloa, J.A., Chiong, M., Criollo, A., Eisner, V., Barros, L.F. & Lavandero, S. (2003) Aldose reductase induced by hyperosmotic stress mediates cardiomyocyte apoptosis: Differential effects of sorbitol and mannitol. *Journal of Biological Chemistry; the Journal of Biological Chemistry,* **278**, 38484-38494.

Geiger, B., Bershadsky, A., Pankov, R. & Yamada, K.M. (2001) Transmembrane crosstalk between the extracellular matrix--cytoskeleton crosstalk. *Nature Reviews. Molecular Cell Biology; Nature Reviews.Molecular Cell Biology,* **2**, 793-805.

Gevaert, K., Goethals, M., Martens, L., Van Damme, J., Staes, A., Thomas, G.R. & Vandekerckhove, J. (2003) Exploring proteomes and analyzing protein processing by mass spectrometric identification of sorted N-terminal peptides. *Nature Biotechnology,* **21**, 566-569.

Giancotti, F.G. (2000) Complexity and specificity of integrin signalling. *Nature Cell Biology,* **2**, E13-4.

Gibson, A.A., Harwood, F.G., Tillman, D.M. & Houghton, J.A. (1998) Selective sensitization to DNA-damaging agents in a human rhabdomyosarcoma cell line with inducible wild-type p53 overexpression. *Clinical Cancer Research : An Official Journal of the American Association for Cancer Research,* **4**, 145-152.

Gibson, A.A., Harwood, F.G., Tillman, D.M. & Houghton, J.A. (1998) Selective sensitization to DNA-damaging agents in a human rhabdomyosarcoma cell line with inducible wild-type p53 overexpression. *Clinical Cancer Research : An Official Journal of the American Association for Cancer Research,* **4**, 145-152.

Giganti, A., Plastino, J., Janji, B., Van Troys, M., Lentz, D., Ampe, C., Sykes, C. & Friederich, E. (2005) Actin-filament cross-linking protein T-plastin increases Arp2/3-mediated actin-based movement. *Journal of Cell Science,* **118**, 1255-1265.

Gilbert, S., Loranger, A. & Marceau, N. (2004) Keratins modulate c-Flip/extracellular signal-regulated kinase 1 and 2 antiapoptotic signaling in simple epithelial cells. *Molecular and Cellular Biology,* **24**, 7072-7081.

Gilkes, D.M., Chen, L. & Chen, J. (2006) MDMX regulation of p53 response to ribosomal stress. *The EMBO Journal,* .

Gilles, A.M., Presecan, E., Vonica, A. & Lascu, I. (1991) Nucleoside diphosphate kinase from human erythrocytes. structural characterization of the two polypeptide chains responsible for heterogeneity of the hexameric enzyme. *The Journal of Biological Chemistry,* **266**, 8784-8789.

GLAZER, R.I. & HARTMAN, K.D. (1981) Analysis of the effect of 5-fluorouracil on the synthesis and translation of polysomal poly(A)RNA from ehrlich ascites cells. *Molecular Pharmacology,* **19**, 117-121.

Glenney, J.R.,Jr, Kaulfus, P. & Weber, K. (1981) F actin assembly modulated by villin: Ca++-dependent nucleation and capping of the barbed end. *Cell,* **24**, 471-480.

Gohla, A. & Bokoch, G.M. (2002) 14-3-3 regulates actin dynamics by stabilizing phosphorylated cofilin. *Current Biology : CB,* **12**, 1704-1710.

Gohla, A. & Bokoch, G.M. (2002) 14-3-3 regulates actin dynamics by stabilizing phosphorylated cofilin. *Current Biology : CB,* **12**, 1704-1710.

Gorman, A.M., Szegezdi, E., Quigney, D.J. & Samali, A. (2005) Hsp27 inhibits 6-hydroxydopamine-induced cytochrome c release and apoptosis in PC12 cells. *Biochemical and Biophysical Research Communications,* **327**, 801-810.

Granes, F., Berndt, C., Roy, C., Mangeat, P., Reina, M. & Vilaro, S. (2003) Identification of a novel ezrin-binding site in syndecan-2 cytoplasmic domain. *FEBS Letters,* **547**, 212-216.

Griffin, R.J., Williams, B.W., Wild, R., Cherrington, J.M., Park, H. & Song, C.W. (2002) Simultaneous inhibition of the receptor kinase activity of vascular endothelial, fibroblast, and platelet-derived growth factors suppresses tumor growth and enhances tumor radiation response. *Cancer Research,* **62**, 1702-1706.

Gruenbaum, Y., Margalit, A., Goldman, R.D., Shumaker, D.K. & Wilson, K.L. (2005) The nuclear lamina comes of age. *Nature Reviews.Molecular Cell Biology,* **6**, 21-31.

Gu, X., Liu, Y. & Santi, D.V. (1999) The mechanism of pseudouridine synthase I as deduced from its interaction with 5-fluorouracil-tRNA. *Proceedings of the National Academy of Sciences of the United States of America; Proceedings of the National Academy of Sciences of the United States of America,* **96**, 14270-14275.

Han, S., Ritzenthaler, J.D., Sitaraman, S.V. & Roman, J. (2006) Fibronectin increases matrix metalloproteinase 9 expression through activation of c-fos via extracellular-regulated kinase and phosphatidylinositol 3-kinase pathways in human lung carcinoma cells. *The Journal of Biological Chemistry,* **281**, 29614-29624.

Haque, F., Lloyd, D.J., Smallwood, D.T., Dent, C.L., Shanahan, C.M., Fry, A.M., Trembath, R.C. & Shackleton, S. (2006) SUN1 interacts with nuclear lamin A and cytoplasmic nesprins to provide a physical connection between the nuclear lamina and the cytoskeleton. *Molecular and Cellular Biology,* **26**, 3738-3751.

HEIDELBERGER, C., CHAUDHURI, N.K., DANNEBERG, P., MOOREN, D., GRIESBACH, L., DUSCHINSKY, R., SCHNITZER, R.J., PLEVEN, E. & SCHEINER, J. (1957) Fluorinated pyrimidines, a new class of tumour-inhibitory compounds. *Nature; Nature,* **179**, 663-666.

Hernandez-Vargas, H., Ballestar, E., Carmona-Saez, P., von Kobbe, C., Banon-Rodriguez, I., Esteller, M., Moreno-Bueno, G. & Palacios, J. (2006) Transcriptional profiling of MCF7 breast cancer cells in response to 5-fluorouracil: Relationship with cell cycle changes and apoptosis, and identification of novel targets of p53. *International Journal of Cancer. Journal International Du Cancer; International Journal of Cancer.Journal International Du Cancer,* **119**, 1164-1175.

Holcik, M. & Sonenberg, N. (2005) Translational control in stress and apoptosis. *Nature Reviews.Molecular Cell Biology,* **6**, 318-327.

Hood, J.D. & Cheresh, D.A. (2002) Role of integrins in cell invasion and migration. *Nature Reviews.Cancer,* **2**, 91-100.

Hsu, M.C., Chang, H.C. & Hung, W.C. (2006) HER-2/neu represses the metastasis suppressor RECK via ERK and sp transcription factors to promote cell invasion. *The Journal of Biological Chemistry,* **281**, 4718-4725.

Ingraham, H.A. & Goulian, M. (1982) Deoxyuridine triphosphatase: A potential site of interaction with pyrimidine nucleotide analogues. *Biochemical and*

Biophysical Research Communications; Biochemical and Biophysical Research Communications, **109**, 746-752.

Irie, F. & Yamaguchi, Y. (2004) EPHB receptor signaling in dendritic spine development. *Frontiers in Bioscience : A Journal and Virtual Library,* **9**, 1365-1373.

Ivaska, J. & Heino, J. (2000) Adhesion receptors and cell invasion: Mechanisms of integrin-guided degradation of extracellular matrix. *Cellular and Molecular Life Sciences : CMLS,* **57**, 16-24.

Izawa, I. & Inagaki, M. (2006) Regulatory mechanisms and functions of intermediate filaments: A study using site- and phosphorylation state-specific antibodies. *Cancer Science,* **97**, 167-174.

Jackson, R.J. (2005) Alternative mechanisms of initiating translation of mammalian mRNAs. *Biochemical Society Transactions,* **33**, 1231-1241.

Johnsen, J.I., Aurelio, O.N., Kwaja, Z., Jorgensen, G.E., Pellegata, N.S., Plattner, R., Stanbridge, E.J. & Cajot, J.F. (2000) p53-mediated negative regulation of stathmin/Op18 expression is associated with G(2)/M cell-cycle arrest. *International Journal of Cancer.Journal International Du Cancer,* **88**, 685-691.

Jung, M., Kondratyev, A.D. & Dritschilo, A. (1994) Elongation factor 1 delta is enhanced following exposure to ionizing radiation. *Cancer Research,* **54**, 2541-2543.

Kawaguchi, Y., Kato, K., Tanaka, M., Kanamori, M., Nishiyama, Y. & Yamanashi, Y. (2003) Conserved protein kinases encoded by herpesviruses and cellular protein kinase cdc2 target the same phosphorylation site in eukaryotic elongation factor 1delta. *Journal of Virology,* 77, 2359-2368.

Kim, Y.M., Kim, H.J., Song, E.J. & Lee, K.J. (2004) Glucuronic acid is a novel inducer of heat shock response. *Molecular and Cellular Biochemistry,* **259**, 23-33.

Klampfer, L., Swaby, L.A., Huang, J., Sasazuki, T., Shirasawa, S. & Augenlicht, L. (2005) Oncogenic ras increases sensitivity of colon cancer cells to 5-FU-induced apoptosis. *Oncogene; Oncogene,* **24**, 3932-3941.

Ku, N.O., Liao, J. & Omary, M.B. (1998) Phosphorylation of human keratin 18 serine 33 regulates binding to 14-3-3 proteins. *The EMBO Journal,* **17**, 1892-1906.

Ku, N.O., Michie, S., Resurreccion, E.Z., Broome, R.L. & Omary, M.B. (2002) Keratin binding to 14-3-3 proteins modulates keratin filaments and hepatocyte mitotic progression. *Proceedings of the National Academy of Sciences of the United States of America,* **99**, 4373-4378.

Ku, N.O., Michie, S., Resurreccion, E.Z., Broome, R.L. & Omary, M.B. (2002) Keratin binding to 14-3-3 proteins modulates keratin filaments and hepatocyte mitotic progression. *Proceedings of the National Academy of Sciences of the United States of America,* **99**, 4373-4378.

Kumagai, J., Fukuda, J., Kodama, H., Murata, M., Kawamura, K., Itoh, H. & Tanaka, T. (2000) Germ cell-specific heat shock protein 105 binds to p53 in a temperature-sensitive manner in rat testis. *European Journal of Biochemistry / FEBS; European Journal of Biochemistry / FEBS,* **267**, 3073-3078.

Kusano, Y., Yoshitomi, Y., Munesue, S., Okayama, M. & Oguri, K. (2004) Cooperation of syndecan-2 and syndecan-4 among cell surface heparan sulfate proteoglycans in the actin cytoskeletal organization of lewis lung carcinoma cells. *Journal of Biochemistry,* **135**, 129-137.

Langlands, K., Yin, X., Anand, G. & Prochownik, E.V. (1997) Differential interactions of id proteins with basic-helix-loop-helix transcription factors. *The Journal of Biological Chemistry,* **272**, 19785-19793.

Larsson, C. (2006) Protein kinase C and the regulation of the actin cytoskeleton. *Cellular Signalling,* **18**, 276-284.

Larsson, C. (2006) Protein kinase C and the regulation of the actin cytoskeleton. *Cellular Signalling,* **18**, 276-284.

Le Sourd, F., Boulben, S., Le Bouffant, R., Cormier, P., Morales, J., Belle, R. & Mulner-Lorillon, O. (2006) eEF1B: At the dawn of the 21st century. *Biochimica Et Biophysica Acta,* **1759**, 13-31.

Leary, J.A., Kerr, J., Chenevix-Trench, G., Doris, C.P., Hurst, T., Houghton, C.R. & Friedlander, M.L. (1995) Increased expression of the NME1 gene is associated with metastasis in epithelial ovarian cancer. *International Journal of Cancer.Journal International Du Cancer,* **64**, 189-195.

Lebart, M.C. & Benyamin, Y. (2006) Calpain involvement in the remodeling of cytoskeletal anchorage complexes. *The FEBS Journal,* **273**, 3415-3426.

LeFebvre, A.K., Korneeva, N.L., Trutschl, M., Cvek, U., Duzan, R.D., Bradley, C.A., Hershey, J.W. & Rhoads, R.E. (2006) Translation initiation factor eIF4G-1 binds to eIF3 through the eIF3e subunit. *The Journal of Biological Chemistry,* **281**, 22917-22932.

Lenz, H.J., Manno, D.J., Danenberg, K.D. & Danenberg, P.V. (1994) Incorporation of 5-fluorouracil into U2 and U6 snRNA inhibits mRNA precursor splicing. *Journal of Biological Chemistry; the Journal of Biological Chemistry,* **269**, 31962-31968.

Liao, J., Lowthert, L.A., Ghori, N. & Omary, M.B. (1995) The 70-kDa heat shock proteins associate with glandular intermediate filaments in an ATP-dependent manner. *Journal of Biological Chemistry; the Journal of Biological Chemistry,* **270**, 915-922.

Liaudet-Coopman, E., Beaujouin, M., Derocq, D., Garcia, M., Glondu-Lassis, M., Laurent-Matha, V., Prebois, C., Rochefort, H. & Vignon, F. (2006) Cathepsin D: Newly discovered functions of a long-standing aspartic protease in cancer and apoptosis. *Cancer Letters,* **237**, 167-179.

Ling, J., Morley, S.J. & Traugh, J.A. (2005) Inhibition of cap-dependent translation via phosphorylation of eIF4G by protein kinase Pak2. *The EMBO Journal,* **24**, 4094-4105.

Liotta, L.A. & Kohn, E.C. (2001) The microenvironment of the tumour-host interface. *Nature; Nature,* **411**, 375-379.

Longley, D.B. & Johnston, P.G. (2005) Molecular mechanisms of drug resistance. *The Journal of Pathology,* **205**, 275-292.

Longley, D.B., Harkin, D.P. & Johnston, P.G. (2003) 5-fluorouracil: Mechanisms of action and clinical strategies. **3**, 330-338.

Longley, D.B., Harkin, D.P. & Johnston, P.G. (2003) 5-fluorouracil: Mechanisms of action and clinical strategies. *Nature Reviews.Cancer,* **3**, 330-338.

MacLeod, J.C., Sayer, R.J., Lucocq, J.M. & Hubbard, M.J. (2004) ERp29, a general endoplasmic reticulum marker, is highly expressed throughout the brain. *The Journal of Comparative Neurology,* **477**, 29-42.

Malet-Martino, M. & Martino, R. (2002) Clinical studies of three oral prodrugs of 5-fluorouracil (capecitabine, UFT, S-1): A review. *The Oncologist,* **7**, 288-323.

Manceau, V., Gavet, O., Curmi, P. & Sobel, A. (1999) Stathmin interaction with HSC70 family proteins. *Electrophoresis; Electrophoresis,* **20**, 409-417.

Matias, P.M., Gorynia, S., Donner, P. & Carrondo, M.A. (2006) Crystal structure of the human AAA+ protein RuvBL1. *Journal of Biological Chemistry,* .

Maxwell, P.J., Longley, D.B., Latif, T., Boyer, J., Allen, W., Lynch, M., McDermott, U., Harkin, D.P., Allegra, C.J. & Johnston, P.G. (2003) Identification of 5-fluorouracil-inducible target genes using cDNA microarray profiling. *Cancer Research; Cancer Research,* **63**, 4602-4606.

McBride, S., Walsh, D., Meleady, P., Daly, N. & Clynes, M. (1999) Bromodeoxyuridine induces keratin protein synthesis at a posttranscriptional level in human lung tumour cell lines. *Differentiation; Research in Biological Diversity; Differentiation; Research in Biological Diversity,* **64**, 185-193.

McBride, S., Meleady, P., Baird, A., Dinsdale, D. & Clynes, M. (1998) Human lung carcinoma cell line DLKP contains 3 distinct subpopulations with different

growth and attachment properties. *Tumour Biology : The Journal of the International Society for Oncodevelopmental Biology and Medicine; Tumour Biology : The Journal of the International Society for Oncodevelopmental Biology and Medicine,* **19**, 88-103.

Meleady, P. & Clynes, M. (2001) Bromodeoxyuridine induces integrin expression at transcriptional (alpha2 subunit) and post-transcriptional (beta1 subunit) levels, and alters the adhesive properties of two human lung tumour cell lines. *Cell Communication & Adhesion,* **8**, 45-59.

Meleady, P. & Clynes, M. (2001) Bromodeoxyuridine increases keratin 19 protein expression at a posttranscriptional level in two human lung tumor cell lines. *in vitro Cellular & Developmental Biology. Animal; in vitro Cellular & Developmental Biology.Animal,* **37**, 536-542.

Meunier, L., Usherwood, Y.K., Chung, K.T. & Hendershot, L.M. (2002) A subset of chaperones and folding enzymes form multiprotein complexes in endoplasmic reticulum to bind nascent proteins. *Molecular Biology of the Cell; Molecular Biology of the Cell,* **13**, 4456-4469.

Meunier, L., Usherwood, Y.K., Chung, K.T. & Hendershot, L.M. (2002) A subset of chaperones and folding enzymes form multiprotein complexes in endoplasmic reticulum to bind nascent proteins. *Molecular Biology of the Cell; Molecular Biology of the Cell,* **13**, 4456-4469.

Misra, U.K., Deedwania, R. & Pizzo, S.V. (2005) Binding of activated alpha2-macroglobulin to its cell surface receptor GRP78 in 1-LN prostate cancer cells regulates PAK-2-dependent activation of LIMK. *Journal of Biological Chemistry; the Journal of Biological Chemistry,* **280**, 26278-26286.

Misra, U.K., Deedwania, R. & Pizzo, S.V. (2005) Binding of activated alpha2-macroglobulin to its cell surface receptor GRP78 in 1-LN prostate cancer cells regulates PAK-2-dependent activation of LIMK. *The Journal of Biological Chemistry,* **280**, 26278-26286.

Miwa, M., Ura, M., Nishida, M., Sawada, N., Ishikawa, T., Mori, K., Shimma, N., Umeda, I. & Ishitsuka, H. (1998) Design of a novel oral fluoropyrimidine carbamate, capecitabine, which generates 5-fluorouracil selectively in tumours by enzymes concentrated in human liver and cancer tissue. *European Journal of Cancer; European Journal of Cancer (Oxford, England : 1990),* **34**, 1274-1281.

Miyazaki, T., Kato, H., Faried, A., Sohda, M., Nakajima, M., Fukai, Y., Masuda, N., Manda, R., Fukuchi, M., Ojima, H., Tsukada, K. & Kuwano, H. (2005) Predictors of response to chemo-radiotherapy and radiotherapy for esophageal squamous cell carcinoma. *Anticancer Research,* **25**, 2749-2755.

Molitoris, B.A., Leiser, J. & Wagner, M.C. (1997) Role of the actin cytoskeleton in ischemia-induced cell injury and repair. *Pediatric Nephrology (Berlin, Germany),* **11**, 761-767.

Mollinedo, F. & Gajate, C. (2003) Microtubules, microtubule-interfering agents and apoptosis. *Apoptosis : An International Journal on Programmed Cell Death,* **8**, 413-450.

Monnier, A., Belle, R., Morales, J., Cormier, P., Boulben, S. & Mulner-Lorillon, O. (2001) Evidence for regulation of protein synthesis at the elongation step by CDK1/cyclin B phosphorylation. *Nucleic Acids Research,* **29**, 1453-1457.

Mori, K. (2004) Unfolded protein response as a quality control mechanism of proteins. *Tanpakushitsu Kakusan Koso.Protein, Nucleic Acid, Enzyme,* **49**, 992-997.

Moumen, A., Masterson, P., O'Connor, M.J. & Jackson, S.P. (2005) hnRNP K: An HDM2 target and transcriptional coactivator of p53 in response to DNA damage. *Cell,* **123**, 1065-1078.

Moumen, A., Masterson, P., O'Connor, M.J. & Jackson, S.P. (2005) hnRNP K: An HDM2 target and transcriptional coactivator of p53 in response to DNA damage. *Cell,* **123**, 1065-1078.

Nakshatri, H., Bhat-Nakshatri, P. & Currie, R.A. (1996) Subunit association and DNA binding activity of the heterotrimeric transcription factor NF-Y is regulated by cellular redox. *The Journal of Biological Chemistry,* **271**, 28784-28791.

Nie, Q., Zhou, Q.H., Zhu, W., Liu, L.X., Fu, J.K., Li, D.B., Li, Y. & Che, G.W. (2006) nm23-H1 gene inhibits lung cancer cell invasion through down-regulation of PKC signal pathway. *Zhonghua Zhong Liu Za Zhi [Chinese Journal of Oncology],* **28**, 334-336.

Nyman, T., Schuler, H., Korenbaum, E., Schutt, C.E., Karlsson, R. & Lindberg, U. (2002) The role of MeH73 in actin polymerization and ATP hydrolysis. *Journal of Molecular Biology,* **317**, 577-589.

Okubo, Y., Hamada, J., Takahashi, Y., Tada, M., Tsutsumida, A., Furuuchi, K., Aoyama, T., Sugihara, T. & Moriuchi, T. (2002) Transduction of HOXD3-antisense into human melanoma cells results in decreased invasive and motile activities. *Clinical & Experimental Metastasis,* **19**, 503-511.

Ono, S., Mohri, K. & Ono, K. (2004) Microscopic evidence that actin-interacting protein 1 actively disassembles actin-depolymerizing factor/Cofilin-bound actin filaments. *The Journal of Biological Chemistry,* **279**, 14207-14212.

Ostareck-Lederer, A., Ostareck, D.H., Cans, C., Neubauer, G., Bomsztyk, K., Superti-Furga, G. & Hentze, M.W. (2002) c-src-mediated phosphorylation of hnRNP K drives translational activation of specifically silenced mRNAs. *Molecular and Cellular Biology,* **22**, 4535-4543.

Pacaud, M. & Derancourt, J. (1993) Purification and further characterization of macrophage 70-kDa protein, a calcium-regulated, actin-binding protein identical to L-plastin. *Biochemistry,* **32**, 3448-3455.

Palacios, I.M., Gatfield, D., St Johnston, D. & Izaurralde, E. (2004) An eIF4AIII-containing complex required for mRNA localization and nonsense-mediated mRNA decay. *Nature,* **427**, 753-757.

Pan, S., Wang, R., Zhou, X., He, G., Koomen, J., Kobayashi, R., Sun, L., Corvera, J., Gallick, G.E. & Kuang, J. (2006) Involvement of the adaptor protein alix in actin cytoskeleton assembly. *Journal of Biological Chemistry,* .

Pandolfi, P.P., Sonati, F., Rivi, R., Mason, P., Grosveld, F. & Luzzatto, L. (1995) Targeted disruption of the housekeeping gene encoding glucose 6-phosphate dehydrogenase (G6PD): G6PD is dispensable for pentose synthesis but essential for defense against oxidative stress. *The EMBO Journal,* **14**, 5209-5215.

Parcellier, A., Brunet, M., Schmitt, E., Col, E., Didelot, C., Hammann, A., Nakayama, K., Nakayama, K.I., Khochbin, S., Solary, E. & Garrido, C. (2006) HSP27 favors ubiquitination and proteasomal degradation of p27Kip1 and helps S-phase re-entry in stressed cells. *The FASEB Journal : Official Publication of the Federation of American Societies for Experimental Biology; the FASEB Journal : Official Publication of the Federation of American Societies for Experimental Biology,* **20**, 1179-1181.

Patel, M.M. & Anchordoquy, T.J. (2006) Ability of spermine to differentiate between DNA sequences--preferential stabilization of A-tracts. *Biophysical Chemistry,* **122**, 5-15.

Pelletier, M.F., Marcil, A., Sevigny, G., Jakob, C.A., Tessier, D.C., Chevet, E., Menard, R., Bergeron, J.J. & Thomas, D.Y. (2000) The heterodimeric structure of glucosidase II is required for its activity, solubility, and localization in vivo. *Glycobiology,* **10**, 815-827.

Peng, Y., Chen, L., Li, C., Lu, W. & Chen, J. (2001) Inhibition of MDM2 by hsp90 contributes to mutant p53 stabilization. *Journal of Biological Chemistry; the Journal of Biological Chemistry,* **276**, 40583-40590.

Poullet, P., Gautreau, A., Kadare, G., Girault, J.A., Louvard, D. & Arpin, M. (2001) Ezrin interacts with focal adhesion kinase and induces its activation independently of cell-matrix adhesion. *The Journal of Biological Chemistry,* **276**, 37686-37691.

Pupa, S.M., Menard, S., Forti, S. & Tagliabue, E. (2002) New insights into the role of extracellular matrix during tumor onset and progression. *Journal of Cellular Physiology; Journal of Cellular Physiology,* **192**, 259-267.

Qu, L., Huang, S., Baltzis, D., Rivas-Estilla, A.M., Pluquet, O., Hatzoglou, M., Koumenis, C., Taya, Y., Yoshimura, A. & Koromilas, A.E. (2004) Endoplasmic reticulum stress induces p53 cytoplasmic localization and prevents p53-dependent apoptosis by a pathway involving glycogen synthase kinase-3beta. *Genes & Development,* **18**, 261-277.

Rabilloud, T., Strub, J.M., Luche, S., van Dorsselaer, A. & Lunardi, J. (2001) A comparison between sypro ruby and ruthenium II tris (bathophenanthroline disulfonate) as fluorescent stains for protein detection in gels. *Proteomics,* **1**, 699-704.

Rahman, F.B. & Yamauchi, K. (2006) Uncompetitive inhibition of xenopus laevis aldehyde dehydrogenase 1A1 by divalent cations. *Zoological Science,* **23**, 239-244.

Rahman, L., Voeller, D., Rahman, M., Lipkowitz, S., Allegra, C., Barrett, J.C., Kaye, F.J. & Zajac-Kaye, M. (2004) Thymidylate synthase as an oncogene: A novel role for an essential DNA synthesis enzyme. *Cancer Cell,* **5**, 341-351.

Ramalho, L.N., Ribeiro-Silva, A., Cassali, G.D. & Zucoloto, S. (2006) The expression of p63 and cytokeratin 5 in mixed tumors of the canine mammary gland provides new insights into the histogenesis of these neoplasms. *Veterinary Pathology; Veterinary Pathology,* **43**, 424-429.

Renton, A., Llanos, S. & Lu, X. (2003) Hypoxia induces p53 through a pathway distinct from most DNA-damaging and stress-inducing agents. *Carcinogenesis; Carcinogenesis,* **24**, 1177-1182.

Rhee, H.J., Kim, G.Y., Huh, J.W., Kim, S.W. & Na, D.S. (2000) Annexin I is a stress protein induced by heat, oxidative stress and a sulfhydryl-reactive agent. *European Journal of Biochemistry / FEBS,* **267**, 3220-3225.

Rubin, C.I. & Atweh, G.F. (2004) The role of stathmin in the regulation of the cell cycle. *Journal of Cellular Biochemistry,* **93**, 242-250.

Rubin, C.I. & Atweh, G.F. (2004) The role of stathmin in the regulation of the cell cycle. *Journal of Cellular Biochemistry,* **93**, 242-250.

RUTMAN, R.J., CANTAROW, A. & PASCHKIS, K.E. (1954) Studies in 2-acetylaminofluorene carcinogenesis. III. the utilization of uracil-2-C14 by preneoplastic rat liver and rat hepatoma. *Cancer Research; Cancer Research,* **14**, 119-123.

Sampath, D., Rao, V.A. & Plunkett, W. (2003) Mechanisms of apoptosis induction by nucleoside analogs. *Oncogene; Oncogene,* **22**, 9063-9074.

Sang Lee, J., Gyu Park, S., Park, H., Seol, W., Lee, S. & Kim, S. (2002) Interaction network of human aminoacyl-tRNA synthetases and subunits of elongation factor 1 complex. *Biochemical and Biophysical Research Communications,* **291**, 158-164.

Santoni, V., Kieffer, S., Desclaux, D., Masson, F. & Rabilloud, T. (2000) Membrane proteomics: Use of additive main effects with multiplicative interaction model to classify plasma membrane proteins according to their solubility and electrophoretic properties. *Electrophoresis,* **21**, 3329-3344.

Sarkaria, J.N., Busby, E.C., Tibbetts, R.S., Roos, P., Taya, Y., Karnitz, L.M. & Abraham, R.T. (1999) Inhibition of ATM and ATR kinase activities by the radiosensitizing agent, caffeine. *Cancer Research,* **59**, 4375-4382.

Schafer, Z.T. & Kornbluth, S. (2006) The apoptosome: Physiological, developmental, and pathological modes of regulation. *Developmental Cell,* **10**, 549-561.

Scheufler, C., Brinker, A., Bourenkov, G., Pegoraro, S., Moroder, L., Bartunik, H., Hartl, F.U. & Moarefi, I. (2000) Structure of TPR domain-peptide complexes: Critical elements in the assembly of the Hsp70-Hsp90 multichaperone machine. *Cell; Cell,* **101**, 199-210.

Schuler, H., Nyakern, M., Schutt, C.E., Lindberg, U. & Karlsson, R. (2000) Mutational analysis of arginine 177 in the nucleotide binding site of beta-actin. *European Journal of Biochemistry / FEBS,* **267**, 4054-4062.

Schultz, M.C. (2003) DNA damage regulation of the RNA components of the translational apparatus: New biology and mechanisms. *IUBMB Life,* **55**, 243-247.

Schumm, K., Rocha, S., Caamano, J. & Perkins, N.D. (2006) Regulation of p53 tumour suppressor target gene expression by the p52 NF-kappaB subunit. *The EMBO Journal,* **25**, 4820-4832.

Seiler, N. (2004) Catabolism of polyamines. *Amino Acids,* **26**, 217-233.

Selkirk, J.K., Merrick, B.A., Stackhouse, B.L. & He, C. (1994) Multiple p53 protein isoforms and formation of oligomeric complexes with heat shock proteins Hsp70 and Hsp90 in the human mammary tumor, T47D, cell line. *Applied and Theoretical Electrophoresis : The Official Journal of the International Electrophoresis Society; Applied and Theoretical Electrophoresis : The Official Journal of the International Electrophoresis Society,* **4**, 11-18.

Sengupta, S. & Harris, C.C. (2005) p53: Traffic cop at the crossroads of DNA repair and recombination. *Nature Reviews. Molecular Cell Biology,* **6**, 44-55.

Sengupta, S. & Harris, C.C. (2005) p53: Traffic cop at the crossroads of DNA repair and recombination. *Nature Reviews. Molecular Cell Biology,* **6**, 44-55.

Sept, D., Xu, J., Pollard, T.D. & McCammon, J.A. (1999) Annealing accounts for the length of actin filaments formed by spontaneous polymerization. *Biophysical Journal,* 77, 2911-2919.

Sharma, A., Patrick, B., Li, J., Sharma, R., Jeyabal, P.V., Reddy, P.M., Awasthi, S. & Awasthi, Y.C. (2006) Glutathione S-transferases as antioxidant enzymes: Small cell lung cancer (H69) cells transfected with hGSTA1 resist doxorubicin-induced apoptosis. *Archives of Biochemistry and Biophysics,* **452**, 165-173.

Sharpe, P.M. & Ferguson, M.W. (1988) Mesenchymal influences on epithelial differentiation in developing systems. *Journal of Cell Science. Supplement; Journal of Cell Science.Supplement,* **10**, 195-230.

Sheu, G.T. & Traugh, J.A. (1999) A structural model for elongation factor 1 (EF-1) and phosphorylation by protein kinase CKII. *Molecular and Cellular Biochemistry,* **191**, 181-186.

Sheu, G.T. & Traugh, J.A. (1997) Recombinant subunits of mammalian elongation factor 1 expressed in escherichia coli. subunit interactions, elongation activity, and phosphorylation by protein kinase CKII. *The Journal of Biological Chemistry,* **272**, 33290-33297.

Shi, J., Feng, Y., Goulet, A.C., Vaillancourt, R.R., Sachs, N.A., Hershey, J.W. & Nelson, M.A. (2003) The p34cdc2-related cyclin-dependent kinase 11 interacts with the p47 subunit of eukaryotic initiation factor 3 during apoptosis. *The Journal of Biological Chemistry,* **278**, 5062-5071.

Shuster, C.B. & Herman, I.M. (1995) Indirect association of ezrin with F-actin: Isoform specificity and calcium sensitivity. *The Journal of Cell Biology,* **128**, 837-848.

Sis, B., Sagol, O., Kupelioglu, A., Sokmen, S., Terzi, C., Fuzun, M., Ozer, E. & Bishop, P. (2004) Prognostic significance of matrix metalloproteinase-2, cathepsin D, and tenascin-C expression in colorectal carcinoma. *Pathology, Research and Practice,* **200**, 379-387.

Soosairajah, J., Maiti, S., Wiggan, O., Sarmiere, P., Moussi, N., Sarcevic, B., Sampath, R., Bamburg, J.R. & Bernard, O. (2005) Interplay between components of a novel LIM kinase-slingshot phosphatase complex regulates cofilin. *The EMBO Journal,* **24**, 473-486.

Spychala, J., Datta, N.S., Takabayashi, K., Datta, M., Fox, I.H., Gribbin, T. & Mitchell, B.S. (1996) Cloning of human adenosine kinase cDNA: Sequence similarity to microbial ribokinases and fructokinases. *Proceedings of the National Academy of Sciences of the United States of America,* **93**, 1232-1237.

Sreedhar, A.S. & Csermely, P. (2004) Heat shock proteins in the regulation of apoptosis: New strategies in tumor therapy: A comprehensive review. *Pharmacology & Therapeutics*, **101**, 227-257.

Steinmetz, M.O. (2006) Structure and thermodynamics of the tubulin-stathmin interaction. *Journal of Structural Biology*, .

Steinmetz, M.O. (2006) Structure and thermodynamics of the tubulin-stathmin interaction. *Journal of Structural Biology*, .

Stoeltzing, O., Liu, W., Reinmuth, N., Fan, F., Parry, G.C., Parikh, A.A., McCarty, M.F., Bucana, C.D., Mazar, A.P. & Ellis, L.M. (2003) Inhibition of integrin alpha5beta1 function with a small peptide (ATN-161) plus continuous 5-FU infusion reduces colorectal liver metastases and improves survival in mice. *International Journal of Cancer. Journal International Du Cancer; International Journal of Cancer.Journal International Du Cancer*, **104**, 496-503.

Tanaka, T., Akatsuka, S., Ozeki, M., Shirase, T., Hiai, H. & Toyokuni, S. (2004) Redox regulation of annexin 2 and its implications for oxidative stress-induced renal carcinogenesis and metastasis. *Oncogene*, **23**, 3980-3989.

Tani, N., Higashiyama, S., Kawaguchi, N., Madarame, J., Ota, I., Ito, Y., Ohoka, Y., Shiosaka, S., Takada, Y. & Matsuura, N. (2003) Expression level of integrin alpha 5 on tumour cells affects the rate of metastasis to the kidney. *British Journal of Cancer*, **88**, 327-333.

Teodori, L., Tirindelli-Danesi, D., Mauro, F., De Vita, R., Uccelli, R., Botti, C., Modini, C., Nervi, C. & Stipa, S. (1983) Non-small-cell lung carcinoma: Tumor characterization on the basis of flow cytometrically determined cellular heterogeneity. *Cytometry : The Journal of the Society for Analytical Cytology; Cytometry*, **4**, 174-183.

Thiery, J.P. & Sleeman, J.P. (2006) Complex networks orchestrate epithelial-mesenchymal transitions. *Nature Reviews. Molecular Cell Biology; Nature Reviews.Molecular Cell Biology*, **7**, 131-142.

Thornalley, P.J. (2003) Protecting the genome: Defence against nucleotide glycation and emerging role of glyoxalase I overexpression in multidrug resistance in cancer chemotherapy. *Biochemical Society Transactions,* **31**, 1372-1377.

Torimura, T., Ueno, T., Kin, M., Sakisaka, S., Tanikawa, K. & Sata, M. (1999) beta1-integrin mediates cell adhesion, haptotaxis, and chemokinesis of hepatoma cells. **32**, 2-10.

Tourriere, H., Gallouzi, I.E., Chebli, K., Capony, J.P., Mouaikel, J., van der Geer, P. & Tazi, J. (2001) RasGAP-associated endoribonuclease G3Bp: Selective RNA degradation and phosphorylation-dependent localization. *Molecular and Cellular Biology,* **21**, 7747-7760.

Troester, M.A., Hoadley, K.A., Parker, J.S. & Perou, C.M. (2004) Prediction of toxicant-specific gene expression signatures after chemotherapeutic treatment of breast cell lines. *Environmental Health Perspectives; Environmental Health Perspectives,* **112**, 1607-1613.

Troester, M.A., Hoadley, K.A., Sorlie, T., Herbert, B.S., Borresen-Dale, A.L., Lonning, P.E., Shay, J.W., Kaufmann, W.K. & Perou, C.M. (2004) Cell-type-specific responses to chemotherapeutics in breast cancer. *Cancer Research; Cancer Research,* **64**, 4218-4226.

Troester, M.A., Hoadley, K.A., Sorlie, T., Herbert, B.S., Borresen-Dale, A.L., Lonning, P.E., Shay, J.W., Kaufmann, W.K. & Perou, C.M. (2004) Cell-type-specific responses to chemotherapeutics in breast cancer. *Cancer Research; Cancer Research,* **64**, 4218-4226.

Troester, M.A., Hoadley, K.A., Sorlie, T., Herbert, B.S., Borresen-Dale, A.L., Lonning, P.E., Shay, J.W., Kaufmann, W.K. & Perou, C.M. (2004) Cell-type-specific responses to chemotherapeutics in breast cancer. *Cancer Research; Cancer Research,* **64**, 4218-4226.

Uchiumi, T., Honma, S., Nomura, T., Dabbs, E.R. & Hachimori, A. (2002) Translation elongation by a hybrid ribosome in which proteins at the GTPase

center of the escherichia coli ribosome are replaced with rat counterparts. *The Journal of Biological Chemistry,* **277**, 3857-3862.

Valasek, L., Nielsen, K.H. & Hinnebusch, A.G. (2002) Direct eIF2-eIF3 contact in the multifactor complex is important for translation initiation in vivo. *The EMBO Journal,* **21**, 5886-5898.

Vandekerckhove, J., Schering, B., Barmann, M. & Aktories, K. (1988) Botulinum C2 toxin ADP-ribosylates cytoplasmic beta/gamma-actin in arginine 177. *The Journal of Biological Chemistry,* **263**, 696-700.

Villena, J., Berndt, C., Granes, F., Reina, M. & Vilaro, S. (2003) Syndecan-2 expression enhances adhesion and proliferation of stably transfected swiss 3T3 cells. *Cell Biology International,* **27**, 1005-1010.

Vulimiri, S.V. & Nayak, R. (1993) 5-fluorouracil modulates aminoacylation of rat liver tRNA. *Biochemistry and Molecular Biology International; Biochemistry and Molecular Biology International,* **31**, 1121-1128.

Wadhwa, R., Yaguchi, T., Hasan, M.K., Mitsui, Y., Reddel, R.R. & Kaul, S.C. (2002) Hsp70 family member, mot-2/mthsp70/GRP75, binds to the cytoplasmic sequestration domain of the p53 protein. *Experimental Cell Research; Experimental Cell Research,* **274**, 246-253.

Walsh, D., Meleady, P., Power, B., Morley, S.J. & Clynes, M. (2003) Increased levels of the translation initiation factor eIF4E in differentiating epithelial lung tumor cell lines. *Differentiation; Research in Biological Diversity; Differentiation; Research in Biological Diversity,* **71**, 126-134.

Wang, C. & Chen, J. (2003) Phosphorylation and hsp90 binding mediate heat shock stabilization of p53. *Journal of Biological Chemistry; the Journal of Biological Chemistry,* **278**, 2066-2071.

Warusavitarne, J., Ramanathan, P., Kaufman, A., Robinson, B.G. & Schnitzler, M. (2006) 5-fluorouracil (5FU) treatment does not influence invasion and metastasis

in microsatellite unstable (MSI-H) colorectal cancer. *International Journal of Colorectal Disease; International Journal of Colorectal Disease,* **21**, 625-631.

Weaver, A.M., Karginov, A.V., Kinley, A.W., Weed, S.A., Li, Y., Parsons, J.T. & Cooper, J.A. (2001) Cortactin promotes and stabilizes Arp2/3-induced actin filament network formation. *Current Biology : CB,* **11**, 370-374.

Wennerberg, K. & Der, C.J. (2004) Rho-family GTPases: It's not only rac and rho (and I like it). *Journal of Cell Science,* **117**, 1301-1312.

Wiest, L. & Pegg, A.E. (1998) Assay of spermidine and spermine synthases. *Methods in Molecular Biology (Clifton, N.J.),* **79**, 51-57.

Wu, Y., Pan, S., Luo, W., Lin, S.H. & Kuang, J. (2002) Hp95 promotes anoikis and inhibits tumorigenicity of HeLa cells. *Oncogene,* **21**, 6801-6808.

Xu, L. & Deng, X. (2006) Suppression of cancer cell migration and invasion by protein phosphatase 2A through dephosphorylation of mu - and m-calpains. *Journal of Biological Chemistry,* .

Yamamoto, I., Muto, N., Murakami, K. & Akiyama, J. (1992) Collagen synthesis in human skin fibroblasts is stimulated by a stable form of ascorbate, 2-O-alpha-D-glucopyranosyl-L-ascorbic acid. *The Journal of Nutrition,* **122**, 871-877.

Yin, X., Fontoura, B.M., Morimoto, T. & Carroll, R.B. (2003) Cytoplasmic complex of p53 and eEF2. *Journal of Cellular Physiology,* **196**, 474-482.

Yu, F.X., Zhou, D.M. & Yin, H.L. (1991) Chimeric and truncated gCap39 elucidate the requirements for actin filament severing and end capping by the gelsolin family of proteins. *The Journal of Biological Chemistry,* **266**, 19269-19275.

Zink, D., Mayr, C., Janz, C. & Wiesmuller, L. (2002) Association of p53 and MSH2 with recombinative repair complexes during S phase. *Oncogene; Oncogene,* **21**, 4788-4800.

Zuzarte-Luis, V., Montero, J.A., Kawakami, Y., Izpisua-Belmonte, J.C. & Hurle, J.M. (2006) Lysosomal cathepsins in embryonic programmed cell death. *Developmental Biology*, .